IDENTIFICATION AND CHARACTERIZATION OF THE TBX5 PROTEOME PROVIDES MECHANISTIC INSIGHT INTO HOLT-ORAM SYNDROME

Lauren Waldron

A dissertation submitted to the faculty at the University of North Carolina at Chapel Hill in partial fulfillment of the requirements for the degree of Doctor of Philosophy in the department of Genetics in the School of Medicine

Chapel Hill
2015

Approved by:

Frank Conlon

Ileana Cristea

Bob Duronio

Lee Graves

Greg Wang

ABSTRACT

Lauren Waldron: Identification and Characterization of the TBX5 proteome provides mechanistic insight into Holt-Oram syndrome
(Under the direction of Frank Conlon)

Congenital heart disease (CHD) remains the most common congenital malformation, with defects in cardiac chamber septation accounting for almost half of all CHD-related deaths in children. The health problem is compounded by the fact that most children are otherwise asymptomatic. The cardiac transcription factor TBX5 has been shown to be causative in patients with septal defects; however, its mechanism of action in normal development and in CHD has not been determined. To begin to address this question we have developed two different model systems that express an epitope-tagged version of TBX5 for in vivo isolation of endogenous tissue. In the *Xenopus* model, I have developed lines in two different species with the intent to isolate endogenous TBX5 protein complexes. In the mouse model, we have isolated and characterized the endogenous TBX5 cardiac interactome and report that TBX5, long considered to be a cardiac transcriptional activator, interacts biochemically and genetically with the chromatin remodeling repressor machinery of the Nucleosome Remodeling and Deacetylase (NuRD) complex. We report that the TBX5-NuRD interaction is essential for normal heart development and that patients with atrioventricular septal defects (AVSD) have mutations that disrupt the TBX5-

NuRD interaction. We identify the direct transcriptional targets of TBX5 and show TBX5 acts to repress expression of neural and cancer associated gene programs in cardiac tissue and that a subset of these genes are disregulated by CHD patient mutations. We also define a new structural-functional domain of TBX5 that is essential for interaction with the NuRD complex and show through phylogenetic analysis that this domain, and hence the interaction with NuRD, evolved during the early diversification of the vertebrates, simultaneous with the evolution of atrial septation. Thus, we report that the TBX5-NuRD interaction identified here plays a central role in cardiac development and in human CHD, as well as in the evolution of the mammalian heart.

To my Opa, for teaching me to love math and science using any scrap paper he could find, including but not limited to: receipts, napkins, wrapping paper and tablecloths.

To Joshua, for reminding me every day how much I love to learn.

ACKNOWLEDGEMENTS

There are many people who have been instrumental to the success of my studies in graduate school. First and foremost, I would like to thank all of the current and previous members of the Conlon Lab for all of their advice, questions, motivation, support, help, and wine: Chris Showell, Kathleen Christine, Erika Paden, Erin Kaltenbrun, Kerry Dorr, Panna Tandon, Nirav Amin, Chris Slagle, Michelle Villasmil, Leslie Kennedy, Carrie Wilczewski, and Lauren Kuchenbrod. I would especially like to acknowledge Kathleen Christine and Erin Kaltenbrun for taking me under their wings and teaching me all of the tips and tricks to being a successful, somewhat sane graduate student. The Conlon lab is very much like my second family and I would like to both thank everybody and apologize for them having to come to year after year of very similar practice talks. Their advice and helpful critique has helped not only my public speaking, but also my confidence in myself as a scientist.

I cannot even put into words the thanks and acknowledgments that I have for Frank Conlon. He has taught me to be independent and to have faith in myself. He always made time for me when I was struggling with an experiment and provided helpful guidance, encouragement, and a viewpoint that I had not previously

considered. Frank always believed in me and my science and made (almost) every day in the lab fun and exciting. I would also like to thank my committee members Bob Duronio, Ileana Cristea, Lee Graves, Greg Wang, and former committee member Jason Lieb. My committee was extremely instrumental in paving the direction in which my work would go, and I really felt they were on my side every step of the way. For this I am very grateful.

Lastly, I would like to thank my friends and family who have given me ongoing love, encouragement, support, and cheese fries throughout these last seven years. I'd like to thank my dad; although he is not a scientist, he always asked about the next experiment and caused me to think outside of the box. I'd like to thank my mom for her unwavering emotional support. I'd like to thank my friends inside and outside of graduate school for providing moral support and wine whenever I needed it. I'd like to thank my Opa, who taught me how to think logically and question everything from a very young age. Finally, I'd like to thank my husband Joshua, who was always there for me through good science days and bad science days. His love and encouragement was crucial to the completion of my degree.

TABLE OF CONTENTS

LIST OF FIGURES

LIST OF TABLES

LIST OF ABBREVIATIONS

Atrial Natriuretic Factor/Peptide	ANF/Nppa
Atrial septal defects	ASD
Atrio-ventricular	AV
Atrioventricular canal	AVC
Atrioventricular septal defect	AVSD
Bone Morphogenetic Protein	BMP
Cardiac conduction system	CCS
Congenital heart disease	CHD
Chromatin immunoprecipitation	ChIP
Dorsal mesenchymal protrusion	DMP
Down Syndrome	DS
Embryonic day	E
Endocardial cushion	EC
Extra-cellular matrix	ECM
Epithelial-mesenchymal transition	EMT
Enhanced green fluorescent protein	EGFP

Facilitates Chromatin Transcription	FACT
Foramen ovale	FO
Holt-Oram syndrome	HOS
Mesenchymal cap	MC
NuRD interaction domain	NID
Nucleosome Remodeling and Deaceylase	NuRD
Ostium primum	OP
Ostium secundum	OS
Persistent foramen ovale	PFO
Plant homeodomain	Phd
Posterior second heart field	pSHF
Restriction Enzyme Mediated Integration	REMI
Second heart field	SHF
Sonic hedgehog	Shh
Smoothened	*Smo*
Septum primum	SP
Septum secundum	SS

Transcription activator-like effector nucleases	TALEN
T-box containing protein	TBX
Transforming Growth Factor Beta	TGFβ
Untranslated region	UTR
Vascular Endothelial Growth Factor	VEGF
Ventricular septal defect	VSD

CHAPTER 1

Introduction

Congenital malformations, or structural birth defects, are the leading cause of infant mortality in the US and Europe (Dolk et al., 2010; Heron and Tejada-Vera, 2009). Congenital heart disease (CHD) is the most common congenital malformation, occurring in 10 per 1000 (or 1%) of live births. Of these, atrial septal defects (ASD) are the most common, accounting for 11.6% of all congenital heart malformations (Morris et al., 2010). This health problem is compounded by the fact that most children are otherwise asymptomatic and that the disease has no identifiable cause in most cases. It is crucial to understand the molecular mechanism involved in atrial septum formation in order to properly treat patients with ASD.

Development of the atrial septum

Formation of the atrial septum begins early in development, during the process of cardiac looping. Atrial septation is a multi-phase process, and perturbation at any stage can lead to a subtype of ASD (Dhanantwari et al., 2009; Krishnan et al., 2014). At embryonic day (E) 10.5 in the developing mouse, the process of atrial septation begins with the formation of a muscular septum primum (SP), that grows from the roof of the atrium toward the atrioventricular canal (AVC). There is a mesenchymal cap (MC) at the lower end of the SP that is similar to an

endocardial cushion (EC). Initially, the MC does not connect to the AVC, which leaves an opening between the atria called the ostium primum (OP) (Figure 1.1A) (Lin et al., 2006). As development proceeds through E11.5, a secondary septum called the septum secundum (SS) is formed to the right of the SP by atrial roof infolding at the dorsal end. The SS then expands from the EC at the ventral end. Concurrently, the SP undergoes apoptosis to form a secondary ostium called the ostium secondum (OS) (Figure 1.1B). Eventually by E14.5, the EC has fused to the MC, and with the addition of the second-heart field (SHF)-derived mesenchyme to the base of the atrial septum, the OP is fused shut. This fusion is referred to as the dorsal mesenchymal protrusion (DMP). The SS does not fuse to the AVC, leaving an opening known as the foramen ovale (FO) (Figure 1.1C). The FO allows for the bypass of blood from the right atrium to the left atrium, bypassing the lungs to allow continued systemic circulation of the blood. The FO fuses shut after birth via the valvula foraminis ovalis, which is a fold projecting from the FO to the atrium, due to increased pressure in the left atrium resulting from pulmonary circulation (Lin et al., 2006).

Clinically, there are many different types of ASD. The most prevalent type is called ASD type 2, or ostium secundum atrial septal defect. ASD type 2 generates an incomplete connection between the SP and the SS (Figure 1.1D), and is caused by defects in the formation of either, or both, structures (Blom et al., 2005). This leads to defects in the formation of the OS and the FO. Many times, ASD type 2 is often difficult to distinguish from another type of cardiac defect called patent foramen ovale (PFO). PFO occurs when there is an incomplete connection between the

valvula formainis ovalis and the SS even though both are fully developed. PFO can refer to either a delayed closure of the FO, or in many cases the FO never fuses shut, as observed in approximately 25% of adults (Blom et al., 2005). This is different from ASD type 2 in that the valvula foraminis ovalis is underdeveloped in ASD type 2 and therefore incapable of closing the FO.

A second type of ASD, called ASD type 1, occurs at the formation of the OP. ASD type 1 rarely occurs in isolation: it is commonly occurs within a larger context of an atrioventricular septal defect (AVSD). AVSD is a more severe type of cardiac defect, in which the atrial septum does not fuse with the ventricular septum via the DMP (Figure 1.1E). There are many AVSD subtypes: incomplete AVSD, transitional AVSD, and complete AVSD, which is the most severe form (Jacobs et al., 2000). All AVSDs have a common valve between the atria and ventricles; the differences between AVSD subtypes are the amounts of shunting that occurs between chambers, as well as the AV valve morphology (Anderson et al., 1998). The valve defects are primarily due to defective in the EC development; therefore, AVSD is also referred to as an EC defect.

Incomplete AVSD is a lack of OP closure, which allows blood to shunt between both atria. Incomplete AVSDs primarily affect primarily the mitral valve, causing mitral insufficiency, but all other valves are present and functional (Jacobs et al., 2000). Transitional AVSD is more similar to complete AVSD, but the leaflets of the common AV valve are fused to the ventricular septum, which essentially creates two distinct valvular orifices. Small ventricular septal defects (VSD) are

commonly observed in transitional AVSD. This also allows blood to shunt between ventricles, but fusion of AV valve leaflets to the ventricular septum prevents a more severe phenotype (Jacobs et al., 2000). Complete AVSD is characterized by the presence of a common AV valve, which results in a severely affected phenotype (Jacobs et al., 2000) (Anderson et al., 1998).

Molecular mechanisms of atrial and atrioventricular septation

Four distinct mesenchymal tissues are required for the atrial and atrioventricular septa: the ECs (superior and inferior), MC, and DMP (Webb et al., 1998). Defects in the formation or differentiation of any of these tissues will result in atrial or atrioventricular septation defects. Sequencing the DNA of patients with syndromic CHD has identified a number of genes responsible for atrial and atrioventricular septation (Table 1.1), whereas sequencing the DNA of patients with non-syndromic CHD has identified an additional subset of genes involved in septation (Table 1.2.). There are several mouse models of defective septation that have not yet been identified in humans (Table 1.3). The following sections briefly summarize the molecular mechanisms underlying AV septal complex formation.

EC defects lead to septation defects

The primary heart tube separates into different layers as it develops. The inner endocardium develops beneath the myocardium and is separated by a layer of extra-cellular matrix (ECM). The developing myocardium secretes additional ECM components, which results in the local formation of four ECs: the superior and

inferior cushions form first, followed by two lateral cushions in the left and right sides of the AV junction (de Lange et al., 2004; Wessels et al., 1996). The superior and inferior cushions form via an epithelial-mesenchymal transition (EMT) (Manasek, 1970; Markwald et al., 1977; Markwald and Smith, 1972). Further development of the superior and inferior ECs produces the mitral valve aortic leaflet and the tricuspid valve septal leaflet. The developmental mechanism of the lateral ECs is still unknown although they are crucial for AV septum formation. The right lateral cushion is important for tricuspid valve leaflet development, whereas the left lateral cushion is important for mitral valve formation and development (de Lange et al., 2004).

The endocardium undergoes EMT via signaling through the underlying myocardium. Signaling pathways regulating EMT include Notch, BMP (*BMP2* and *BMP4*), *TGFβ2*, *TGFβ3* and *VEGF* (Camenisch et al., 2002; Jiao et al., 2003; Liebner et al., 2004; Luna-Zurita et al., 2010; Ma et al., 2005; McCormack et al., 2013; Rivera-Feliciano and Tabin, 2006; Rodgers et al., 2006; Timmerman et al., 2004). Endocardial tissues in the cushions express downstream receptors and effectors of the myocardial signaling pathways, including ALK2 (ACVR1), ALK3 (BMPR1A), and NOTCH-1, and thereby promote EMT. Defects in these signaling pathways have been linked to septation defects (Tables 1.1- 1.3). Myocardial tissues in the cushions express genes such as *BMP2*, *TBX2*, *NFATC2, NFATC3,* and *NFATC4*, which are important for EMT completion, and mutations in these genes have also been linked to septation defects (Chang et al., 2004; Harrelson et al., 2004; Ma et al., 2005) (Tables 1.1-1.3).

One of the most common AVSD mouse models is the Trisomy 16 mouse, which is the mouse model of Down syndrome (DS) (Epstein et al., 1985; Miyabara et al., 1982). Trisomy 16 null ECs have different morphology and are larger than wild type ECs, which may interfere with DMP fusion with the ECs (Webb et al., 1996). In Trisomy 16 mice, the DMP is hypoplastic and does not bridge the space between the MC and the ECs, thereby leading to AVSD. AVSD is the most common cardiac malformation in DS (up to 30-40% of affected probands), and DS is commonly associated with AVSD, (Blom et al., 2003). Many studies have investigated the genetic cause of AVSD in DS. Recent work associated mutations in the VEGFA pathway (*COL6A1, COL6A2, CRELD1, FBLN2, FRZB,* and *GATA5*) with AVSD in DS by sequencing the DNA of 141 patients with AVSD/DS and comparing with the DNA sequence of DS patients without AVSD (Ackerman et al., 2012; Redig et al., 2014; Robinson et al., 2003). Cell biological studies utilizing cell lines from DS patients found that the Sonic hedgehog (Shh) pathway and pathways involved in ciliogenesis are involved in AVSD-related DS (Ripoll et al., 2012). It is evident that there are many potential candidate genes related to cardiac defects in DS, including genes important for EC formation. However, DS is a very complex disorder and requires more research into the candidate genes.

MC formation defects lead to septation defects

MS formation defects lead to defective EC development and septation. The MC initially forms off of the SP: as the SP grows and elongates the MC obtains a more prominent ridge-like structure (Arrechedera et al., 1987; Wessels et al., 2000)

that helps to close the OP. The MC is contiguous with the DMP and the superior AV cushion at its posterior and anterior ends, respectively. (Wessels et al., 2000). The MC and the DMP are both mesenchymal structures on a molecular level, although they appear to originate from different lineages. Using a *Tie2-Cre* reporter mouse it was demonstrated that the MC is derived from endocardial lineage via EMT (Mommersteeg et al., 2006). This suggests that mutations in proteins required for ECM or EMT may lead to defects in ECs and the MC, which thereby lead to septation defects.

DMP malformations lead to AVSD

The most well-studied event during septation is DMP formation. The MC originates from an endocardial lineage, whereas the DMP is derived from the SHF. The SHF is a population of cardiac progenitor cells located in the pharyngeal mesoderm that contributes to the elongating heart tube, a subset of the developing atrial myocardium, the developing DMP, cardiac smooth muscle cells, and endothelial cells (Cai et al., 2003; Kelly et al., 2001; Mjaatvedt et al., 2001; Waldo et al., 2001).

Many genes and pathways that are required for DMP formation have been identified. One of these is the hedgehog signaling pathway. *Shh* null embryos have defects in the SP and SS, and some null embryos also have defects in AV valve formation (Washington Smoak et al., 2005). *Shh* null embryos exhibit AVSD, and *Shh* signaling within the DMP is required to prevent AVSD (Goddeeris et al., 2008). Knockout of the hedgehog receptor smoothened (*Smo*) in atrial progenitor cells

leads to AVSD (Hoffmann et al., 2009). Fate mapping of *Shh* receiving cells using a *Gli1*^{CreERT2} driver reveals contributions to the PS and DMP, and *Shh* signaling occurs in atrial septum progenitor cells before atrial septation begins (Hoffmann et al., 2009). *Shh* is also required in the pulmonary endoderm for atrial septation (Hoffmann et al., 2009).

Numerous studies have investigated hedgehog-dependent pathways involved in atrial septation and AVSD. Genetic studies indicate that *Isl1* acts upstream of hedgehog signaling during atrial septum formation (Lin et al., 2006). *Isl1* and *Shh* are expressed in the posterior SHF (pSHF); therefore, Hoffmann et al. defined a SHF hedgehog-dependent regulatory network using transcriptional profiling to begin to elucidate the pathway. They found that *Foxf1a* and *Foxf2*, which are Forkhead box transcription factors, are Hedgehog targets in the SHF. Depletion of one copy each of *Foxf1a* and *Foxf2* leads to AVSD and abolishes the DMP. A SHF-specific *Foxf1a* regulatory element was shown to bind both TBX5 and the hedgehog transcriptional regulators GLI1 and GLI3 *in vivo* (Hoffmann et al., 2014).

In addition to *Shh* and the VEGF pathways, mutations in the *Wnt* pathway also lead to DMP malformation and AVSD. Wnt signaling functions via β-catenin to maintain ISL1^{+} SHF progenitor cells in the anterior portion of the developing heart (Ai et al., 2007; Cohen et al., 2007; Kwon et al., 2007; Lin et al., 2007). *Wnt2* ligand characterization and knockout in a mouse model indicates that WNT2 regulates expansion of SHF progenitors via β-catenin in the venous pole of the heart (Tian et al., 2010). Global *Wnt2* depletion reduces the number of ISL1^{+} SHF progenitors,

reduces proliferation in the DMP, reduces DMP hypoplasia, and therefore leads to AVSD (Tian et al., 2010).

Mutations in cardiac transcription factors lead to septation defects

Cardiac septation is mediated by a number of specific cardiac transcription factors in addition to proteins required for ECM, EMT, and AV septal complex formation. Members of the Nkx, Tbox, and Gata families are considered as canonical transcription factors that are required for multiple aspects of cardiogenesis. TBX5, NKX2-5, and GATA4 are expressed in the atria during septation, physically interact with each other at the correct time and place, and coordinately activate additional atrial genes (Bruneau et al., 2001; Garg et al., 2003; Hiroi et al., 2001; Takeuchi and Bruneau, 2009). Mutations in TBX5, NKX2-5, GATA4, TBX20, and GATA6 lead to septation defects in both humans and mice (Tables 1.1-1.3).

TBX5 is required for atrial septation

ASD is often observed in a proband in the context of a congenital syndrome. For example, the Holt-Oram syndrome (HOS), which is caused by mutations in TBX5, is characterized primarily by septal defects (Baban et al., 2014a; Basson et al., 1997; Basson et al., 1994; Basson et al., 1999; Cross et al., 2000; Li et al., 1997; Newbury-Ecob et al., 1996). Mice that are heterozygous for *Tbx5* expression display ASD type 2 and, less abundantly, AVSD (Bruneau et al., 2001).

TBX5 is required in the SHF for atrial septation (Hoffmann et al., 2014; Xie et al., 2012). *Tbx5* is expressed in the pSHF, DMP, and DMP-surrounding mesocardium as observed by *in situ* hybridization. Lineage tracing shows that *Tbx5* is not required in the myocardium or the endocardium for atrial septation; using a *Tnt-Cre* or *Tie2-Cre* driver to deplete *Tbx5* in the myocardium or endocardium, respectively, results in normal septation in mice. However, *Tbx5* depletion in the pSHF using a *Gli1-Cre* driver results in approximately 40% penetrance of ASD (Xie et al., 2012). Xie et al. also performed fate-mapping to show that *Tbx5* is essential for DMP development, and *Tbx5* is required for atrial septum progenitor cell proliferation. The pathway involved in *Tbx5*-mediated atrial septation development has recently been elucidated. *Tbx5* regulates hedgehog signaling in cardiac progenitor cells by regulating *Gas1* and *Osr* expression (Xie et al., 2012), which drives atrial septation.

Molecular genetics of Holt-Oram syndrome (HOS)

HOS (OMIM 142900) is a heart-hand syndrome first described by Mary Holt and Samuel Oram in 1960 (Holt and Oram, 1960). HOS is the most common of three heart-hand syndromes, and affects approximately one in 100,000 live births (Csaba E, 1991). HOS has an autosomal dominant inheritance pattern, and probands have a variety of congenital heart defects and limb defects. To be formally diagnosed with HOS, patients must present with an upper limb defect involving the carpal bone and in many cases, radial or thenar bones (Basson et al., 1994; Li et al., 1997). Approximately 80% of HOS patients have CHD (Basson et al., 1999). The severity of

the limb and cardiac defects do not appear to be correlated, and while HOS is highly penetrant, the phenotype of probands seems to vary widely, even in families (Brassington et al., 2003).

Cardiac defects in HOS patients

The most common CHDs observed in HOS patients are ASDs, VSDs, or defects in the cardiac conduction system (CCS) (Basson et al., 1994; Bruneau et al., 1999; Cross et al., 2000) (Newbury-Ecob et al., 1997). Approximately 40% of cases have CCS abnormalities alone (Newbury-Ecob et al., 1996). Disease severity and prognosis depends primarily on the cardiac defect severity; many ASDs and VSDs can be surgically corrected.

More recent studies of HOS patients report more severe cardiac defects, such as AVSD (Figure 1.1E) (Baban et al., 2014a). These recent HOS cases were identified prenatally, or before the first year of the proband's life, whereas probands in previous HOS case reports were diagnosed later in life. HOS prevalence may be statistically underreported because HOS is often undetected prenatally in spite of the existence of major structural anomalies. When a HOS diagnosis is discovered, up to 55% of parents (11/20) are reported to electively terminate the pregnancy (Barisic et al., 2014). The linkage between AVSD and HOS prompted reexamination of earlier case reports, and nine patients with AVSD were re-discovered but not validated genetically, making AVSD a more common diagnostic phenotype of HOS (Baban et al., 2014a; Basson et al., 1994; Boehme and Shotar, 1989; Del Corso et al., 1991;

Holmes, 1965; Kumar et al., 1994; Marcus et al., 1985; Newbury-Ecob et al., 1996; Sletten and Pierpont, 1996; Smith et al., 1979; Terrett et al., 1994)

The TBX5 mutation spectrum in HOS

Linkage analysis of HOS in two affected families localized the HOS genetic defect on chromosome 12q (Basson et al., 1994; Basson et al., 1995; Bonnet et al., 1994; Terrett et al., 1994; Terrett et al., 1996). Further analysis and direct sequencing of affected families determined that the causative gene was *Tbx5*, a member of the T-box transcription factor family (Li., 1997) (Basson 1997). Currently, there are approximately 200 cases of HOS with a molecular diagnosis by sequence analysis (Table 1.4). The most common TBX5 mutations are those affecting *Tbx5* mRNA splicing, or frameshift mutations caused by nucleic acid insertions or deletions. These mutations lead to truncation or premature stop of TBX5 protein. In most cases, truncated TBX5 is degraded by the nonsense-mediated decay system (Mori et al., 2006). In rare cases, translation of the TBX5 protein is extended, resulting in a gain-of-function phenotype that manifests as atypical HOS, which has a similar phenotype to that of loss-of-function TBX5 mutations (Bohm et al., 2008; Muru et al., 2011). TBX5 overexpression also leads to atypical HOS. Because TBX5 overexpression and null mutation both have the same phenotype, one can hypothesize that proper TBX5 levels are crucial for cardiogenesis. (Fan et al., 2003a; Fan et al., 2003b; Patel et al., 2012; Porto et al., 2010; Postma et al., 2008).

A substantial number of probands contain a point mutation in TBX5. The overwhelming majority of TBX5 missense mutations are located in the T-box DNA-

binding domain. Functional analysis of many of these mutations (e.g., M74I, G80R, L94R, A143T, S154A, R237P, R237Q, R237W, R279X, and 1333delC) indicates that these mutant proteins cannot bind and activate downstream target genes such as *Atrial natriuretic peptide* (*ANF*/*Nppa*) (Baban et al., 2014a; Bohm et al., 2008; Fan et al., 2003b; Ghosh et al., 2001; Hiroi et al., 2001; Zhang et al., 2015; Zhou et al., 2015). Many of these same missense mutations affect TBX5 interaction with partner proteins NKX2.5 and GATA4 (Boogerd et al., 2010; Fan et al., 2003a; Fan et al., 2003b; Hiroi et al., 2001). Outside of the T-box DNA-binding domain, there are additional TBX5 missense mutations with unknown CHD molecular mechanisms: however, it was hypothesized that mutations in the TBX5 C-terminus affects the binding of TBX5 to the minor groove of DNA (Muller and Herrmann, 1997). My recent work identified a novel molecular mechanism for CHD in patients with mutations in the TBX5 C-terminus via interaction of TBX5 with a chromatin-remodeling network.

Recent studies have discovered *TBX5* mutations in a subset of CHD patients who do not meet the strict limb-related criteria for HOS. These patients exhibit a wide array of cardiac defects. Two studies concurrently reported two patients with dilated cardiomyopathy resulting from two different TBX5 missense mutations (Zhang et al., 2015; Zhou et al., 2015) An additional study was performed on probands with septation defects that were not diagnosed with HOS. The DNA of these patients was sequenced for mutations in *Tbx5*. This study identified almost 30 TBX5 mutations that were associated with VSD, ASD, and AVSD. These include missense mutations, silent mutations, and intronic mutations. This study is

confounded by the fact that many of these were DS patients: because DS patients have a very high prevalence of AVSD, it is difficult to correlate genotype with phenotype in these cases. However, the study suggests a high prevalence of TBX5 mutations in DS patients, which should be investigated further (Reamon-Buettner and Borlak, 2004b).

Approximately 70% of individuals who meet the diagnostic criteria for HOS have a mutation in the TBX5 coding region (Basson et al., 1997; Basson et al., 1999; McDermott et al., 2005). This suggests that the remaining 30% of HOS patients may have a mutation in either a regulatory (non-coding) region of *Tbx5*, in a direct target gene of TBX5, or in a TBX5-interacting protein partner. Precedence for this was reported by Smemo et al who identified a variation in a *Tbx5* enhancer in a patient with congenital heart disease (Smemo et al., 2012). To understand the mechanisms underlying HOS, it is crucial to identify the gene regulatory regions, the *in vivo* cardiac protein partners, and the downstream targets of TBX5.

TBX5-interacting protein partners

TBX5-interacting protein partners have been identified in *in vitro* experiments (e.g., GST-pulldowns) and in tissue culture cells. TBX5 contains two protein-protein interaction domains, one at the N-terminus into the T-box, and the other at the C-terminal end. At the N-terminus, TBX5 interacts with the cardiac transcription factors TBX20 (Brown et al., 2005; Goetz et al., 2006), GATA4 (Garg et al., 2003; Maitra et al., 2009), NKX2.5 (Hiroi et al., 2001), and MEF2C (Ghosh et al., 2009). The TBX5-TBX20 interaction is required to repress ectopic expression of *ANF/Nppa* (Brown et

al., 2005; Plageman and Yutzey, 2004). Further evidence suggests that the TBX5-TBX20 interaction is important for the regulation of cell polarity and adhesion genes. Depletion of both TBX20 and TBX5 protein in *Xenopus* embryos results in more severe cardiac defects than depletion of either protein alone, but cardiomyocyte marker expression is maintained (Brown et al., 2005). *Tbx5* and *Gata4* interact genetically; mice that are compound heterozygous for both genes exhibit atrioventricular septal defects and a thinning of the myocardial wall, which is a more severe phenotype than the ASD observed in *Tbx5* heterozygous mice (Maitra et al., 2009). Additionally TBX5 and GATA4 have also been shown to interact biochemically with NKX2.5 to activate downstream expression of *ANF/Nppa* (Bruneau et al., 2001; Garg et al., 2003; Hiroi et al., 2001) and the gap junction protein GJA5/CX40 (Linhares et al., 2004). TBX5 also interacts with the transcription factor MEF2C to drive expression of *alpha myosin heavy chain* (*Myh6*) which patterns the heart (Ghosh et al., 2009).

The TBX5 C-terminus interacts with non-cardiac specific proteins, and these interactions may have roles in protein regulation. TBX5 interacts with LMP4 to regular TBX5 nuclear localization (Camarata et al., 2006; Krause et al., 2004; Kulisz and Simon, 2008). In zebrafish, it has been demonstrated that the zebrafish ortholog of LMP4 (Pdlim7) interacts with zTbx5 to regulate the zTbx5 target genes *nppa* and *tbx2b* at the AV-boundary, and this interaction is required for AV valve formation (Camarata et al., 2010). The TBX5 C-terminus also interacts with TAZ and YAP to regulate TBX5-dependent promoters via the histone acetyltransferases p300 and PCAF (Murakami et al., 2005). The effects of these interactions on the developing

heart are unknown. My work shows that the TBX5 C-terminus also interacts with the NuRD complex to repress aberrant gene transcription of neural- and cancer- related genes. This suggests that the C-terminal TBX5 protein interaction domain may be important for TBX5 protein regulation.

TBX5 interacts with a number of chromatin-remodeling proteins to modulate *Tbx5* transcriptional activity. *Tbx5* genetically interacts with the SWI/SNF protein BRG1, and depletion of BRG1 in mice using an *Nkx2.5-Cre* driver leads to embryonic lethality by E10.5 due to cardiac defects (VSD, double outlet right ventricle, patent foramen ovale, and dilation of the ventricles) and defective cardiomyocyte migration and shape (Takeuchi et al., 2011). TBX5 interacts with the BRG1-interacting factor BAF60C in tissue culture to mediate cardiac gene expression (Lickert et al., 2004). TBX5 also interacts with the histone-modifying protein HDAC3 to reduce *Tbx5* transcriptional activity. Specifically, the interaction between HDAC3 and TBX5 leads to proper regulation of cardiac differentiation; mice lacking HDAC3 in cardiac progenitor cells display overdifferentiation of precursor cells, cardiac defects, and upregulation of TBX5 target genes (Lewandowski et al., 2014).

Dissertation goals

TBX5 is required during many phases of cardiac development, from the cardiac precursor cell stage to atrial septum. However, very little is known about the *in vivo* TBX5 protein interaction partners and gene targets. This is partially due to the fact that isolation and purification of TBX5 protein is difficult. TBX5 shares high

sequence homology with other T-box transcription factors within the T-box DNA-binding domain (Papaioannou and Silver, 1998). TBX5 is sequestered in the nucleus (Zaragoza et al., 2004), which makes the protein difficult to solubilize. A high affinity, high specificity antibody for TBX5 has not been produced. TBX5 has been difficult to purify; the complete crystal structure of TBX5 or any other T-box DNA-binding protein has not been obtained. However, the T-box domains of TBX5 and TBX3 have been purified in the presence and absence of DNA (Coll et al., 2002; Stirnimann et al., 2010). .

We felt that it was necessary to bridge the current knowledge gap by determining the *in vivo* molecular mechanisms by which TBX5 regulates cardiogenesis. For the first step, we developed in vivo methods to isolate endogenous TBX5 protein using the Avi-tag/BirA system in *Xenopus* (Chapter 2) and mouse (Chapter 3) model systems. Chapter 2 describes the generation of *Xenopus laevis* and *Xenopus tropicalis* lines containing TBX5-Avitag. These frog lines are the first to express an epitope-tagged protein under its endogenous cardiac promoter, and this is the first *Xenopus tropicalis* line of any kind to display germline transmission. These frogs can be utilized to determine the *in vivo* TBX5 protein interaction partners and target genes. Chapter 3 describes a comprehensive study of the murine TBX5 cardiac proteome using a $Tbx5^{Avi/Avi};ROSA26^{HA\text{-}BirA/BirA}$ mouse line. We determine that TBX5 interacts with the Nucleosome Remodeling and Deacetylase (NuRD) complex in the heart. We establish a new role for TBX5 as a repressor of neural- and cancer- related genes and validated 11 new transcriptional targets of TBX5. We show that the TBX5-NuRD interaction is essential for normal

heart development, and patients with AVSD have mutations that disrupt the TBX5-NuRD interaction. We also define a new structure-function domain of TBX5 that is essential for interaction with the NuRD complex and perform phylogenetic analysis to show that this domain, and hence the interaction with NuRD, evolved during early diversification of vertebrates, simultaneously with the evolution of atrial septation. Finally, we report that the TBX5-NuRD interaction has a central role in cardiac development, in human CHD, and in evolution of the mammalian heart. Collectively this work enhances the understanding of the molecular mechanisms of TBX5 function in the developing heart.

Table 1.1 Genes involved in septum-related human syndromic CHD.

Gene	Syndrome	OMIM	Mouse Model available	Phenotype	Reference
ATR	Seckel Syndrome	210600	Yes (no cardiac phenotype)	ASD type 2, AVSD, VSD	(Howanietz et al., 1989; Ucar et al., 2004)
BBS12, BBS10, TMEM67, MKS1	Bardet-Biedl Syndrome	209900	Yes (no cardiac phenotype)	ASD type 2, AVSD, VSD	(Willaredt et al., 2012)
B9D1, TEMEM67, MKS1	Mechel-Gruber Syndrome	249000	Yes (no cardiac phenotype)	ASD type 2, VSD	(Weatherbee et al., 2009; Willaredt et al., 2012)
CHD7, SEMA3E	CHARGE Syndrome	214800	Yes	ASD type 2, VSD, AVSD	(Bosman et al., 2005; Corsten-Janssen et al., 2014; D'Alessandro et al., 2015; Issekutz et al., 2005; Jongmans et al., 2006)
CREBBP, EP300	Rubenstein-Schinzel Syndrome	180849	Yes	ASD type 2, VSD	(Oike et al., 1999; Stevens and Bhakta, 1995)
CRELD (VEGA pathway)*, CALL*	3p Syndrome	606217	No	AVSD	(Ackerman et al., 2012; Drumheller et al., 1996; Green et al., 2000; Kozma et al., 2004; Maslen et al., 2006; Robinson et al., 2003; Zatyka et al., 2005)
CTNND2	Cri-Du-Chat Syndrome	123450	No	ASD type 2, VSD	(Chang et al., 2007)
DHCR7	Smith-Lemli-Poitz Syndrome	270400	Yes (no cardiac phenotype)	ASD type 2, AVSD, VSD	(Ryan et al., 1998; Smith et al., 1964; Wassif et al., 2001)
ETS1	Jacobsen Syndrome	147791	Yes (no reported atrial septal defect)	ASD type 2, VSD	(Ye et al., 2010)
EVC, EVC2	Ellis-van Creveld Syndrome	225500	Yes (no cardiac phenotype)	AVSD	(Kamesui et al., 1997; Ruiz-Perez et al., 2007; Tompson et al., 2007)

FGF8	22q11 deletion syndrome (DiGeorge)	188400	Yes	ASD type 2, VSD	(Abu-Issa et al., 2002; Frank et al., 2002)
GDF1	Ivemark Syndrome	208530	Yes	ASD type 2, AVSD	(Calabro et al., 1988; Rankin et al., 2000)
GPC3	Simpson-Golabi-Behmel Syndrome	312870	Yes	ASD type 2, AVSD (mouse), VSD	(Cano-Gauci et al., 1999; Lin et al., 1999; Ng et al., 2009)
JAG1,NOTCH	Alagille Syndrome	118450	Yes (no reported atrial septal defect)	ASD, VSD	(High et al., 2009; Hofmann et al., 2012; Xie et al., 2015)
Kras pathway (*KRAS, BRAF, MEK1, MEK2)*	Cardio-facio-cutaneous Syndrome	115150	Yes	ASD type 2, VSD	(Armour and Allanson, 2008; Inoue et al., 2014)
MKKS	Kaufman-McKusick Syndrome	236700	Yes (no reported septal defect)	AVSD	(Fath et al., 2005; Owens et al., 2009)
MLL2/KMT2D/ KDM6A	Kabuki Syndrome	147920	Yes (no reported cardiac defect)	ASD type 2, VSD	(Bjornsson et al., 2014; Digilio et al., 2001; McMahon and Reardon, 2006; Niikawa et al., 1988)
NIPBL	Cornelia de Lange Syndrome/Brachmann de Lange Syndrome	122470	Yes	ASD type 2, AVSD	(D'Alessandro et al., 2015; Kawauchi et al., 2009; Selicorni et al., 2009)
NOTCH2	Alagille Syndrome 2	610205	Yes	ASD type 2	(McCright et al., 2002; McDaniell et al., 2006)
PITX2	Axenfield-Reiger Syndrome	180500	Yes	ASD type 2, VSD, AVSD	(Ammirabile et al., 2012; Cunningham et al., 1998; Feldt, 1995; Kitamura et al., 1999)
PTPN11 (KRAS, SOS1, RAF1, BRAF, MKEK1, HRAS, NRAS, SHOC2, CBL,	Noonan Syndrome	163950	Yes	ASD type 2, VSD, AVSD	(Araki et al., 2004; Burch et al., 1993; Croonen et al., 2008; Marino et al., 1999; Sznajer et al., 2007)

NF1)					
TBX1	DiGeorge Syndrome	188400	Yes	AVSD, VSD	(Rana et al., 2014)
TBX5	Holt-Oram Syndrome	142900	Yes	AVSD, ASD type 2, VSD	(Baban et al., 2014a; Bruneau et al., 2001; Cross et al., 2000; Holt and Oram, 1960; Newbury-Ecob et al., 1996)
TMEM67, KIF7	Joubert Syndrome	213300	Yes (no atrial septal defects reported)	ASD type 2, VSD	(Abdelhamed et al., 2015; Elmali et al., 2007)
Trisomy 13	Patau Syndrome	-	No	ASD type 2, VSD	(Musewe et al., 1990; Springett et al., 2015)
Trisomy 18	Edwards Syndrome	-	No	ASD type 2, VSD	(Bruns and Martinez, 2015; Oppenheimer-Dekker et al., 1985; Springett et al., 2015)
Trisomy 21 (AUTS2, CNN2, DSCR3, DYNLT3, NQO1, OFD1, PDIA4, PIGP, TTC3, TUBB2B, *CRELD1, VEGFA* pathway: *COL6A1, COL6A2, FBLN2, FRZB, GATA5, SHH*)	Down Syndrome	190685	Yes	AVSD, VSD, ASD type 2	(Ackerman et al., 2012; Blom et al., 2003; Epstein et al., 1985; Freeman et al., 1998; Maslen et al., 2006; Miyabara et al., 1982; O'Doherty et al., 2005; Park et al., 1977; Ripoll et al., 2012; Stoll et al., 1998)
Unknown (1q41-1q42)	Fryns Syndrome	229850	No	ASD type 2, VSD	(Fryns et al., 1979; Lin et al., 2005)
Unknown (8q24.13)	Ritscher-Schinzel Syndrome/ Cranial-cerebello-	220210	No	AVSD, ASD type I, ASD type 2	(Hoo et al., 1994; Orstavik et al., 1998; Ritscher et al., 1987)

	cardiac (3C) Syndrome				
WHSC1	Wolf-Hirschhorn Syndrome	194190	Yes	ASD type 2, VSD	(Hirschhorn et al., 1965; Nimura et al., 2009)

Table 1.2. Human genetic mutations associated with non-syndromic ASD.

Gene	OMIM	Mouse Model?	Phenotype	Reference
ACTC1	102540	Yes (no septal defect reported)	ASD type 2, VSD	(Matsson et al., 2008; Monserrat et al., 2007; Song et al., 2010)
ALK2/ACVR1	102576	Yes	AVSD	(Smith et al., 2009; Wang et al., 2005)
ALK3/BMPR1A	601299	Yes	AVSD	(Briggs et al., 2013; D'Alessandro et al., 2015; Ma et al., 2005; Smith et al., 2009; Yang et al., 2006)
ALK4/ACVR1B	601300	Yes (no cardiac defect reported)	AVSD	(Jornvall et al., 2004; Tomita-Mitchell et al., 2012)
APC	611371	Yes (no cardiac defect reported)	AVSD	(Oshima et al., 1995; Smith et al., 2009; Su et al., 1992)
AVCR2B	602730	Yes	ASD type 2, AVSD, VSD	(Ma et al., 2012; Oh and Li, 1997)
BMP4	112262	Yes	AVSD, ASD type 2, VSD	(Jiao et al., 2003; Posch et al., 2008)
CEP152	613529	No	AVSD	(D'Alessandro et al., 2015)
CFC1	605194	Yes	ASD type 2, VSD, AVSD	(Gaio et al., 1999; Ozcelik et al., 2006; Wang et al., 2011)
CITED2	602937	Yes	ASD type 2, VSD	(Bamforth et al., 2001; Bamforth et al., 2004; Barbera et al., 2002; Sperling et al., 2005; Yin et al., 2002)
CRELD1	607171	No	ASD type 2, AVSD, VSD	(Maslen et al., 2006; Robinson et al., 2003; Zatyka et al., 2005)
GATA4	600576	Yes	ASD type 2, AVSD, VSD	(Garg et al., 2003; Hirayama-Yamada et al., 2005; Moskowitz et al., 2011; Posch et al., 2008; Reamon-Buettner and Borlak, 2005; Tomita-Mitchell

				et al., 2007)
GATA6	601656	Yes (no atrial septal defect reported)	ASD type 2, AVSD, VSD	(Lepore et al., 2006; Lin et al., 2010; Maitra et al., 2010; Morrisey et al., 1998; Wang et al., 2012; Zheng et al., 2012)
GJA1	121014	Yes (no septal defect reported)	ASD type 2, AVSD	(Dasgupta et al., 2001; Reaume et al., 1995; Ya et al., 1998)
HEY2	604674	Yes (no atrial septal defect reported)	AVSD, VSD	(Donovan et al., 2002; Fischer et al., 2004; Reamon-Buettner and Borlak, 2006)
IFT25	-	Yes	AVSD	(Keady et al., 2012)
IFT88	600595	Yes	ASD type 2, AVSD, VSD	(Willaredt et al., 2012; Willaredt et al., 2008)
LEFTY1/2	601877	Yes (no septal defect reported)	AVSD	(Kosaki et al., 1999; Meno et al., 2001)
MDM4	602274	Yes (no cardiac defects reported)	AVSD	(D'Alessandro et al., 2015; Xiong, 2013)
MYH6	160710	Yes (no septal defect reported)	ASD type 2	(Ching et al., 2005; Jiang et al., 2013)
MYH7	160760	Yes (no septal defect reported)	ASD type 2, VSD	(Budde et al., 2007; Postma et al., 2011)
NKX2.5	600584	Yes (no septal defect reported)	ASD type 2, AVSD, VSD	(Benson et al., 1999; Gutierrez-Roelens et al., 2006; Inga et al., 2005; Reamon-Buettner and Borlak, 2004a; Schott et al., 1998; Tanaka et al., 1999)
TBX5	601620	Yes	ASD type 2, AVSD, VSD	(Garg et al., 2003; Reamon-Buettner and Borlak, 2004b)
TBX20	606061	Yes (no septal defect reported)	ASD type 2	(Cai et al., 2005; Kirk et al., 2007; Posch et al., 2010; Singh et al., 2005; Stennard et al., 2005)
ZIC3	300265	Yes	ASD type 2, AVSD, VSD	(Ma et al., 2012; Purandare et al., 2002; Ware et al., 2004)

ZPFM2 (*FOG2*)	603693	Yes	ASD type 2, AVSD, VSD	(D'Alessandro et al., 2015; Svensson et al., 2000)
3q22.1-3q26.1 (*FOXL2, NPHP3, FAM62C, CEP70, FAIM, PIK3CB, BPESC1)*	-	No	AVSD	(Erdogan et al., 2008; Priest et al., 2012)
8p23.1 (*GATA4, NEIL2, FDFT1, CSTB, SOX7*)	-	No	AVSD	(Soemedi et al., 2012) (Tomita-Mitchell et al., 2007)
15q11.2 (*TUBGCP5, CYFIP1, NIPA1, NIPA2*)	-	No	ASD type 2, VSD	(Soemedi et al., 2012)
Xp22.2 (*MID1*)	-	No	AVSD	(Silversides et al., 2012)

Table 1.3. Mouse genetic mutations associated with non-syndromic ASD.

These defects are currently not associated with human patients with ASD.

Gene	OMIM	Phenotype	Reference
Adam19	603640	ASD type 2, VSD	(Zhou et al., 2004)
Bmpr2	600799	ASD type 2, VSD	(Beppu et al., 2009)
Bmp6/7	112266/112267	ASD, VSD	(Kim et al., 2001)
Crtl1/Hapln1	118888	ASD type 2, AVSD, VSD	(Watanabe and Yamada, 1999; Wirrig et al., 2007)
Ctnnb1	116806	ASD type 2, VSD	(Huh and Ornitz, 2010; Liebner et al., 2004; Lin et al., 2007)
Cx40/Cx43	121013/121014	ASD type 2, AVSD	(Kirchhoff et al., 2000)
Ep300	602700	ASD type 2	(Shikama et al., 2003)
EphA3	179611	ASD type 2, AVSD	(Stephen et al., 2007)
Ezh2	601573	AVSD type 2, VSD, AVSD	(Chen et al., 2012)
Fbln1	135820	ASD type 2, VSD	(Cooley et al., 2008)
Foxf1a/Fox2	-	AVSD	(Hoffmann et al., 2009)
Has2	601636	Partial AVSD	(Camenisch et al., 2000)
Id2	600386	AVSD	(Moskowitz et al., 2011)
Nfatc	600489	AVSD, VSD	(de la Pompa et al., 1998)
Nt3	162600	ASD type 2, VSD	(Donovan et al., 1996)
Pdgfrα	173490	ASD type 2	(Bleyl et al., 2010)

Postn	608777	ASD type 2	(Norris et al., 2008)
Rxrα	180245	AVSD, VSD	(Dyson et al., 1995; Gruber et al., 1996)
Shh	600725	ASD type 2/ AVSD	(Goddeeris et al., 2008; Goddeeris et al., 2007; Washington Smoak et al., 2005)
Sirt1	604479	ASD type 2, VSD	(Cheng et al., 2003)
Smo	601500	AVSD	(Hoffmann et al., 2009)
Tbx2	600747	AVSD	(Harrelson et al., 2004)
Tgfbr2	190182	ASD, VSD	(Robson et al., 2010)
Wnt2	147870	AVSD	(Goss et al., 2009; Tian et al., 2010)

Table 1.4. TBX5 mutations found in human patients with heart defects.

Mutation	Type of Mutation	Cardiac phenotype	Reference
100delG (exon 2)	Frameshift	1) ASD, VSD 2) AVSD, VSD	(Brassington et al., 2003)
100-101insG (exon 2)	Frameshift	1) ASD (2 patients) 2) AV dissociation 3) ASD, mitral valve defect	(Borozdin et al., 2006; Brassington et al., 2003)
Q49K	Missense	ASD (2 patients)	(Yang et al., 2000)
IVS2-1G>C	Splice Mutation	1) VSD 2) Unknown	(Basson et al., 1999; Guo et al., 2015)
IVS2-2C->A	Splice Mutation	Unknown	(Basson et al., 1999)
I54T	Missense	1) ASD 2) AVSD	(Reamon-Buettner and Borlak, 2004b; Yang et al., 2000)
D61Y	Missense	Aortic/mitral valve prolapse	(Dias et al., 2007)
W64X	Nonsense	Unknown	(Fan et al., 2003a)
E69X	Nonsense	1) AVSD 2) Unknown (2 patients)	(Basson et al., 1997; Basson et al., 1999; He et al., 2004)
M74I	Missense	VSD, LV hypertrophy, ventricular tachycardia	(Boogerd et al., 2010)
M74V	Missense	ASD	(Debeer et al., 2007)
A79V	Missense	ASD	(Reamon-Buettner and Borlak, 2004b)
G80R	Missense	Composite cardiac defects (19 patients)	(Basson et al., 1999)
IVS3-1 G>A	Splice Mutation	VSD	(McDermott et al., 2005)
IVS3-2 A>G	Splice Mutation	Conductive heart failure	(Heinritz et al., 2005)
246G>AA	Frameshift	Unknown	(Basson et al., 1999)

K88X	Nonsense	1) ASD, mitral valve prolapse 2) None 3) ASD	(Garavelli et al., 2008)
V89E	Missense	None	(Furniss et al., 2009)
280delC (exon 4)	Frameshift	1) VSD (2 patients) 2) ASD, VSD	(Heinritz et al., 2005)
aa83insM	Insertion	Unknown	(Basson et al., 1999)
L94R	Missense	ASD, VSD	(Boogerd et al., 2010)
P96L	Missense	AVSD, Down Syndrome	(Reamon-Buettner and Borlak, 2004b)
Y100C	Missense	ASD	(Reamon-Buettner and Borlak, 2004b)
L102P	Missense	AVSD, Down Syndrome	(Reamon-Buettner and Borlak, 2004b)
I106V	Missense	None (2 patients)	(Boogerd et al., 2010; McDermott et al., 2005)
P108T	Missense	Tricuspid atresia	(Yoshida et al., 2015)
D111Y	Missense	DORV, VSD, ASD, PDA	(Granados-Riveron et al., 2012)
Y114X	Nonsense	Conduction	(McDermott et al., 2005)
W121G	Missense	1) ASD (3 patients) 2) ASD, VSD	(Brassington et al., 2003)
IVS4+1G>T	Splice Mutation	VSD	(McDermott et al., 2005)
IVS4+2T->C	Splice Mutation	Unknown	(Cross et al., 2000)
G125R	Missense	1) None (3 patients) 2) atrial fibrillation (13 patients) 3) ASD 4) VSD 5) incomplete right bundle branch block	(Postma et al., 2008)
374delG (exon 5)	Frameshift	ASD, VSD	(Porto et al., 2010)

381-408del	Deletion	ASD, VSD, bradycardia, mitral valve prolapse (25 patients)	(Fan et al., 2003a)
400-401insC (exon 5)	Frameshift	1) VSD (3 patients) 2) ASD 3) ASD, VSD	(Brassington et al., 2003)
R134C	Missense	AVSD, Down Syndrome	(Reamon-Buettner and Borlak, 2004b)
Y136X	Nonsense	1) ASD (6 patients) 2) Conduction system defects, TOF	(Gruenauer-Kloevekorn and Froster, 2003; Heinritz et al., 2005; McDermott et al., 2005)
416delC	Deletion	ASD	(Yang et al., 2000)
aa140delD	Deletion	Unknown	(Basson et al., 1999)
420-432del	Deletion	Unknown	(Basson et al., 1999)
A143T	Missense	Dilated Cardiomyopathy	(Zhou et al., 2015)
T144I	Missense	AVSD, Down Syndrome	(Reamon-Buettner and Borlak, 2004b)
426-427insC (exon 5)	Frameshift	1) ASD 2) VSD (2 patients) 3) ASD, VSD	(Brassington et al., 2003)
Q151X	Nonsense	ASD, mitral valve	(Borozdin et al., 2006)
456delC (exon 5)	Frameshift	ASD	(Brassington et al., 2003)
S154A	Missense	Dilated Cardiomyopathy	(Zhang et al., 2015)
467insA (exon 5)	Frameshift	ASD	(Heinritz et al., 2005)
475-480dup6	Insertion	ASD	(Debeer et al., 2007)
484ins46bp (exon5)	Frameshift	Aneurysm of the AS, brachycardia	(Heinritz et al., 2005)
504delT	Frameshift	1) ASD, VSD, PDA 2) mitral/tricuspid valve prolapse	(Borozdin et al., 2006)
G169R	Missense	Conotruncal malformation	(Cross et al., 2000)

H170L	Missense	ASD, VSD	(McDermott et al., 2005)
E190X	Missense	Unknown	(Basson et al., 1999)
G195A	Missense	1) PFO, assymetrical aortic valve 2) Unknown	(Brassington et al., 2003; Li et al., 1997)
S196X	Nonsense	1) VSD, TOF 2) Unknown (2 patients) 3) VSD (2 patients)	(Basson et al., 1999; Brassington et al., 2003; Debeer et al., 2007; Li et al., 1997; McDermott et al., 2005)
aa198insN	Insertion	Unknown	(Basson et al., 1999)
614-615 insCCGT (exon 6)	Frameshift	1) murmor in childhood, normal 2) VSD	(Brassington et al., 2003)
641delG	Frameshift	1) AVSD 2) none 3) Unknown	(Borozdin et al., 2006)
H220del	Deletion	AVSD, hypoplastic RV, AV insufficiency, pulmonary valve stenosis	(Boogerd et al., 2010)
T223M	Missense	1) None (2 patients) 2) ASD, VSD (4 patients) 3) VSD (2 patients)	(Brassington et al., 2003)
K226N	Missense	1) ASD, pulmonary stenosis, mitral valve prolapse (2 patients)	(Porto et al., 2010)
T233M	Missense	ASD, VSD	(McDermott et al., 2005)
R237P	Missense	1) ASD, persistent left superior vena cava 2) ASD, VSD	(Boogerd et al., 2010)
R237Q	Missense	1) PFO 2) ASD (6 patients) 3) ASD, incomplete right bundle branch block	(Basson et al., 1997; Basson et al., 1999; Brassington et al., 2003; Debeer et al., 2007)
R237W	Missense	1) AVSD, VSD 2) None 3) ASD	(Basson et al., 1999; Brassington et al., 2003)
726-710del5	Deletion	ASD	(Debeer et al., 2007)
727delG (exon 8)	Frameshift	Unknown	(Basson et al., 1999)

Q250X	Nonsense	ASD	(McDermott et al., 2005)
S252I	Missense	VSD	(Cross et al., 2000)
IVS7-1 G>A	Splice Mutation	VSD, conduction	(McDermott et al., 2005)
IVS7-3 C>G	Splice Mutation	ASD, VSD	(Heinritz et al., 2005)
IVS7+2 T>G	Splice Mutation	VSD	(McDermott et al., 2005)
S261C	Missense	1) None (2 patients) 2) DORV, AVSD	(Brassington et al., 2003)
V263M	Missense	Complete right bundle branch block, ASD, tricuspid valve prolapse, hypoplastic left ventricle	(Faria et al., 2008)
R264L	Missense	1) VSD 2) VSD, pulmonary atresia	(Yoshida et al., 2015)
K266R	Missense	AVSD, Down Syndrome	(Reamon-Buettner and Borlak, 2004b)
798delA (exon 8)	Frameshift	ASD, VSD	(Brassington et al., 2003)
805delT	Deletion	Unknown	(Cross et al., 2000)
813-814 delCA	Frameshift	ASD, Conduction system, LQT	(McDermott et al., 2005)
R279X	Nonsense	1) Unknown 2) ASD, VSD (2 patients) 3) AVSD 4) VSD 5) AVSD, aortic coarction, valve defects	(Baban et al., 2014b; Brassington et al., 2003; Heinritz et al., 2005; Li et al., 1997; Porto et al., 2010)
Y291X	Nonsense	1) VSD 2) ASD	(Borozdin et al., 2006)
Q292R	Missense	AVSD	(Reamon-Buettner and Borlak, 2004b)
939delG	Frameshift	1) ASD 2) ASD, VSD	(Borozdin et al., 2006)
Q315X	Nonsense	ASD, VSD	(McDermott et al., 2005)

E316X	Nonsense	Unknown	(Cross et al., 2000)
1024delT	Frameshift	ASD, VSD	(Borozdin et al., 2006)
Q362X	Nonsense	ASD, VSD, pulmonary vein anomaly	(Heinritz et al., 2005)
S372L	Missense	ASD, conduction	(Baban et al., 2014b)
1128delA	Frameshift	VSD, pulmonary hypertension	(Debeer et al., 2007)
aa 383insA	Insertion	Unknown	(Li et al., 1997)
aa 387insS	Insertion	Unknown	(Basson et al., 1999)
1304delT	Deletion	ASD, VSD, PDA, conduction	(Muru et al., 2011)
1333delC	Frameshift (protein extended)	ASD, VSD	(Bohm et al., 2008)
V452M	Missense	1) None 2) Truncus arteriosis	(Brassington et al., 2003)
Q456X	Missense	Patent ductus arteriosus	(Borozdin et al., 2006)
Exon 6 del	Deletion	1) None 2) ASD, VSD	(Borozdin et al., 2006)
Exon 9 del	Deletion	ASD (2 patients)	(Borozdin et al., 2006)
Ex3_9_del	Deletion	VSD	(Akrami et al., 2001)
Large intragenic duplication	Duplication	AVSD, pulmonary stenosis	(Patel et al., 2012)
Dup 12.q13.1->24.2	Duplication	VSD, FO	(Dixon et al., 1993)
T5:12	Translocation	AVSD	(Basson et al., 1999)

Figure 1.1: Formation of the atrial septum and atrial septal defects. (A) At E10.5, cardiac development at the beginning of atrial septation. (**B**) At E11.0 OS formation begins by apoptosis, and the SS arises to the right of the SP. (**C**) At E14.5, septation is complete. The SS comes together leaving a space called the FO, which is responsible for shunting of blood until birth, when it is fused shut. The second heart field contributes to the dorsal mesenchymal protrusion, fusing the septum to the ECs, forming the AV septal complex. The valves are formed at this stage. Defects in this process lead to ASD type 2 (**D**) and ASD type 1/AVSD (**E**).

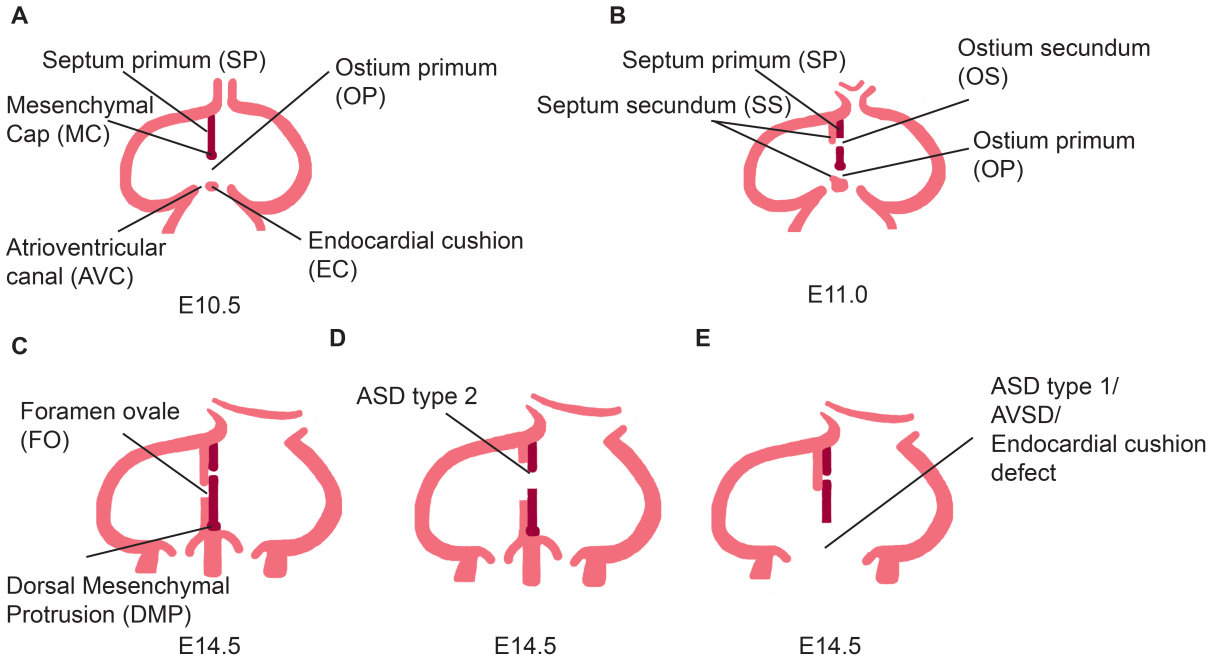

REFERENCES

Abdelhamed, Z.A., Natarajan, S., Wheway, G., Inglehearn, C.F., Toomes, C., Johnson, C.A., and Jagger, D.J. (2015). The Meckel-Gruber syndrome protein TMEM67 controls basal body positioning and epithelial branching morphogenesis in mice via the non-canonical Wnt pathway. Dis Model Mech *8*, 527-541.

Abu-Issa, R., Smyth, G., Smoak, I., Yamamura, K., and Meyers, E.N. (2002). Fgf8 is required for pharyngeal arch and cardiovascular development in the mouse. Development *129*, 4613-4625.

Ackerman, C., Locke, A.E., Feingold, E., Reshey, B., Espana, K., Thusberg, J., Mooney, S., Bean, L.J., Dooley, K.J., Cua, C.L.*, et al.* (2012). An excess of deleterious variants in VEGF-A pathway genes in Down-syndrome-associated atrioventricular septal defects. Am J Hum Genet *91*, 646-659.

Ai, D., Fu, X., Wang, J., Lu, M.F., Chen, L., Baldini, A., Klein, W.H., and Martin, J.F. (2007). Canonical Wnt signaling functions in second heart field to promote right ventricular growth. Proc Natl Acad Sci U S A *104*, 9319-9324.

Akrami, S.M., Winter, R.M., Brook, J.D., and Armour, J.A. (2001). Detection of a large TBX5 deletion in a family with Holt-Oram syndrome. J Med Genet *38*, E44.

Ammirabile, G., Tessari, A., Pignataro, V., Szumska, D., Sutera Sardo, F., Benes, J., Jr., Balistreri, M., Bhattacharya, S., Sedmera, D., and Campione, M. (2012). Pitx2 confers left morphological, molecular, and functional identity to the sinus venosus myocardium. Cardiovasc Res *93*, 291-301.

Anderson, R.H., Ho, S.Y., Falcao, S., Daliento, L., and Rigby, M.L. (1998). The diagnostic features of atrioventricular septal defect with common atrioventricular junction. Cardiol Young *8*, 33-49.

Araki, T., Mohi, M.G., Ismat, F.A., Bronson, R.T., Williams, I.R., Kutok, J.L., Yang, W., Pao, L.I., Gilliland, D.G., Epstein, J.A.*, et al.* (2004). Mouse model of Noonan syndrome reveals cell type- and gene dosage-dependent effects of Ptpn11 mutation. Nat Med *10*, 849-857.

Armour, C.M., and Allanson, J.E. (2008). Further delineation of cardio-facio-cutaneous syndrome: clinical features of 38 individuals with proven mutations. J Med Genet *45*, 249-254.

Arrechedera, H., Alvarez, M., Strauss, M., and Ayesta, C. (1987). Origin of mesenchymal tissue in the septum primum: a structural and ultrastructural study. J Mol Cell Cardiol *19*, 641-651.

Baban, A., Pitto, L., Pulignani, S., Cresci, M., Mariani, L., Gambacciani, C., Digilio, M.C., Pongiglione, G., and Albanese, S. (2014a). Holt-Oram syndrome with intermediate atrioventricular canal defect, and aortic coarctation: functional characterization of a de novo TBX5 mutation. Am J Med Genet A *164A*, 1419-1424.

Baban, A., Postma, A.V., Marini, M., Trocchio, G., Santilli, A., Pelegrini, M., Sirleto, P., Lerone, M., Albanese, S.B., Barnett, P.*, et al.* (2014b). Identification of TBX5 mutations in a series of 94 patients with Tetralogy of Fallot. Am J Med Genet A *164A*, 3100-3107.

Bamforth, S.D., Braganca, J., Eloranta, J.J., Murdoch, J.N., Marques, F.I., Kranc, K.R., Farza, H., Henderson, D.J., Hurst, H.C., and Bhattacharya, S. (2001). Cardiac malformations, adrenal agenesis, neural crest defects and exencephaly in mice lacking Cited2, a new Tfap2 co-activator. Nat Genet *29*, 469-474.

Bamforth, S.D., Braganca, J., Farthing, C.R., Schneider, J.E., Broadbent, C., Michell, A.C., Clarke, K., Neubauer, S., Norris, D., Brown, N.A.*, et al.* (2004). Cited2 controls left-right patterning and heart development through a Nodal-Pitx2c pathway. Nat Genet *36*, 1189-1196.

Barbera, J.P., Rodriguez, T.A., Greene, N.D., Weninger, W.J., Simeone, A., Copp, A.J., Beddington, R.S., and Dunwoodie, S. (2002). Folic acid prevents exencephaly in Cited2 deficient mice. Hum Mol Genet *11*, 283-293.

Barisic, I., Boban, L., Greenlees, R., Garne, E., Wellesley, D., Calzolari, E., Addor, M.C., Arriola, L., Bergman, J.E., Braz, P.*, et al.* (2014). Holt Oram syndrome: a registry-based study in Europe. Orphanet J Rare Dis *9*, 156.

Basson, C.T., Bachinsky, D.R., Lin, R.C., Levi, T., Elkins, J.A., Soults, J., Grayzel, D., Kroumpouzou, E., Traill, T.A., Leblanc-Straceski, J.*, et al.* (1997). Mutations in human TBX5 [corrected] cause limb and cardiac malformation in Holt-Oram syndrome. Nat Genet *15*, 30-35.

Basson, C.T., Cowley, G.S., Solomon, S.D., Weissman, B., Poznanski, A.K., Traill, T.A., Seidman, J.G., and Seidman, C.E. (1994). The clinical and genetic spectrum of the Holt-Oram syndrome (heart-hand syndrome). N Engl J Med *330*, 885-891.

Basson, C.T., Huang, T., Lin, R.C., Bachinsky, D.R., Weremowicz, S., Vaglio, A., Bruzzone, R., Quadrelli, R., Lerone, M., Romeo, G.*, et al.* (1999). Different TBX5 interactions in heart and limb defined by Holt-Oram syndrome mutations. Proc Natl Acad Sci U S A *96*, 2919-2924.

Basson, C.T., Solomon, S.D., Weissman, B., MacRae, C.A., Poznanski, A.K., Prieto, F., Ruiz de la Fuente, S., Pease, W.E., Levin, S.E., Holmes, L.B.*, et al.* (1995). Genetic heterogeneity of heart-hand syndromes. Circulation *91*, 1326-1329.

Benson, D.W., Silberbach, G.M., Kavanaugh-McHugh, A., Cottrill, C., Zhang, Y., Riggs, S., Smalls, O., Johnson, M.C., Watson, M.S., Seidman, J.G.*, et al.* (1999).

Mutations in the cardiac transcription factor NKX2.5 affect diverse cardiac developmental pathways. J Clin Invest *104*, 1567-1573.

Beppu, H., Malhotra, R., Beppu, Y., Lepore, J.J., Parmacek, M.S., and Bloch, K.D. (2009). BMP type II receptor regulates positioning of outflow tract and remodeling of atrioventricular cushion during cardiogenesis. Dev Biol *331*, 167-175.

Bjornsson, H.T., Benjamin, J.S., Zhang, L., Weissman, J., Gerber, E.E., Chen, Y.C., Vaurio, R.G., Potter, M.C., Hansen, K.D., and Dietz, H.C. (2014). Histone deacetylase inhibition rescues structural and functional brain deficits in a mouse model of Kabuki syndrome. Sci Transl Med *6*, 256ra135.

Bleyl, S.B., Saijoh, Y., Bax, N.A., Gittenberger-de Groot, A.C., Wisse, L.J., Chapman, S.C., Hunter, J., Shiratori, H., Hamada, H., Yamada, S.*, et al.* (2010). Dysregulation of the PDGFRA gene causes inflow tract anomalies including TAPVR: integrating evidence from human genetics and model organisms. Hum Mol Genet *19*, 1286-1301.

Blom, N.A., Ottenkamp, J., Jongeneel, T.H., DeRuiter, M.C., and Gittenberger-de Groot, A.C. (2005). Morphogenetic differences of secundum atrial septal defects. Pediatr Cardiol *26*, 338-343.

Blom, N.A., Ottenkamp, J., Wenink, A.G., and Gittenberger-de Groot, A.C. (2003). Deficiency of the vestibular spine in atrioventricular septal defects in human fetuses with down syndrome. Am J Cardiol *91*, 180-184.

Boehme, D.H., and Shotar, A.O. (1989). A complex deformity of appendicular skeleton and shoulder with congenital heart disease in three generations of a Jordanian family. Clin Genet *36*, 442-450.

Bohm, J., Heinritz, W., Craig, A., Vujic, M., Ekman-Joelsson, B.M., Kohlhase, J., and Froster, U. (2008). Functional analysis of the novel TBX5 c.1333delC mutation resulting in an extended TBX5 protein. BMC Med Genet *9*, 88.

Bonnet, D., Pelet, A., Legeai-Mallet, L., Sidi, D., Mathieu, M., Parent, P., Plauchu, H., Serville, F., Schinzel, A., Weissenbach, J.*, et al.* (1994). A gene for Holt-Oram syndrome maps to the distal long arm of chromosome 12. Nat Genet *6*, 405-408.

Boogerd, C.J., Dooijes, D., Ilgun, A., Mathijssen, I.B., Hordijk, R., van de Laar, I.M., Rump, P., Veenstra-Knol, H.E., Moorman, A.F., Barnett, P.*, et al.* (2010). Functional analysis of novel TBX5 T-box mutations associated with Holt-Oram syndrome. Cardiovasc Res *88*, 130-139.

Borozdin, W., Bravo Ferrer Acosta, A.M., Bamshad, M.J., Botzenhart, E.M., Froster, U.G., Lemke, J., Schinzel, A., Spranger, S., McGaughran, J., Wand, D.*, et al.* (2006). Expanding the spectrum of TBX5 mutations in Holt-Oram syndrome: detection of two intragenic deletions by quantitative real time PCR, and report of eight novel point mutations. Hum Mutat *27*, 975-976.

Bosman, E.A., Penn, A.C., Ambrose, J.C., Kettleborough, R., Stemple, D.L., and Steel, K.P. (2005). Multiple mutations in mouse Chd7 provide models for CHARGE syndrome. Hum Mol Genet *14*, 3463-3476.

Brassington, A.M., Sung, S.S., Toydemir, R.M., Le, T., Roeder, A.D., Rutherford, A.E., Whitby, F.G., Jorde, L.B., and Bamshad, M.J. (2003). Expressivity of Holt-Oram syndrome is not predicted by TBX5 genotype. Am J Hum Genet *73*, 74-85.

Briggs, L.E., Phelps, A.L., Brown, E., Kakarla, J., Anderson, R.H., van den Hoff, M.J., and Wessels, A. (2013). Expression of the BMP receptor Alk3 in the second heart field is essential for development of the dorsal mesenchymal protrusion and atrioventricular septation. Circ Res *112*, 1420-1432.

Brown, D.D., Martz, S.N., Binder, O., Goetz, S.C., Price, B.M., Smith, J.C., and Conlon, F.L. (2005). Tbx5 and Tbx20 act synergistically to control vertebrate heart morphogenesis. Development *132*, 553-563.

Bruneau, B.G., Logan, M., Davis, N., Levi, T., Tabin, C.J., Seidman, J.G., and Seidman, C.E. (1999). Chamber-specific cardiac expression of Tbx5 and heart defects in Holt-Oram syndrome. Dev Biol *211*, 100-108.

Bruneau, B.G., Nemer, G., Schmitt, J.P., Charron, F., Robitaille, L., Caron, S., Conner, D.A., Gessler, M., Nemer, M., Seidman, C.E*., et al.* (2001). A murine model of Holt-Oram syndrome defines roles of the T-box transcription factor Tbx5 in cardiogenesis and disease. Cell *106*, 709-721.

Bruns, D.A., and Martinez, A. (2015). An analysis of cardiac defects and surgical interventions in 84 cases with full trisomy 18. Am J Med Genet A.

Budde, B.S., Binner, P., Waldmuller, S., Hohne, W., Blankenfeldt, W., Hassfeld, S., Bromsen, J., Dermintzoglou, A., Wieczorek, M., May, E*., et al.* (2007). Noncompaction of the ventricular myocardium is associated with a de novo mutation in the beta-myosin heavy chain gene. PLoS One *2*, e1362.

Burch, M., Sharland, M., Shinebourne, E., Smith, G., Patton, M., and McKenna, W. (1993). Cardiologic abnormalities in Noonan syndrome: phenotypic diagnosis and echocardiographic assessment of 118 patients. J Am Coll Cardiol *22*, 1189-1192.

Cai, C.L., Liang, X., Shi, Y., Chu, P.H., Pfaff, S.L., Chen, J., and Evans, S. (2003). Isl1 identifies a cardiac progenitor population that proliferates prior to differentiation and contributes a majority of cells to the heart. Dev Cell *5*, 877-889.

Cai, C.L., Zhou, W., Yang, L., Bu, L., Qyang, Y., Zhang, X., Li, X., Rosenfeld, M.G., Chen, J., and Evans, S. (2005). T-box genes coordinate regional rates of proliferation and regional specification during cardiogenesis. Development *132*, 2475-2487.

Calabro, A., Taraschi, A., Lungarotti, M.S., and Ferdinandi, A. (1988). Familial situs inversus and congenital heart defects. Am J Med Genet *31*, 689-690.

Camarata, T., Bimber, B., Kulisz, A., Chew, T.L., Yeung, J., and Simon, H.G. (2006). LMP4 regulates Tbx5 protein subcellular localization and activity. J Cell Biol *174*, 339-348.

Camarata, T., Krcmery, J., Snyder, D., Park, S., Topczewski, J., and Simon, H.G. (2010). Pdlim7 (LMP4) regulation of Tbx5 specifies zebrafish heart atrio-ventricular boundary and valve formation. Dev Biol *337*, 233-245.

Camenisch, T.D., Molin, D.G., Person, A., Runyan, R.B., Gittenberger-de Groot, A.C., McDonald, J.A., and Klewer, S.E. (2002). Temporal and distinct TGFbeta ligand requirements during mouse and avian endocardial cushion morphogenesis. Dev Biol *248*, 170-181.

Camenisch, T.D., Spicer, A.P., Brehm-Gibson, T., Biesterfeldt, J., Augustine, M.L., Calabro, A., Jr., Kubalak, S., Klewer, S.E., and McDonald, J.A. (2000). Disruption of hyaluronan synthase-2 abrogates normal cardiac morphogenesis and hyaluronan-mediated transformation of epithelium to mesenchyme. J Clin Invest *106*, 349-360.

Cano-Gauci, D.F., Song, H.H., Yang, H., McKerlie, C., Choo, B., Shi, W., Pullano, R., Piscione, T.D., Grisaru, S., Soon, S.*, et al.* (1999). Glypican-3-deficient mice exhibit developmental overgrowth and some of the abnormalities typical of Simpson-Golabi-Behmel syndrome. J Cell Biol *146*, 255-264.

Chang, C.P., Neilson, J.R., Bayle, J.H., Gestwicki, J.E., Kuo, A., Stankunas, K., Graef, I.A., and Crabtree, G.R. (2004). A field of myocardial-endocardial NFAT signaling underlies heart valve morphogenesis. Cell *118*, 649-663.

Chang, C.Y., Lin, S.P., Lin, H.Y., Chen, Y.J., Kao, H.A., Yeung, C.Y., Hsu, C.H., and Chi, H. (2007). Cri-du-chat syndrome. Acta Paediatr Taiwan *48*, 328-331.

Chen, L., Ma, Y., Kim, E.Y., Yu, W., Schwartz, R.J., Qian, L., and Wang, J. (2012). Conditional ablation of Ezh2 in murine hearts reveals its essential roles in endocardial cushion formation, cardiomyocyte proliferation and survival. PLoS One *7*, e31005.

Cheng, H.L., Mostoslavsky, R., Saito, S., Manis, J.P., Gu, Y., Patel, P., Bronson, R., Appella, E., Alt, F.W., and Chua, K.F. (2003). Developmental defects and p53 hyperacetylation in Sir2 homolog (SIRT1)-deficient mice. Proc Natl Acad Sci U S A *100*, 10794-10799.

Ching, Y.H., Ghosh, T.K., Cross, S.J., Packham, E.A., Honeyman, L., Loughna, S., Robinson, T.E., Dearlove, A.M., Ribas, G., Bonser, A.J.*, et al.* (2005). Mutation in myosin heavy chain 6 causes atrial septal defect. Nat Genet *37*, 423-428.

Cohen, E.D., Wang, Z., Lepore, J.J., Lu, M.M., Taketo, M.M., Epstein, D.J., and Morrisey, E.E. (2007). Wnt/beta-catenin signaling promotes expansion of Isl-1-positive cardiac progenitor cells through regulation of FGF signaling. J Clin Invest *117*, 1794-1804.

Coll, M., Seidman, J.G., and Muller, C.W. (2002). Structure of the DNA-bound T-box domain of human TBX3, a transcription factor responsible for ulnar-mammary syndrome. Structure *10*, 343-356.

Cooley, M.A., Kern, C.B., Fresco, V.M., Wessels, A., Thompson, R.P., McQuinn, T.C., Twal, W.O., Mjaatvedt, C.H., Drake, C.J., and Argraves, W.S. (2008). Fibulin-1 is required for morphogenesis of neural crest-derived structures. Dev Biol *319*, 336-345.

Corsten-Janssen, N., du Marchie Sarvaas, G.J., Kerstjens-Frederikse, W.S., Hoefsloot, L.H., van Beynum, I.M., Kapusta, L., and van Ravenswaaij-Arts, C.M. (2014). CHD7 mutations are not a major cause of atrioventricular septal and conotruncal heart defects. Am J Med Genet A *164A*, 3003-3009.

Croonen, E.A., van der Burgt, I., Kapusta, L., and Draaisma, J.M. (2008). Electrocardiography in Noonan syndrome PTPN11 gene mutation--phenotype characterization. Am J Med Genet A *146A*, 350-353.

Cross, S.J., Ching, Y.H., Li, Q.Y., Armstrong-Buisseret, L., Spranger, S., Lyonnet, S., Bonnet, D., Penttinen, M., Jonveaux, P., Leheup, B.*, et al.* (2000). The mutation spectrum in Holt-Oram syndrome. J Med Genet *37*, 785-787.

Csaba E, M.V., and Endre C (1991). Holt-Oram syndroma. Orvosi Hetilap *132*, 73-78.

Cunningham, E.T., Jr., Eliott, D., Miller, N.R., Maumenee, I.H., and Green, W.R. (1998). Familial Axenfeld-Rieger anomaly, atrial septal defect, and sensorineural hearing loss: a possible new genetic syndrome. Arch Ophthalmol *116*, 78-82.

D'Alessandro, L.C., Al Turki, S., Manickaraj, A.K., Manase, D., Mulder, B.J., Bergin, L., Rosenberg, H.C., Mondal, T., Gordon, E., Lougheed, J.*, et al.* (2015). Exome sequencing identifies rare variants in multiple genes in atrioventricular septal defect. Genet Med.

Dasgupta, C., Martinez, A.M., Zuppan, C.W., Shah, M.M., Bailey, L.L., and Fletcher, W.H. (2001). Identification of connexin43 (alpha1) gap junction gene mutations in patients with hypoplastic left heart syndrome by denaturing gradient gel electrophoresis (DGGE). Mutat Res *479*, 173-186.

de la Pompa, J.L., Timmerman, L.A., Takimoto, H., Yoshida, H., Elia, A.J., Samper, E., Potter, J., Wakeham, A., Marengere, L., Langille, B.L.*, et al.* (1998). Role of the NF-ATc transcription factor in morphogenesis of cardiac valves and septum. Nature *392*, 182-186.

de Lange, F.J., Moorman, A.F., Anderson, R.H., Manner, J., Soufan, A.T., de Gier-de Vries, C., Schneider, M.D., Webb, S., van den Hoff, M.J., and Christoffels, V.M. (2004). Lineage and morphogenetic analysis of the cardiac valves. Circ Res *95*, 645-654.

Debeer, P., Race, V., Gewillig, M., Devriendt, K., and Frijns, J.P. (2007). Novel TBX5 mutations in patients with Holt-Oram syndrome. Clin Orthop Relat Res *462*, 20-26.

Del Corso, L., Vannini, A., De Marco, S., Gnesi, A., and Pentimone, F. (1991). [Complete endocardial cushion defect and bone malformations of the hands. Holt-Oram syndrome]. Minerva Med *82*, 683-686.

Dhanantwari, P., Lee, E., Krishnan, A., Samtani, R., Yamada, S., Anderson, S., Lockett, E., Donofrio, M., Shiota, K., Leatherbury, L.*, et al.* (2009). Human cardiac development in the first trimester: a high-resolution magnetic resonance imaging and episcopic fluorescence image capture atlas. Circulation *120*, 343-351.

Dias, R.R., Albuquerque, J.M., Pereira, A.C., Stolf, N.A., Krieger, J.E., Mady, C., and Oliveira, S.A. (2007). Holt-Oram syndrome presenting as agenesis of the left pericardium. Int J Cardiol *114*, 98-100.

Digilio, M.C., Marino, B., Toscano, A., Giannotti, A., and Dallapiccola, B. (2001). Congenital heart defects in Kabuki syndrome. Am J Med Genet *100*, 269-274.

Dixon, J.W., Costa, T., and Teshima, I.E. (1993). Mosaicism for duplication 12q (12q13-->q24.2) in a dysmorphic male infant. J Med Genet *30*, 70-72.

Dolk, H., Loane, M., and Garne, E. (2010). The prevalence of congenital anomalies in Europe. Adv Exp Med Biol *686*, 349-364.

Donovan, J., Kordylewska, A., Jan, Y.N., and Utset, M.F. (2002). Tetralogy of fallot and other congenital heart defects in Hey2 mutant mice. Curr Biol *12*, 1605-1610.

Donovan, M.J., Hahn, R., Tessarollo, L., and Hempstead, B.L. (1996). Identification of an essential nonneuronal function of neurotrophin 3 in mammalian cardiac development. Nat Genet *14*, 210-213.

Drumheller, T., McGillivray, B.C., Behrner, D., MacLeod, P., McFadden, D.E., Roberson, J., Venditti, C., Chorney, K., Chorney, M., and Smith, D.I. (1996). Precise localisation of 3p25 breakpoints in four patients with the 3p-syndrome. J Med Genet *33*, 842-847.

Dyson, E., Sucov, H.M., Kubalak, S.W., Schmid-Schonbein, G.W., DeLano, F.A., Evans, R.M., Ross, J., Jr., and Chien, K.R. (1995). Atrial-like phenotype is associated with embryonic ventricular failure in retinoid X receptor alpha -/- mice. Proc Natl Acad Sci U S A *92*, 7386-7390.

Elmali, M., Ozmen, Z., Ceyhun, M., Tokatlioglu, O., Incesu, L., and Diren, B. (2007). Joubert syndrome with atrial septal defect and persistent left superior vena cava. Diagn Interv Radiol *13*, 94-96.

Epstein, C.J., Cox, D.R., and Epstein, L.B. (1985). Mouse trisomy 16: an animal model of human trisomy 21 (Down syndrome). Ann N Y Acad Sci *450*, 157-168.

Erdogan, F., Larsen, L.A., Zhang, L., Tumer, Z., Tommerup, N., Chen, W., Jacobsen, J.R., Schubert, M., Jurkatis, J., Tzschach, A.*, et al.* (2008). High frequency of submicroscopic genomic aberrations detected by tiling path array comparative genome hybridisation in patients with isolated congenital heart disease. J Med Genet *45*, 704-709.

Fan, C., Duhagon, M.A., Oberti, C., Chen, S., Hiroi, Y., Komuro, I., Duhagon, P.I., Canessa, R., and Wang, Q. (2003a). Novel TBX5 mutations and molecular mechanism for Holt-Oram syndrome. J Med Genet *40*, e29.

Fan, C., Liu, M., and Wang, Q. (2003b). Functional analysis of TBX5 missense mutations associated with Holt-Oram syndrome. J Biol Chem *278*, 8780-8785.

Faria, M.H., Rabenhorst, S.H., Pereira, A.C., and Krieger, J.E. (2008). A novel TBX5 missense mutation (V263M) in a family with atrial septal defects and postaxial hexodactyly. Int J Cardiol *130*, 30-35.

Fath, M.A., Mullins, R.F., Searby, C., Nishimura, D.Y., Wei, J., Rahmouni, K., Davis, R.E., Tayeh, M.K., Andrews, M., Yang, B.*, et al.* (2005). Mkks-null mice have a phenotype resembling Bardet-Biedl syndrome. Hum Mol Genet *14*, 1109-1118.

Feldt, R.H., Porter, C.J., Edwards, W.D., Puga, F.J., and Seward, J.B (1995). Atrioventricular septal defects. In Heart Disease in Infants, Children and Adolescents, G.C.E.e. al, ed. (Baltimore: Williams & Wilkins), pp. 704-710.

Fischer, A., Schumacher, N., Maier, M., Sendtner, M., and Gessler, M. (2004). The Notch target genes Hey1 and Hey2 are required for embryonic vascular development. Genes Dev *18*, 901-911.

Frank, D.U., Fotheringham, L.K., Brewer, J.A., Muglia, L.J., Tristani-Firouzi, M., Capecchi, M.R., and Moon, A.M. (2002). An Fgf8 mouse mutant phenocopies human 22q11 deletion syndrome. Development *129*, 4591-4603.

Freeman, S.B., Taft, L.F., Dooley, K.J., Allran, K., Sherman, S.L., Hassold, T.J., Khoury, M.J., and Saker, D.M. (1998). Population-based study of congenital heart defects in Down syndrome. Am J Med Genet *80*, 213-217.

Fryns, J.P., Moerman, F., Goddeeris, P., Bossuyt, C., and Van den Berghe, H. (1979). A new lethal syndrome with cloudy corneae, diaphragmatic defects and distal limb deformities. Hum Genet *50*, 65-70.

Furniss, D., Kan, S.H., Taylor, I.B., Johnson, D., Critchley, P.S., Giele, H.P., and Wilkie, A.O. (2009). Genetic screening of 202 individuals with congenital limb malformations and requiring reconstructive surgery. J Med Genet *46*, 730-735.

Gaio, U., Schweickert, A., Fischer, A., Garratt, A.N., Muller, T., Ozcelik, C., Lankes, W., Strehle, M., Britsch, S., Blum, M.*, et al.* (1999). A role of the cryptic gene in the correct establishment of the left-right axis. Curr Biol *9*, 1339-1342.

Garavelli, L., De Brasi, D., Verri, R., Guareschi, E., Cariola, F., Melis, D., Calcagno, G., Salvatore, F., Unger, S., Sebastio, G.*, et al.* (2008). Holt-Oram syndrome associated with anomalies of the feet. Am J Med Genet A *146A*, 1185-1189.

Garg, V., Kathiriya, I.S., Barnes, R., Schluterman, M.K., King, I.N., Butler, C.A., Rothrock, C.R., Eapen, R.S., Hirayama-Yamada, K., Joo, K.*, et al.* (2003). GATA4 mutations cause human congenital heart defects and reveal an interaction with TBX5. Nature *424*, 443-447.

Ghosh, T.K., Packham, E.A., Bonser, A.J., Robinson, T.E., Cross, S.J., and Brook, J.D. (2001). Characterization of the TBX5 binding site and analysis of mutations that cause Holt-Oram syndrome. Hum Mol Genet *10*, 1983-1994.

Ghosh, T.K., Song, F.F., Packham, E.A., Buxton, S., Robinson, T.E., Ronksley, J., Self, T., Bonser, A.J., and Brook, J.D. (2009). Physical interaction between TBX5 and MEF2C is required for early heart development. Mol Cell Biol *29*, 2205-2218.

Goddeeris, M.M., Rho, S., Petiet, A., Davenport, C.L., Johnson, G.A., Meyers, E.N., and Klingensmith, J. (2008). Intracardiac septation requires hedgehog-dependent cellular contributions from outside the heart. Development *135*, 1887-1895.

Goddeeris, M.M., Schwartz, R., Klingensmith, J., and Meyers, E.N. (2007). Independent requirements for Hedgehog signaling by both the anterior heart field and neural crest cells for outflow tract development. Development *134*, 1593-1604.

Goetz, S.C., Brown, D.D., and Conlon, F.L. (2006). TBX5 is required for embryonic cardiac cell cycle progression. Development *133*, 2575-2584.

Goss, A.M., Tian, Y., Tsukiyama, T., Cohen, E.D., Zhou, D., Lu, M.M., Yamaguchi, T.P., and Morrisey, E.E. (2009). Wnt2/2b and beta-catenin signaling are necessary and sufficient to specify lung progenitors in the foregut. Dev Cell *17*, 290-298.

Granados-Riveron, J.T., Pope, M., Bu'lock, F.A., Thornborough, C., Eason, J., Setchfield, K., Ketley, A., Kirk, E.P., Fatkin, D., Feneley, M.P.*, et al.* (2012). Combined mutation screening of NKX2-5, GATA4, and TBX5 in congenital heart disease: multiple heterozygosity and novel mutations. Congenit Heart Dis *7*, 151-159.

Green, E.K., Priestley, M.D., Waters, J., Maliszewska, C., Latif, F., and Maher, E.R. (2000). Detailed mapping of a congenital heart disease gene in chromosome 3p25. J Med Genet *37*, 581-587.

Gruber, P.J., Kubalak, S.W., Pexieder, T., Sucov, H.M., Evans, R.M., and Chien, K.R. (1996). RXR alpha deficiency confers genetic susceptibility for aortic sac, conotruncal, atrioventricular cushion, and ventricular muscle defects in mice. J Clin Invest *98*, 1332-1343.

Gruenauer-Kloevekorn, C., and Froster, U.G. (2003). Holt-Oram syndrome: a new mutation in the TBX5 gene in two unrelated families. Ann Genet *46*, 19-23.

Guo, Q., Shen, J., Liu, Y., Pu, T., Sun, K., and Chen, S. (2015). Exome Sequencing Identifies a c.148-1G>C Mutation of TBX5 in a Holt-Oram Family with Unusual Genotype-Phenotype Correlations. Cell Physiol Biochem *37*, 1066-1074.

Gutierrez-Roelens, I., De Roy, L., Ovaert, C., Sluysmans, T., Devriendt, K., Brunner, H.G., and Vikkula, M. (2006). A novel CSX/NKX2-5 mutation causes autosomal-dominant AV block: are atrial fibrillation and syncopes part of the phenotype? Eur J Hum Genet *14*, 1313-1316.

Harrelson, Z., Kelly, R.G., Goldin, S.N., Gibson-Brown, J.J., Bollag, R.J., Silver, L.M., and Papaioannou, V.E. (2004). Tbx2 is essential for patterning the atrioventricular canal and for morphogenesis of the outflow tract during heart development. Development *131*, 5041-5052.

He, J., McDermott, D.A., Song, Y., Gilbert, F., Kligman, I., and Basson, C.T. (2004). Preimplantation genetic diagnosis of human congenital heart malformation and Holt-Oram syndrome. Am J Med Genet A *126A*, 93-98.

Heinritz, W., Moschik, A., Kujat, A., Spranger, S., Heilbronner, H., Demuth, S., Bier, A., Tihanyi, M., Mundlos, S., Gruenauer-Kloevekorn, C*., et al.* (2005). Identification of new mutations in the TBX5 gene in patients with Holt-Oram syndrome. Heart *91*, 383-384.

Heron, M., and Tejada-Vera, B. (2009). Deaths: leading causes for 2005. Natl Vital Stat Rep *58*, 1-97.

High, F.A., Jain, R., Stoller, J.Z., Antonucci, N.B., Lu, M.M., Loomes, K.M., Kaestner, K.H., Pear, W.S., and Epstein, J.A. (2009). Murine Jagged1/Notch signaling in the second heart field orchestrates Fgf8 expression and tissue-tissue interactions during outflow tract development. J Clin Invest *119*, 1986-1996.

Hirayama-Yamada, K., Kamisago, M., Akimoto, K., Aotsuka, H., Nakamura, Y., Tomita, H., Furutani, M., Imamura, S., Takao, A., Nakazawa, M*., et al.* (2005). Phenotypes with GATA4 or NKX2.5 mutations in familial atrial septal defect. Am J Med Genet A *135*, 47-52.

Hiroi, Y., Kudoh, S., Monzen, K., Ikeda, Y., Yazaki, Y., Nagai, R., and Komuro, I. (2001). Tbx5 associates with Nkx2-5 and synergistically promotes cardiomyocyte differentiation. Nat Genet *28*, 276-280.

Hirschhorn, K., Cooper, H.L., and Firschein, I.L. (1965). Deletion of short arms of chromosome 4-5 in a child with defects of midline fusion. Humangenetik *1*, 479-482.

Hoffmann, A.D., Peterson, M.A., Friedland-Little, J.M., Anderson, S.A., and Moskowitz, I.P. (2009). sonic hedgehog is required in pulmonary endoderm for atrial septation. Development *136*, 1761-1770.

Hoffmann, A.D., Yang, X.H., Burnicka-Turek, O., Bosman, J.D., Ren, X., Steimle, J.D., Vokes, S.A., McMahon, A.P., Kalinichenko, V.V., and Moskowitz, I.P. (2014). Foxf genes integrate tbx5 and hedgehog pathways in the second heart field for cardiac septation. PLoS Genet *10*, e1004604.

Hofmann, J.J., Briot, A., Enciso, J., Zovein, A.C., Ren, S., Zhang, Z.W., Radtke, F., Simons, M., Wang, Y., and Iruela-Arispe, M.L. (2012). Endothelial deletion of murine Jag1 leads to valve calcification and congenital heart defects associated with Alagille syndrome. Development *139*, 4449-4460.

Holmes, L.B. (1965). CONGENITAL HEART DISEASE AND UPPER-EXTREMITY DEFORMITIES: A REPORT OF TWO FAMILIES. N Engl J Med *272*, 437-444.

Holt, M., and Oram, S. (1960). Familial heart disease with skeletal malformations. Br Heart J *22*, 236-242.

Hoo, J.J., Kreiter, M., Halverson, N., and Perszyk, A. (1994). 3C (cranio-cerebello-cardiac) syndrome: a recently delineated and easily recognizable congenital malformation syndrome. Am J Med Genet *52*, 66-69.

Howanietz, H., Frisch, H., Jedlicka-Kohler, I., and Steger, H. (1989). [Seckel dwarfism based on a personal case]. Klin Padiatr *201*, 139-141.

Huh, S.H., and Ornitz, D.M. (2010). Beta-catenin deficiency causes DiGeorge syndrome-like phenotypes through regulation of Tbx1. Development *137*, 1137-1147.

Inga, A., Reamon-Buettner, S.M., Borlak, J., and Resnick, M.A. (2005). Functional dissection of sequence-specific NKX2-5 DNA binding domain mutations associated with human heart septation defects using a yeast-based system. Hum Mol Genet *14*, 1965-1975.

Inoue, S., Moriya, M., Watanabe, Y., Miyagawa-Tomita, S., Niihori, T., Oba, D., Ono, M., Kure, S., Ogura, T., Matsubara, Y.*, et al.* (2014). New BRAF knockin mice provide a pathogenetic mechanism of developmental defects and a therapeutic approach in cardio-facio-cutaneous syndrome. Hum Mol Genet *23*, 6553-6566.

Issekutz, K.A., Graham, J.M., Jr., Prasad, C., Smith, I.M., and Blake, K.D. (2005). An epidemiological analysis of CHARGE syndrome: preliminary results from a Canadian study. Am J Med Genet A *133A*, 309-317.

Jacobs, J.P., Burke, R.P., Quintessenza, J.A., and Mavroudis, C. (2000). Congenital Heart Surgery Nomenclature and Database Project: atrioventricular canal defect. Ann Thorac Surg *69*, S36-43.

Jiang, J., Wakimoto, H., Seidman, J.G., and Seidman, C.E. (2013). Allele-specific silencing of mutant Myh6 transcripts in mice suppresses hypertrophic cardiomyopathy. Science *342*, 111-114.

Jiao, K., Kulessa, H., Tompkins, K., Zhou, Y., Batts, L., Baldwin, H.S., and Hogan, B.L. (2003). An essential role of Bmp4 in the atrioventricular septation of the mouse heart. Genes Dev *17*, 2362-2367.

Jongmans, M.C., Admiraal, R.J., van der Donk, K.P., Vissers, L.E., Baas, A.F., Kapusta, L., van Hagen, J.M., Donnai, D., de Ravel, T.J., Veltman, J.A.*, et al.* (2006). CHARGE syndrome: the phenotypic spectrum of mutations in the CHD7 gene. J Med Genet *43*, 306-314.

Jornvall, H., Reissmann, E., Andersson, O., Mehrkash, M., and Ibanez, C.F. (2004). ALK7, a receptor for nodal, is dispensable for embryogenesis and left-right patterning in the mouse. Mol Cell Biol *24*, 9383-9389.

Kamesui, T., Seki, M., Tsubota, M., Endo, M., Watanabe, S., and Sato, H. (1997). [A case of Ellis-van Creveld syndrome with partial atrioventricular septal defect and double orifice mitral valve]. Nihon Kyobu Geka Gakkai Zasshi *45*, 589-593.

Kawauchi, S., Calof, A.L., Santos, R., Lopez-Burks, M.E., Young, C.M., Hoang, M.P., Chua, A., Lao, T., Lechner, M.S., Daniel, J.A.*, et al.* (2009). Multiple organ system defects and transcriptional dysregulation in the Nipbl(+/-) mouse, a model of Cornelia de Lange Syndrome. PLoS Genet *5*, e1000650.

Keady, B.T., Samtani, R., Tobita, K., Tsuchya, M., San Agustin, J.T., Follit, J.A., Jonassen, J.A., Subramanian, R., Lo, C.W., and Pazour, G.J. (2012). IFT25 links the signal-dependent movement of Hedgehog components to intraflagellar transport. Dev Cell *22*, 940-951.

Kelly, R.G., Brown, N.A., and Buckingham, M.E. (2001). The arterial pole of the mouse heart forms from Fgf10-expressing cells in pharyngeal mesoderm. Dev Cell *1*, 435-440.

Kim, R.Y., Robertson, E.J., and Solloway, M.J. (2001). Bmp6 and Bmp7 are required for cushion formation and septation in the developing mouse heart. Dev Biol *235*, 449-466.

Kirchhoff, S., Kim, J.S., Hagendorff, A., Thonnissen, E., Kruger, O., Lamers, W.H., and Willecke, K. (2000). Abnormal cardiac conduction and morphogenesis in connexin40 and connexin43 double-deficient mice. Circ Res *87*, 399-405.

Kirk, E.P., Sunde, M., Costa, M.W., Rankin, S.A., Wolstein, O., Castro, M.L., Butler, T.L., Hyun, C., Guo, G., Otway, R.*, et al.* (2007). Mutations in cardiac T-box factor gene TBX20 are associated with diverse cardiac pathologies, including defects of septation and valvulogenesis and cardiomyopathy. Am J Hum Genet *81*, 280-291.

Kitamura, K., Miura, H., Miyagawa-Tomita, S., Yanazawa, M., Katoh-Fukui, Y., Suzuki, R., Ohuchi, H., Suehiro, A., Motegi, Y., Nakahara, Y.*, et al.* (1999). Mouse Pitx2 deficiency leads to anomalies of the ventral body wall, heart, extra- and periocular mesoderm and right pulmonary isomerism. Development *126*, 5749-5758.

Kosaki, K., Bassi, M.T., Kosaki, R., Lewin, M., Belmont, J., Schauer, G., and Casey, B. (1999). Characterization and mutation analysis of human LEFTY A and LEFTY B, homologues of murine genes implicated in left-right axis development. Am J Hum Genet *64*, 712-721.

Kozma, C., Slavotinek, A.M., and Meck, J.M. (2004). Segregation of a t(1;3) translocation in multiple affected family members with both types of adjacent-1 segregants. Am J Med Genet A *124A*, 118-128.

Krause, A., Zacharias, W., Camarata, T., Linkhart, B., Law, E., Lischke, A., Miljan, E., and Simon, H.G. (2004). Tbx5 and Tbx4 transcription factors interact with a new chicken PDZ-LIM protein in limb and heart development. Dev Biol *273*, 106-120.

Krishnan, A., Samtani, R., Dhanantwari, P., Lee, E., Yamada, S., Shiota, K., Donofrio, M.T., Leatherbury, L., and Lo, C.W. (2014). A detailed comparison of mouse and human cardiac development. Pediatr Res *76*, 500-507.

Kulisz, A., and Simon, H.G. (2008). An evolutionarily conserved nuclear export signal facilitates cytoplasmic localization of the Tbx5 transcription factor. Mol Cell Biol *28*, 1553-1564.

Kumar, A., Van Mierop, L.H., and Epstein, M.L. (1994). Pathogenetic implications of muscular ventricular septal defect in Holt-Oram syndrome. Am J Cardiol *73*, 993-995.

Kwon, C., Arnold, J., Hsiao, E.C., Taketo, M.M., Conklin, B.R., and Srivastava, D. (2007). Canonical Wnt signaling is a positive regulator of mammalian cardiac progenitors. Proc Natl Acad Sci U S A *104*, 10894-10899.

Lepore, J.J., Mericko, P.A., Cheng, L., Lu, M.M., Morrisey, E.E., and Parmacek, M.S. (2006). GATA-6 regulates semaphorin 3C and is required in cardiac neural crest for cardiovascular morphogenesis. J Clin Invest *116*, 929-939.

Lewandowski, S.L., Janardhan, H.P., Smee, K.M., Bachman, M., Sun, Z., Lazar, M.A., and Trivedi, C.M. (2014). Histone deacetylase 3 modulates Tbx5 activity to regulate early cardiogenesis. Hum Mol Genet *23*, 3801-3809.

Li, Q.Y., Newbury-Ecob, R.A., Terrett, J.A., Wilson, D.I., Curtis, A.R., Yi, C.H., Gebuhr, T., Bullen, P.J., Robson, S.C., Strachan, T.*, et al.* (1997). Holt-Oram syndrome is caused by mutations in TBX5, a member of the Brachyury (T) gene family. Nat Genet *15*, 21-29.

Lickert, H., Takeuchi, J.K., Von Both, I., Walls, J.R., McAuliffe, F., Adamson, S.L., Henkelman, R.M., Wrana, J.L., Rossant, J., and Bruneau, B.G. (2004). Baf60c is essential for function of BAF chromatin remodelling complexes in heart development. Nature *432*, 107-112.

Liebner, S., Cattelino, A., Gallini, R., Rudini, N., Iurlaro, M., Piccolo, S., and Dejana, E. (2004). Beta-catenin is required for endothelial-mesenchymal transformation during heart cushion development in the mouse. J Cell Biol *166*, 359-367.

Lin, A.E., Neri, G., Hughes-Benzie, R., and Weksberg, R. (1999). Cardiac anomalies in the Simpson-Golabi-Behmel syndrome. Am J Med Genet *83*, 378-381.

Lin, A.E., Pober, B.R., Mullen, M.P., and Slavotinek, A.M. (2005). Cardiovascular malformations in Fryns syndrome: is there a pathogenic role for neural crest cells? Am J Med Genet A *139*, 186-193.

Lin, L., Bu, L., Cai, C.L., Zhang, X., and Evans, S. (2006). Isl1 is upstream of sonic hedgehog in a pathway required for cardiac morphogenesis. Dev Biol *295*, 756-763.

Lin, L., Cui, L., Zhou, W., Dufort, D., Zhang, X., Cai, C.L., Bu, L., Yang, L., Martin, J., Kemler, R.*, et al.* (2007). Beta-catenin directly regulates Islet1 expression in cardiovascular progenitors and is required for multiple aspects of cardiogenesis. Proc Natl Acad Sci U S A *104*, 9313-9318.

Lin, X., Huo, Z., Liu, X., Zhang, Y., Li, L., Zhao, H., Yan, B., Liu, Y., Yang, Y., and Chen, Y.H. (2010). A novel GATA6 mutation in patients with tetralogy of Fallot or atrial septal defect. J Hum Genet *55*, 662-667.

Linhares, V.L., Almeida, N.A., Menezes, D.C., Elliott, D.A., Lai, D., Beyer, E.C., Campos de Carvalho, A.C., and Costa, M.W. (2004). Transcriptional regulation of the murine Connexin40 promoter by cardiac factors Nkx2-5, GATA4 and Tbx5. Cardiovasc Res *64*, 402-411.

Luna-Zurita, L., Prados, B., Grego-Bessa, J., Luxan, G., del Monte, G., Benguria, A., Adams, R.H., Perez-Pomares, J.M., and de la Pompa, J.L. (2010). Integration of a Notch-dependent mesenchymal gene program and Bmp2-driven cell invasiveness regulates murine cardiac valve formation. J Clin Invest *120*, 3493-3507.

Ma, L., Lu, M.F., Schwartz, R.J., and Martin, J.F. (2005). Bmp2 is essential for cardiac cushion epithelial-mesenchymal transition and myocardial patterning. Development *132*, 5601-5611.

Ma, L., Selamet Tierney, E.S., Lee, T., Lanzano, P., and Chung, W.K. (2012). Mutations in ZIC3 and ACVR2B are a common cause of heterotaxy and associated cardiovascular anomalies. Cardiol Young *22*, 194-201.

Maitra, M., Koenig, S.N., Srivastava, D., and Garg, V. (2010). Identification of GATA6 sequence variants in patients with congenital heart defects. Pediatr Res *68*, 281-285.

Maitra, M., Schluterman, M.K., Nichols, H.A., Richardson, J.A., Lo, C.W., Srivastava, D., and Garg, V. (2009). Interaction of Gata4 and Gata6 with Tbx5 is critical for normal cardiac development. Dev Biol *326*, 368-377.

Manasek, F.J. (1970). Sulfated extracellular matrix production in the embryonic heart and adjacent tissues. J Exp Zool *174*, 415-439.

Marcus, R.H., Marcus, B.D., and Levin, S.E. (1985). The upper limb-cardiovascular syndrome (Holt-Oram syndrome) in a South African family. S Afr Med J *67*, 1013-1014.

Marino, B., Digilio, M.C., Toscano, A., Giannotti, A., and Dallapiccola, B. (1999). Congenital heart diseases in children with Noonan syndrome: An expanded cardiac spectrum with high prevalence of atrioventricular canal. J Pediatr *135*, 703-706.

Markwald, R.R., Fitzharris, T.P., and Manasek, F.J. (1977). Structural development of endocardial cushions. Am J Anat *148*, 85-119.

Markwald, R.R., and Smith, W.N. (1972). Distribution of mucosubstances in the developing rat heart. J Histochem Cytochem *20*, 896-907.

Maslen, C.L., Babcock, D., Robinson, S.W., Bean, L.J., Dooley, K.J., Willour, V.L., and Sherman, S.L. (2006). CRELD1 mutations contribute to the occurrence of cardiac atrioventricular septal defects in Down syndrome. Am J Med Genet A *140*, 2501-2505.

Matsson, H., Eason, J., Bookwalter, C.S., Klar, J., Gustavsson, P., Sunnegardh, J., Enell, H., Jonzon, A., Vikkula, M., Gutierrez, I*., et al.* (2008). Alpha-cardiac actin mutations produce atrial septal defects. Hum Mol Genet *17*, 256-265.

McCormack, N., Molloy, E.L., and O'Dea, S. (2013). Bone morphogenetic proteins enhance an epithelial-mesenchymal transition in normal airway epithelial cells during restitution of a disrupted epithelium. Respir Res *14*, 36.

McCright, B., Lozier, J., and Gridley, T. (2002). A mouse model of Alagille syndrome: Notch2 as a genetic modifier of Jag1 haploinsufficiency. Development *129*, 1075-1082.

McDaniell, R., Warthen, D.M., Sanchez-Lara, P.A., Pai, A., Krantz, I.D., Piccoli, D.A., and Spinner, N.B. (2006). NOTCH2 mutations cause Alagille syndrome, a heterogeneous disorder of the notch signaling pathway. Am J Hum Genet *79*, 169-173.

McDermott, D.A., Bressan, M.C., He, J., Lee, J.S., Aftimos, S., Brueckner, M., Gilbert, F., Graham, G.E., Hannibal, M.C., Innis, J.W.*, et al.* (2005). TBX5 genetic testing validates strict clinical criteria for Holt-Oram syndrome. Pediatr Res *58*, 981-986.

McMahon, C.J., and Reardon, W. (2006). The spectrum of congenital cardiac malformations encountered in six children with Kabuki syndrome. Cardiol Young *16*, 30-33.

Meno, C., Takeuchi, J., Sakuma, R., Koshiba-Takeuchi, K., Ohishi, S., Saijoh, Y., Miyazaki, J., ten Dijke, P., Ogura, T., and Hamada, H. (2001). Diffusion of nodal signaling activity in the absence of the feedback inhibitor Lefty2. Dev Cell *1*, 127-138.

Miyabara, S., Gropp, A., and Winking, H. (1982). Trisomy 16 in the mouse fetus associated with generalized edema and cardiovascular and urinary tract anomalies. Teratology *25*, 369-380.

Mjaatvedt, C.H., Nakaoka, T., Moreno-Rodriguez, R., Norris, R.A., Kern, M.J., Eisenberg, C.A., Turner, D., and Markwald, R.R. (2001). The outflow tract of the heart is recruited from a novel heart-forming field. Dev Biol *238*, 97-109.

Mommersteeg, M.T., Soufan, A.T., de Lange, F.J., van den Hoff, M.J., Anderson, R.H., Christoffels, V.M., and Moorman, A.F. (2006). Two distinct pools of mesenchyme contribute to the development of the atrial septum. Circ Res *99*, 351-353.

Monserrat, L., Hermida-Prieto, M., Fernandez, X., Rodriguez, I., Dumont, C., Cazon, L., Cuesta, M.G., Gonzalez-Juanatey, C., Peteiro, J., Alvarez, N.*, et al.* (2007). Mutation in the alpha-cardiac actin gene associated with apical hypertrophic cardiomyopathy, left ventricular non-compaction, and septal defects. Eur Heart J *28*, 1953-1961.

Mori, A.D., Zhu, Y., Vahora, I., Nieman, B., Koshiba-Takeuchi, K., Davidson, L., Pizard, A., Seidman, J.G., Seidman, C.E., Chen, X.J.*, et al.* (2006). Tbx5-dependent rheostatic control of cardiac gene expression and morphogenesis. Dev Biol *297*, 566-586.

Morrisey, E.E., Tang, Z., Sigrist, K., Lu, M.M., Jiang, F., Ip, H.S., and Parmacek, M.S. (1998). GATA6 regulates HNF4 and is required for differentiation of visceral endoderm in the mouse embryo. Genes Dev *12*, 3579-3590.

Moskowitz, I.P., Wang, J., Peterson, M.A., Pu, W.T., Mackinnon, A.C., Oxburgh, L., Chu, G.C., Sarkar, M., Berul, C., Smoot, L.*, et al.* (2011). Transcription factor genes Smad4 and Gata4 cooperatively regulate cardiac valve development. [corrected]. Proc Natl Acad Sci U S A *108*, 4006-4011.

Muller, C.W., and Herrmann, B.G. (1997). Crystallographic structure of the T domain-DNA complex of the Brachyury transcription factor. Nature *389*, 884-888.

Murakami, M., Nakagawa, M., Olson, E.N., and Nakagawa, O. (2005). A WW domain protein TAZ is a critical coactivator for TBX5, a transcription factor implicated in Holt-Oram syndrome. Proc Natl Acad Sci U S A *102*, 18034-18039.

Muru, K., Kalev, I., Teek, R., Sonajalg, M., Kuuse, K., Reimand, T., and Ounap, K. (2011). A Boy with Holt-Oram Syndrome Caused by Novel Mutation c.1304delT in the TBX5 Gene. Mol Syndromol *1*, 307-310.

Musewe, N.N., Alexander, D.J., Teshima, I., Smallhorn, J.F., and Freedom, R.M. (1990). Echocardiographic evaluation of the spectrum of cardiac anomalies associated with trisomy 13 and trisomy 18. J Am Coll Cardiol *15*, 673-677.

Newbury-Ecob, R.A., Leanage, R., Raeburn, J.A., and Young, I.D. (1996). Holt-Oram syndrome: a clinical genetic study. J Med Genet *33*, 300-307.

Ng, A., Wong, M., Viviano, B., Erlich, J.M., Alba, G., Pflederer, C., Jay, P.Y., and Saunders, S. (2009). Loss of glypican-3 function causes growth factor-dependent defects in cardiac and coronary vascular development. Dev Biol *335*, 208-215.

Niikawa, N., Kuroki, Y., Kajii, T., Matsuura, N., Ishikiriyama, S., Tonoki, H., Ishikawa, N., Yamada, Y., Fujita, M., Umemoto, H.*, et al.* (1988). Kabuki make-up (Niikawa-Kuroki) syndrome: a study of 62 patients. Am J Med Genet *31*, 565-589.

Nimura, K., Ura, K., Shiratori, H., Ikawa, M., Okabe, M., Schwartz, R.J., and Kaneda, Y. (2009). A histone H3 lysine 36 trimethyltransferase links Nkx2-5 to Wolf-Hirschhorn syndrome. Nature *460*, 287-291.

Norris, R.A., Moreno-Rodriguez, R.A., Sugi, Y., Hoffman, S., Amos, J., Hart, M.M., Potts, J.D., Goodwin, R.L., and Markwald, R.R. (2008). Periostin regulates atrioventricular valve maturation. Dev Biol *316*, 200-213.

O'Doherty, A., Ruf, S., Mulligan, C., Hildreth, V., Errington, M.L., Cooke, S., Sesay, A., Modino, S., Vanes, L., Hernandez, D.*, et al.* (2005). An aneuploid mouse strain carrying human chromosome 21 with Down syndrome phenotypes. Science *309*, 2033-2037.

Oh, S.P., and Li, E. (1997). The signaling pathway mediated by the type IIB activin receptor controls axial patterning and lateral asymmetry in the mouse. Genes Dev *11*, 1812-1826.

Oike, Y., Hata, A., Mamiya, T., Kaname, T., Noda, Y., Suzuki, M., Yasue, H., Nabeshima, T., Araki, K., and Yamamura, K. (1999). Truncated CBP protein leads to classical Rubinstein-Taybi syndrome phenotypes in mice: implications for a dominant-negative mechanism. Hum Mol Genet *8*, 387-396.

Oppenheimer-Dekker, A., Gittenberger-de Groot, A.C., Bartelings, M.M., Wenink, A.C., Moene, R.J., and van der Harten, J.J. (1985). Abnormal architecture of the ventricles in hearts with an overriding aortic valve and a perimembranous ventricular septal defect ("Eisenmenger VSD"). Int J Cardiol *9*, 341-355.

Orstavik, K.H., Bechensteen, A.G., Fugelseth, D., and Orderud, W. (1998). Sibs with Ritscher-Schinzel (3C) syndrome and anal malformations. Am J Med Genet *75*, 300-303.

Oshima, M., Oshima, H., Kitagawa, K., Kobayashi, M., Itakura, C., and Taketo, M. (1995). Loss of Apc heterozygosity and abnormal tissue building in nascent intestinal polyps in mice carrying a truncated Apc gene. Proc Natl Acad Sci U S A *92*, 4482-4486.

Owens, G.E., Gomez-Fifer, C., Gelehrter, S., and Owens, S.T. (2009). Outcomes for patients with unbalanced atrioventricular septal defects. Pediatr Cardiol *30*, 431-435.

Ozcelik, C., Bit-Avragim, N., Panek, A., Gaio, U., Geier, C., Lange, P.E., Dietz, R., Posch, M.G., Perrot, A., and Stiller, B. (2006). Mutations in the EGF-CFC gene cryptic are an infrequent cause of congenital heart disease. Pediatr Cardiol *27*, 695-698.

Papaioannou, V.E., and Silver, L.M. (1998). The T-box gene family. Bioessays *20*, 9-19.

Park, S.C., Mathews, R.A., Zuberbuhler, J.R., Rowe, R.D., Neches, W.H., and Lenox, C.C. (1977). Down syndrome with congenital heart malformation. Am J Dis Child *131*, 29-33.

Patel, C., Silcock, L., McMullan, D., Brueton, L., and Cox, H. (2012). TBX5 intragenic duplication: a family with an atypical Holt-Oram syndrome phenotype. Eur J Hum Genet *20*, 863-869.

Plageman, T.F., Jr., and Yutzey, K.E. (2004). Differential expression and function of Tbx5 and Tbx20 in cardiac development. J Biol Chem *279*, 19026-19034.

Porto, M.P., Vergani, N., Carvalho, A.C., Cernach, M.C., Brunoni, D., and Perez, A.B. (2010). Novel mutations in the TBX5 gene in patients with Holt-Oram Syndrome. Genet Mol Biol *33*, 232-236.

Posch, M.G., Gramlich, M., Sunde, M., Schmitt, K.R., Lee, S.H., Richter, S., Kersten, A., Perrot, A., Panek, A.N., Al Khatib, I.H.*, et al.* (2010). A gain-of-function TBX20 mutation causes congenital atrial septal defects, patent foramen ovale and cardiac valve defects. J Med Genet *47*, 230-235.

Posch, M.G., Perrot, A., Schmitt, K., Mittelhaus, S., Esenwein, E.M., Stiller, B., Geier, C., Dietz, R., Gessner, R., Ozcelik, C.*, et al.* (2008). Mutations in GATA4, NKX2.5, CRELD1, and BMP4 are infrequently found in patients with congenital cardiac septal defects. Am J Med Genet A *146A*, 251-253.

Postma, A.V., van de Meerakker, J.B., Mathijssen, I.B., Barnett, P., Christoffels, V.M., Ilgun, A., Lam, J., Wilde, A.A., Lekanne Deprez, R.H., and Moorman, A.F. (2008). A gain-of-function TBX5 mutation is associated with atypical Holt-Oram syndrome and paroxysmal atrial fibrillation. Circ Res *102*, 1433-1442.

Postma, A.V., van Engelen, K., van de Meerakker, J., Rahman, T., Probst, S., Baars, M.J., Bauer, U., Pickardt, T., Sperling, S.R., Berger, F.*, et al.* (2011). Mutations in the sarcomere gene MYH7 in Ebstein anomaly. Circ Cardiovasc Genet *4*, 43-50.

Priest, J.R., Girirajan, S., Vu, T.H., Olson, A., Eichler, E.E., and Portman, M.A. (2012). Rare copy number variants in isolated sporadic and syndromic atrioventricular septal defects. Am J Med Genet A *158A*, 1279-1284.

Purandare, S.M., Ware, S.M., Kwan, K.M., Gebbia, M., Bassi, M.T., Deng, J.M., Vogel, H., Behringer, R.R., Belmont, J.W., and Casey, B. (2002). A complex syndrome of left-right axis, central nervous system and axial skeleton defects in Zic3 mutant mice. Development *129*, 2293-2302.

Rana, M.S., Theveniau-Ruissy, M., De Bono, C., Mesbah, K., Francou, A., Rammah, M., Dominguez, J.N., Roux, M., Laforest, B., Anderson, R.H.*, et al.* (2014). Tbx1 coordinates addition of posterior second heart field progenitor cells to the arterial and venous poles of the heart. Circ Res *115*, 790-799.

Rankin, C.T., Bunton, T., Lawler, A.M., and Lee, S.J. (2000). Regulation of left-right patterning in mice by growth/differentiation factor-1. Nat Genet *24*, 262-265.

Reamon-Buettner, S.M., and Borlak, J. (2004a). Somatic NKX2-5 mutations as a novel mechanism of disease in complex congenital heart disease. J Med Genet *41*, 684-690.

Reamon-Buettner, S.M., and Borlak, J. (2004b). TBX5 mutations in non-Holt-Oram syndrome (HOS) malformed hearts. Hum Mutat *24*, 104.

Reamon-Buettner, S.M., and Borlak, J. (2005). GATA4 zinc finger mutations as a molecular rationale for septation defects of the human heart. J Med Genet *42*, e32.

Reamon-Buettner, S.M., and Borlak, J. (2006). HEY2 mutations in malformed hearts. Hum Mutat *27*, 118.

Reaume, A.G., de Sousa, P.A., Kulkarni, S., Langille, B.L., Zhu, D., Davies, T.C., Juneja, S.C., Kidder, G.M., and Rossant, J. (1995). Cardiac malformation in neonatal mice lacking connexin43. Science *267*, 1831-1834.

Redig, J.K., Fouad, G.T., Babcock, D., Reshey, B., Feingold, E., Reeves, R.H., and Maslen, C.L. (2014). Allelic Interaction between and in the Pathogenesis of Cardiac Atrioventricular Septal Defects. AIMS Genet *1*, 1-19.

Ripoll, C., Rivals, I., Ait Yahya-Graison, E., Dauphinot, L., Paly, E., Mircher, C., Ravel, A., Grattau, Y., Blehaut, H., Megarbane, A.*, et al.* (2012). Molecular signatures of cardiac defects in Down syndrome lymphoblastoid cell lines suggest altered ciliome and Hedgehog pathways. PLoS One *7*, e41616.

Ritscher, D., Schinzel, A., Boltshauser, E., Briner, J., Arbenz, U., and Sigg, P. (1987). Dandy-Walker(like) malformation, atrio-ventricular septal defect and a similar pattern of minor anomalies in 2 sisters: a new syndrome? Am J Med Genet *26*, 481-491.

Rivera-Feliciano, J., and Tabin, C.J. (2006). Bmp2 instructs cardiac progenitors to form the heart-valve-inducing field. Dev Biol *295*, 580-588.

Robinson, S.W., Morris, C.D., Goldmuntz, E., Reller, M.D., Jones, M.A., Steiner, R.D., and Maslen, C.L. (2003). Missense mutations in CRELD1 are associated with cardiac atrioventricular septal defects. Am J Hum Genet *72*, 1047-1052.

Robson, A., Allinson, K.R., Anderson, R.H., Henderson, D.J., and Arthur, H.M. (2010). The TGFbeta type II receptor plays a critical role in the endothelial cells during cardiac development. Dev Dyn *239*, 2435-2442.

Rodgers, L.S., Lalani, S., Hardy, K.M., Xiang, X., Broka, D., Antin, P.B., and Camenisch, T.D. (2006). Depolymerized hyaluronan induces vascular endothelial growth factor, a negative regulator of developmental epithelial-to-mesenchymal transformation. Circ Res *99*, 583-589.

Ruiz-Perez, V.L., Blair, H.J., Rodriguez-Andres, M.E., Blanco, M.J., Wilson, A., Liu, Y.N., Miles, C., Peters, H., and Goodship, J.A. (2007). Evc is a positive mediator of Ihh-regulated bone growth that localises at the base of chondrocyte cilia. Development *134*, 2903-2912.

Ryan, A.K., Bartlett, K., Clayton, P., Eaton, S., Mills, L., Donnai, D., Winter, R.M., and Burn, J. (1998). Smith-Lemli-Opitz syndrome: a variable clinical and biochemical phenotype. J Med Genet *35*, 558-565.

Schott, J.J., Benson, D.W., Basson, C.T., Pease, W., Silberbach, G.M., Moak, J.P., Maron, B.J., Seidman, C.E., and Seidman, J.G. (1998). Congenital heart disease caused by mutations in the transcription factor NKX2-5. Science *281*, 108-111.

Selicorni, A., Colli, A.M., Passarini, A., Milani, D., Cereda, A., Cerutti, M., Maitz, S., Alloni, V., Salvini, L., Galli, M.A.*, et al.* (2009). Analysis of congenital heart defects in 87 consecutive patients with Brachmann-de Lange syndrome. Am J Med Genet A *149A*, 1268-1272.

Shikama, N., Lutz, W., Kretzschmar, R., Sauter, N., Roth, J.F., Marino, S., Wittwer, J., Scheidweiler, A., and Eckner, R. (2003). Essential function of p300 acetyltransferase activity in heart, lung and small intestine formation. EMBO J *22*, 5175-5185.

Silversides, C.K., Lionel, A.C., Costain, G., Merico, D., Migita, O., Liu, B., Yuen, T., Rickaby, J., Thiruvahindrapuram, B., Marshall, C.R.*, et al.* (2012). Rare copy number variations in adults with tetralogy of Fallot implicate novel risk gene pathways. PLoS Genet *8*, e1002843.

Singh, M.K., Christoffels, V.M., Dias, J.M., Trowe, M.O., Petry, M., Schuster-Gossler, K., Burger, A., Ericson, J., and Kispert, A. (2005). Tbx20 is essential for cardiac chamber differentiation and repression of Tbx2. Development *132*, 2697-2707.

Sletten, L.J., and Pierpont, M.E. (1996). Variation in severity of cardiac disease in Holt-Oram syndrome. Am J Med Genet *65*, 128-132.

Smemo, S., Campos, L.C., Moskowitz, I.P., Krieger, J.E., Pereira, A.C., and Nobrega, M.A. (2012). Regulatory variation in a TBX5 enhancer leads to isolated congenital heart disease. Hum Mol Genet *21*, 3255-3263.

Smith, A.T., Sack, G.H., Jr., and Taylor, G.J. (1979). Holt-Oram syndrome. J Pediatr *95*, 538-543.

Smith, D.W., Lemli, L., and Opitz, J.M. (1964). A NEWLY RECOGNIZED SYNDROME OF MULTIPLE CONGENITAL ANOMALIES. J Pediatr *64*, 210-217.

Smith, K.A., Joziasse, I.C., Chocron, S., van Dinther, M., Guryev, V., Verhoeven, M.C., Rehmann, H., van der Smagt, J.J., Doevendans, P.A., Cuppen, E.*, et al.* (2009). Dominant-negative ALK2 allele associates with congenital heart defects. Circulation *119*, 3062-3069.

Soemedi, R., Wilson, I.J., Bentham, J., Darlay, R., Topf, A., Zelenika, D., Cosgrove, C., Setchfield, K., Thornborough, C., Granados-Riveron, J.*, et al.* (2012). Contribution of global rare copy-number variants to the risk of sporadic congenital heart disease. Am J Hum Genet *91*, 489-501.

Song, W., Dyer, E., Stuckey, D., Leung, M.C., Memo, M., Mansfield, C., Ferenczi, M., Liu, K., Redwood, C., Nowak, K.*, et al.* (2010). Investigation of a transgenic mouse model of familial dilated cardiomyopathy. J Mol Cell Cardiol *49*, 380-389.

Sperling, S., Grimm, C.H., Dunkel, I., Mebus, S., Sperling, H.P., Ebner, A., Galli, R., Lehrach, H., Fusch, C., Berger, F.*, et al.* (2005). Identification and functional analysis of CITED2 mutations in patients with congenital heart defects. Hum Mutat *26*, 575-582.

Springett, A., Wellesley, D., Greenlees, R., Loane, M., Addor, M.C., Arriola, L., Bergman, J., Cavero-Carbonell, C., Csaky-Szunyogh, M., Draper, E.S.*, et al.* (2015). Congenital anomalies associated with trisomy 18 or trisomy 13: A registry-based study in 16 european countries, 2000-2011. Am J Med Genet A.

Stennard, F.A., Costa, M.W., Lai, D., Biben, C., Furtado, M.B., Solloway, M.J., McCulley, D.J., Leimena, C., Preis, J.I., Dunwoodie, S.L.*, et al.* (2005). Murine T-box transcription factor Tbx20 acts as a repressor during heart development, and is essential for adult heart integrity, function and adaptation. Development *132*, 2451-2462.

Stephen, L.J., Fawkes, A.L., Verhoeve, A., Lemke, G., and Brown, A. (2007). A critical role for the EphA3 receptor tyrosine kinase in heart development. Dev Biol *302*, 66-79.

Stevens, C.A., and Bhakta, M.G. (1995). Cardiac abnormalities in the Rubinstein-Taybi syndrome. Am J Med Genet *59*, 346-348.

Stirnimann, C.U., Ptchelkine, D., Grimm, C., and Muller, C.W. (2010). Structural basis of TBX5-DNA recognition: the T-box domain in its DNA-bound and -unbound form. J Mol Biol *400*, 71-81.

Stoll, C., Alembik, Y., Dott, B., and Roth, M.P. (1998). Study of Down syndrome in 238,942 consecutive births. Ann Genet *41*, 44-51.

Su, L.K., Kinzler, K.W., Vogelstein, B., Preisinger, A.C., Moser, A.R., Luongo, C., Gould, K.A., and Dove, W.F. (1992). Multiple intestinal neoplasia caused by a mutation in the murine homolog of the APC gene. Science *256*, 668-670.

Svensson, E.C., Huggins, G.S., Lin, H., Clendenin, C., Jiang, F., Tufts, R., Dardik, F.B., and Leiden, J.M. (2000). A syndrome of tricuspid atresia in mice with a targeted mutation of the gene encoding Fog-2. Nat Genet *25*, 353-356.

Sznajer, Y., Keren, B., Baumann, C., Pereira, S., Alberti, C., Elion, J., Cave, H., and Verloes, A. (2007). The spectrum of cardiac anomalies in Noonan syndrome as a result of mutations in the PTPN11 gene. Pediatrics *119*, e1325-1331.

Takeuchi, J.K., and Bruneau, B.G. (2009). Directed transdifferentiation of mouse mesoderm to heart tissue by defined factors. Nature *459*, 708-711.

Takeuchi, J.K., Lou, X., Alexander, J.M., Sugizaki, H., Delgado-Olguin, P., Holloway, A.K., Mori, A.D., Wylie, J.N., Munson, C., Zhu, Y.*, et al.* (2011). Chromatin remodelling complex dosage modulates transcription factor function in heart development. Nat Commun *2*, 187.

Tanaka, M., Chen, Z., Bartunkova, S., Yamasaki, N., and Izumo, S. (1999). The cardiac homeobox gene Csx/Nkx2.5 lies genetically upstream of multiple genes essential for heart development. Development *126*, 1269-1280.

Terrett, J.A., Newbury-Ecob, R., Cross, G.S., Fenton, I., Raeburn, J.A., Young, I.D., and Brook, J.D. (1994). Holt-Oram syndrome is a genetically heterogeneous disease with one locus mapping to human chromosome 12q. Nat Genet *6*, 401-404.

Terrett, J.A., Newbury-Ecob, R., Smith, N.M., Li, Q.Y., Garrett, C., Cox, P., Bonnet, D., Lyonnet, S., Munnich, A., Buckler, A.J.*, et al.* (1996). A translocation at 12q2 refines the interval containing the Holt-Oram syndrome 1 gene. Am J Hum Genet *59*, 1337-1341.

Tian, Y., Yuan, L., Goss, A.M., Wang, T., Yang, J., Lepore, J.J., Zhou, D., Schwartz, R.J., Patel, V., Cohen, E.D.*, et al.* (2010). Characterization and in vivo pharmacological rescue of a Wnt2-Gata6 pathway required for cardiac inflow tract development. Dev Cell *18*, 275-287.

Timmerman, L.A., Grego-Bessa, J., Raya, A., Bertran, E., Perez-Pomares, J.M., Diez, J., Aranda, S., Palomo, S., McCormick, F., Izpisua-Belmonte, J.C.*, et al.* (2004). Notch promotes epithelial-mesenchymal transition during cardiac development and oncogenic transformation. Genes Dev *18*, 99-115.

Tomita-Mitchell, A., Mahnke, D.K., Struble, C.A., Tuffnell, M.E., Stamm, K.D., Hidestrand, M., Harris, S.E., Goetsch, M.A., Simpson, P.M., Bick, D.P.*, et al.* (2012). Human gene copy number spectra analysis in congenital heart malformations. Physiol Genomics *44*, 518-541.

Tomita-Mitchell, A., Maslen, C.L., Morris, C.D., Garg, V., and Goldmuntz, E. (2007). GATA4 sequence variants in patients with congenital heart disease. J Med Genet *44*, 779-783.

Tompson, S.W., Ruiz-Perez, V.L., Blair, H.J., Barton, S., Navarro, V., Robson, J.L., Wright, M.J., and Goodship, J.A. (2007). Sequencing EVC and EVC2 identifies mutations in two-thirds of Ellis-van Creveld syndrome patients. Hum Genet *120*, 663-670.

Ucar, B., Kilic, Z., Dinleyici, E.C., Yakut, A., and Dogruel, N. (2004). Seckel syndrome associated with atrioventricular canal defect: a case report. Clin Dysmorphol *13*, 53-55.

Waldo, K.L., Kumiski, D.H., Wallis, K.T., Stadt, H.A., Hutson, M.R., Platt, D.H., and Kirby, M.L. (2001). Conotruncal myocardium arises from a secondary heart field. Development *128*, 3179-3188.

Wang, B., Wang, J., Liu, S., Han, X., Xie, X., Tao, Y., Yan, J., and Ma, X. (2011). CFC1 mutations in Chinese children with congenital heart disease. Int J Cardiol *146*, 86-88.

Wang, J., Luo, X.J., Xin, Y.F., Liu, Y., Liu, Z.M., Wang, Q., Li, R.G., Fang, W.Y., Wang, X.Z., and Yang, Y.Q. (2012). Novel GATA6 mutations associated with congenital ventricular septal defect or tetralogy of fallot. DNA Cell Biol *31*, 1610-1617.

Wang, J., Sridurongrit, S., Dudas, M., Thomas, P., Nagy, A., Schneider, M.D., Epstein, J.A., and Kaartinen, V. (2005). Atrioventricular cushion transformation is mediated by ALK2 in the developing mouse heart. Dev Biol *286*, 299-310.

Ware, S.M., Peng, J., Zhu, L., Fernbach, S., Colicos, S., Casey, B., Towbin, J., and Belmont, J.W. (2004). Identification and functional analysis of ZIC3 mutations in heterotaxy and related congenital heart defects. Am J Hum Genet *74*, 93-105.

Washington Smoak, I., Byrd, N.A., Abu-Issa, R., Goddeeris, M.M., Anderson, R., Morris, J., Yamamura, K., Klingensmith, J., and Meyers, E.N. (2005). Sonic hedgehog is required for cardiac outflow tract and neural crest cell development. Dev Biol *283*, 357-372.

Wassif, C.A., Zhu, P., Kratz, L., Krakowiak, P.A., Battaile, K.P., Weight, F.F., Grinberg, A., Steiner, R.D., Nwokoro, N.A., Kelley, R.I.*, et al.* (2001). Biochemical, phenotypic and neurophysiological characterization of a genetic mouse model of RSH/Smith--Lemli--Opitz syndrome. Hum Mol Genet *10*, 555-564.

Watanabe, H., and Yamada, Y. (1999). Mice lacking link protein develop dwarfism and craniofacial abnormalities. Nat Genet *21*, 225-229.

Weatherbee, S.D., Niswander, L.A., and Anderson, K.V. (2009). A mouse model for Meckel syndrome reveals Mks1 is required for ciliogenesis and Hedgehog signaling. Hum Mol Genet *18*, 4565-4575.

Webb, S., Anderson, R.H., and Brown, N.A. (1996). Endocardial cushion development and heart loop architecture in the trisomy 16 mouse. Dev Dyn *206*, 301-309.

Webb, S., Brown, N.A., and Anderson, R.H. (1998). Formation of the atrioventricular septal structures in the normal mouse. Circ Res *82*, 645-656.

Wessels, A., Anderson, R.H., Markwald, R.R., Webb, S., Brown, N.A., Viragh, S., Moorman, A.F., and Lamers, W.H. (2000). Atrial development in the human heart:

an immunohistochemical study with emphasis on the role of mesenchymal tissues. Anat Rec *259*, 288-300.

Wessels, A., Markman, M.W., Vermeulen, J.L., Anderson, R.H., Moorman, A.F., and Lamers, W.H. (1996). The development of the atrioventricular junction in the human heart. Circ Res *78*, 110-117.

Willaredt, M.A., Gorgas, K., Gardner, H.A., and Tucker, K.L. (2012). Multiple essential roles for primary cilia in heart development. Cilia *1*, 23.

Willaredt, M.A., Hasenpusch-Theil, K., Gardner, H.A., Kitanovic, I., Hirschfeld-Warneken, V.C., Gojak, C.P., Gorgas, K., Bradford, C.L., Spatz, J., Wolfl, S.*, et al.* (2008). A crucial role for primary cilia in cortical morphogenesis. J Neurosci *28*, 12887-12900.

Wirrig, E.E., Snarr, B.S., Chintalapudi, M.R., O'Neal J, L., Phelps, A.L., Barth, J.L., Fresco, V.M., Kern, C.B., Mjaatvedt, C.H., Toole, B.P.*, et al.* (2007). Cartilage link protein 1 (Crtl1), an extracellular matrix component playing an important role in heart development. Dev Biol *310*, 291-303.

Xie, L., Hoffmann, A.D., Burnicka-Turek, O., Friedland-Little, J.M., Zhang, K., and Moskowitz, I.P. (2012). Tbx5-hedgehog molecular networks are essential in the second heart field for atrial septation. Dev Cell *23*, 280-291.

Xie, X., Lu, Y., Wang, X., Wu, B., and Yu, H. (2015). JAGGED1 gene variations in Chinese twin sisters with Alagille syndrome. Int J Clin Exp Pathol *8*, 8506-8511.

Xiong, S. (2013). Mouse models of Mdm2 and Mdm4 and their clinical implications. Chin J Cancer *32*, 371-375.

Ya, J., Erdtsieck-Ernste, E.B., de Boer, P.A., van Kempen, M.J., Jongsma, H., Gros, D., Moorman, A.F., and Lamers, W.H. (1998). Heart defects in connexin43-deficient mice. Circ Res *82*, 360-366.

Yang, J., Hu, D., Xia, J., Yang, Y., Ying, B., Hu, J., and Zhou, X. (2000). Three novel TBX5 mutations in Chinese patients with Holt-Oram syndrome. Am J Med Genet *92*, 237-240.

Yang, L., Cai, C.L., Lin, L., Qyang, Y., Chung, C., Monteiro, R.M., Mummery, C.L., Fishman, G.I., Cogen, A., and Evans, S. (2006). Isl1Cre reveals a common Bmp pathway in heart and limb development. Development *133*, 1575-1585.

Ye, M., Coldren, C., Liang, X., Mattina, T., Goldmuntz, E., Benson, D.W., Ivy, D., Perryman, M.B., Garrett-Sinha, L.A., and Grossfeld, P. (2010). Deletion of ETS-1, a gene in the Jacobsen syndrome critical region, causes ventricular septal defects and abnormal ventricular morphology in mice. Hum Mol Genet *19*, 648-656.

Yin, Z., Haynie, J., Yang, X., Han, B., Kiatchoosakun, S., Restivo, J., Yuan, S., Prabhakar, N.R., Herrup, K., Conlon, R.A.*, et al.* (2002). The essential role of Cited2, a negative regulator for HIF-1alpha, in heart development and neurulation. Proc Natl Acad Sci U S A *99*, 10488-10493.

Yoshida, A., Morisaki, H., Nakaji, M., Kitano, M., Kim, K.S., Sagawa, K., Ishikawa, S., Satokata, I., Mitani, Y., Kato, H.*, et al.* (2015). Genetic mutation analysis in Japanese patients with non-syndromic congenital heart disease. J Hum Genet.

Zaragoza, M.V., Lewis, L.E., Sun, G., Wang, E., Li, L., Said-Salman, I., Feucht, L., and Huang, T. (2004). Identification of the TBX5 transactivating domain and the nuclear localization signal. Gene *330*, 9-18.

Zatyka, M., Priestley, M., Ladusans, E.J., Fryer, A.E., Mason, J., Latif, F., and Maher, E.R. (2005). Analysis of CRELD1 as a candidate 3p25 atrioventicular septal defect locus (AVSD2). Clin Genet *67*, 526-528.

Zhang, X.L., Qiu, X.B., Yuan, F., Wang, J., Zhao, C.M., Li, R.G., Xu, L., Xu, Y.J., Shi, H.Y., Hou, X.M.*, et al.* (2015). TBX5 loss-of-function mutation contributes to familial dilated cardiomyopathy. Biochem Biophys Res Commun *459*, 166-171.

Zheng, G.F., Wei, D., Zhao, H., Zhou, N., Yang, Y.Q., and Liu, X.Y. (2012). A novel GATA6 mutation associated with congenital ventricular septal defect. Int J Mol Med *29*, 1065-1071.

Zhou, H.M., Weskamp, G., Chesneau, V., Sahin, U., Vortkamp, A., Horiuchi, K., Chiusaroli, R., Hahn, R., Wilkes, D., Fisher, P.*, et al.* (2004). Essential role for ADAM19 in cardiovascular morphogenesis. Mol Cell Biol *24*, 96-104.

Zhou, W., Zhao, L., Jiang, J.Q., Jiang, W.F., Yang, Y.Q., and Qiu, X.B. (2015). A novel TBX5 loss-of-function mutation associated with sporadic dilated cardiomyopathy. Int J Mol Med *36*, 282-288.

CHAPTER 2

Generating a *Xenopus* line expressing *Tbx5*^{Avi} to study TBX5 functional mechanisms *in vivo*

Overview

This work was performed by myself, Erika Paden (a previous graduate student in the lab), Michelle Villasmil (a previous postdoc in the lab), and Lauren Kuchenbrod (our lab technician). Erika Paden performed data mining for phosphorylated TBX5 and generated the *Tbx5* enhancer construct driving GFP expression. I generated the TBX5 phosphorylation mutations and performed all of the transient transcriptional assays. I also generated the *Tbx5*^{Avi} construct and performed all *Xenopus tropicalis* transgenic injections, genotyping, and animal husbandry. Lauren Kuchenbrod performed *Xenopus laevis* injections and is currently maintaining all transgenic lines in our *Xenopus* facility. Michelle performed subsequent protein expression analysis of TBX5^{Avi}. The mouse experiment was performed in the laboratory of Benoit Bruneau. The project was conceived by Frank Conlon.

Clinical studies provide direct evidence for a role for T-box transcription factors in heart development and human disease. Specifically, mutations in *Tbx5* have been associated with the human congenital heart disease Holt-Oram syndrome

(HOS), which is characterized by a wide array of cardiac abnormalities. HOS mutations can lead to TBX5 overexpression and depletion, which increases and decreases TBX5 activity, indicating that proper TBX5 levels are essential for normal cardiac development. Despite the crucial role for TBX5 in development and disease, little is known about TBX5 functional mechanisms. We performed data mining of phosphoproteomes and identified a set of *in vivo* phosphorylated residues in a previously uncharacterized region of the TBX5 protein. Transcriptional analysis and bioassays indicate that phosphorylation of TBX5 at a single threonine residue inhibits its transcriptional activity. Preliminary data suggests that phosphorylation at this residue reduces protein stability. We hypothesize that TBX5 phosphorylation mediates novel protein-protein interactions that regulate TBX5 levels and activity. We have generated a novel *Xenopus* line expressing epitope-tagged $Tbx5^{Avi}$ to determine the TBX5 protein interactome.

INTRODUCTION

The T-box gene family is a large family of transcription factors that are required for early cell fate decision, differentiation and organogenesis (Papaioannou and Silver, 1998; Smith, 1999; Wilson and Conlon, 2002). T-box gene mutation studies in mice and zebrafish result in dramatic phenotypes and suggest that these genes may have crucial roles in a number of human congenital malformations (Wilson and Conlon, 2002). Clinical studies provided direct evidence for a role for T-box genes in human congenital heart disease (CHD). *Tbx1* is deleted in most patients with DiGeorge syndrome (Chieffo et al., 1997; Lindsay et al., 2001), *Tbx20*

mutations that reduce or up-regulate TBX20 expression are associated with a wide range of cardiac abnormalities (Kirk et al., 2007; Posch et al., 2010; Qian et al., 2008), and *Tbx5* mutations are associated with the CHD Holt-Oram syndrome (HOS) (Hammer et al., 2008; Kirk et al., 2007; Li et al., 1997; Lindsay et al., 2001; Mandel et al., 2005; Qian et al., 2008; Scambler, 2000). This dissertation investigates the molecular mechanism of TBX5 activity in HOS.

Tbx5 was initially identified in mouse (Bollag et al., 1994), and its homologs have been characterized in a number of vertebrate organisms including zebrafish (Begemann and Ingham, 2000; Ruvinsky et al., 2000; Tamura et al., 1999), *Xenopus* (Brown et al., 2005; Goetz et al., 2006; Horb and Thomsen, 1999), chicken (Gibson-Brown et al., 1998; Ohuchi et al., 1998), and human (Basson et al., 1997; Li et al., 1997). Amino acid sequence homology analysis indicates that *Tbx5* is highly conserved throughout evolution, with approximately 70% conservation between human and *Xenopus* full length *Tbx5,* and more than 90% conservation within the T-box DNA-binding domain. Initial studies in mouse showed that *Tbx5* expression was restricted to a subset of cells in the developing eye, heart, and limb (Chapman et al., 1996). Similar results have been observed in other vertebrates (Begemann and Ingham, 2000; Brown et al., 2005; Gibson-Brown et al., 1998; Horb and Thomsen, 1999; Li et al., 1997). Studies in *Xenopus* (Brown et al., 2005; Horb and Thomsen, 1999; Showell et al., 2006) report that *Tbx5* is expressed in the migrating heart primordia of the neurula stage (stage 20) embryo. By stage 24, the *Tbx5* expression pattern becomes restricted to the developing heart, a dorsal stripe corresponding to the common cardinal vein, and the dorsal part of the eye. Whole-mount and

sectioned *in situ* tissue samples at tadpole stages show high levels of *Tbx5* expression in the common cardinal vein, hepatic vein, and the ventricle, with lower levels detected in the atria and the in-flow tract (Horb and Thomsen, 1999; Showell et al., 2006). TBX5 is one of the earliest markers of the cardiac lineage in all vertebrates. Recent studies show that TBX5 is one of three cardiac transcription factors (along with GATA4 and MEF2C) that coordinately function to directly reprogram fibroblasts into differentiated cardiomyocytes. These differentiated cardiomyocytes have similar molecular, anatomical, and physiological properties as endogenous cardiomyocytes (Ieda et al., 2010; Qian et al., 2012).

Holt-Oram syndrome (HOS), also known as heart-hand syndrome, is a congenital autosomal dominant disorder that primarily affects the heart and upper limbs (Holt and Oram, 1960). The cardiac defects include atrial septal defects (ASD), ventricular septal defects (VSD), and/or defects in the cardiac conduction system (Basson et al., 1994; Benson et al., 1996; Cross et al., 2000; McDermott et al., 2005; Newbury-Ecob et al., 1996). HOS is often caused by mutations in the coding region of the T-box transcription factor *Tbx5* (Basson et al., 1997; Basson et al., 1999; Li et al., 1997). More than 70% of patients with HOS have a mutation in the *Tbx5* coding region, and 85% of those mutations occur *de novo* (McDermott et al., 2005). Most HOS mutations are predicted to result in TBX5 haploinsufficiency (Basson et al., 1999; Li et al., 1997); however, TBX5 overexpression also can result in HOS (termed atypical HOS) (Brassington et al., 2003; Dixon et al., 1993; Garavelli et al., 2008; Lehner et al., 2003; McDermott et al., 2005; Newbury-Ecob et al., 1996; Postma et al., 2008; Sletten and Pierpont, 1996; van Bever et al., 1996). These

results are consistent with numerous overexpression and depletion experiments in a number of model organisms, including mouse (Bruneau et al., 2001; Liberatore et al., 2000; Moskowitz et al., 2004), chicken (Hatcher et al., 2004; Hatcher et al., 2001), *Xenopus* (Brown et al., 2005; Goetz et al., 2006; Horb and Thomsen, 1999), and zebrafish (Garrity et al., 2002). Collectively, these studies demonstrate that proper TBX5 levels are essential for proper heart development, and even a slight alteration in TBX5 levels can lead to human congenital heart disease. These results suggest that human CHD is likely associated with TBX5 function.

In this chapter, we determined how alterations in TBX5 levels could lead to CHD. We performed data mining studies and showed that TBX5 is phosphorylated *in vivo*. We characterized the phosphorylated residues, and observed that mutated TBX5 at T278 increases TBX5-mediated transcriptional activation of the downstream target genes in *Xenopus*. We showed that the increase in transcriptional activity is not due to changes in nuclear localization; rather, it seems likely that mutation at this residue leads to changes in protein stability. We hypothesized that TBX5 phosphorylation mediates protein-protein interactions that regulate protein turnover. For further analysis, it is crucial to isolate the TBX5 transcriptional complex from *Xenopus* heart tissue by immunoisolation. Due to the lack of a high specificity, high affinity TBX5 antibody, past attempts at purifying endogenous TBX5 transcriptional complexes by our lab and others have been unsuccessful. To circumvent this problem we have generated *Xenopus laevis* and *Xenopus troplicalis* transgenic lines expressing epitope-tagged TBX5 under the control of a novel endogenous cardiac enhancer. These studies are currently ongoing.

MATERIALS AND METHODS

Plasmid Construction

Xenopus tropicalis TBX5 was cloned into pcDNA3.1-C-HA using NheI and NotI restriction sites. Site-directed mutagenesis was performed using the QuikChange II Site Directed Mutagenesis kit (Agilent, Santa Clara, USA). Primer sequences are presented in Table S2.1.

Xenopus transcriptional assays

For transient transcription assays, all *Xenopus* embryos were injected at the one-cell stage with 100 pg UAS-SV40-Luciferase reporter plasmid, 10 pg Renilla reporter plasmid, and in the presence or absence of 1 ng of wild type *Tbx5*, mutant *Tbx5* mRNA (1ng). Injected embryos were cultured until stage 10.5 (Nieuwkoop, 1994). Ten injected embryos (in triplicate) were lysed in 50 μL Passive Lysis Buffer (Promega, Madison, USA). Then, 20 μL of cleared lysate were assayed using the Dual-Luciferase Reporter Assay System (Promega, Madison, USA). The results of transcriptional assays are plotted as the average relative transcription ± SEM. Statistical significance was determined by Student's t-test.

Cell transfection and nuclear isolation

COS-7 cells were transfected using FuGene6 according to the manufacturer's protocol (Promega, Madison, USA). Cells were harvested 48 hours after transfection. Nuclear extracts were prepared using the CelLytic NuCLEAR Extraction Kit according to the manufacturer's protocol (Sigma, St. Louis, USA). Briefly, cells

were washed in PBS, scraped, and isolated. Cells were lysed in 5x cell pellet volume of lysis buffer (5 mM Tris HCl, pH 7.5, 1 mM $MgCl_2$, 1.5 mM $CaCl_2$, 150 mM sucrose, 1 mM DTT, 0.1 μL Sigma protease inhibitor cocktail P8340) for 15 minutes on ice. Then, 10% IGEPAL was added to the cell lysate to a final concentration of 0.6%, and the lysate was vortexed for 10 s and centrifuged for 30 s at 10,000 x g. The cytoplasmic supernatant was collected and the nuclear pellet was extracted using extraction buffer (2/3 volume of total cell pellet, 70 uL) (20 mM HEPES, pH 7.9, 4.5 mM $MgCl_2$, 0.42 M NaCl, 0.2 mM EDTA, 25% glycerol, 1 mM DTT and 1μL Sigma protease inhibitor cocktail P8340). Protein concentrations in cytoplasmic and nuclear fractions were determined by Bradford assays to ensure equal protein loading.

Xenopus tropicalis transgenesis

Xenopus tropicalis embryos were transformed using restricted emzyme mediated-integration (REMI). DNA constructs were linearized using SalI, and transgenesis was performed according to Kroll and Amaya as described previously (Amaya and Kroll, 1999; Amin et al., 2014; Kroll and Amaya, 1996; Mandel et al., 2010). Frogs were genotyped using primers (forward, CTAACCACAGCCCATTCTCT; reverse, ACAGAGCCTGTACCATCC. Primers were designed for *Xenopus tropicalis Tbx5* exons 8 and 9.

Xenopus protein extraction

Batches of 10 embryos were lysed in a minimal volume of lysis buffer (50mM Tris pH 7.6, 150 mM NaCl, 6 mM EDTA, 1% Triton X-100, 1x protease inhibitor (Sigma, St. Louis, USA)). Lysate was sonicated for 15 minutes, (30s on/30s off) at

4C°, and centrifuged for 10 min at 15,000rpm. The supernatant was then collected and isolated from the lipid layer on top of the lysate and the insoluble pellet and then prepared for western blot.

RESULTS

TBX5 is phosphorylated in vivo

Data mining was performed in our laboratory to identify the phosphproteome of adult mice. These results indicated that TBX5 is phosphorylated *in vivo* at four residues (S261, T262, S276, and T278) (Villen et al., 2007). Three of these residues (S261, T262, and T278) are evolutionarily conserved across all TBX5 orthologs including *Xenopus*, mouse, and human (Table 2.1). The phosphorylation sites map to an uncharacterized region of the TBX5 protein in the C-terminal region, located 3' to the T-box DNA binding domain (Figure 2.1).

Mutation of phosphorylation residue T278 increases transcriptional activity.

To determine the importance of the potentially phosphorylated residues for TBX5-mediated transcriptional activation of target genes, we mutated all three residues to alanine, which generates the triple phospho-dead mutant TBX5$^{S261A-T262A-T278A}$) in the *Xenopus tropicalis* ortholog of TBX5. Combinatorial mutation of all three residues significantly increased the level of TBX5-mediated transcriptional activation of its downstream target *ANF*/Nppa (Bruneau et al., 2001; Fan et al., 2003; Garg et al., 2003; Hiroi et al., 2001) in *Xenopus* transcriptional assays (Figure

2.2A). By contrast, mutation of all three residues to aspartic acid or glutamic acid generates the triple phospho-mimetic mutant TBX5$^{S261D-T262E-T278E}$ /TBX5$^{S261E-T262E-T278E}$), which results in transcriptional activity similar to that of wild type TBX5. Therefore, we conclude that TBX5 phosphorylation at these residues reduces TBX5 transcriptional activity.

To determine the crucial residues involved in TBX5 transcriptional activity, we performed transcriptional assays in *Xenopus* expressing single point mutations of TBX5 (TBX5^{S261A}, TBX5^{T262A}, or TBX5^{T278A}). Mutation of residues S261 and T262 had minimal effects on TBX5 transcriptional activity, whereas mutation of T278 to alanine recapitulated the increased TBX5 transcriptional activity observed in the triple phospho-dead mutant (Figure 2.2B). We conclude that residue T278 is phosphorylated to reduce TBX5-mediated transcriptional activation of the *ANF* promoter.

Mutation of phosphorylation residue T278 does not affect TBX5 localization

There are a number of processes that can explain changes in the transcriptional activity of a transcription factor. Phosphorylation of TBX5 may change TBX5 nuclear localization, and thereby affect TBX5-mediated transcriptional activation of downstream target genes. To determine whether TBX5 phosphorylation changes the protein localization, we overexpressed wild type TBX5 and TBX5^{T278A} in COS-7 cells and isolated nuclear and cytoplasmic extracts. Endogenous TBX5 is predominantly expressed in the nucleus, but cytoplasmic localization of TBX5 is also

observed when TBX5 is overexpressed. However, we detected no change in TBX5 localization in the mutated TBX5^{T278} protein (Figure S2.1).

Mutation of TBX5 at T278 may affect TBX5 stability

Ubiquitin-mediated degradation pathways are known to process phosphorylated proteins. To assess the effects of TBX5 phosphorylation on protein stability, we expressed HA-tagged wild type TBX5 and TBX5^{T278A} in *Xenopus* embryos. Embryos were collected at gastrulation (stage 10), early neurula (stage 20), mid neurula (stage 26), and at the formation of the three-chambered heart (stage 33/34). At early gastrulation both wild type TBX5 and mutated TBX5$^{T278A\text{-}HA}$ proteins are expressed. However, we were not able to detect TBX5 protein in any samples after gastrulation (Figure 2.3, data at later stages not shown). We do consistently observe greater levels of TBX5^{T278A} protein expression at early stages even after normalizing for total protein level via Bradford assay (Figure 2.3 and Figure S2.1). Therefore, we hypothesize that phosphorylation of TBX5 may affect the protein half-life, turnover, or degradation.

Isolating the endogenous cardiac regulatory element of Tbx5

We hypothesize that phosphorylation of TBX5 mediates protein-protein interactions that regulate protein turnover. To test this, it is crucial to isolate the endogenous TBX5 transcriptional complex from *Xenopus* heart tissue by

immunoisolation. Currently, there is no high specificity, high affinity TBX5 antibody, and all previous attempts to isolate endogenous TBX5 and TBX5 protein complexes by us and others have failed. Therefore, it is necessary to express tagged TBX5 under its endogenous cardiac enhancer element to isolate TBX5.

To determine the endogenous cardiac regulatory elements of TBX5, we fused 11 kB of the *Xenopus tropicalis Tbx5* promoter and intragenic region, a non-coding exon, and the beginning of the first coding exon in frame to drive EGFP expression (Figure 2.4A). EGFP is expressed in the developing heart (Figure 2.4B-D) and the developing eye (data not shown) with the correct spatiotemporal localization and patterning as that of endogenous TBX5 expression. To confirm that this sequence contains a true enhancer, we utilized the same region to generate transgenic mouse embryos. The results show that EGFP expression in the mouse is the same as EGFP expression in *Xenopus* embryos (Figure 2.4 E-J). These data indicate that reporter constructs containing the *Tbx5* 5' UTR and promoter sequence faithfully recapitulate endogenous *Tbx5* expression in living *Xenopus* and mouse embryos.

Generation of transgenic Xenopus expressing Tbx5^{Avi}

To isolate endogenous TBX5 from *Xenopus* embryos, we utilized the endogenous cardiac enhancer element to express TBX5 protein labeled with the biotin acceptor peptide (Avi), V5, and 6x His tags (Figure 2.5A). The Avi tag is a small peptide tag that is biotinylated in the presence of the bacterial enzyme BirA. Thus, the Avitag/BirA system combines minimal structural invasiveness with the

robust specificity of the biotin-streptavidin interaction. This is the strongest non-covalent peptide-ligand interaction in nature; the affinity of this interaction greatly exceeds that of any antibody-antigen interaction (Bayer and Wilchek, 1980; Maine et al., 2010; Roesli et al., 2006; van Werven and Timmers, 2006; Wang et al., 2006).

Both *Xenopus laevis* and *Xenopus tropicalis* eggs were injected with the *Tbx5*^{Avi} construct using restriction enzyme mediated integration transgenesis. Briefly, sperm nuclei are incubated with linearized DNA and a restriction enzyme, along with egg extract that promotes chromatin decondensation. The sperm nuclei/DNA/egg extract mixture is then injected into an unfertilized egg, where the foreign DNA randomly integrates into multiple genomic loci during the DNA repair process, ideally before the first cleavage (Kroll and Amaya, 1996).

Tadpoles were genotyped for the presence of the *Tbx5*^{Avi} transgene using primers designed to *Tbx5* exons 8 and 9 (Figure 2.5B). Designing primer sequences that flank intron 8 allows us to distinguish between wild type *Tbx5* genomic DNA and the *Tbx5*^{Avi} transgene. Approximately 70% of our transgenic tadpoles were positive for *Tbx5*^{Avi}.

To determine if *Tbx5*^{Avi} transmits through the germline, transgenic *Tbx5*^{Avi} *Xenopus* tadpoles were grown to sexual maturity. Five *X. tropicalis* females and one male were backcrossed to wild type frogs to test for germline transmission. Approximately 50% of the founder frogs (three females) transmitted *Tbx5*^{Avi} through the germline. In the F1 population, more than 90% of tadpoles genotyped from these three females were positive for *Tbx5*^{Avi}. Fourteen *X. laevis* males and five females

were backcrossed to wild type and 74% of the founder frogs (nine males and five females) transmitted *Tbx5*^{Avi} through the germline. These results germline transmission, and we are continuing to expand the *Tbx5*^{Avi} lines. We also generated *X, laevis* transgenic lines expressing the BirA biotin ligase (Amin et al., 2014), and are working to cross these lines to generate frogs expressing endogenously biotinylated TBX5^{Avi} in the cardiac lineage.

TBX5^{Avi} *is expressed in Xenopus*

The presence of the *Tbx5*^{Avi} transgene does not necessarily correlate with protein expression. Although TBX5^{Avi} protein expression is driven by the endogenous Tbx5 cardiac enhancer, it is still possible that the transgene integrated into a locus where TBX5^{Avi} protein cannot be expressed. To confirm that TBX5^{Avi} protein is expressed in our developing embryos, we tested protein expression in *Tbx5*^{Avi} *X. laevis* tadpoles during heart development. Western blot analysis shows that TBX5^{Avi} is expressed in embryos from both founder females by stage 46 (Figure 2.6).

DISCUSSION

The genetic requirement for for *Tbx5* during cardiogenesis is evolutionarily conserved from *Xenopus* to human, and TBX5 is mutated in a large percentage of HOS patients. Some patients with HOS express TBX5 mutations that lead to protein depletion, whereas others lead to protein and overexpression, but both cases result in similar phenotypes (Cross et al., 2000; Postma et al., 2008). These observations

are consistent with numerous overexpression and depletion experiments in a number of model organisms, including mouse (Bruneau et al., 2001; Liberatore et al., 2000; Moskowitz et al., 2004), chicken (Hatcher et al., 2004; Hatcher et al., 2001), *Xenopus* (Brown et al., 2005; Goetz et al., 2006; Horb and Thomsen, 1999), and zebrafish (Garrity et al., 2002). Collectively, these studies indicate that the proper gene dosage of *Tbx5* and appropriate levels of TBX5 protein are required for cardiogenesis, and slight alteration in levels of TBX5 can lead to CHD.

Analysis of TBX5 phosphorylation in *Xenopus*

A large percentage of TBX5 mutations resulting in HOS are missense mutations, which are less likely to result loss of TBX5 protein than a truncation or a frameshift mutation. Many of these mutations affect serine or threonine residues. Therefore, we therefore hypothesized that TBX5 phosphorylation could have a role in protein regulation. We performed data mining to analyze the phospho-proteome and found that TBX5 is phosphorylated in the mouse liver in vivo (Villen et al., 2007) at four residues, three of which are conserved in *Xenopus*. Mutation of T278 to the phospho-dead alanine increases the levels of TBX5-mediated transcriptional activation of the target gene *Anf* promoter. TBX5 phosphorylation affects protein nuclear localization, protein stability, and the ability to interact with additional proteins. We suggest that the point mutant $TBX5^{T278A}$ is more stable than wild type TBX5, but this requires further validation by performing protein stability assays using cycloheximide.

Characterization of the endogenous *Tbx5* cardiac enhancer region

Xenopus embryos are an ideal system for characterizing enhancer elements; it is a relatively inexpensive system for introducing potential regulatory regions into the developing embryo, and hundreds of transgenic embryos can be generated in a matter of days. A number of studies have utilized *Xenopus* embryos to analyze enhancer elements for a number of cardiac genes, including studies from our lab on *Tbx20* (Amaya and Kroll, 1999; Garriock et al., 2005; Latinkić et al., 2004; Latinkić et al., 2002; Mandel et al., 2010; Small and Krieg, 2003; Smith et al., 2005; Smith et al., 2006; Sparrow et al., 2000). The current studies have identified the enhancer element region of *Tbx5*, which can be added to the small number of crucial cardiac genes with known regulatory elements.

Generation of TBX5^{Avi} transgenic lines and future studies

Our studies are among the first to generate a *Xenopus* line expressing an epitope-tagged protein under its endogenous cardiac promoter. There are a number of uses for this animal model that will provide a deeper understanding of TBX5 function and activity in the developing heart.

We hypothesized that phosphorylation of TBX5 at residue T278 mediates protein-protein interactions that regulate protein turnover. We intend to isolate epitope-tagged TBX5 protein from the developing *Xenopus* heart and perform phosphoproteomics analysis to confirm that T278 is phosphorylated in the heart. We then will utilize these transgenic frogs to isolate epitope-tagged TBX5 transcriptional complexes from the heart. We will construct a TBX5 transcriptional network of

proteins required for cardiogenesis. In the future, we intend to generate a similar line of frogs expressing *Tbx5*$^{T278A\text{-}Avi}$. Analysis of the TBX5 transcriptional network and interactome in these transgenic frogs expressing the phospho-dead *Tbx5*$^{T278A\text{-}Avi}$ protein will provide more information about the function of TBX5 phosphorylation during cardiogenesis.

FIGURES

Figure 2.1. Schematic of *Xenopus tropicalis* TBX5 structure. TBX5 contains a T-box DNA binding domain, characteristic of all T-box transcription factors. It also contains a small N-terminal protein-protein interaction (PPI) domain and a larger putative C-terminal PPI, two nuclear localization signals (NLS), and a C-terminal transcription activation domain (AD). Phosphorylation residues S261, T262, and T278 are not located inside a known functional domain.

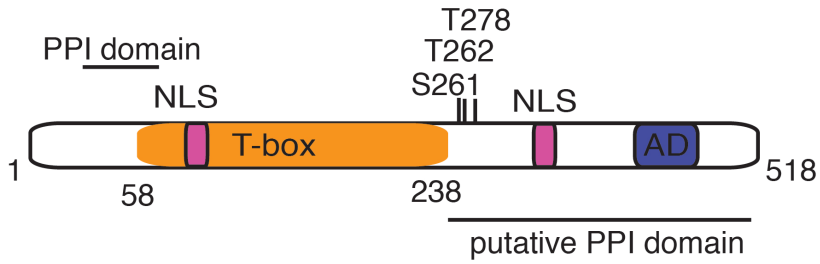

Figure 2.2. Mutation of phosphorylation residue T278 increases TBX5-mediated transcriptional actvity. Transcription assays were performed by microinjection of *Tbx5* mRNA (wild type or mutant), along with *ANF-Firefly Luciferase* and *Renilla Luciferase* reporter plasmids into *Xenopus* embryos at the one cell stage. All values are normalized to *ANF-luciferase* alone (bar 1), and all values are statistically significant compared to *ANF-luciferase* alone (p-values not shown). **(A)** Mutation of all three phosphorylation residues combinatorially. (**B**) Mutation of each phosphorylation residue individually.

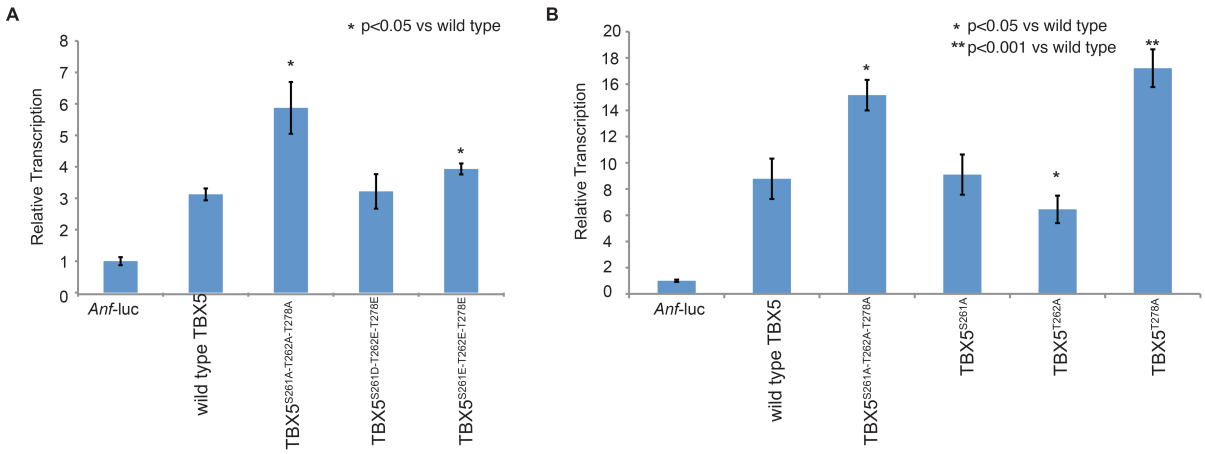

Figure 2.3. Mutation of phosphorylation residue T278 may affect protein stability. Western blot shows more phospho-dead mutant TBX5 than wild type TBX5 at early stages, suggesting that mutant protein may be more stable. Beta-Tubulin was used to demonstrate equal loading of protein.

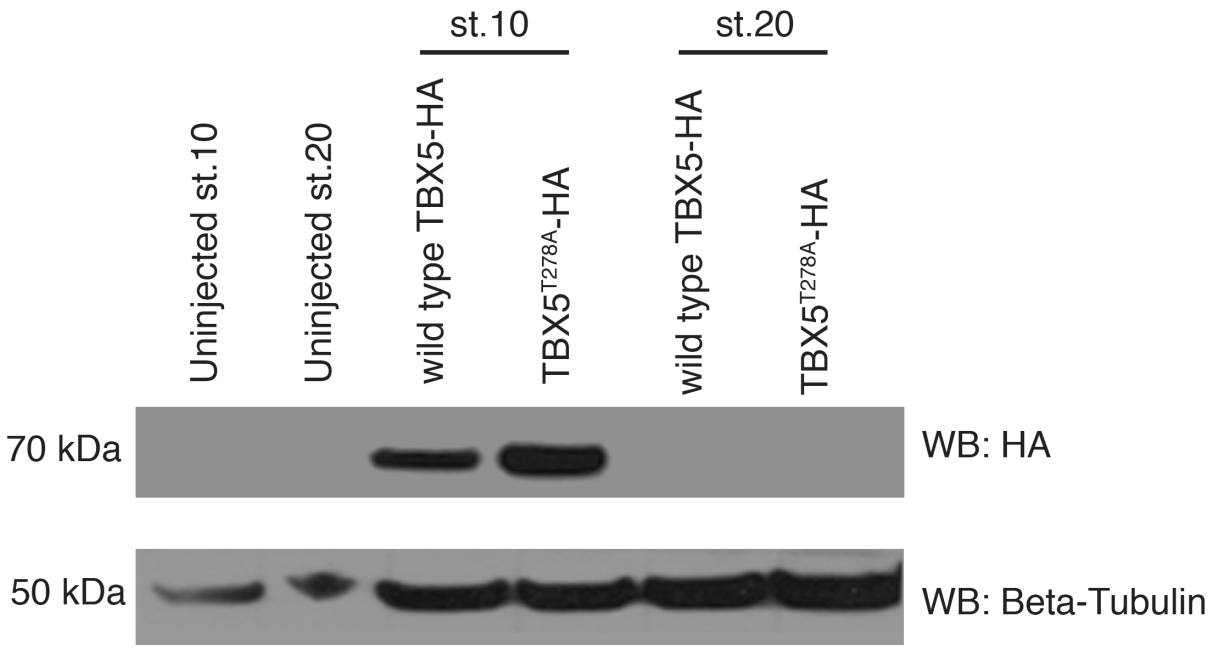

Figure 2.4. Characterization of the *Tbx5* enhancer regulatory element. (**A**) Schematic of 11 KB of *Tbx5* promoter/intragenic region, a non-coding exon, and the beginning of a coding exon fused in frame to drive EGFP expression. (**B-D**) Ventral view of a late tadpole stage transgenic embryo. (**C**) EGFP is expressed in the heart (white box) under the control of the *Tbx5* regulatory element. Autofluorescence is seen in the gut (white arrow). (**D**) Enlargement of the heart shows EGFP expression in the atria (A) and the ventricle (V). (**E-G**) Bright field images of E10.5 transgenic mouse embryo. (**H-J**) EGFP is expressed in the heart under the control of the *Tbx5* regulatory element in the left ventricle and both atria.

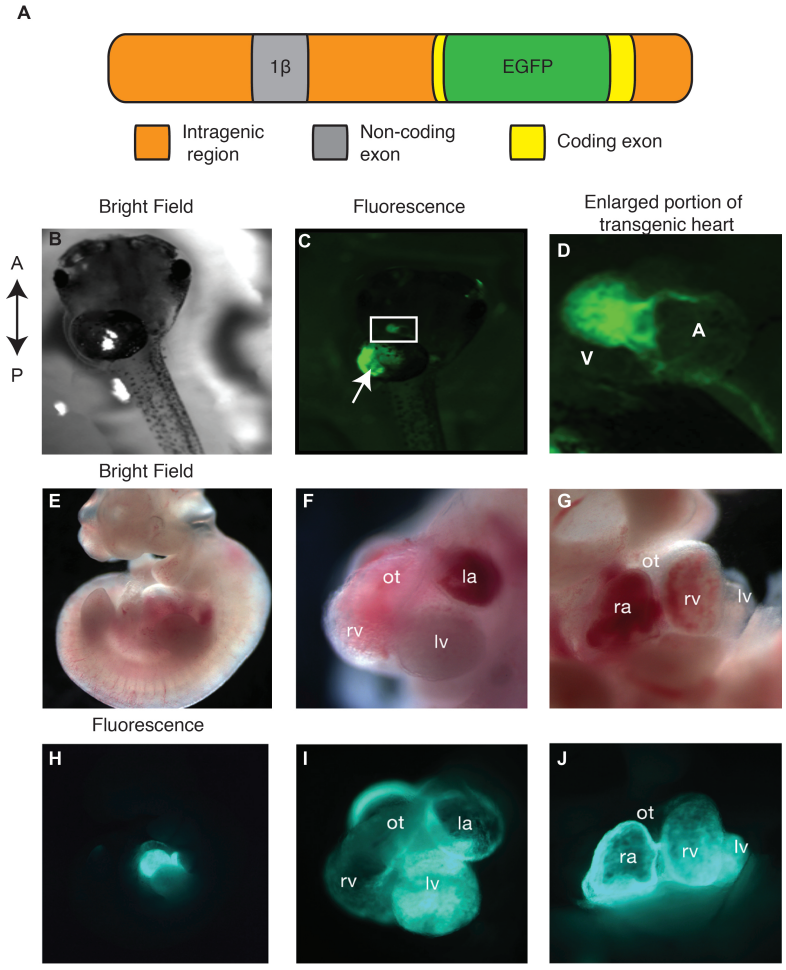

Figure 2.5. Generation of *Tbx5*^{Avi} *Xenopus* transgenic lines. (**A**) Schematic of the *Tbx5*^{Avi} transgenic construct. 11 KB of *Tbx5* regulatory region now drives expression of *Xenopus tropicalis Tbx5* fused in frame to the Avi, V5, and 6XHis tags. (**B**) Genotyping analysis of *Tbx5*^{Avi} tadpoles. DNA was isolated from tails clipped from late tadpole stage embryos. Tadpoles were genotyped for the presence of *Tbx5*^{Avi} (top panel) and the presence of DNA using *Xenopus Twist* (bottom panel).

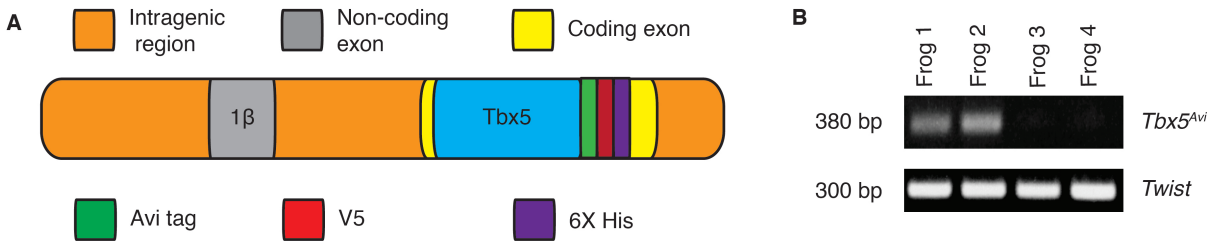

Figure 2.6. TBX5^{Avi} protein is expressed at stage 46 in *Xenopus* embryos.

Western blot analysis shows TBX5^{Avi} protein from two different founder females by stage 46. TBX5^{Avi} expression is notably decreased before this stage. GAPDHexpression levels were examined to ensure equal protein loading.

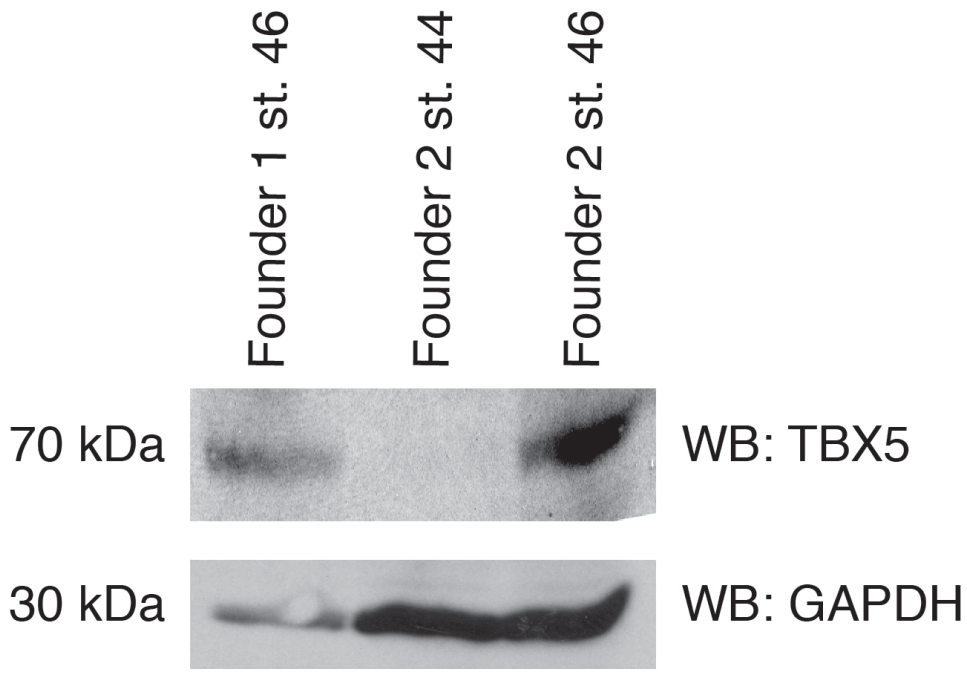

Tables

Table 2.1: Evolutionary Conservation of amino acid sequence flanking TBX5 phosphorylation sites. Phosphorylation residues (red, bold) are conserved from *Xenopus* to human.

Organism	Sequence
Xenopus laevis	256 PVVPR **ST** VRQKVSSNHSPFSQE **T** RNITG 283
Xenopus tropicalis	256 PVVPR **ST** VRQKVSSNHSPFSQE **T** RNITG 283
Mus musculus	256 PVVPR **ST** VRHKVTSNHSPFSSE **T** RALST 283
Homo sapiens	253 PVVPR **ST** VRQKVASNHSPFSSE **T** RALST 280

Supplemental Figure

Figure S2.1. Phosphorlyation of Tbx5 has no effect on Tbx5 localization. COS-7 cells were transfected with HA-tagged wild type Tbx5 or Tbx5^{T278A}. Nuclear extracts were prepared and all protein samples were normalized using Bradford assays.

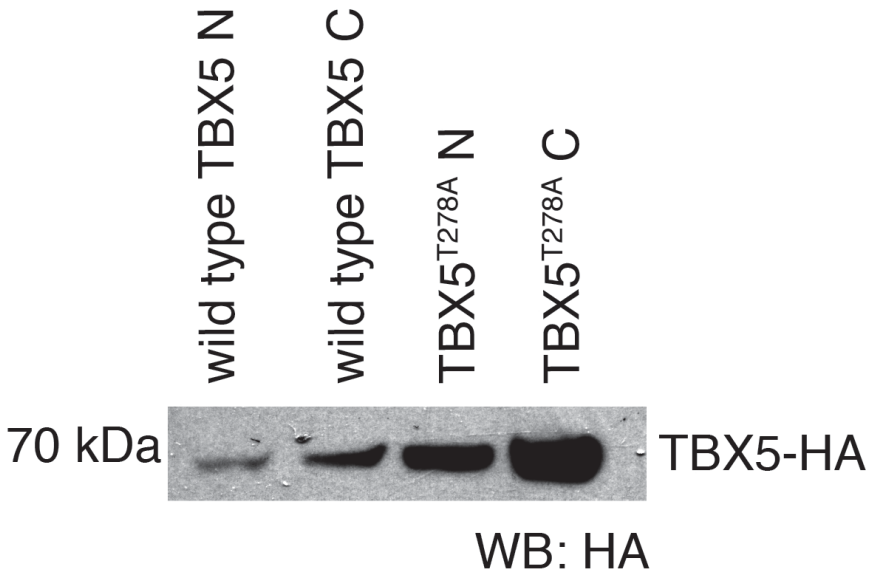

Supplemental Tables

Table S2.1. Site directed mutagenesis primers

Mutation	Forward Primer Sequence	Reverse Primer Sequence
S261A	CAGTAGTCCCTAGGGCCACAGTCC	CAGTAGTCCCTAGGGCCACAGTCC
S261A-T262A	TACCCAGTAGTCCCAAGAGCCGCAGTCCGTCAGAAGGTGTCC	GGACACCTTCTGACGGACTGCGGCTCTTGGGACTACTGGGTA
S261D-T262E	CCCAGTAGTCCCAAGAGACGAAGTCCGTCAGAAGGTG	CACCTTCTGACGGACTTCGTCTCTTGGGACTACTGGG
S261E-T262E	CACCTTCTGACGGACTTCCTCTCTTGGGACTACTGGG	CCCAGTAGTCCCAAGAGAGGAAGTCCGTCAGAAGGTG
T262A	CCAGTAGTCCCAAGAAGCGCAGTCCGTCAGAAG	CTTCTGACGGACTGCGCTTCTTGGGACTACTGG
T278A	CCATTCTCTCAAGAAGCACGCAACATTACAGGATCC	GGATCCTGTAATGTTGCGTGCTTCTTGAGAGAATGG
T278E	GCCCATTCTCTCAAGAAGAACGCAACATTACAGGATCCTC	GAGGATCCTGTAATGTTGCGTTCTTCTTGAGAGAATGGGC

REFERENCES

Amaya, E., and Kroll, K.L. (1999). A method for generating transgenic frog embryos. Methods Mol Biol *97*, 393-414.

Amin, N.M., Greco, T.M., Kuchenbrod, L.M., Rigney, M.M., Chung, M.I., Wallingford, J.B., Cristea, I.M., and Conlon, F.L. (2014). Proteomic profiling of cardiac tissue by isolation of nuclei tagged in specific cell types (INTACT). Development *141*, 962-973.

Basson, C.T., Bachinsky, D.R., Lin, R.C., Levi, T., Elkins, J.A., Soults, J., Grayzel, D., Kroumpouzou, E., Traill, T.A., Leblanc-Straceski, J.*, et al.* (1997). Mutations in human TBX5 [corrected] cause limb and cardiac malformation in Holt-Oram syndrome. Nat Genet *15*, 30-35.

Basson, C.T., Cowley, G.S., Solomon, S.D., Weissman, B., Poznanski, A.K., Traill, T.A., Seidman, J.G., and Seidman, C.E. (1994). The clinical and genetic spectrum of the Holt-Oram syndrome (heart-hand syndrome). N Engl J Med *330*, 885-891.

Basson, C.T., Huang, T., Lin, R.C., Bachinsky, D.R., Weremowicz, S., Vaglio, A., Bruzzone, R., Quadrelli, R., Lerone, M., Romeo, G.*, et al.* (1999). Different TBX5 interactions in heart and limb defined by Holt-Oram syndrome mutations. Proc Natl Acad Sci U S A *96*, 2919-2924.

Bayer, E.A., and Wilchek, M. (1980). The use of the avidin-biotin complex as a tool in molecular biology. Methods Biochem Anal *26*, 1-45.

Begemann, G., and Ingham, P.W. (2000). Developmental regulation of Tbx5 in zebrafish embryogenesis. Mech Dev *90*, 299-304.

Benson, D.W., Basson, C.T., and MacRae, C.A. (1996). New understandings in the genetics of congenital heart disease. Curr Opin Pediatr *8*, 505-511.

Bollag, R.J., Siegfried, Z., Cebra-Thomas, J.A., Garvey, N., Davison, E.M., and Silver, L.M. (1994). An ancient family of embryonically expressed mouse genes sharing a conserved protein motif with the T locus. Nat Genet *7*, 383-389.

Brassington, A.M., Sung, S.S., Toydemir, R.M., Le, T., Roeder, A.D., Rutherford, A.E., Whitby, F.G., Jorde, L.B., and Bamshad, M.J. (2003). Expressivity of Holt-Oram syndrome is not predicted by TBX5 genotype. Am J Hum Genet *73*, 74-85.

Brown, D.D., Martz, S.N., Binder, O., Goetz, S.C., Price, B.M., Smith, J.C., and Conlon, F.L. (2005). Tbx5 and Tbx20 act synergistically to control vertebrate heart morphogenesis. Development *132*, 553-563.

Bruneau, B.G., Nemer, G., Schmitt, J.P., Charron, F., Robitaille, L., Caron, S., Conner, D.A., Gessler, M., Nemer, M., Seidman, C.E.*, et al.* (2001). A murine model

of Holt-Oram syndrome defines roles of the T-box transcription factor Tbx5 in cardiogenesis and disease. Cell *106*, 709-721.

Chapman, D.L., Garvey, N., Hancock, S., Alexiou, M., Agulnik, S.I., Gibson-Brown, J.J., Cebra-Thomas, J., Bollag, R.J., Silver, L.M., and Papaioannou, V.E. (1996). Expression of the T-box family genes, Tbx1-Tbx5, during early mouse development. Dev Dyn *206*, 379-390.

Chieffo, C., Garvey, N., Gong, W., Roe, B., Zhang, G., Silver, L., Emanuel, B.S., and Budarf, M.L. (1997). Isolation and characterization of a gene from the DiGeorge chromosomal region homologous to the mouse Tbx1 gene. Genomics *43*, 267-277.

Cross, S.J., Ching, Y.H., Li, Q.Y., Armstrong-Buisseret, L., Spranger, S., Lyonnet, S., Bonnet, D., Penttinen, M., Jonveaux, P., Leheup, B.*, et al.* (2000). The mutation spectrum in Holt-Oram syndrome. J Med Genet *37*, 785-787.

Dixon, J.W., Costa, T., and Teshima, I.E. (1993). Mosaicism for duplication 12q (12q13-->q24.2) in a dysmorphic male infant. J Med Genet *30*, 70-72.

Fan, C., Liu, M., and Wang, Q. (2003). Functional analysis of TBX5 missense mutations associated with Holt-Oram syndrome. J Biol Chem *278*, 8780-8785.

Garavelli, L., De Brasi, D., Verri, R., Guareschi, E., Cariola, F., Melis, D., Calcagno, G., Salvatore, F., Unger, S., Sebastio, G.*, et al.* (2008). Holt-Oram syndrome associated with anomalies of the feet. Am J Med Genet A *146A*, 1185-1189.

Garg, V., Kathiriya, I.S., Barnes, R., Schluterman, M.K., King, I.N., Butler, C.A., Rothrock, C.R., Eapen, R.S., Hirayama-Yamada, K., Joo, K.*, et al.* (2003). GATA4 mutations cause human congenital heart defects and reveal an interaction with TBX5. Nature *424*, 443-447.

Garriock, R.J., Meadows, S.M., and Krieg, P.A. (2005). Developmental expression and comparative genomic analysis of Xenopus cardiac myosin heavy chain genes. Dev Dyn *233*, 1287-1293.

Garrity, D.M., Childs, S., and Fishman, M.C. (2002). The heartstrings mutation in zebrafish causes heart/fin Tbx5 deficiency syndrome. Development *129*, 4635-4645.

Gibson-Brown, J.J., S, I.A., Silver, L.M., and Papaioannou, V.E. (1998). Expression of T-box genes Tbx2-Tbx5 during chick organogenesis. Mech Dev *74*, 165-169.

Goetz, S.C., Brown, D.D., and Conlon, F.L. (2006). TBX5 is required for embryonic cardiac cell cycle progression. Development *133*, 2575-2584.

Hammer, S., Toenjes, M., Lange, M., Fischer, J.J., Dunkel, I., Mebus, S., Grimm, C.H., Hetzer, R., Berger, F., and Sperling, S. (2008). Characterization of TBX20 in human hearts and its regulation by TFAP2. J Cell Biochem *104*, 1022-1033.

Hatcher, C.J., Diman, N.Y., Kim, M.S., Pennisi, D., Song, Y., Goldstein, M.M., Mikawa, T., and Basson, C.T. (2004). A role for Tbx5 in proepicardial cell migration during cardiogenesis. Physiol Genomics *18*, 129-140.

Hatcher, C.J., Kim, M.S., Mah, C.S., Goldstein, M.M., Wong, B., Mikawa, T., and Basson, C.T. (2001). TBX5 transcription factor regulates cell proliferation during cardiogenesis. Dev Biol *230*, 177-188.

Hiroi, Y., Kudoh, S., Monzen, K., Ikeda, Y., Yazaki, Y., Nagai, R., and Komuro, I. (2001). Tbx5 associates with Nkx2-5 and synergistically promotes cardiomyocyte differentiation. Nat Genet *28*, 276-280.

Holt, M., and Oram, S. (1960). Familial heart disease with skeletal malformations. Br Heart J *22*, 236-242.

Horb, M.E., and Thomsen, G.H. (1999). Tbx5 is essential for heart development. Development *126*, 1739-1751.

Ieda, M., Fu, J.D., Delgado-Olguin, P., Vedantham, V., Hayashi, Y., Bruneau, B.G., and Srivastava, D. (2010). Direct reprogramming of fibroblasts into functional cardiomyocytes by defined factors. Cell *142*, 375-386.

Kirk, E.P., Sunde, M., Costa, M.W., Rankin, S.A., Wolstein, O., Castro, M.L., Butler, T.L., Hyun, C., Guo, G., Otway, R.*, et al.* (2007). Mutations in cardiac T-box factor gene TBX20 are associated with diverse cardiac pathologies, including defects of septation and valvulogenesis and cardiomyopathy. Am J Hum Genet *81*, 280-291.

Kroll, K.L., and Amaya, E. (1996). Transgenic Xenopus embryos from sperm nuclear transplantations reveal FGF signaling requirements during gastrulation. Development *122*, 3173-3183.

Latinkić , B.V., Cooper, B., Smith, S., Kotecha, S., Towers, N., Sparrow, D., and Mohun, T.J. (2004). Transcriptional regulation of the cardiac-specific MLC2 gene during Xenopus embryonic development. Development *131*, 669-679.

Latinkić, B.V., Cooper, B., Towers, N., Sparrow, D., Kotecha, S., and Mohun, T.J. (2002). Distinct enhancers regulate skeletal and cardiac muscle-specific expression programs of the cardiac alpha-actin gene in Xenopus embryos. Dev Biol *245*, 57-70.

Lehner, R., Goharkhay, N., Tringler, B., Fasching, C., and Hengstschlager, M. (2003). Pedigree analysis and descriptive investigation of three classic phenotypes associated with Holt-Oram syndrome. J Reprod Med *48*, 153-159.

Li, Q.Y., Newbury-Ecob, R.A., Terrett, J.A., Wilson, D.I., Curtis, A.R., Yi, C.H., Gebuhr, T., Bullen, P.J., Robson, S.C., Strachan, T.*, et al.* (1997). Holt-Oram syndrome is caused by mutations in TBX5, a member of the Brachyury (T) gene family. Nat Genet *15*, 21-29.

Liberatore, C.M., Searcy-Schrick, R.D., and Yutzey, K.E. (2000). Ventricular expression of tbx5 inhibits normal heart chamber development. Dev Biol *223*, 169-180.

Lindsay, E.A., Vitelli, F., Su, H., Morishima, M., Huynh, T., Pramparo, T., Jurecic, V., Ogunrinu, G., Sutherland, H.F., Scambler, P.J.*, et al.* (2001). Tbx1 haploinsufficieny in the DiGeorge syndrome region causes aortic arch defects in mice. Nature *410*, 97-101.

Maine, G.N., Li, H., Zaidi, I.W., Basrur, V., Elenitoba-Johnson, K.S., and Burstein, E. (2010). A bimolecular affinity purification method under denaturing conditions for rapid isolation of a ubiquitinated protein for mass spectrometry analysis. Nat Protoc *5*, 1447-1459.

Mandel, E.M., Callis, T.E., Wang, D.Z., and Conlon, F.L. (2005). Transcriptional mechanisms of congenital heart disease. Drug Discov Today *2*, 33-38.

Mandel, E.M., Kaltenbrun, E., Callis, T.E., Zeng, X.X., Marques, S.R., Yelon, D., Wang, D.Z., and Conlon, F.L. (2010). The BMP pathway acts to directly regulate Tbx20 in the developing heart. Development *137*, 1919-1929.

McDermott, D.A., Bressan, M.C., He, J., Lee, J.S., Aftimos, S., Brueckner, M., Gilbert, F., Graham, G.E., Hannibal, M.C., Innis, J.W.*, et al.* (2005). TBX5 genetic testing validates strict clinical criteria for Holt-Oram syndrome. Pediatr Res *58*, 981-986.

Moskowitz, I.P., Pizard, A., Patel, V.V., Bruneau, B.G., Kim, J.B., Kupershmidt, S., Roden, D., Berul, C.I., Seidman, C.E., and Seidman, J.G. (2004). The T-Box transcription factor Tbx5 is required for the patterning and maturation of the murine cardiac conduction system. Development *131*, 4107-4116.

Newbury-Ecob, R.A., Leanage, R., Raeburn, J.A., and Young, I.D. (1996). Holt-Oram syndrome: a clinical genetic study. J Med Genet *33*, 300-307.

Nieuwkoop, P., Faber, J (1994). Normal Table of Xenopus laevis (New York, Garland Publishing).

Ohuchi, H., Takeuchi, J., Yoshioka, H., Ishimaru, Y., Ogura, K., Takahashi, N., Ogura, T., and Noji, S. (1998). Correlation of wing-leg identity in ectopic FGF-induced chimeric limbs with the differential expression of chick Tbx5 and Tbx4. Development *125*, 51-60.

Papaioannou, V.E., and Silver, L.M. (1998). The T-box gene family. Bioessays *20*, 9-19.

Posch, M.G., Gramlich, M., Sunde, M., Schmitt, K.R., Lee, S.H., Richter, S., Kersten, A., Perrot, A., Panek, A.N., Al Khatib, I.H.*, et al.* (2010). A gain-of-function TBX20

mutation causes congenital atrial septal defects, patent foramen ovale and cardiac valve defects. J Med Genet *47*, 230-235.

Postma, A.V., van de Meerakker, J.B., Mathijssen, I.B., Barnett, P., Christoffels, V.M., Ilgun, A., Lam, J., Wilde, A.A., Lekanne Deprez, R.H., and Moorman, A.F. (2008). A gain-of-function TBX5 mutation is associated with atypical Holt-Oram syndrome and paroxysmal atrial fibrillation. Circ Res *102*, 1433-1442.

Qian, L., Huang, Y., Spencer, C.I., Foley, A., Vedantham, V., Liu, L., Conway, S.J., Fu, J.D., and Srivastava, D. (2012). In vivo reprogramming of murine cardiac fibroblasts into induced cardiomyocytes. Nature *485*, 593-598.

Qian, L., Mohapatra, B., Akasaka, T., Liu, J., Ocorr, K., Towbin, J.A., and Bodmer, R. (2008). Transcription factor neuromancer/TBX20 is required for cardiac function in Drosophila with implications for human heart disease. Proc Natl Acad Sci U S A *105*, 19833-19838.

Roesli, C., Neri, D., and Rybak, J.N. (2006). In vivo protein biotinylation and sample preparation for the proteomic identification of organ- and disease-specific antigens accessible from the vasculature. Nat Protoc *1*, 192-199.

Ruvinsky, I., Oates, A.C., Silver, L.M., and Ho, R.K. (2000). The evolution of paired appendages in vertebrates: T-box genes in the zebrafish. Dev Genes Evol *210*, 82-91.

Scambler, P.J. (2000). The 22q11 deletion syndromes. Hum Mol Genet *9*, 2421-2426.

Showell, C., Christine, K.S., Mandel, E.M., and Conlon, F.L. (2006). Developmental expression patterns of Tbx1, Tbx2, Tbx5, and Tbx20 in Xenopus tropicalis. Dev Dyn *235*, 1623-1630.

Sletten, L.J., and Pierpont, M.E. (1996). Variation in severity of cardiac disease in Holt-Oram syndrome. Am J Med Genet *65*, 128-132.

Small, E.M., and Krieg, P.A. (2003). Transgenic analysis of the atrialnatriuretic factor (ANF) promoter: Nkx2-5 and GATA-4 binding sites are required for atrial specific expression of ANF. Dev Biol *261*, 116-131.

Smith, J. (1999). T-box genes: what they do and how they do it. Trends Genet *15*, 154-158.

Smith, S.J., Ataliotis, P., Kotecha, S., Towers, N., Sparrow, D.B., and Mohun, T.J. (2005). The MLC1v gene provides a transgenic marker of myocardium formation within developing chambers of the Xenopus heart. Dev Dyn *232*, 1003-1012.

Smith, S.J., Fairclough, L., Latinkic, B.V., Sparrow, D.B., and Mohun, T.J. (2006). Xenopus laevis transgenesis by sperm nuclear injection. Nat Protoc *1*, 2195-2203.

Sparrow, D.B., Cai, C., Kotecha, S., Latinkic, B., Cooper, B., Towers, N., Evans, S.M., and Mohun, T.J. (2000). Regulation of the tinman homologues in Xenopus embryos. Dev Biol *227*, 65-79.

Tamura, K., Yonei-Tamura, S., and Izpisua Belmonte, J.C. (1999). Differential expression of Tbx4 and Tbx5 in Zebrafish fin buds. Mech Dev *87*, 181-184.

van Bever, Y., Dijkstra, P.F., and Hennekam, R.C. (1996). Autosomal dominant familial radial luxation, carpal fusion and scapular dysplasia with variable heart defects. Am J Med Genet *65*, 213-217.

van Werven, F.J., and Timmers, H.T. (2006). The use of biotin tagging in Saccharomyces cerevisiae improves the sensitivity of chromatin immunoprecipitation. Nucleic Acids Res *34*, e33.

Villen, J., Beausoleil, S.A., Gerber, S.A., and Gygi, S.P. (2007). Large-scale phosphorylation analysis of mouse liver. Proc Natl Acad Sci U S A *104*, 1488-1493.

Wang, J., Rao, S., Chu, J., Shen, X., Levasseur, D.N., Theunissen, T.W., and Orkin, S.H. (2006). A protein interaction network for pluripotency of embryonic stem cells. Nature *444*, 364-368.

Wilson, V., and Conlon, F.L. (2002). The T-box family. Genome Biol *3*, REVIEWS3008.

CHAPTER 3

The cardiac TBX5 interactome reveals a chromatin remodeling network essential for atrial septation

Overview

This work was submitted to *Developmental Cell*. The project was conceived by myself, Frank Conlon, Ileana Cristea and Ivan Moskowitz. Kerry Dorr performed Southern analysis to determine $Tbx5^{Avi}$ positive clones. Junghun Kweon and Jeffrey Steimle performed all experiments and analysis related to the $Tbx5^{+/-}$; $Mta1^{+/-}$ mouse, and Caralynn Wilczewski performed the $Mta1^{-/-}$ experiment and analysis. Brenda Temple modeled the TBX5 protein structure, and generated the TBX5 evolutionary tree, Todd Greco and I analyzed proteomics data. Nicholas Gomez performed large scale bioinformatics analysis of TBX5 binding motifs and pathway analysis. Ian Davis provided additional bioinformatics expertise. Ileana Cristea provided additional proteomics expertise. Ivan Moskowitz provided RNA-seq data. I performed all other experiments. Frank Conlon and I wrote the manuscript with contributions and comments from all authors.

Lauren Waldron, Junghun Kweon, Todd M. Greco, Nicholas C. Gomez, Kerry M. Dorr, Jeffrey D. Steimle, Brenda Temple, Xinan Holly Yang, Caralynn M. Wilczewski, Ian J. Davis, Ileana M. Cristea, Ivan P. Moskowitz, and Frank L. Conlon**.** (2015) The cardiac TBX5 interactome reveals a chromatin remodeling network essential for atrial septation. *Developmental Cell* [submitted]

Congenital heart disease (CHD) is the most common congenital malformation, with defects in cardiac chamber septation accounting for almost half of all CHD-related deaths in children. The cardiac transcription factor TBX5 has been shown to be causative in patients with septal defects; however, its mechanism of action in normal development and in CHD has not been determined. We have isolated and characterized the endogenous TBX5 cardiac interactome and report that TBX5, long considered to be a cardiac transcriptional activator, interacts biochemically and genetically with the chromatin remodeling repressor machinery of the Nucleosome Remodeling and Deacetylase (NuRD) complex. We report that the TBX5-NuRD interaction is essential for normal heart development and that patients with atrioventricular septal defects (AVSD) have mutations that disrupt the TBX5-NuRD interaction. We identify the direct transcriptional targets of TBX5 and show that TBX5 acts to repress expression of neural- and cancer- associated gene programs in cardiac tissue. Furthermore, a subset of these genes are disregulated by CHD patient mutations. We also define a new structural-functional domain of TBX5 essential for interaction with the NuRD complex, and show through phylogenetic analysis that this domain

evolved during the early diversification of vertebrates, simultaneous with the evolution of atrial septation. We define a novel TBX5-NuRD interaction that is essential to cardiac development and the evolution of the mammalian heart, and that when altered may contribute to human CHD.

INTRODUCTION

Congenital malformations, or structural birth defects, are the leading cause of infant mortality in the US and Europe (Dolk et al., 2010; Heron and Tejada-Vera, 2009). Congenital heart disease (CHD) remains the most common congenital malformation, with atrial septal defects present in 56 per 100,000 live births (Morris, 2010). Holt Oram Syndrome (HOS) is an autosomal disorder associated with cardiac septal defects and is caused by dominant mutations in the T-box transcription factor *Tbx5* (Basson et al., 1997; Basson et al., 1994; Basson et al., 1999; Cross et al., 2000; Holt and Oram, 1960; Li et al., 1997). Mice heterozygous for a null mutation in *Tbx5* display many of the phenotypic abnormalities of HOS, while mice homozygous for a null mutation in *Tbx5* die by E10.5 due to cardiac defects (Bruneau et al., 1999; Bruneau et al., 2001; Moskowitz et al., 2007; Moskowitz et al., 2004). In addition to its role in cardiogenesis, *Tbx5* is one of the key factors essential for cellular reprogramming of fibroblasts into induced cardiomyocytes (Ieda et al., 2010; Qian et al., 2012).

While *Tbx5* is an essential transcription factor for heart development and reprogramming, and its disease relevance is well established, there are many critical unanswered questions about the mechanism of TBX5 function. For

example, it is not understood what proteins complex with TBX5 during different stages of cardiac development and homeostasis, how these interactions regulate TBX5's choice of distinct transcriptional targets, or how these interactions function to activate and/or repress target gene transcription. It is also not known how these events, when disrupted, manifest as CHD. To these ends, we initiated a directed proteomic-based approach to identify endogenous cardiac proteins that function in physical association with TBX5.

Here we report the discovery that TBX5 interacts biochemically and genetically with the transcriptional repression machinery of the Nucleosome Remodeling and Deacetylase (NuRD) complex to repress inappropriate expression of neural and cancer related genes in the developing heart. We have further uncovered a novel domain of TBX5, show that it forms an α-Helix, and show that TBX5 mis-sense mutations associated with septal defects in human patients map to this domain. Moreover, we demonstrate that HOS patient mis-sense mutations in this domain disrupt the TBX5-NuRD interaction and elicit misexpression of neural and cancer genes that are normally repressed by TBX5. Through phylogenetic analysis across numerous vertebrate species, we find that the NuRD-interaction domain of TBX5, and hence the interaction of TBX5 with NuRD, evolved during the early diversification of vertebrates, simultaneous with the evolution of atrial septation. Thus, the TBX5-NuRD interaction identified here plays a central role in both cardiac development and human congenital heart defects, as well as the evolution of the mammalian heart.

MATERIALS AND METHODS

Generation of Tbx5^{Avi} mice

The targeting construct used to create a conditional knock-in allele of *Tbx5^{Avi}* was created in collaboration with the UNC Animal Models Core and the UNC BAC Core (Chapel Hill). Briefly, the biotin acceptor peptide (Avi) targeting cassette was inserted in frame to the terminal exon of the *Tbx5* gene. Targeted ES cells were selected and introduced into B6 mouse blastocysts. High-chimera males were mated with B6 females to produce F1 heterozygotes (*Tbx5$^{Avi\text{-}Neo/+}$*). Incorporation of the *Tbx5^{Avi}* construct was confirmed by PCR and Southern analysis (Figure S3.1B), while presence of *Tbx5^{Avi}* mRNA was confirmed by RT-PCR (Figure S3.1D). F1 heterozygotes were crossed with *Sox2-Cre* mice (Hayashi et al., 2002) to remove the neomycin selection cassette in the F2 generation (Figure S3.1C). F2 compound heterozygous mice were intercrossed to remove the *Sox2-Cre* allele and establish *Tbx5$^{Avi/Avi}$* homozygous lines. *Tbx5$^{Avi/Avi}$* mice were crossed to *Rosa26^{BirA}* mice (JAX), which have been previously described (Driegen et al., 2005), and those progeny intercrossed to obtain compound homozygotes. Genotyping was performed by PCR. Genotyping primers can be found in Supplemental Experimental Procedures. Southern probe was designed to *Tbx5* intron 8. Genomic DNA was digested with EcoRV or BamHI. Animal care and animal experiments were conducted in accordance with the Animal Care Committee at the University of North Carolina, Chapel Hill.

Preparation of cardiac nuclei

Frozen hearts from 4 week old *Tbx5*$^{Avi/Avi}$*; Rosa26*$^{BirA/BirA}$ (n=3, 2 replicates) and *Tbx5*$^{Avi/Avi}$ or *Rosa26*$^{BirA/BirA}$ control mice (n=3, 1 replicate per genotype) were homogenized using a mortar and pestle in liquid nitrogen. Nuclei were prepared as previously described (Franklin et al., 2011) and snap frozen in liquid N_2.

Solubilization of protein complexes

Plasmids were transfected into HEK-293 cells, which were harvested and lysed as previously described (Kaltenbrun et al., 2013). E9.5 hearts were harvested in PBS and lysed as previously described (Kaltenbrun et al., 2013). Cells and nuclear pellets were resuspended in lysis buffer (200mM K-HEPES pH 7.4, 1.1M KOAc, 20mM $MgCl_2$, 1% Tween-20, 10μM $ZnCl_2$, 10mM $CaCl_2$, 0.5% Triton X-100, 500 mM NaCl, 1X protease inhibitors (Roche), 1X phosphatase inhibitors (Sigma), optimized for TBX5 complexes. Nuclei were then homogenized using a Polytron (Kinematica), and processed for affinity purification or immunoprecipitation as previously described (Kaltenbrun et al., 2013).

Conjugation of magnetic beads and affinity purification

Conjugation of V5 (Invitrogen R960-CUS) or TBX5 (Aviva ARP33403-P050) antibody to magnetic beads (Invitrogen), and immunoisolation of protein

complexes was performed as previously described (Cristea et al., 2005; Kaltenbrun et al., 2013), but modified as follows for streptavidin-coated beads. Affinity purifications were performed using streptavidin conjugated Dynabeads (Invitrogen) by slow rocking at RT for 30 minutes. The isolated protein complex was eluted from the beads for 20 min at 95°C in 40μL elution buffer (80mM NaOAc pH 9.0, 95% formamide). Western blots were probed with mouse anti-V5 (1:5000, Invitrogen R960-CUS), rabbit anti-CHD4 (1:500, Active Motif 39289), mouse anti-HDAC2 (1:1000, Abcam Ab51832), rabbit anti-MTA1 (1:5000, Bethyl A300-280A), rabbit anti-TBX5 (1:1000, Aviva ARP33403-P050, using light chain-specific rabbit secondary), goat anti-TBX5 (1:500, Santa Cruz SC-17866), and mouse anti-GFP (1:10000, Clontech 63281).

Mass spectrometry

Isolated protein complexes were analyzed by mass spectrometry as previously described (Kaltenbrun et al., 2013). Briefly, tandem mass spectra were extracted by Proteome Discoverer (Thermo Fisher Scientific), and all MS/MS samples were analyzed with SEQUEST (Thermo Fisher Scientific; version 1.2.0.208), set up to search the human and mouse UniProt-SwissProt protein sequence database, assuming digestion pattern with trypsin. Scaffold (version Scaffold_3_00_06, Proteome Software Inc., Portland, OR) was used to validate MS/MS-based peptide and protein identifications. Peptide sequences were deemed a match if they could be established at >95.0% probability as specified by the Peptide Prophet algorithm (Keller et al., 2002). In turn, protein

identifications were deemed a match if they could be established at >99.0% probability by the ProteinProphet algorithm and have at least two sequenced peptides. Protein identifications and associated spectral counts were exported to Excel for further data processing.

Interaction bioinformatics analysis

Protein identifications were filtered to exclude non-specific associations. Proteins were retained as specific candidates if they (1) had at least two spectral counts in both *Tbx5*$^{Avi/Avi}$*; Rosa26*$^{BirA/BirA}$ replicates with at least 4 spectral counts in one replicate, and (2) were uniquely identified or had at least a 2.5-fold spectral count enrichment in the *Tbx5*$^{Avi/Avi}$*; Rosa26*$^{BirA/BirA}$ condition versus the controls. Candidates were assigned gene ontology classification using the UniProt GOA annotations from within the Cytoscape (v3.2) platform (Cline et al., 2007). Gene symbols were submitted to the web-based STRING database (Franceschini et al., 2013) for interaction network analysis. Interactions with a combined STRING score of > 0.4 (medium confidence) were retained, exported, and further visualized in Cytoscape.

RNA extraction and RT-PCR

Adult (n=2) hearts were cryolysed (2.5 min/cycle, 30 Hz, 20 cycles) in Trizol (Invitrogen) to macerate heart tissue. RNA was extracted using Trizol and purified on RNeasy columns (Qiagen). cDNA synthesis was performed from 0.5-

1 µg of RNA using random primers and SuperScript II reverse transcriptase (Invitrogen). Expression levels were assessed using GoTaq Green Master Mix (Promega) and Taq polymerase on a GeneAmp PCR System (Applied Biosystems). PCR products were analyzed by 1.5% agarose gel electrophoresis. RT-PCR primer sequences are provided in supplemental Experimental Procedures.

Transcriptional assays

ChIP peak regions from our candidate genes of interest were amplified from mouse genomic DNA and subcloned into the PGL3-Promoter Luciferase vector (Promega). Primer sequences for each candidate gene are provided in Supplemental Experimental Procedures. HEK-293 cells were transfected with 600ng total DNA in 12 well plates using FuGene6 (Promega) and harvested 48 hours later for transcription assay. Transcriptional assays were performed using Dual Reporter Assay System (Promega) according to the manufacturer's protocol in three biological and three technical replicates per assay.

DNA constructs

Generation of the *Tbx5*^{Avi} targeting construct for embryonic stem cells and generation of chimeric mice was performed by JrGang Chen (UNC BAC Core-Chapel Hill). *Tbx5-Avi-V5* was generated by synthesizing an oligo encoding the Avi tag (5' ggc ctg aac gac atc ttc gag gct cag aaa atc gaa tgg cac gaa 3') and subcloning it into the pcDNA3.1/V5-His TOPO vector (Invitrogen). Full length and

truncated versions of mouse *Tbx5* were then subcloned into pcDNA3.1-Avi-V5. pEF1α-BirA-V5-Neo was generously provided by Stuart Orkin (Harvard University) (Kim et al., 2009). GFP tagged full length, C-terminal, and N-terminal human CHD4 constructs were generously provided by Stephen Jackson (Cambridge) (Polo et al., 2010). Site-directed mutagenesis primers are available in Supplemental Experimental Procedures.

Genetic interaction and histology

Tbx5$^{fl/fl}$ mice were generously provided by Jon and Christine Seidman (Harvard Medical School). The *Tbx5*$^{+/-}$ mouse has been previously reported (Bruneau et al., 2001). The *Mta1*$^{+/-}$ mouse line was generated by Harold Olivey (Indiana University Northwest) and generously provided by Eric Svensson (Novartis Institutes for Biomedial Research). All mice are in a mixed B6/129/SvEv/CD-1 background and all mouse experiments were performed according to a protocol reviewed and approved by the Institutional Animal Care and Use Committee of the University of Chicago, in compliance with the USA Public Health Service Policy on Humane Care and Use of Laboratory Animals. E13.5 and E14.5 wild type, *Tbx5*$^{+/-}$, *Mta1*$^{+/,-}$ and *Tbx5*$^{+/-}$;*Mta1*$^{+/-}$ embryos were dissected from timed matings. Embryos were fixed in 4% PFA overnight and sent to the Human Tissue Resource Center at the University of Chicago for paraffin embedding, sectioning, and H&E staining. Slides were imaged on a Leica DM2500 microscope and QImaging Retiga 2000R 1394 Color Cooled camera.

Mta1$^{-/-}$ null hearts were sectioned and prepared as previously described (Dorr et al., 2015).

RNA-seq

Heart tube dissections were performed as described previously (Hoffmann et al., 2014). Briefly, E9.5 *Tbx5*$^{+/+}$ and *Tbx5*$^{-/-}$ heart tubes were dissected away from the body nearest the myocardial reflections and four heart tubes were pooled to isolate sufficient RNA. Genotypes were assigned via PCR. Pools of tissue were mechanically homogenized in TRIzol Reagent (Invitrogen, Carlsbad CA) and then RNA was isolated in accordance with the manufacturer's instructions. RNA resuspended in water was further purified with 500 µl of 1-butanol (4 times) and 500 µl diethyl ether (twice) (Krebs et al., 2009). Isolated RNA underwent library preparation and 51-bp single-ended RNA sequencing at the Genomics Core Facility at The University of Chicago. Briefly, mRNA was selected using an oligo-dT pulldown, and barcoded libraries were prepared according to Illumina's instructions accompanying the TruSeq RNA Sample prep kit v2 (Part# RS-122-2001). Library fragments of ~275 bps (insert plus adaptor and PCR primer sequences) were quantitated using the Agilent Bio-analyzer 2100 and pooled in equimolar amounts. The pooled libraries were sequenced on the HiSeq2500 in Rapid Run Mode following the manufacturer's protocols (Invitrogen, 2013).

The raw data output from the Illumina Genome Analyzer was in phred-scaled base-64 fastq format, representing the sequence and quality scores for each read. The single-ended 51-bp reads were filtered based on their quality

scores using FastQC toolkit (Andrews S, 2010) , selecting for the 37-bp reads on the right with a minimum quality score of 35 in 75% of the bases of the read. The reads passing the filter were aligned to the mouse genome mm10 assembly by Tophat (version 2.0.6) using default parameters (Kim et al., 2013). The output SAM files were filtered for alignment sorted, and converted to BAM files using Samtools (Li et al., 2009). Hit counts were estimated and normalized by both each transcript's length and the total yield of the sequencer using Cufflinks (version 2.1.1, default parameters and “-p 2”) (Trapnell et al., 2012). Among all Cufflinks reported transcript abundances, the Fragments Per Kilobase of exon per Million fragments mapped (FPKM), values larger than 0.125 in all samples were kept for the following statistical analysis. This filter guaranteed the median correlation coefficient >0.96 between any two biological replicates while kept ~65% of all transcripts, including 11789 coding genes (Ensembl annotation, mm10, 2014 April version). Differential expression between mutant samples (n=2) and wild types (n=4) was tested using Cuffdiff (v2.1.1) (Trapnell et al., 2012) Although Cuffdiff lacks power for designs with fewer than three replicates per group, the low variability of the two biological replicates in all cases (r>0.96) guarantees the statistic power of a fold change to reveal biologically meaningful results. All genes with an adjusted p-value less than 0.05 and the absolute fold change larger than 1.57 were called significant.

Large Scale bioinformatics analysis of TBX5 binding sites

Differentially expressed genes were determined by q-value (<0.05) and status ("OK"). Those genes that did not meet the status threshold were given a non-significant q-value (qval=1). TBX5 ChIP-Seq FASTQ data was downloaded from GEO (GSE21529). Tags were filtered using Tag-dust (Lassmann et al., 2009) and aligned to the mouse genome (mm9) using bowtie (Langmead et al., 2009). Peaks were called using MACS2 (Zhang et al., 2008) with default parameters. Peaks were associated with differentially expressed genes and differential motif enrichment was determined using BETA (Wang et al., 2013) with the following options –-pn 40000 and –-df 0.05 –-da 1. Because BETA uses a curated database that lacks the TBX5 motif, TBX5 peaks associated with differentially regulated genes were also analyzed for motif enrichment using HOMER (Heinz et al., 2010). Genes associated with TBX5 regulation were then analyzed for pathway enrichment using DAVID (Huang da et al., 2009). The top 10 (by p-value) KEGG pathways are shown for both activated and repressed genes.

Chromatin IP

HEK-293 cells were transfected with the *Kctd16-Luciferase* construct used in transcriptional assays, as well as wild type TBX5 or $TBX5^{S261C}$ (20 μg total DNA) using FuGene 6 (Promega). Cells were fixed in 1% PFA for 10 minutes at RT. 10 million cells were used per ChIP. Cells were lysed in ChIP Buffer (50mM Tris pH 7.5, 140 mM NaCl, 1mM EDTA, 1 mM EGTA, 0.1% sodium

deoxycholate, 0.1% SDS), sonicated using a Branson 450d, 12 cycles, 30s/cycle (1s on, 0.5s off), 30% amplitude), and spun at top speed to isolate chromatin. Triton X-100 was added to 1%, and the chromatin was added to CHD4-conjugated Protein G beads (Life Technologies) at 4°C O/N. ChIP was resumed using ChIP Protocol (Agilent). ChIP primer sequence is available in Supplemental Experimental Procedures.

TBX5 NID Modelling

The mouse TBX5 sequence was submitted to the DisProt PONDR-FIT disorder predictor in order to identify disordered regions in the protein. Both the entire protein and just the NID region were submitted to the fold recognition server HHpred (http://toolkit.tuebingen.mpg.de/hhpred) to determine if any suitable templates were available for structural modeling. A small coil-to-helical region involving residues 255-264 was predicted by HHpred. This region of TBX5 was modeled based on the correspondingly small region of the structure of the CRISPR-associated protein [PDB ID 3VZI].

RESULTS

Generation of the Tbx5^{Avi} allele

Past attempts to isolate endogenous T-box protein complexes have been hampered by their relative low abundance and insolubility. Therefore, we introduced an Avitag epitope into the murine *Tbx5* locus via homologous

recombination to generate a *Tbx5*^{Avi} allele (Figure S3.1). The Avitag is a small peptide tag that is biotinylated in the presence of the bacterial enzyme BirA. Thus, the Avitag/BirA system combines minimal structural invasiveness with the specificity and strength of the biotin-streptavidin interaction. This is the strongest non-covalent peptide-ligand interaction in nature, and therefore the affinity greatly exceeds that of any antibody-antigen interaction (Bayer and Wilchek, 1980; Maine et al., 2010; Roesli et al., 2006; van Werven and Timmers, 2006; Wang et al., 2006); *Tbx5*^{Avi} mice were mated to mice ubiquitously expressing BirA (*Rosa26*^{BirA}) (Driegen et al., 2005). The *Tbx5*^{Avi}; *Rosa26*^{BirA} compound homozygous mice show no overt phenotype, have no cardiac phenotype, and are fertile. Thus, the Avitag appears to have no effect on TBX5 activity, and expression of biotinylated TBX5^{Avi} is not deleterious to embryonic development.

Isolation and characterization of the endogenous TBX5 interactome

To define the TBX5 cardiac interactome, we performed mass spectrometry analysis of affinity-purified TBX5 complexes from *Tbx5*$^{Avi/Avi}$;*Rosa26*$^{BirA/BirA}$ cardiac nuclei (Figure 3.1A). We used an unbiased gene ontology-based bioinformatics classification to screen the functions of proteins associated with TBX5 at a statistical relevance versus *Tbx5*$^{Avi/Avi}$ alone (no BirA) and *Rosa26*$^{BirA/BirA}$ alone. This analysis defined a subset of 58 candidate interactions (Table S3.1). We analyzed these candidates by functional network analysis; drawing upon the STRING database of protein-protein interactions, 40

out of the 58 candidates were assigned to a single interconnected network (Figure 3.1B, S3.2).

TBX5 interacts with components of the Nucleosome Remodeling and Deacetylase (NuRD) complex in vivo

Analysis of the TBX5 interaction network identified the Heterodimeric Facilitates Chromatin Transcription (FACT) complex and several members of the transcription initiation factor TFIID complex, both of which play roles in RNA Pol II-dependent gene transcription (Berk, 1999; Saunders et al., 2003) (Figure 3.1B). TBX5 has been long considered to be a cardiac transcriptional activator. Surprisingly, in our analysis we identified TBX5 in association with multiple components of the NuRD complex (Figure 3.1B, C), which in most instances functions as a chromatin modifying complex that represses gene transcription (Wade et al., 1998; Xue et al., 1998). We find TBX5 in association with six components of the NuRD transcriptional repression complex: CHD4, MTA1, RBBP4, GATAD2a, GATAD2b, and HDAC2. All the components required for a functional NuRD complex were identified in association with TBX5, as CHD3 commonly acts in a mutually exclusive manner with CHD4, RBBP7 and RBBP4 act redundantly, and an additional component of the NuRD complex, MBD3, has been suggested to be dispensable for transcription factor recruitment (e.g., by hunchback (Kehle et al., 1998)). We confirmed the interaction of TBX5 with multiple members of the NuRD complex in adult cardiac nuclear extracts (Figure 3.1C).

As TBX5 has been shown to be required for cardiogenesis at E9.5 (Bruneau et al., 2001), we established expression of components of the NuRD complex in cardiac tissue at E9.5 (Figure S3.2B). We found that members of the NuRD complex are ubiquitously expressed in the heart at this stage. We further demonstrate that endogenous TBX5 (untagged TBX5) interacts with CHD4 at E9.5 (Figure 3.1D).

TBX5 and MTA1 and atrial septation

To further define the relationship between TBX5 and the NuRD complex, we generated mice heterozygous null for *Tbx5* and a central component of the NuRD complex, *Mta1* (Figure 3.2, S3.3, 3.4). At E13.5, $Mta1^{+/-}$ mice have no apparent cardiac defects (Figure 3.2C), whereas $Tbx5^{+/-}$ mice exhibit partially penetrant cardiac defects as previously described, including atrial septal defects (ASD), ventricular septal defects (VSD) and atrioventricular septal defects (AVSDs) (Figure 3.2D) (Baban et al., 2014; Basson et al., 1994; Basson et al., 1999; Benson et al., 1996; Bruneau et al., 1999; Bruneau et al., 2001; McDermott et al., 2005). $Tbx5^{+/-}$; $Mta1^{+/-}$ heterozygous null embryos demonstrated a higher frequency of AVSDs than either single heterozygote alone (n=12/14 heterozygous null vs 4/10 $Tbx5^{-/-}$) ($p<0.03$) (Figure 3.2E, S3.3D). Furthermore, $Mta1^{-/-}$ hearts also do not have AVSDs at this stage (Figure S3.4). $Tbx5^{+/-}$; $Mta1^{+/-}$ heterozygous null embryos also showed defects in the formation of the dorsal mesenchymal protrusion (DMP), similar to $Tbx5^{+/-}$ mice. We find no change in the left ventricular chamber width or left ventricular wall thickness (Figure S3.3E-F)

and further observe that the inferior and superior cushions are present and normal in size, and that the AV valves are apparent (Figure S3.3G-L). To rule out a developmental delay in septation in the *Tbx5*$^{+/-}$; *Mta1*$^{+/-}$ heterozygous null embryos, we examined *Tbx5*$^{+/-}$; *Mta1*$^{+/-}$ heterozygous null embryos at E14.5 and consistently observe AVSDs at this time point (Figure S3.3M-N). Taken together, these results demonstrate an additive genetic requirement for *Tbx5* and *Mta1*, providing genetic evidence for a role for the TBX5-NuRD interaction in atrial septum formation.

TBX5 acts to repress neural and cancer related genes in cardiac tissue

The finding that TBX5 and components of the NuRD complex interact biochemically and genetically led us to hypothesize that TBX5 can function to repress aberrant gene expression in the developing heart. To test this hypothesis, we performed transcriptional profiling of embryonic *Tbx5* null hearts to determine the gene targets of TBX5 repression. We performed RNA-seq analysis at E9.5 from wild type and *Tbx5*$^{-/-}$ hearts to define genes differentially expressed between wild type and *Tbx5* null hearts (Figure 3.3A, Table S3.2). From this data, we found 1171 genes significantly downregulated in the *Tbx5* null heart and 1361 genes significantly upregulated in the *Tbx5* null heart (Table S3.2). We overlaid TBX5 ChIP-seq data (He et al., 2011) with genes upregulated in the *Tbx5* null heart. From this analysis, we identified 928 genes that were potentially directly repressed by TBX5 (Table S3.3).

To validate the genes putatively repressed by TBX5, we rank ordered the 928 genes based first on relative change in expression between wild-type and *Tbx5*$^{-/-}$ hearts and then the number of reads in the ChIP-seq data set (Table S3.3). From this list, we cloned the top 15 of the ChIP peak sequence elements from 14 genes and performed transcriptional assays (Figure 3.3B-M, S3.5). Of the candidate genes tested, 11 were repressed by TBX5. This set of genes could be divided into two categories: *Casz1*, *Fgf11*, *Gad1, Kcne3, Kctd16, Nxph4, Plekha2,* and *Sncb* are expressed in neural lineages (Diez-Roux et al., 2011; Dorr et al., 2015; Liu et al., 2011; Metz et al., 2011; Smallwood et al., 1996; Sopher et al., 2001; Trifonov et al., 2014; Wang et al., 2014), while *Casz1*, *Col20a1, Fgf11*, *Gad1*, *Klf4, Mef2b,* and *Plekha2* are expressed in a divergent subset of cancers (Costantini et al., 2009; Evans and Liu, 2008; Hu et al., 2015; Huang et al., 2013; Kimura et al., 2013; Ying et al., 2013). Altogether, these data demonstrate that TBX5 function is essential for *in vivo* transcriptional repression and prevention of ectopic expression of neural and cancer related genes in the heart.

TBX5 binds to the same consensus site in activated and repressed target genes

As we have now shown TBX5 to act as both a transcriptional activator and a transcriptional repressor, we sought to characterize differences between TBX5 activated genes and TBX5 repressed genes. Therefore, we performed bioinformatics analysis on TBX5 binding sites on a larger scale. From our ChIP-seq and RNA-seq data, 71,624 TBX5 peak regions were identified by enrichment

of signal using MACS2 (Zhang et al., 2008). These peak regions demonstrated a significant association with genes that were differentially regulated between *Tbx5* wild type and *Tbx5*$^{-/-}$ hearts. Given that a large number of peaks can skew results in gene-association analyses, we varied the number of analyzed peaks from 10,000 to 70,000 in increments of 10,000. In every instance, TBX5 was significantly associated with differentially expressed genes (data not shown). We selected the top 40,000 peaks for subsequent analyses since the inclusion of additional peaks minimally increased the number of associated genes (data not shown). We identified an association between TBX5 and 82% of genes differentially expressed between *Tbx5* wild type and *Tbx5*$^{-/-}$ hearts (2988 of 3634, Figure S3.6A). Of these genes, about half were activated and half were repressed by TBX5. Both groups demonstrated a statistically significant enrichment in TBX5 binding sites in the TBX5 ChIP-peak regions (activated 4.88 x 10^{-141}, repressed p = 1.29 x 10^{-142}, KS test, Figure S6B). Genes repressed by TBX5 were enriched in pathways involved in cancer as well as cardiac diseases, while genes activated by TBX5 were enriched in pathways involved in cell cycle and DNA replication, a known function of TBX5 (Figure S3.6C) (Goetz et al., 2006). Interestingly, the TBX5 consensus motif was found equally abundant at regions associated with activated and repressed genes (Figure S3.6D).

TBX5 interacts with the NuRD complex through a coil-α-helix domain

To gain insight into the mechanisms of TBX5-NuRD mediated repression, we mapped the protein interaction domains of TBX5 and the catalytic core

component of the NuRD complex, CHD4 (Figure 3.4). Streptavidin pulldown of TBX5 complexes demonstrated that an N-terminal human CHD4 region containing one pair of plant homeodomains (Phd) and one pair of chromo domains was required for interaction with mouse TBX5 (Figure 3.4A, C). However, we found that deletion of either the Phd or chromo domains does not ablate the interaction between TBX5 and CHD4, demonstrating that the Phd and chromo domains are not required for the interaction between TBX5 and CHD4 (Figure 3.4D). We further demonstrated that a TBX5 region C-terminal to the T-box was necessary and sufficient for interaction with CHD4 (amino acids 238-340) (Figure 3.4B, E-F). As the majority of the TBX5 protein interactions occur N-terminal to and within the T-box, we sought to characterize this protein-protein interaction motif. We noted that this previously uncharacterized region was highly conserved across 48 TBX5 orthologues (Figure 3.5B), and that this domain was predicted to form a Coil followed by an α-Helix (Figure 3.5C, D). We have termed this structural-functional region of TBX5 the NuRD Interaction Domain ($TBX5^{NID}$) (Figure 3.5A).

The TBX5-NuRD interaction is essential for cardiac development and function in humans

The majority of TBX5 mutations associated with CHD are located within the T-box, with most causing either a loss of TBX5 DNA binding or degradation by non-sense mediated decay (Fan et al., 2003a; Fan et al., 2003b; Mori and Bruneau, 2004). In addition, there exists a subset of CHD-associated mutations

that lie in the C-terminus of TBX5, outside the T-box; the resulting mutant forms of TBX5 are stable, nuclear localized and bind DNA. The molecular basis for these CHD-associated mutations however, has been unknown. We found mis-sense mutations that correspond to TBX5-associated CHD in the C-terminal region of TBX5 that fall within the $TBX5^{NID}$ including: $TBX5^{S252I}$, $TBX5^{S261C}$, $TBX5^{V263M}$, $TBX5^{K266R}$, and $TBX5^{Q292R}$ (Heinritz et al., 2005) (Figure 3.5A). We investigated the physical location of these TBX5 amino acids on the predicted NID structural domain and observed that the amino acids align along a single interaction surface of the $TBX5^{NID}$ α-Helix (Figure 3.5D). We hypothesized the CHD mis-sense mutations in the $TBX5^{NID}$ disrupt the TBX5-CHD4 interaction.

We tested the prediction that TBX5 mis-sense mutations in the $TBX5^{NID}$ alter the TBX5-NuRD association. Three single mis-sense mutations within the $TBX5^{NID}$ ($TBX5^{S261C}$, $TBX5^{V263M}$, and $TBX5^{K266R}$) each abolished the interaction between TBX5 and both CHD4 and MTA1, and an additional two other CHD single mis-sense mutations ($TBX5^{S252I}$ and $TBX5^{Q292R}$) reduced the interactions (Figure 3.5E). These results support the hypothesis that disruption of the TBX5-NuRD complex *in vivo* leads to cardiac abnormalities associated with HOS.

TBX5 represses a neural and cancer associated target gene in a NuRD dependent manner

Having demonstrated that the TBX5-NuRD interaction is disrupted in CHD-associated mutations in the NID, we queried if repression of TBX5 target genes was NuRD dependent. We performed transcriptional assays and observed

that, of the 11 validated targets repressed by TBX5, *Kctd16* and *Mef2b* fail to be repressed by TBX5 containing the CHD associated mutation $TBX5^{S261C}$ (Figure 3.6A-B, S3.5). Moreover, $TBX5^{S261C}$ failed to repress transcription of multiple elements of the *Mef2b* gene (Figure 3.6B-D). Taken together, with results showing that we were able to ChIP CHD4 in the presence of TBX5 to these elements (Figure 3.6E-F), these results imply the TBX5-NuRD complex is required to repress inappropriate gene expression in the heart and further suggest a subset of CHD mutants leads to the mis-expression of genes including *Mef2b* in the developing heart.

The TBX5-NuRD interaction arose concomitantly with the evolution of atrial septation

Phylogenetic analysis of forty-eight TBX5 orthologues demonstrates there is a complete conservation of the $TBX5^{NID}$ amino acids mutated in TBX5-associated CHD in animals with a septated heart ($TBX5^{S261}$, $TBX5^{V263}$, $TBX5^{K266}$) (e.g. *Xenopus* to human) (Figure 3.7). In contrast, orthologues of TBX5 in vertebrates that lack a septated heart (e.g. zebrafish) have amino acid substitutions present in human CHD patients that we show ablate the TBX5-NuRD interaction (Figure 3.5E). We hypothesized that the *Xenopus* ortholog of Tbx5 would interact with the NuRD complex, but a *Xenopus* Tbx5 ortholog with zebrafish NID amino acid substitutions would fail to interact with the NuRD complex. To test this hypothesis we generated the K266R mutation in the *Xenopus* ortholog of Tbx5 ($xTbx5^{K266R}$) and found that while mTBX5 and xTbx5

interact with the NuRD complex, xTbx5^{K266R} has a disrupted interaction with CHD4 (Figure 3.7B). Thus, our data suggested that the TBX5-NuRD interaction arose coincidentally with the evolution of atrial septation and it is an essential component of an evolutionarily conserved mechanism for atrial septum formation.

DISCUSSION

Here we report the isolation and characterization of the first *in vivo* TBX5 interactome. For over 20 years, studies have defined TBX5 as an activator of transcription. However, our analysis shows that TBX5 interacts biochemically and genetically with the transcriptional repression machinery of the NuRD complex. We further report that TBX5 acts to repress neural and cancer related genes in cardiac tissue. Our observation that only a subset of TBX5-repressed target genes failed to be repressed by the TBX5 HOS mutation TBX5^{S261C} (Figure 3.6A-D, S3.7) implies that TBX5-mediated repression occurs in both a NuRD-dependent and NuRD-independent manner. We favor a model by which TBX5 regulates growth and differentiation of cardiomyocytes in part through the repression of alternate lineage-specific gene regulatory networks, including neural and cancer networks. This model is consistent with the observation that *Tbx5* null mice and human HOS patients display defects in atrial and ventricular septal growth, as well as cardiac conduction abnormalities.

We note we did not identify at statistical relevance (95% peptide identity and 99% protein identity) proteins previously shown to interact with TBX5

through in vitro studies (BRG1, NKX2.5, GATA4, TBX20, Myocardin, TAZ and BAF60C). However, if we relax the statistical cutoffs we were able to identify BRG1 (SMARCA4) in complex with TBX5 interaction partners (Takeuchi et al., 2011). There are several reasons why we may not have identified these proteins. First, the proteins may not be soluble in the lysis buffer that was optimized for TBX5 and therefore lost. Second, they may not interact with TBX5 at the time points we performed the study. Third, although their interactions may be essential for TBX5 function, their kinetics may not allow the complex to be isolated by pulldown as we have performed. It remains a formal possibility that these proteins do not physically associate in vivo.

TBX5 and atrial septation

We have previously shown that *Tbx5* is specifically required in second heart field (SHF) derivatives for atrio-ventricular septation (Xie et al., 2012). A crucial aspect of atrio-ventricular septation is the development of the dorsal mesenchymal protrusion (DMP), a structure derived from the SHF. We observed DMP abnormalities in $Tbx5^{+/-}$ mice (Xie et al., 2012) and further observed absence of the DMP in $Tbx5^{+/-}; Mta1^{+/-}$ compound heterozygotes. This suggests the AVSDs in $Tbx5^{+/-}; Mta1^{+/-}$ compound heterozygotes may result from absence of a SHF-derived structure. Taken together, our data suggest that the TBX5-NuRD interaction arose coincidentally with cardiac atrial septation. This hypothesis is further supported by our observations that $Tbx5^{+/-}; Mta1^{+/-}$ compound heterozygous mice have a higher frequency of AVSDs than either

single heterozygote (Figure S3.3D). AVSDs have been reported in 18 HOS patients, and 10 have been characterized to date (Baban et al., 2014). Of these, 6 of the mutations lead to the introduction of a stop codon before the $TBX5^{NID}$, and one mis-sense mutation maps within the $TBX5^{NID}$ and ablates the TBX5-NuRD interaction (Figure 3.5E). Thus, we find a correlation between the phenotype of patients displaying AVSD and the genotype of those TBX5 patient mutations specifically lacking or altering the $TBX5^{NID}$.

CONCLUSIONS

Our studies demonstrate that a proteomic-based approach coupled with protein modeling provides a powerful predictive strategy in prioritizing patient mutations. This type of approach should be broadly applicable to the analysis of protein complexes in any cell or tissue type. The power of such an approach is underscored by recent high-throughput sequencing studies that have led to the identification of a vast number of somatic mutations in coding regions of potential disease causing genes. Exploiting such large datasets has proved problematic because it has not been possible to determine which mutations are naturally occurring, non-disease associated variants and which are disease-causing. Results presented here demonstrate a novel proteomic-modeling based strategy that can serve to prioritize mis-sense mutations and, therefore, correlate disease associated phenotypes with specific mutations.

The authors declare no financial interests.

FIGURES

Figure 3.1. TBX5 interacts with the NuRD complex.

(A) Overview of the isolation and characterization of the endogenous cardiac TBX5 interactome. (**B**) TBX5 transcriptional interaction network. Network nodes, labeled with mouse gene symbols, are candidate direct or indirect TBX5 protein interactions identified from affinity enrichment of biotinylated TBX5. Network edges represent known and/or predicted functional interactions in the STRING database. Edge thickness reflects the combined STRING evidence score for each binary relationship. Thicker edges represent increased interaction evidence. Selected transcriptional complexes within the network are highlighted in red dashed boxes. (**C**) Affinity isolation of endogenous $TBX5^{Avi}$ from 4 week cardiac nuclei confirms interaction of TBX5 with endogenous components of the NuRD complex. (**D**) Affinity isolation of TBX5 from E9.5 hearts further confirms interaction of TBX5 with the NuRD component CHD4 in the embryonic heart.

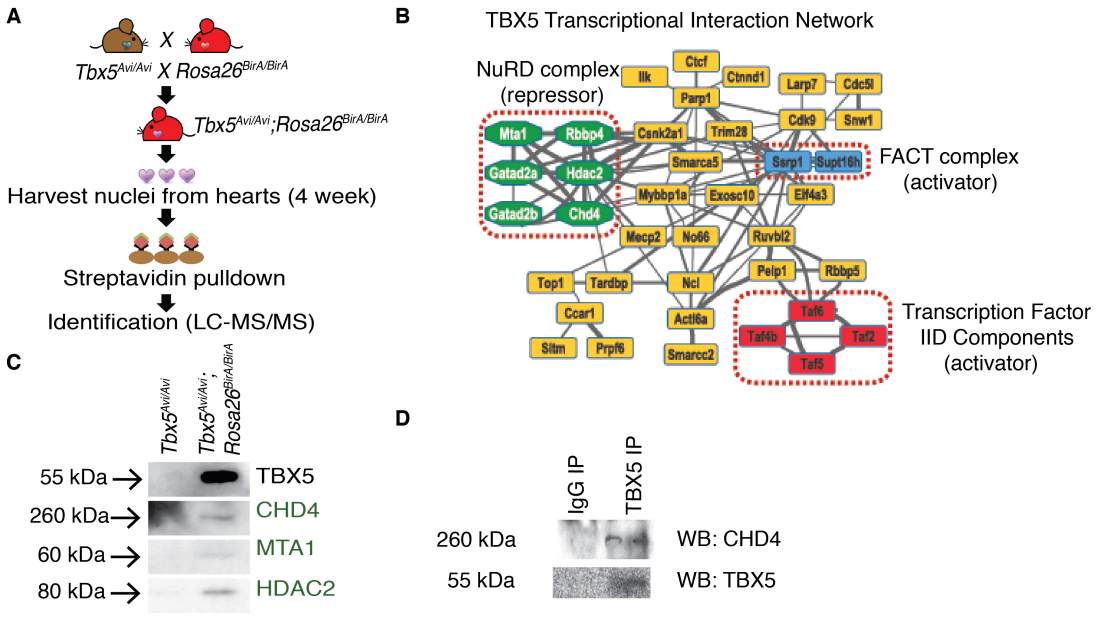

Figure 3.2. TBX5 and the NuRD complex genetically interact.

Histology staining (Hematoxylin and Eosin) of heart tissue at E13.5 (**A**) Low magnification of a wild type heart. (**B**) High magnification of a wild type, (**C**) *Mta1*$^{+/-}$, (**D**) *Tbx5*$^{+/-}$ and, (**E**) *Tbx5*$^{+/-}$*; Mta1*$^{+/}$ heart. Note that the *Tbx5*$^{+/-}$*; Mta1*$^{+/}$ hearts exhibited cardiac defects including ASD and AVSD (asterisk). Cardiac defects are characterized and quantified in Figure S3. as = atrial septum, ivs = intervectricular septum, la = left atrium, lv = left ventricle, ra = right atrium, rv = right ventricle.

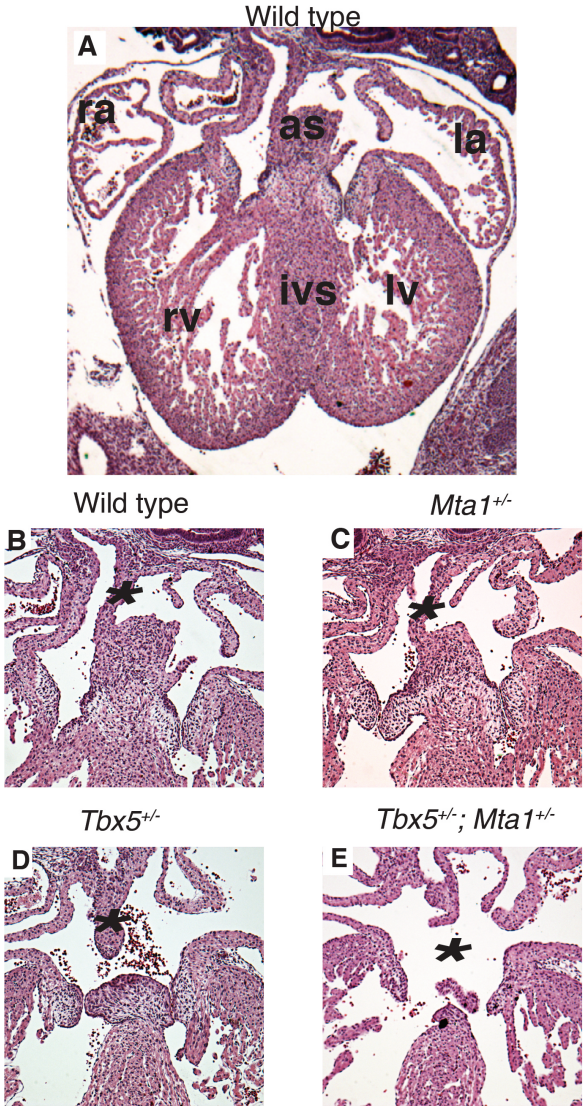

Figure 3.3. TBX5 functions to repress neural and cancer genes in cardiac tissue.

(**A**) Schematic overlay between genes upregulated in RNA-seq between wild type and *Tbx5*$^{-/-}$ heart tissue and TBX5 ChIP-seq data (He et al., 2011) reveals 928 genes that are both upregulated in a *Tbx5*$^{-/-}$ null and bound by TBX5. (**B**) Summary of fold change (RNA-seq) and ChIP-seq peak values of the 15 top rank ordered genes. (**C-M**) Gene reporter elements cloned from potential TBX5

targets in the presence or absence of TBX5. Transcriptional assays of target genes show TBX5 acts as a transcriptional repressor in 11 of 15 elements tested (additional data in Figure S6). Genes defined as neural are shown in red, expressed in cancer as blue, or both as purple. Graphs are plotted as the mean luciferase value ± SEM. Student's two tailed t-test was used to perform statistical analysis. * p< 0.05 *** p < 0.001.

A

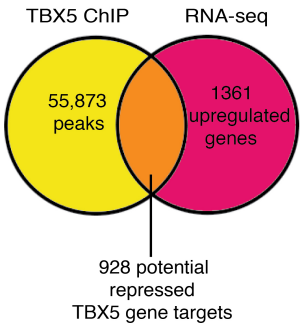

B

Gene	Log2 fold change	ChIP peak location	ChIP peak value(s)	Size of element
Sncb	5.01	intron 4	18	321 bp
Nxph4	4.93	5' UTR (5.7 kb from TSS)	41	490 bp
Mef2b	4.61	5' UTR (7.4 kb from TSS)	27	347 bp
Kctd16	4.53	5' UTR (1.4 kb from TSS)	17	426 bp
Gad1	4.19	intron 1	17	276 bp
Kcne3	3.63	5' UTR (100bp from TSS)	23	350 bp
Fgf11	3.49	intron 1	45	1,200 bp
Col20a1	1.95	5' UTR (2.7 kb from TSS)	17, 35	1,100 bp
Klf4	1.74	exon 3	57, 56	3,291 bp
Fgf8	1.71	5' UTR (2.8 kb from TSS)	80	384 bp
Fbxl20	1.37	5' UTR/ exon 1/ intron 1	25, 56, 30	1,600 bp
Casz1-1	1.26	exon 1/ intron 1	60, 29, 43	3,200 bp
Casz1-2	1.26	intron 1	32, 22, 18	2,400 bp
Kcnn2	1.23	exon 1	13	140 bp
Plekha2	1.21	5' UTR (1.3 kb from TSS)	49, 33	1,700 bp

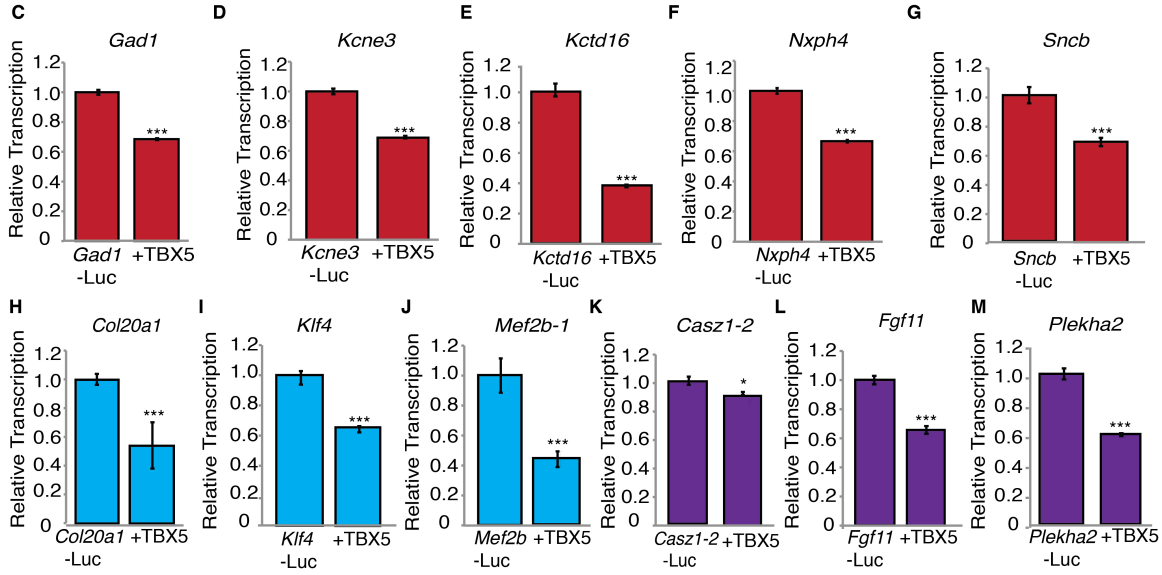

Figure 3.4. Mapping the interaction domains of CHD4 and TBX5

(**A**) Schematic of CHD4 deletion constructs. Phd= Plant homeo domain. CHD4 FL = aa 1-1937, CHD4 N = aa 1-758, CHD4 C = aa 1183-1937, TBX5 FL = aa 1-518, TBX5 N = aa 1-237, TBX5 C = aa 238-518. (**B**) Schematic of TBX5 deletion constructs. NLS = Nuclear Localization Signal. AD = Activation domain. (**C-D**) Affinity isolation of full-length TBX5-Avi-V5 with GFP-tagged CHD4 deletions reveals that CHD4 interacts with TBX5 via sequences in the N-terminus of CHD4, but that the Phd and chromo domains are not individually required for the TBX5-CHD4 interaction. **(E-F**) Affinity isolation of CHD4 with a TBX5-Avi-V5 deletion series demonstrates TBX5 sequences aa 238-340 are both necessary and sufficient for interaction with CHD4. This region has been termed the NuRD interaction domain (NID).

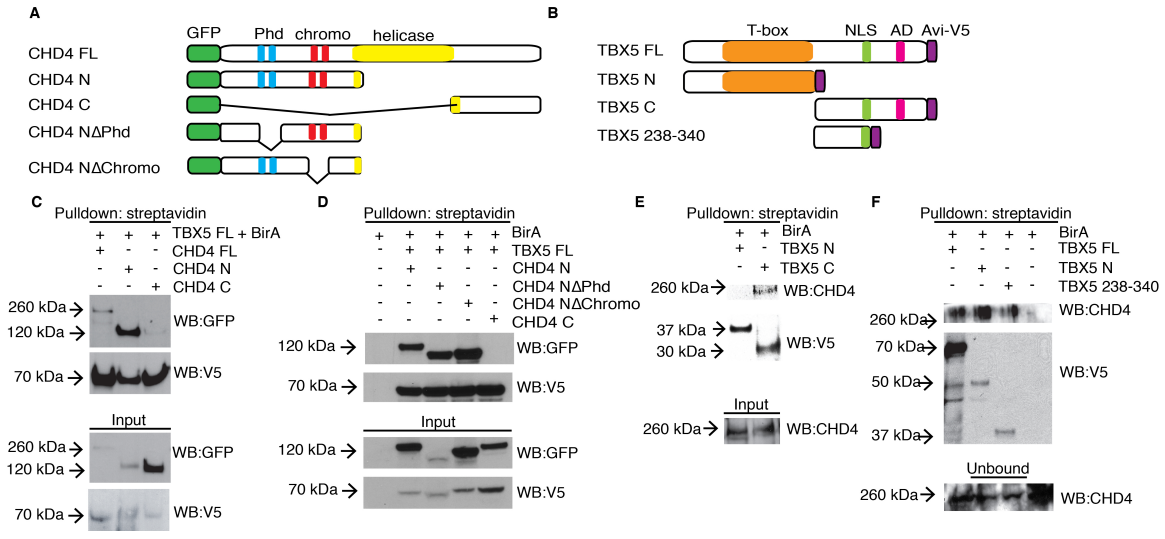

Figure 3.5. Congenital heart disease associated mutations of TBX5 disrupt the TBX5-NuRD interaction.

(**A**) Schematic of human TBX5 protein showing location of a subset of CHD associated mis-sense mutations. NID= NuRD interacting domain (aa 238-340). (**B**) Sequence alignment of the TBX5^{NID} from 48 TBX5 ortholgues**.** Height of letters is relative conservation at that residue. (**C**) Structural prediction of the TBX5^{NID} shows the TBX5^{NID} is comprised of a coil region followed an α-helix. (**D**) CHD associated mis-sense mutations align along a single surface of the α-helix and are predicted to disrupt protein-protein interactions (representative residues TBX5^{S261}, TBX5^{V263}, and TBX5^{K266} shown in dark blue). (**E**) Immunoisolation of V5-tagged CHD associated mis-sense mutations of TBX5 probed for CHD4 and MTA1.

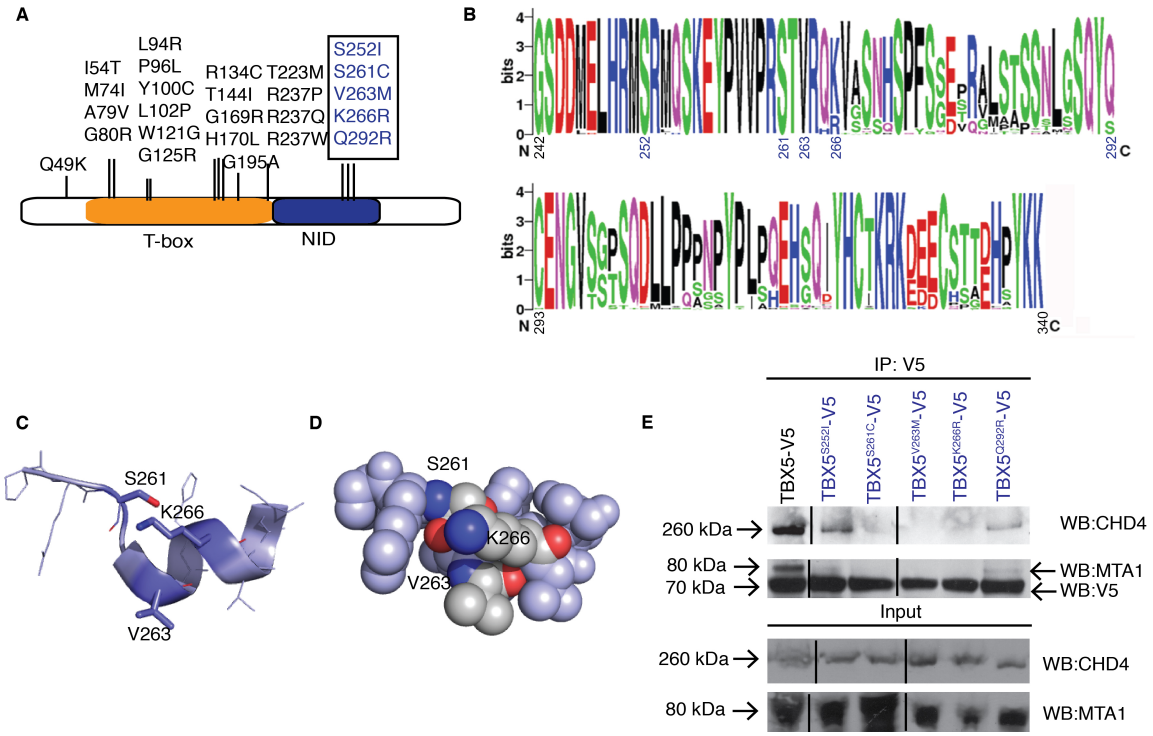

Figure 3.6. Congenital heart disease associated mutations of TBX5 disrupt TBX5-NuRD complex activity.

(**A-D**) Transcription of the regulatory regions of TBX5 target genes in response to wild type TBX5 (second column) or TBX5^{S261C} (third column). Additional gene targets shown in Figure S7. n= 9 per transcriptional assay. Graphs are plotted as the mean luciferase value ± SEM. Student's two tailed t-test was used to perform statistical analysis. *** $p < 0.001$. (**E**) Schematic of ChIP primer location on *Kctd16* element. The T-box binding element (asterisk) is noted. (**c**) ChIP of CHD4 from cells co-transfected with *Kctd16-Luciferase* in the presence of absence of TBX5.

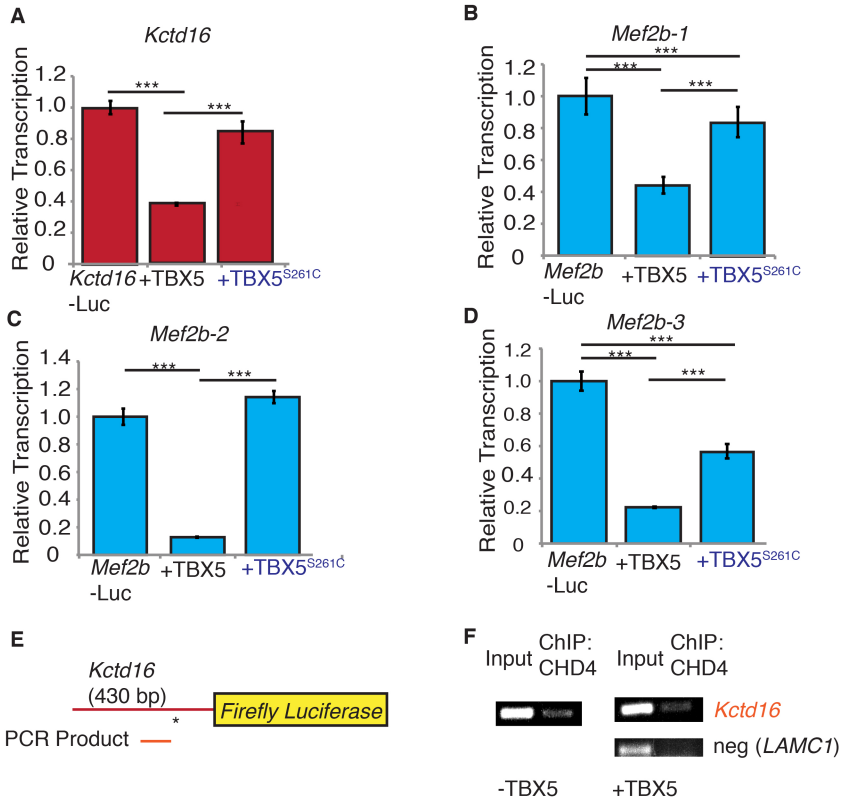

Figure 3.7. The TBX5-NuRD interaction evolved concurrently with atrial septation. (A**)** Phylogenetic comparison of TBX5 orthologues with boot-strap values. Dark green brackets represent animals with a septated heart. Light green brackets represent animals without a septated heart. Sequence of core amino acid residues required for the TBX5-NuRD interaction are shown to the right. Amino acid residues mutated in TBX5-associated CHD are bolded, and a K->R substitution from fish to frog is highlighted in pink. (**B**) Immunoisolation of V5-tagged TBX5 orthologs probed for CHD4.

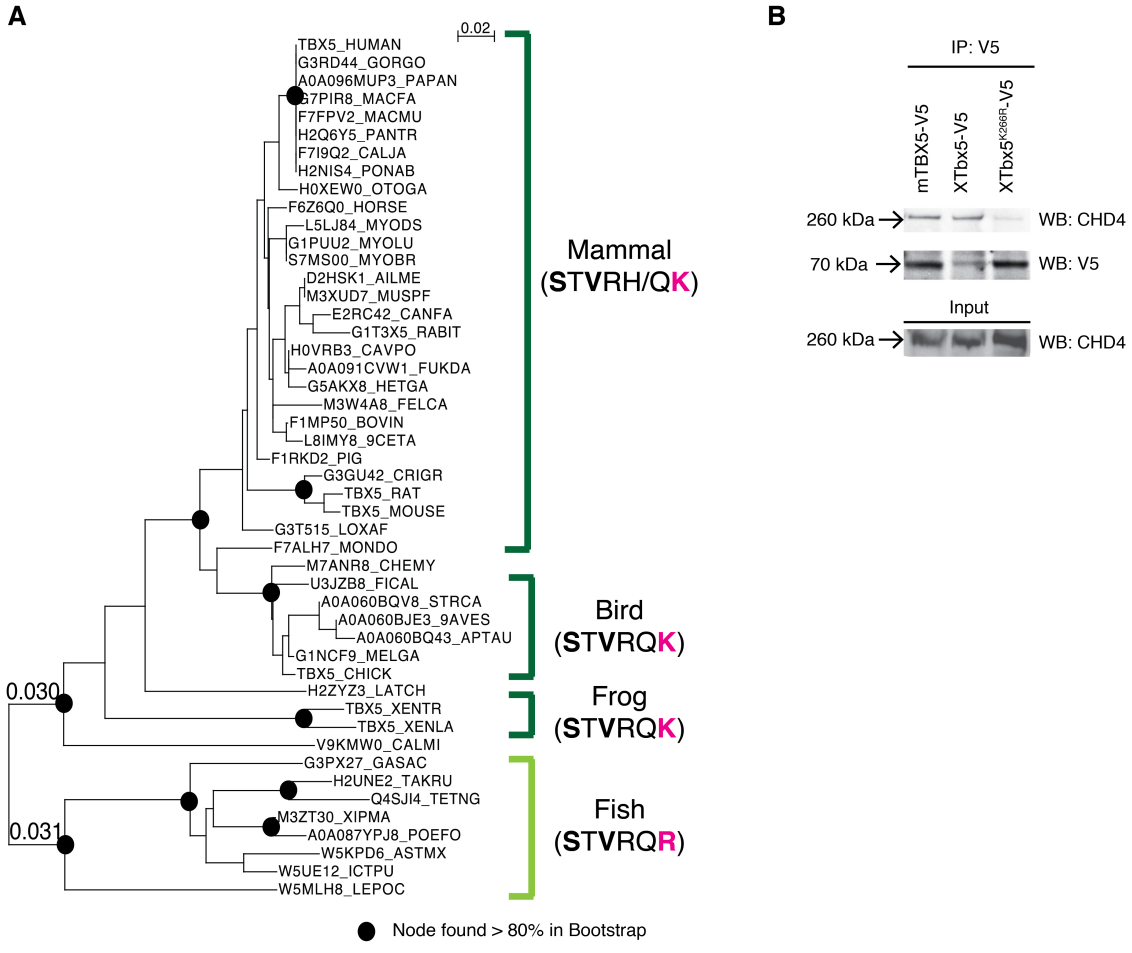

Figure S3.1, Related to Figure 3.1. Generation of a *Tbx5*^{Avi} knock-in mouse

(**A**) (Top) The *Tbx5-Avi* targeting cassette contains the biotin acceptor peptide (Avi) fused in frame to the terminal coding exon of *Tbx5*. Neo-neomycin resistance gene. PGK- phosphoglycerate kinase-1 promoter. Amp-Ampicillan resistance gene. Exons colored brown represent untranslated exons (5' and 3' UTR). Exons colored orange represent the T-box DNA binding domain. Exons colored green represent the nuclear localization signal. Exons colored pink represent the activation domain. (Middle) Schematic of the *Tbx5* recombined locus (*Tbx5*$^{Avi\text{-}Neo}$) upon homologous recombination. (Bottom) Schematic of the *Tbx5* locus upon introduction of *Cre* (*Tbx5*^{Avi}). (**B**) Southern blot of positive embryonic stem cell clone confirms homologous recombination. (**C**) Southern blot of F2 mice confirms removal of Neo cassette upon introduction of *Cre*. Samples were run on the same gel but were noncontiguous. (**D**) RT-PCR analysis of *Tbx5*$^{Avi/+}$ adult hearts demonstrates presence of *Tbx5*^{Avi} mRNA.

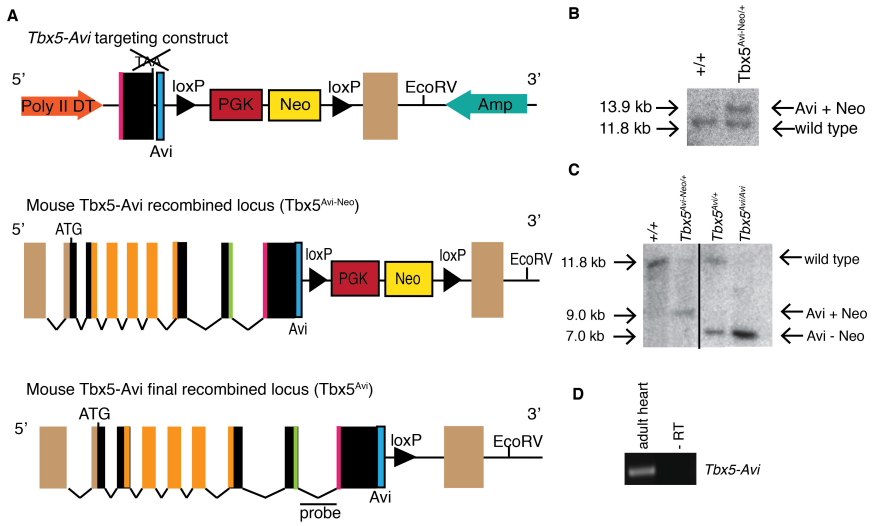

Figure S3.2, Related to Figure 3.1. The TBX5 transcription interaction network.

(**A**) Sixty mouse genes corresponding to TBX5 candidate interactions as identified by the gene ontology function of transcription were uploaded to the STRING database (www.string-db.org). STRING functional relationships were evaluated with default settings with text mining disabled. Forty proteins were clustered in a single protein interaction network, reflecting a minimum combined STRING score of > 0.4 (medium confidence) between each binary relationship (left). This network was imported to Cytoscape for further processing (see Figure 1). The remaining 20 nodes with scores < 0.4 are illustrated as disconnected (bottom). (**B**) RT-PCR analysis of all possible members of the NuRD complex demonstrates the NuRD complex is present in both the adult and embryonic heart.

A

Functional connectivity (direct and indirect) among the 60 proteins co-isolated with TBX5 that have transcription-related functions was displayed using the STRING knowledgebase.

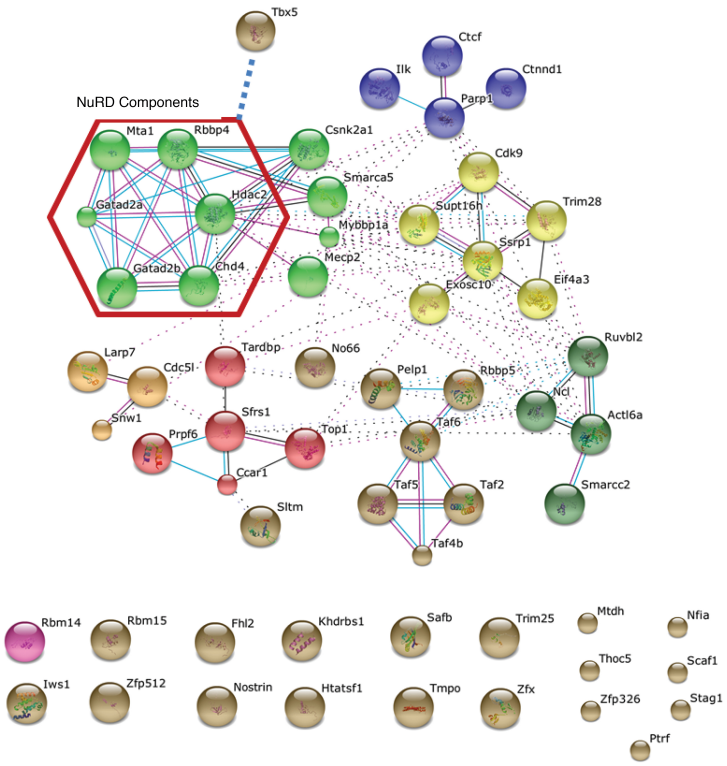

B

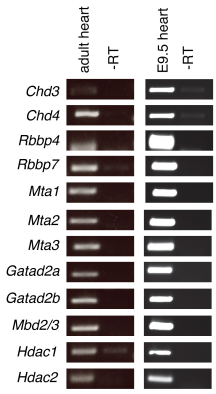

Figure S3.3, Related to Figure 3.2. TBX5 and MTA1 and atrial septation. Histology staining (Hematoxylin and Eosin) of (**A**) *Mta1*$^{+/-}$, (**B**) *Tbx5*$^{+/-}$ and, (**C**) *Tbx5*$^{+/-}$*; Mta1*$^{+/-}$ mice at E13.5. (**D**) Quantification of cardiac defects seen in all mice. Both chi-squared and Fisher's exact test show that the cardiac defects seen in *Tbx5*$^{+/-}$*; Mta1*$^{+/-}$ are significant as compared to wild type and *Tbx5*$^{+/-}$. (**E-F**) Measurements of left ventricular (LV) chamber width (**E**) and wall thickness (**F**) of wild type and *Tbx5*$^{+/-}$; *Mta1*$^{+/-}$ embryonic hearts (n=11 per genotype) at E13.5 from the 4-chamber view at the widest part. Data is reported as either chamber width or wall thickness in millimeters ± SEM. P value was determined by Student's T- test. (**G-L**) Histology staining at E13.5 through the entirety of one *Tbx5*$^{+/-}$*; Mta1*$^{+/-}$ heart from superior to inferior orientation demonstrates that the inferior and superior cushions are present and appear normal in size. The cushions are normally populated by mesenchymal cells, and both AV valves are apparent. (**M**-**N**) Histology staining of (**M**) wild type and (**N**) *Tbx5*$^{+/-}$*; Mta1*$^{+/-}$ mice at E14.5 demonstrates AVSD at this stage (asterisk).

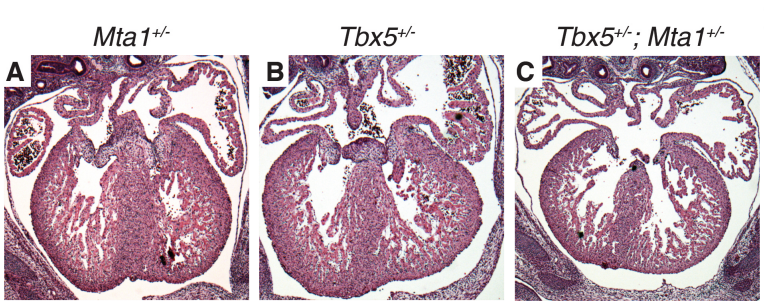

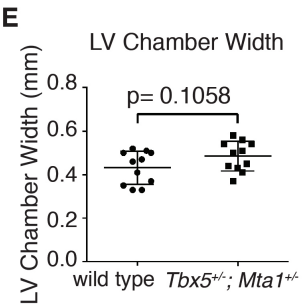

D

	Wild type	*Mta1*$^{+/-}$	*Tbx5*$^{+/-}$	*Tbx5*$^{+/-}$; *Mta1*$^{+/-}$
Intact	10	8	4	0
1° ASD	0	0	1	1
AVSD	0	0	4	12
VSD only	0	0	1	1
Total	10	8	10	14
χ^2 (vs wild type)			0.0034	0.0001
Fisher's exact test (vs wild type)		1	0.0108	0.0001
χ^2 (vs *Tbx5*$^{+/-}$)				0.0095
Fisher's exact test (vs *Tbx5*$^{+/-}$)				0.0198

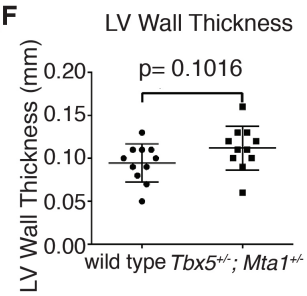

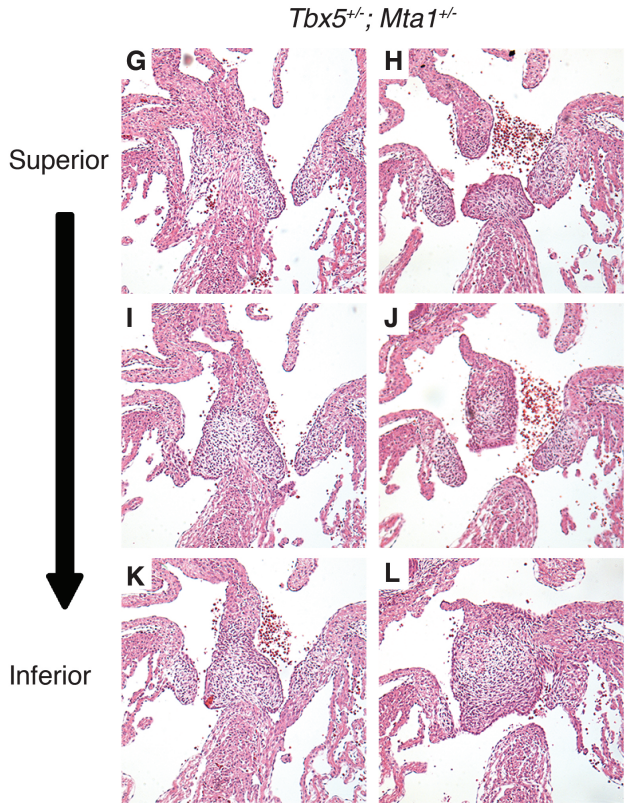

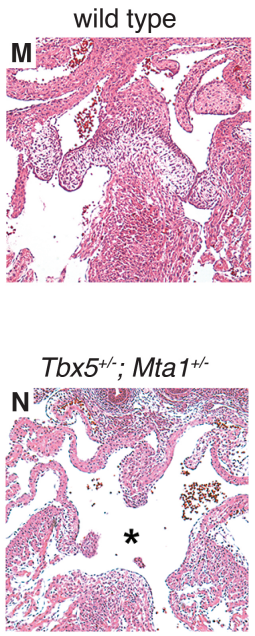

Figure S3.4, Related to Figure 3.2. *Mta1*$^{-/-}$ embryos undergo normal heart chamber septation. Histology staining (Hematoxylin and Eosin) of heart tissue at E13.5. Low magnification transverse section through (**A**) wild-type heart and (**B**) *Mta1*$^{-/-}$ heart. Asterisks denote region of higher magnification, arrows denote leaflets of venous valve of inferior vena cava, scale bar=310μm. High magnification of asterisk region in (**C**) wild-type heart and (**D**) *Mta1*$^{-/-}$ heart at point of chamber septation. Scale bar=130μm. la = left atrium, lv = left ventricle, ra = right atrium, rv = right ventricle.

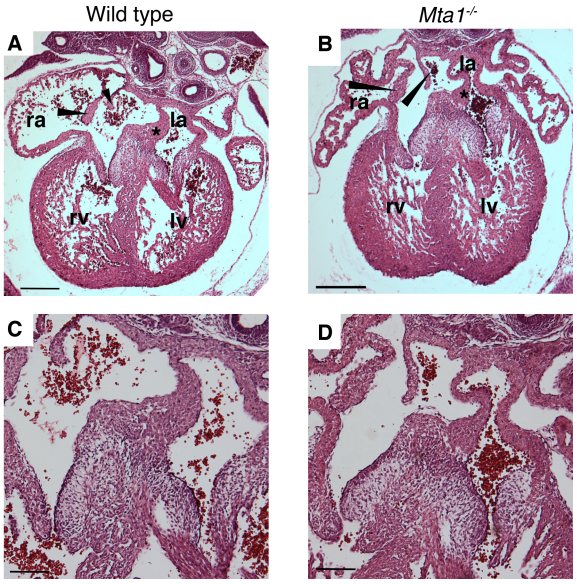

Figure S3.5, Related to Figure 3.3. Transcriptional targets not repressed by TBX5.

(**A-D)** Gene reporter elements cloned from potential TBX5 targets in the presence or absence of TBX5. Data is reported as the mean ± SEM. Student's T-test was used to determine significance. *** $p < 0.001$.

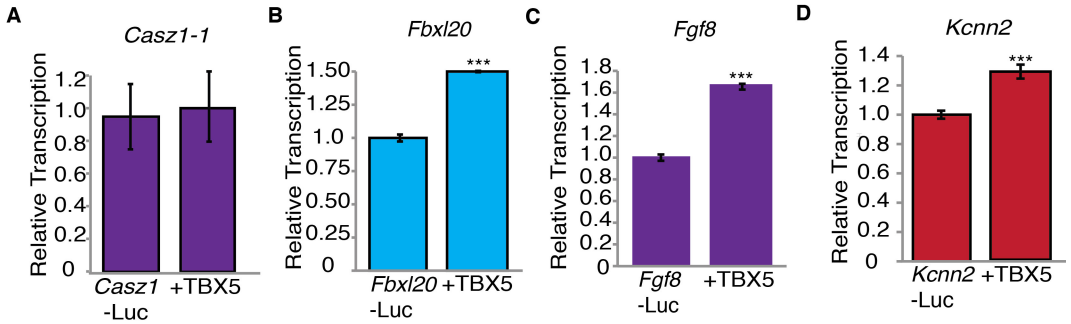

Figure S3.6, Related to Figure 3.3. Analysis of TBX5 binding motifs in activated vs repressed genes. (**A**) Schematic overlay between TBX5 peaks (He et al., 2011) and differentially expressed genes between wild-type and *Tbx5* null heart tissue. 2988 genes are differentially expressed and associated with a TBX5 peak. Inset is number of up and downregulated genes. (**B**) Activating/Repressive function prediction of TBX5 peaks. Red and purple lines represent up and down-regulated genes. Black dashed line represents background (static genes). Genes are ranked from high to low based on their regulatory potential score (RPS) determined by BETA. P values represent significance of up or down-regulated group relative to background (static genes) by Kolmogorov-Smirnov test. (**C**) Kegg Pathway enrichment of down-regulated genes associated with TBX5 binding ranked by $-\log_{10}$(pvalue). (**D**) TBX5 consensus motif (top) and top motif from de novo identification (bottom) and its presence at ChIP-seq peaks associated with activated or repressed genes.

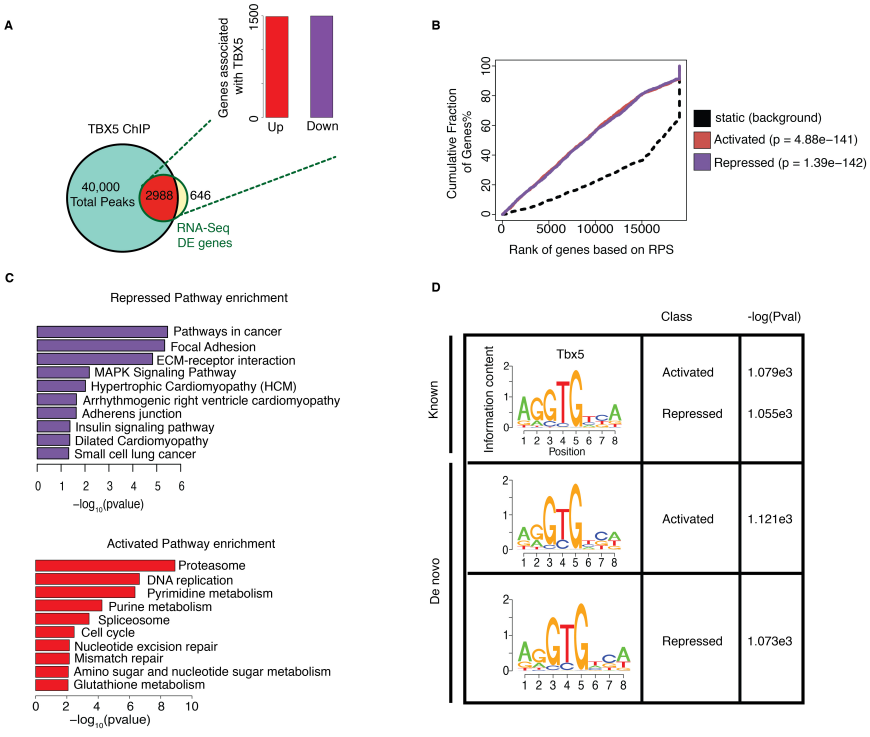
A
Genes associated with TBX5
1500
0
Up
Down
TBX5 ChIP
40,000
Total Peaks
2988
646
RNA-Seq
DE genes
B
Cumulative Fraction of Genes%
0
20
40
60
80
100
0
5000
10000
15000
Rank of genes based on RPS
static (background)
Activated (p = 4.88e−141)
Repressed (p = 1.39e−142)
C
Repressed Pathway enrichment
Pathways in cancer
Focal Adhesion
ECM-receptor interaction
MAPK Signaling Pathway
Hypertrophic Cardiomyopathy (HCM)
Arrhythmogenic right ventricle cardiomyopathy
Adherens junction
Insulin signaling pathway
Dilated Cardiomyopathy
Small cell lung cancer
0 1 2 3 4 5 6
−log10(pvalue)
Activated Pathway enrichment
Proteasome
DNA replication
Pyrimidine metabolism
Purine metabolism
Spliceosome
Cell cycle
Nucleotide excision repair
Mismatch repair
Amino sugar and nucleotide sugar metabolism
Glutathione metabolism
0 2 4 6 8 10
−log10(pvalue)
D
Class
-log(Pval)
Known
De novo
Tbx5
Information content
Position
Activated
1.079e3
Repressed
1.055e3
Activated
1.121e3
Repressed
1.073e3

Figure S3.7, Related to Figure 3.6. Targets repressed by TBX5 in a NuRD independent manner.

(**A-I)** TBX5-repressed gene reporter elements and in the co-transfected with wild type TBX5 or TBX5^{S261C}. Genes sorted into neural (red), cancer (blue), or both (purple). Data is reported as the mean ± SEM. Student's T-test was used to determine significance * p< 0.05 *** p < 0.001.

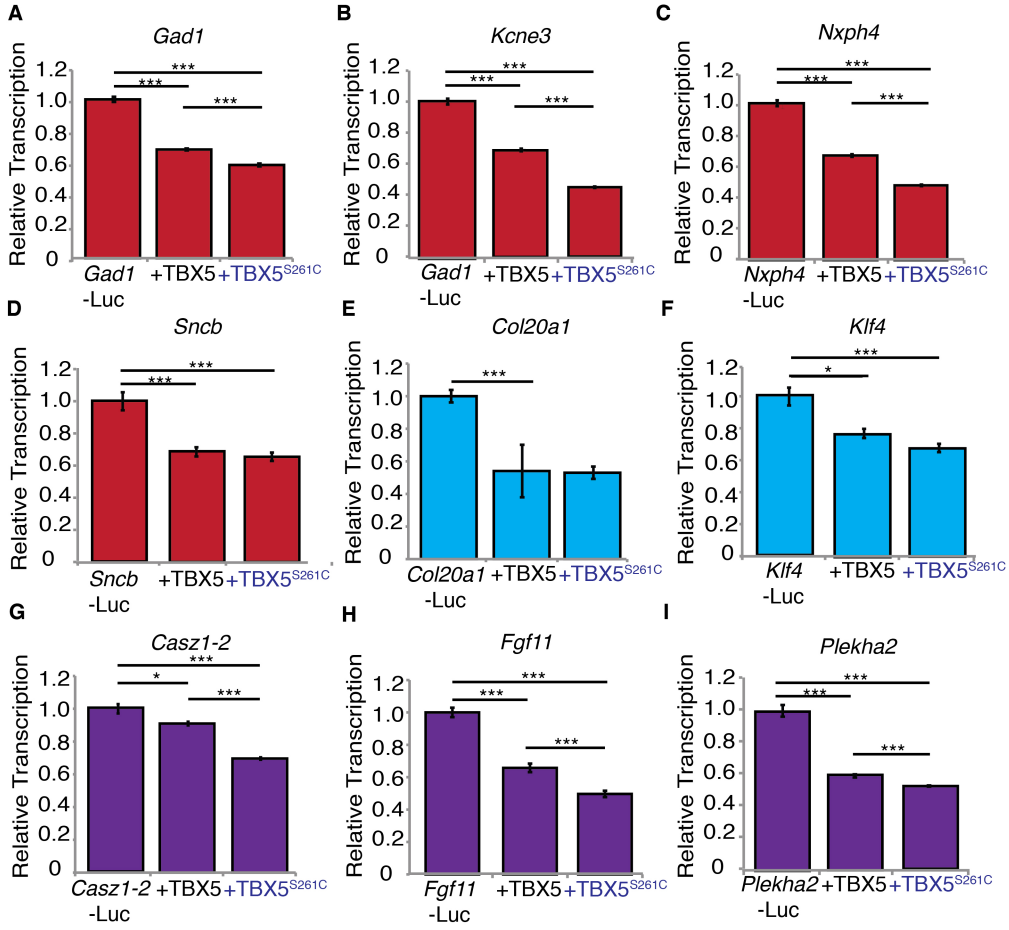

Table S3.1. Spectral counts for TBX5 interacting proteins

Cytoscape Node ID	Input Gene	Description	Protein Length	Complex Annotation	$TBX5^{Avi}$ IP1, Spectral Counts	$TBX5^{Avi}$ IP2, Spectral Counts	$TBX5^{Avi}$, Avg Spectral Counts	$TBX5^{Avi/Avi}$ Negative Control IP, Spectral Counts	$Rosa26^{BirA/BirA}$ Negative Control IP, Spectral Counts
Actl6a	Actl6a	Actin-like protein 6A	429		4	7	6	0	0
Ccar1	Ccar1	Cell division cycle and apoptosis regulator protein 1	1146		11	4	8	0	0
Cdc5l	Cdc5l	Cell division cycle 5-related protein	802		8	33	21	2	0
Cdk9	Cdk9	Cell division protein kinase 9	372		3	8	6	0	0
Chd4	Chd4	Chromodomain-helicase-DNA-binding protein 4	1915	NuRD	18	11	15	0	0
Csnk2a1	Csnk2a1	Casein kinase II subunit alpha	391		13	36	25	8	0
Ctcf	Ctcf	Transcriptional repressor CTCF	736		4	24	14	1	0
Ctnnd1	Ctnnd1	Catenin delta-1	938		2	10	6	1	0
Eif4a3	Eif4a3	Eukaryotic initiation factor 4A-III	411		19	8	14	1	1
Exosc10	Exosc10	Exosome component 10	887		9	7	8	1	0
Gatad2a	Gatad2a	Transcriptional repressor p66 alpha	629	NuRD	2	4	3	0	0
Gatad2b	Gatad2b	Transcriptional repressor p66-beta	594	NuRD	7	14	11	0	0
Hdac2	Hdac2	Histone deacetylase 2	488	NuRD	8	3	6	2	0
Ilk	Ilk	Integrin-linked protein kinase	452		7	30	19	2	0
Larp7	Larp7	La-related protein 7	570		21	20	21	7	2
Mecp2	Mecp2	Methyl-CpG-binding protein 2	484		14	88	51	5	2
Mta1	Mta1	Metastasis-associated protein MTA1	715	NuRD	7	5	6	1	0
Mybbp1a	Mybbp1a	Myb-binding protein 1A	1344		35	383	209	29	0
Ncl	Ncl	Nucleolin	707		3	23	13	0	0
No66	2410016O06Rik	Lysine-specific demethylase NO66	603		10	5	8	2	0
Parp1	Parp1	Poly [ADP-ribose] polymerase 1	1013		8	30	19	0	0
Pelp1	Pelp1	Proline-, glutamic acid- and leucine-rich protein 1	1123		23	25	24	6	0
Prpf6	Prpf6	Pre-mRNA-processing factor 6	941		5	20	13	1	0
Rbbp4	Rbbp4	Histone-binding protein RBBP4	425	NuRD	3	8	6	2	1
Rbbp5	Rbbp5	Retinoblastoma-binding protein 5	538		4	2	3	0	0
Ruvbl2	Ruvbl2	RuvB-like 2	463		3	22	13	0	0
Sltm	Sltm	SAFB-like transcription modulator	1031		9	11	10	0	0
Smarca5	Smarca5	SWI/SNF-related matrix-associated actin-dependent regulator of c	1051		10	46	28	1	0
Smarcc2	Smarcc2	SWI/SNF complex subunit SMARCC2	1213		10	29	20	0	0
Snw1	Snw1	SNW domain-containing protein 1	536		8	3	6	0	0
Ssrp1	Ssrp1	FACT complex subunit SSRP1	708	FACT	3	6	5	0	0
Supt16h	Supt16h	FACT complex subunit SPT16	1047	FACT	13	17	15	3	0
Taf2	Taf2	Transcription initiation factor TFIID subunit 2	1104	TFIID	5	5	5	0	0
Taf4b	Taf4b	Transcription initiation factor TFIID subunit 4	855	TFIID	5	5	5	0	0
Taf5	Taf5	Transcription initiation factor TFIID subunit 5	801	TFIID	10	6	8	3	1
Taf6	Taf6	Transcription initiation factor TFIID subunit 6	678	TFIID	12	6	9	0	1
Tardbp	Tardbp	TAR DNA-binding protein 43	414		5	4	5	0	0
Top1	Top1	DNA topoisomerase 1	767		3	170	87	4	0
Trim28	Trim28	Transcription intermediary factor 1-beta	834		11	47	29	1	1
-	Htatsf1	HIV Tat-specific factor 1 homolog	757		4	23	14	0	0
-	Iws1	Protein IWS1 homolog	766		12	15	14	2	0
-	Khdrbs1	KH domain-containing, RNA-binding, signal transduction-associate	443		7	11	9	3	0
-	Mtdh	Protein LYRIC	579		6	34	20	2	0
-	Nfia	Nuclear factor 1 A-type	532		2	7	5	0	0
-	Nostrin	Nostrin	506		2	17	10	0	0
-	Ptrf	Polymerase I and transcript release factor	392		20	618	319	8	14
-	Rbm14	RNA-binding protein 14	669		15	5	10	2	1
-	Rbm15	Putative RNA-binding protein 15	977		5	14	10	1	0
-	Scaf1	Splicing factor, arginine/serine-rich 19	1256		10	2	6	0	0
-	Stag1	Cohesin subunit SA-1	1258		2	5	4	0	0
-	Tbx5	T-box transcription factor TBX5	518		11	9	10	0	0
-	Tmpo	Lamina-associated polypeptide 2, isoforms beta/delta/epsilon/gar	452		3	24	14	0	0
-	Trim25	E3 ubiquitin/ISG15 ligase TRIM25	634		7	3	5	1	0
-	Zfp326	Zinc finger protein 326	580		14	8	11	0	3
-	Zfp512	Zinc finger protein 512	562		7	29	18	5	1
-	Zfx	Zinc finger X-chromosomal protein	799		3	5	4	0	3
-	Safb	Scaffold attachment factor B1	937		4	2	3	1	1
-	Thoc5	THO complex subunit 5 homolog	683		5	2	4	1	0

Table S3.2. Complete list of genes misregulated in *Tbx5* null hearts

This excel spreadsheet can be found on Frank Conlon's lab website

(http://www.unc.edu/~fconlon/index.htm)

Table S3.3. Complete list of genes misregulated in *Tbx5* null hearts

This excel spreadsheet can be found on Frank Conlon's lab website

(http://www.unc.edu/~fconlon/index.htm)

Table S3.4. Ranked gene list of TBX5-mediated repressed genes for validation. Genes highlighted in orange were cloned and validated by transcriptional assay.

Gene Name	Relative Change in Gene Expression	Peak Start	Peak End	Peak Location	Peak Value	Rank
Sncb	5.01002	54861810	54862049	intron 4	18	1
Nxph4	4.92698	126992730	126992999	intron 1	41	2
Mef2b	4.61428	72682470	72682709	intron 1	27	3
Ndufa4l2	4.58836	126948480	126949559	5' UTR (3kb from TSS)	77	4
Kctd16	4.52734	40416420	40416839	5' UTR (1.5kb from TSS)	17	5
Espn	4.43154	151505580	151505849	intron 1	23	6
Gad1	4.19206	70404180	70404419	intron 1	17	7
Ndrg1	3.84096	66800910	66801839	5' UTR (<1kb from TSS)	86	8
Kcne3	3.63127	107326920	107327249	5' UTR (<1kb from TSS)	23	9
Gipr	3.56164	19751340	19751879	5' UTR (<1kb from TSS)	70	10
Fgf11	3.48673	69614130	69615299	Intron 1	45	11
Rora	3.07638	69137880	69138659	intron 1	42	12
Col20a1	1.95346	180730080	180730289	5' UTR (3kb from TSS)	17	13
Klf4	1.73917	55543110	55543979	exon 3	57, 56	14
Fgf8	1.71411	45819990	45820349	5' UTR (3kb from TSS)	80	15
Fbxl20	1.36908	98010180	98011799	5'UTR/exon1/intron1	25, 56, 30	16
Casz1	1.26372	148178250	148181429	exon/intron 1	60, 29, 43	17
Casz1	1.26372	148209150	148211279	intron 1	32, 22, 18	18
Kcnn2	1.22744	45719130	45719399	exon 1	13	19
Plekha2	1.21231	26211930	26213129	5' UTR (1.2kb from TSS)	49, 33	20
Trim66	4.28947	116634840	116635019	intron 1	17	21
Aldh1l2	3.91811	82996020	82996409	intron 1	23	22
Nags	3.69031	102007440	102007679	5'UTR(<1kb from TSS)	14	23
Guca2b	3.30223	119335590	119335919	5' UTR(4kb from TSS)	23	24
Ier3	3.29257	35958450	35958659	5' UTR(<1kb from TSS)	25	25
Cyp2s1	3.08233	26601510	26602049	5' UTR(<1kb from TSS)	30	26
Unc13a	3.0467	74153250	74153429	5' UTR(<1kb from TSS)	18	27
Egln3	2.96697	55292070	55292549	intron 1	37	28
Tesc	2.85569	118477710	118478819	intron 1	52, 45	29
Lrrc2	2.84378	76552590	76553489	5' UTR(<1kb from TSS)	15, 35	30
Ddit4	2.83727	59414220	59415299	5' UTR(<1kb from TSS)	64	31
Kcnb1	2.81069	167014200	167014649	5' UTR(<1kb from TSS)	17	32
Serpine1	2.80374	137549010	137549309	5' UTR(1kb from TSS)	36	33
Kbtbd11	2.80136	15020880	15021089	5' UTR(6kb from TSS)	34	34
Car9	2.78354	43520910	43521119	intron 1	13	35
Lamb3	2.76341	195127920	195128219	5' UTR(<1kb from TSS)	29	36
Etnk2	2.67908	135261000	135261299	5' UTR(<1kb from TSS)	12	37
Cdsn	2.64553	35686650	35686919	5' UTR(2kb from TSS)	31	38
Vldlr	2.61734	27292020	27292379	intron 1	100	39
Ankrd37	2.59871	47085060	47085419	5' UTR(<1kb from TSS)	36	40
Pltp	2.58051	164682210	164683019	intron 1	27	41
Gfod1	2.56865	43364280	43364759	intron 1	78	42
Lgals3	2.56457	47993280	47993789	5' UTR(<1kb from TSS)	50	43
Lims2	2.55671	32090730	32091329	5' UTR(<1kb from TSS)	30	44
Cyp26a1	2.54431	37772100	37772309	5' UTR(<1kb from TSS)	13	45
Snai3	2.52939	124984470	124985999	5' UTR(<1kb from TSS)	82, 46	46
Trib3	2.52645	152169180	152169989	exon1/intron1	19, 89	47
Sema3g	2.48507	32030850	32031089	5' UTR(<1kb from TSS)	15	48
Ace	2.4802	105828630	105829739	5' UTR(<1kb from TSS)	72	49
Hspa1b	2.47804	35096280	35096699	5' UTR(<1kb from TSS)	37	50

SUPPLEMENTAL EXPERIMENTAL PROCEDURES

Generation of *Tbx5^{Avi}* mice

Genotyping primers for *Tbx5$^{Avi/Avi}$; Rosa26$^{BirA/BirA}$* mice.

Genotyping Primers	Sequence
Wild type *Tbx5*	F: CGGCGTGCCCAGGACCCTGT R: GGCACAGGTCAGCCTTTAGC
Tbx5^{Avi}	F: CGGCGTGCCCAGGACCCTGT R: GCGCGCCTTCGTGCCATTCGA
Sox2-Cre	F: GTCCCCTTCTCCATCTCCAG R: GCAAACGGACAGAAGCATTT
Neo	F: AGGATCTCCTGTCATCTCACCTT R: CTAGAGAATTGATCCCCTCAGAAG
Presence of BirA	F: TTACGCAAGCTGGGTGCAGA R: TTACGCAAGCTGGGTGCAGA
Absence of BirA	F: GTGTAACTGTGGACAGAGGAG R: GAACTTGATGTGTAGACCAGG

Transcriptional assays

TBX5 target gene primers for transcriptional assays.

ChIP cloning PCR Primers	Sequence
Casz1-1	F: ATCGGGTACCTGTCCCTTTCTTCTGTCCCA R: ATCGGGTACCAGGCATAAGATCGCTGGAAA
Casz1-2	F: ATCGGGTACCACCATCCATCCTCGTGTAGC R: ATCGGCTAGCGCCAAAAACAGTGGCCTAAA
Col20a1	F: ATCGGCTAGCATCGAGTGTGTCAGCTGTGG R: ATCGAAGCTTCCGTGGTGCTGTGTTCTTAC
Fbxl20	F: GATCACGCGTGGCCCAAGGAATGGGTACT R: GATCACGCGTCCACAGTCGCCTCTATCGTC
Fgf8	F: CGAGGCTAGCCCAGCTCCCTCCTTCCTTTA R: CGAGGGTACCGGCAGCTTTCTGTCTTGGTT
Fgf11	F: GCACAGATCTGGGACTCCCTAACTGTCGTACC R: GCACACGCGTCCGCTGGAGCTAGTCAGG
Gad1	F: CGAGGGTACCCACTGGAATTCCTACCGTGA R: CGAGGCTAGCCAAGGCGTTCTGGTCTAAGG
Kcne3	F: CGCTACGCGTGTGCCACACAGCTACAATAA R: CGCTCTCGAGTCCGGTGAACACTGCAATAA
Kcnn2	F: GATCGGTACCCTGGTCTCCCTGCAGCTTTA R: GATCGCTACGGTTGTCCTGGCTCTGTTGCT
Kctd16	F: AGGACGCGTTGCTTGTGCAAACTCCAGAC R: GACCAGATCTAGGCAGGGCGACAGATAGAT
Klf4	F: ATCGACGCGTCTTGGCGTGAGGAACTCTCT R: ATCGAGATCTCGCTCAAATGGGCCTCTA
Mef2b-1	F: CGAGGTACCTCTTCTCTCGGACGGACCTA R: CGAGGCTAGCCACACACACTCACGGCTCTC
Mef2b-2	F: CGAGGCTAGCCTGCACAGGGACCCACAG

	R: CGAGGCTAGCCTGCACAGGGACCCACAG
Mef2b-3	F: CGAGGGTACCGCGTGCGATCACCATAACT R: CGAGGCTAGCAGGGGCTGCGATGTAGGT
Nxph-4	F: CGAGGGTACCGCTTGCAGAAGGGTATCTGG R: CGAGGCTAGCTAAGCCTCCAGGCATTCAAC
Plekha2	F: GATCGGTACCTAACTTGGAACCGACCTACG R: GATCGCTAGCTTTCACACCTGAGCGAACTG
Sncb	F: CACGGGTACCTCCCTCCACTGCCTCCAC R: CAGCGCTAGCGCTCCAGGGTCCTCCTAGTC

DNA constructs

Site directed mutagenesis primer pairs. Amino acid changes are represented in bold.

mTBX5^{S252I}	F: GATGTCTCGGATGCAA**ATT**AAAGAGTATCCTGTGGTTC R: GAACCACAGGATACTCTTT**AAT**TTGCATCCGAGACATC
mTBX5^{S261C}	F: GTATCCTGTGGTTCCCAGG**TCG**ACAGTGAGGCACAAAG R: CTTTGTGCCTCACTGT**CGA**CCTGGGAACCACAGGATAC
mTBX5^{V263M}	F: GGTTCCCAGGAGCACA**ATG**AGGCACAAAGTCACCTCC R: GGAGGTGACTTTGTGCCT**CAT**TGTGCTCCTGGGAACC
mTBX5^{K266R}	F: GAGCACAGTGAGGCAC**AGA**GTCACCTCCAACCACAGC R: GCTGTGGTTGGAGGTGAC**TCT**GTGCCTCACTGTGCTC
mTBX5^{Q292R}	F: CAATTTAGGGTCCCAGTAC**CGG**TGTGAGAATGGTGTC R: GACACCATTCTCACA**CCG**GTACTGGGACCCTAAATTG
xTbx5^{K266R}	F: GTCCGTCAG**AGG**GTGTCCTCT R: TGTGCATCTTGGGACTAC

Chromatin IP

Kctd16 intron 1 ChIP-PCR primer sequences

Kctd16 intron 1	F: GTTTCTTGCCTGCACTGCT R: GAAGGAAAAGCAGCCGGGAA

RT-PCR

Primer sequences for NuRD complex members

Chd3	F: AGAAGGAAAACAAGCCAGG R: TTGTGTCCCCCATCCCCTT
Chd4	F: GGGTGAAATGAATCGTGGC R: TTGTGTAGGACTGCATTGGC
Rbbp4	F: ACTGTTGCCTTGTGGGATCT R: AGATCCCAGACATTCAGCCT
Rbbp7	F: GGTGGTTGCTCGAGTTCATA R: GTGGCAATGATGTGAGGATTC
Mta1	F: AGAGCCCACTGGTGCTGAAG R: CATCTACCCCATTGTGCTGC
Mta2	F: GCTCGATCCGACTTCCTAAG R: GTCTCATAGGAACGTTTCACC
Mta3	F: TGAGAATTCCTCCAGCAACCC R: TTAGCATGCTTGTCGGCGAG
Gatad2a	F: GCCCAGTGCTGCCAATAATG R: CAGCGGCATGTGAAGTCTGT
Gatad2b	F: TTACAGCAGCAGGCAGCA R: GCCACCTGGCACAGACAATT
Mbd2/3	F: GGAGAAGAACCCTGGTGTGT R: ACAGGCCTTGTCCAGTGGT

Hdac2	F: ATGAGGCTTCATGGGATGAC R: CATGGCGTACAGTCAAGGAG

REFERENCES

Andrews S. FastQC: a quality control tool for high throughput sequence data. 2010. Available from: http://www.bioinformatics.babraham.ac.uk/projects/fastqc.

Baban, A., Pitto, L., Pulignani, S., Cresci, M., Mariani, L., Gambacciani, C., Digilio, M.C., Pongiglione, G., and Albanese, S. (2014). Holt-Oram syndrome with intermediate atrioventricular canal defect, and aortic coarctation: Functional characterization of a de novo TBX5 mutation. Am J Med Genet A.

Basson, C.T., Bachinsky, D.R., Lin, R.C., Levi, T., Elkins, J.A., Soults, J., Grayzel, D., Kroumpouzou, E., Traill, T.A., Leblanc-Straceski, J.*, et al.* (1997). Mutations in human TBX5 [corrected] cause limb and cardiac malformation in Holt-Oram syndrome. Nat Genet *15*, 30-35.

Basson, C.T., Cowley, G.S., Solomon, S.D., Weissman, B., Poznanski, A.K., Traill, T.A., Seidman, J.G., and Seidman, C.E. (1994). The clinical and genetic spectrum of the Holt-Oram syndrome (heart-hand syndrome). N Engl J Med *330*, 885-891.

Basson, C.T., Huang, T., Lin, R.C., Bachinsky, D.R., Weremowicz, S., Vaglio, A., Bruzzone, R., Quadrelli, R., Lerone, M., Romeo, G.*, et al.* (1999). Different TBX5 interactions in heart and limb defined by Holt-Oram syndrome mutations. Proc Natl Acad Sci U S A *96*, 2919-2924.

Bayer, E.A., and Wilchek, M. (1980). The use of the avidin-biotin complex as a tool in molecular biology. Methods Biochem Anal *26*, 1-45.

Benson, D.W., Basson, C.T., and MacRae, C.A. (1996). New understandings in the genetics of congenital heart disease. Curr Opin Pediatr *8*, 505-511.

Berk, A.J. (1999). Activation of RNA polymerase II transcription. Curr Opin Cell Biol *11*, 330-335.

Bruneau, B.G., Logan, M., Davis, N., Levi, T., Tabin, C.J., Seidman, J.G., and Seidman, C.E. (1999). Chamber-specific cardiac expression of Tbx5 and heart defects in Holt-Oram syndrome. Dev Biol *211*, 100-108.

Bruneau, B.G., Nemer, G., Schmitt, J.P., Charron, F., Robitaille, L., Caron, S., Conner, D.A., Gessler, M., Nemer, M., Seidman, C.E.*, et al.* (2001). A murine model of Holt-Oram syndrome defines roles of the T-box transcription factor Tbx5 in cardiogenesis and disease. Cell *106*, 709-721.

Cline, M.S., Smoot, M., Cerami, E., Kuchinsky, A., Landys, N., Workman, C., Christmas, R., Avila-Campilo, I., Creech, M., Gross, B.*, et al.* (2007). Integration of biological networks and gene expression data using Cytoscape. Nat Protoc *2*, 2366-2382.

Costantini, J.L., Cheung, S.M., Hou, S., Li, H., Kung, S.K., Johnston, J.B., Wilkins, J.A., Gibson, S.B., and Marshall, A.J. (2009). TAPP2 links phosphoinositide 3-kinase signaling to B-cell adhesion through interaction with the cytoskeletal protein utrophin: expression of a novel cell adhesion-promoting complex in B-cell leukemia. Blood *114*, 4703-4712.

Cristea, I.M., Williams, R., Chait, B.T., and Rout, M.P. (2005). Fluorescent proteins as proteomic probes. Mol Cell Proteomics *4*, 1933-1941.

Cross, S.J., Ching, Y.H., Li, Q.Y., Armstrong-Buisseret, L., Spranger, S., Lyonnet, S., Bonnet, D., Penttinen, M., Jonveaux, P., Leheup, B.*, et al.* (2000). The mutation spectrum in Holt-Oram syndrome. J Med Genet *37*, 785-787.

Diez-Roux, G., Banfi, S., Sultan, M., Geffers, L., Anand, S., Rozado, D., Magen, A., Canidio, E., Pagani, M., Peluso, I.*, et al.* (2011). A high-resolution anatomical atlas of the transcriptome in the mouse embryo. PLoS Biol *9*, e1000582.

Dolk, H., Loane, M., and Garne, E. (2010). The prevalence of congenital anomalies in Europe. Adv Exp Med Biol *686*, 349-364.

Dorr, K.M., Amin, N.M., Kuchenbrod, L.M., Labiner, H., Charpentier, M.S., Pevny, L.H., Wessels, A., and Conlon, F.L. (2015). Casz1 is required for cardiomyocyte G1-to-S phase progression during mammalian cardiac development. Development *142*, 2037-2047.

Driegen, S., Ferreira, R., van Zon, A., Strouboulis, J., Jaegle, M., Grosveld, F., Philipsen, S., and Meijer, D. (2005). A generic tool for biotinylation of tagged proteins in transgenic mice. Transgenic Res *14*, 477-482.

Evans, P.M., and Liu, C. (2008). Roles of Krupel-like factor 4 in normal homeostasis, cancer and stem cells. Acta Biochim Biophys Sin (Shanghai) *40*, 554-564.

Fan, C., Duhagon, M.A., Oberti, C., Chen, S., Hiroi, Y., Komuro, I., Duhagon, P.I., Canessa, R., and Wang, Q. (2003a). Novel TBX5 mutations and molecular mechanism for Holt-Oram syndrome. J Med Genet *40*, e29.

Fan, C., Liu, M., and Wang, Q. (2003b). Functional analysis of TBX5 missense mutations associated with Holt-Oram syndrome. J Biol Chem *278*, 8780-8785.

Franceschini, A., Szklarczyk, D., Frankild, S., Kuhn, M., Simonovic, M., Roth, A., Lin, J., Minguez, P., Bork, P., von Mering, C.*, et al.* (2013). STRING v9.1: protein-protein interaction networks, with increased coverage and integration. Nucleic Acids Res *41*, D808-815.

Franklin, S., Zhang, M.J., Chen, H., Paulsson, A.K., Mitchell-Jordan, S.A., Li, Y., Ping, P., and Vondriska, T.M. (2011). Specialized compartments of cardiac nuclei exhibit distinct proteomic anatomy. Mol Cell Proteomics *10*, M110 000703.

Goetz, S.C., Brown, D.D., and Conlon, F.L. (2006). TBX5 is required for embryonic cardiac cell cycle progression. Development *133*, 2575-2584.

Hayashi, S., Lewis, P., Pevny, L., and McMahon, A.P. (2002). Efficient gene modulation in mouse epiblast using a Sox2Cre transgenic mouse strain. Mech Dev *119 Suppl 1*, S97-S101.

He, A., Kong, S.W., Ma, Q., and Pu, W.T. (2011). Co-occupancy by multiple cardiac transcription factors identifies transcriptional enhancers active in heart. Proc Natl Acad Sci U S A *108*, 5632-5637.

Heinritz, W., Shou, L., Moschik, A., and Froster, U.G. (2005). The human TBX5 gene mutation database. Hum Mutat *26*, 397.

Heinz, S., Benner, C., Spann, N., Bertolino, E., Lin, Y.C., Laslo, P., Cheng, J.X., Murre, C., Singh, H., and Glass, C.K. (2010). Simple combinations of lineage-determining transcription factors prime cis-regulatory elements required for macrophage and B cell identities. Mol Cell *38*, 576-589.

Heron, M., and Tejada-Vera, B. (2009). Deaths: leading causes for 2005. Natl Vital Stat Rep *58*, 1-97.

Hoffmann, A.D., Yang, X.H., Burnicka-Turek, O., Bosman, J.D., Ren, X., Steimle, J.D., Vokes, S.A., McMahon, A.P., Kalinichenko, V.V., and Moskowitz, I.P. (2014). Foxf genes integrate tbx5 and hedgehog pathways in the second heart field for cardiac septation. PLoS Genet *10*, e1004604.

Holt, M., and Oram, S. (1960). Familial heart disease with skeletal malformations. Br Heart J *22*, 236-242.

Hu, S., Li, L., Yeh, S., Cui, Y., Li, X., Chang, H.C., Jin, J., and Chang, C. (2015). Infiltrating T cells promote prostate cancer metastasis via modulation of FGF11-->miRNA-541-->androgen receptor (AR)-->MMP9 signaling. Mol Oncol *9*, 44-57.

Huang, C.C., Tu, S.H., Lien, H.H., Jeng, J.Y., Huang, C.S., Huang, C.J., Lai, L.C., and Chuang, E.Y. (2013). Concurrent gene signatures for han chinese breast cancers. PLoS One *8*, e76421.

Huang da, W., Sherman, B.T., and Lempicki, R.A. (2009). Systematic and integrative analysis of large gene lists using DAVID bioinformatics resources. Nat Protoc *4*, 44-57.

Ieda, M., Fu, J.D., Delgado-Olguin, P., Vedantham, V., Hayashi, Y., Bruneau, B.G., and Srivastava, D. (2010). Direct reprogramming of fibroblasts into functional cardiomyocytes by defined factors. Cell *142*, 375-386.

Kaltenbrun, E., Greco, T.M., Slagle, C.E., Kennedy, L.M., Li, T., Cristea, I.M., and Conlon, F.L. (2013). A Gro/TLE-NuRD corepressor complex facilitates Tbx20-dependent transcriptional repression. J Proteome Res *12*, 5395-5409.

Kehle, J., Beuchle, D., Treuheit, S., Christen, B., Kennison, J.A., Bienz, M., and Muller, J. (1998). dMi-2, a hunchback-interacting protein that functions in polycomb repression. Science *282*, 1897-1900.

Keller, A., Nesvizhskii, A.I., Kolker, E., and Aebersold, R. (2002). Empirical statistical model to estimate the accuracy of peptide identifications made by MS/MS and database search. Anal Chem *74*, 5383-5392.

Kim, D., Pertea, G., Trapnell, C., Pimentel, H., Kelley, R., and Salzberg, S.L. (2013). TopHat2: accurate alignment of transcriptomes in the presence of insertions, deletions and gene fusions. Genome Biol *14*, R36.

Kim, J., Cantor, A.B., Orkin, S.H., and Wang, J. (2009). Use of in vivo biotinylation to study protein-protein and protein-DNA interactions in mouse embryonic stem cells. Nat Protoc *4*, 506-517.

Kimura, R., Kasamatsu, A., Koyama, T., Fukumoto, C., Kouzu, Y., Higo, M., Endo-Sakamoto, Y., Ogawara, K., Shiiba, M., Tanzawa, H.*, et al.* (2013). Glutamate acid decarboxylase 1 promotes metastasis of human oral cancer by beta-catenin translocation and MMP7 activation. BMC Cancer *13*, 555.

Krebs, S., Fischaleck, M., and Blum, H. (2009). A simple and loss-free method to remove TRIzol contaminations from minute RNA samples. Anal Biochem *387*, 136-138.

Langmead, B., Trapnell, C., Pop, M., and Salzberg, S.L. (2009). Ultrafast and memory-efficient alignment of short DNA sequences to the human genome. Genome Biol *10*, R25.

Lassmann, T., Hayashizaki, Y., and Daub, C.O. (2009). TagDust--a program to eliminate artifacts from next generation sequencing data. Bioinformatics *25*, 2839-2840.

Li, H., Handsaker, B., Wysoker, A., Fennell, T., Ruan, J., Homer, N., Marth, G., Abecasis, G., and Durbin, R. (2009). The Sequence Alignment/Map format and SAMtools. Bioinformatics *25*, 2078-2079.

Li, Q.Y., Newbury-Ecob, R.A., Terrett, J.A., Wilson, D.I., Curtis, A.R., Yi, C.H., Gebuhr, T., Bullen, P.J., Robson, S.C., Strachan, T.*, et al.* (1997). Holt-Oram syndrome is caused by mutations in TBX5, a member of the Brachyury (T) gene family. Nat Genet *15*, 21-29.

Liu, Z., Yang, X., Li, Z., McMahon, C., Sizer, C., Barenboim-Stapleton, L., Bliskovsky, V., Mock, B., Ried, T., London, W.B.*, et al.* (2011). CASZ1, a

candidate tumor-suppressor gene, suppresses neuroblastoma tumor growth through reprogramming gene expression. Cell Death Differ *18*, 1174-1183.

Maine, G.N., Li, H., Zaidi, I.W., Basrur, V., Elenitoba-Johnson, K.S., and Burstein, E. (2010). A bimolecular affinity purification method under denaturing conditions for rapid isolation of a ubiquitinated protein for mass spectrometry analysis. Nat Protoc *5*, 1447-1459.

McDermott, D.A., Bressan, M.C., He, J., Lee, J.S., Aftimos, S., Brueckner, M., Gilbert, F., Graham, G.E., Hannibal, M.C., Innis, J.W.*, et al.* (2005). TBX5 genetic testing validates strict clinical criteria for Holt-Oram syndrome. Pediatr Res *58*, 981-986.

Metz, M., Gassmann, M., Fakler, B., Schaeren-Wiemers, N., and Bettler, B. (2011). Distribution of the auxiliary GABAB receptor subunits KCTD8, 12, 12b, and 16 in the mouse brain. J Comp Neurol *519*, 1435-1454.

Mori, A.D., and Bruneau, B.G. (2004). TBX5 mutations and congenital heart disease: Holt-Oram syndrome revealed. Curr Opin Cardiol *19*, 211-215.

Morris, C. (2010). Epidemiology of congenital heart disease. In Cardiology, D.J. Crawford MH, Paulus WJ, ed. (Philadelphia, Mosby), pp. 1381-1389.

Moskowitz, I.P., Kim, J.B., Moore, M.L., Wolf, C.M., Peterson, M.A., Shendure, J., Nobrega, M.A., Yokota, Y., Berul, C., Izumo, S.*, et al.* (2007). A molecular pathway including Id2, Tbx5, and Nkx2-5 required for cardiac conduction system development. Cell *129*, 1365-1376.

Moskowitz, I.P., Pizard, A., Patel, V.V., Bruneau, B.G., Kim, J.B., Kupershmidt, S., Roden, D., Berul, C.I., Seidman, C.E., and Seidman, J.G. (2004). The T-Box transcription factor Tbx5 is required for the patterning and maturation of the murine cardiac conduction system. Development *131*, 4107-4116.

Polo, S.E., Kaidi, A., Baskcomb, L., Galanty, Y., and Jackson, S.P. (2010). Regulation of DNA-damage responses and cell-cycle progression by the chromatin remodelling factor CHD4. EMBO J *29*, 3130-3139.

Qian, L., Huang, Y., Spencer, C.I., Foley, A., Vedantham, V., Liu, L., Conway, S.J., Fu, J.D., and Srivastava, D. (2012). In vivo reprogramming of murine cardiac fibroblasts into induced cardiomyocytes. Nature *485*, 593-598.

Roesli, C., Neri, D., and Rybak, J.N. (2006). In vivo protein biotinylation and sample preparation for the proteomic identification of organ- and disease-specific antigens accessible from the vasculature. Nat Protoc *1*, 192-199.

Saunders, A., Werner, J., Andrulis, E.D., Nakayama, T., Hirose, S., Reinberg, D., and Lis, J.T. (2003). Tracking FACT and the RNA polymerase II elongation complex through chromatin in vivo. Science *301*, 1094-1096.

Sedmera, D., and Thompson, R.P. (2011). Myocyte proliferation in the developing heart. Dev Dyn *240*, 1322-1334.

Smallwood, P.M., Munoz-Sanjuan, I., Tong, P., Macke, J.P., Hendry, S.H., Gilbert, D.J., Copeland, N.G., Jenkins, N.A., and Nathans, J. (1996). Fibroblast growth factor (FGF) homologous factors: new members of the FGF family implicated in nervous system development. Proc Natl Acad Sci U S A *93*, 9850-9857.

Sopher, B.L., Koszdin, K.L., McClain, M.E., Myrick, S.B., Martinez, R.A., Smith, A.C., and La Spada, A.R. (2001). Genomic organization, chromosome location, and expression analysis of mouse beta-synuclein, a candidate for involvement in neurodegeneration. Cytogenet Cell Genet *93*, 117-123.

Trapnell, C., Roberts, A., Goff, L., Pertea, G., Kim, D., Kelley, D.R., Pimentel, H., Salzberg, S.L., Rinn, J.L., and Pachter, L. (2012). Differential gene and transcript expression analysis of RNA-seq experiments with TopHat and Cufflinks. Nat Protoc *7*, 562-578.

Trifonov, S., Yamashita, Y., Kase, M., Maruyama, M., and Sugimoto, T. (2014). Glutamic acid decarboxylase 1 alternative splicing isoforms: characterization, expression and quantification in the mouse brain. BMC Neurosci *15*, 114.

van Werven, F.J., and Timmers, H.T. (2006). The use of biotin tagging in Saccharomyces cerevisiae improves the sensitivity of chromatin immunoprecipitation. Nucleic Acids Res *34*, e33.

Wade, P.A., Jones, P.L., Vermaak, D., and Wolffe, A.P. (1998). A multiple subunit Mi-2 histone deacetylase from Xenopus laevis cofractionates with an associated Snf2 superfamily ATPase. Curr Biol *8*, 843-846.

Wang, J., Rao, S., Chu, J., Shen, X., Levasseur, D.N., Theunissen, T.W., and Orkin, S.H. (2006). A protein interaction network for pluripotency of embryonic stem cells. Nature *444*, 364-368.

Wang, S., Sun, H., Ma, J., Zang, C., Wang, C., Wang, J., Tang, Q., Meyer, C.A., Zhang, Y., and Liu, X.S. (2013). Target analysis by integration of transcriptome and ChIP-seq data with BETA. Nat Protoc *8*, 2502-2515.

Wang, W., Kim, H.J., Lee, J.H., Wong, V., Sihn, C.R., Lv, P., Perez Flores, M.C., Mousavi-Nik, A., Doyle, K.J., Xu, Y.*, et al.* (2014). Functional significance of K+ channel beta-subunit KCNE3 in auditory neurons. J Biol Chem *289*, 16802-16813.

Xie, L., Hoffmann, A.D., Burnicka-Turek, O., Friedland-Little, J.M., Zhang, K., and Moskowitz, I.P. (2012). Tbx5-hedgehog molecular networks are essential in the second heart field for atrial septation. Dev Cell *23*, 280-291.

Xue, Y., Wong, J., Moreno, G.T., Young, M.K., Cote, J., and Wang, W. (1998). NURD, a novel complex with both ATP-dependent chromatin-remodeling and histone deacetylase activities. Mol Cell *2*, 851-861.

Ying, C.Y., Dominguez-Sola, D., Fabi, M., Lorenz, I.C., Hussein, S., Bansal, M., Califano, A., Pasqualucci, L., Basso, K., and Dalla-Favera, R. (2013). MEF2B mutations lead to deregulated expression of the oncogene BCL6 in diffuse large B cell lymphoma. Nat Immunol *14*, 1084-1092.

Zhang, Y., Liu, T., Meyer, C.A., Eeckhoute, J., Johnson, D.S., Bernstein, B.E., Nusbaum, C., Myers, R.M., Brown, M., Li, W.*, et al.* (2008). Model-based analysis of ChIP-Seq (MACS). Genome Biol *9*, R137.

CHAPTER 4

DISCUSSION AND FUTURE DIRECTIONS

TBX5 is required for heart development in a number of vertebrates from zebrafish humans (Basson et al., 1997; Bruneau et al., 1999; Bruneau et al., 2001; Garrity et al., 2002; Horb and Thomsen, 1999; Li et al., 1997; Liberatore et al., 2000). TBX5 is one of the first cardiac transcription factors expressed in the developing heart (Basson et al., 1999; Brown et al., 2005; Horb and Thomsen, 1999), and it interacts with other early-expressing cardiac transcription factors like TBX20, GATA4, and NKX2.5 to regulate cardiogenesis (Brown et al., 2005; Garg et al., 2003; Hiroi et al., 2001). TBX5 is required for proper cardiac looping to occur by E9.5 (Bruneau et al., 2001), cell proliferation and differentiation (Fijnvandraat et al., 2003; Goetz et al., 2006; Misra et al., 2014), and subsequent chamber formation (Bruneau et al., 1999; Christoffels et al., 2000; Koshiba-Takeuchi et al., 2009; Liberatore et al., 2000; Rothschild et al., 2009). Later in development, TBX5 is required in the pSHF for the development of the atrial septum (Hoffmann et al., 2014; Horb and Thomsen, 1999; Misra et al., 2014; Xie et al., 2012; Zhou et al., 2015). However, the in vivo molecular mechanisms of TBX5 function are not yet established. This dissertation comprises a set of studies designed to understand the TBX5 *in vivo* protein interaction partners and how the TBX5 interactome leads to

HOS patient defects. These studies were performed in parallel in both *Xenopus* and mouse model systems.

Generation of a TBX5^{Avi} *Xenopus* line

In Chapter 2, I described our caracterization of a novel *Tbx5* enhancer in *Xenopus.* We generated a line of frogs expressing TBX5^{Avi} under the endogenous *Tbx5* enhancer element. I designed a construct containing the *Xenopus* 5' UTR, *Tbx5*^{Avi} coding sequence, *Tbx*5 alternative exon 1b sequence and the *Tbx5* intron 1 sequence. This construct with the enhancer sequence expressed EGFP at the time and place that TBX5 is endogenously expressed in *Xenopus* embryos. The TBX5^{Avi} construct was injected into *Xenopus* embryos at the one cell stage by Restriction Enzyme Mediated Integration (REMI) transgenesis (Amaya and Kroll, 1999), and then the embryos were allowed to reach sexual maturity. Frogs that carried *Tbx5*^{Avi} were backcrossed to wild-type frogs to demonstrate that the construct was transmissible through the germline.

REMI transgenesis has been used extensively for promoter-enhancer analysis, because integration of the transgene into the *Xenopus* genome is random. Therefore, this is an ideal system to characterize enhancers and other cis-regulatory regions. Enhancers and regulatory regions have been identified for a number of cardiac factors, such as *Anf, Cardiac* α*-actinin, Mlc2, Mlc1v, Nkx2-5,* and *Tbx20* (Amaya and Kroll, 1999; Garriock et al., 2005; Latinkić et al., 2004; Latinkić et al., 2002; Mandel et al., 2010; Small and Krieg, 2003; Smith et al., 2005; Smith et al.,

2006; Sparrow et al., 2000). My *in vivo* studies add *Tbx5* to this small list of cardiac factors with known enhancer/regulatory regions in *Xenopus*.

By defining the endogenous enhancer of *Tbx5* we are now able to express $TBX5^{Avi}$ under the control of this element. This tool provides us with a unique opportunity to isolate endogenous TBX5 protein in vivo. However, $TBX5^{Avi}$ is not currently biotinylated endogenously in this line of frogs. Instead, we can perform microinjections of *BirA* mRNA into developing embryos to biotinylate TBX5 in the current generation of frogs. We have since established a *Xenopus* line that ubiquitously expresses the BirA enzyme, and we will cross these lines together to generate a $Tbx5^{Avi}$*; BirA* line with endogenously biotinylated TBX5.

Having biotinylated TBX5 in vivo, we could isolate TBX5 protein complexes using steptavidin-coated beads (Chapter 3). We would then conduct similar proteomics experiments to answer a number of questions about the role of TBX5 in cardiogenesis. We could determine the TBX5 interactome in IP, identify novel TBX5 target genes using ChIP, and determine a new mechanism for TBX5 in the developing heart. More excitingly, we can use the *Xenopus* line to do a comparative analysis of the mouse and *Xenopus* proteomes to determine a role for TBX5 in ventricular septation. The developing mouse and *Xenopus* hearts have critical differences, and a comparative proteomics analysis could illuminate those differences. In both organisms, the heart begins as two bilateral patches of mesoderm that migrate to the ventral midline from the anterior of the embryo and fuse to form the cardiac crescent (Dale and Slack, 1987; Lawson et al., 1991; Moody, 1987; Parameswaran and Tam, 1995; Sater and Jacobson, 1989; Tam et

al., 1997). The cardiac crescent fuses to form a linear heart tube, which undergoes looping to form the developing chambers (de Boer et al., 2012; Kolker et al., 2000; Mohun et al., 2000; Moorman et al., 2003). However, the *Xenopus* heart only has three chambers (two atria and a ventricle) while the mouse heart has a four-chambered heart (two atria and two ventricles)(Mohun et al., 2000; Moorman et al., 2003). TBX5 is expressed predominantly in the left ventricle, and its expression pattern boundary with TBX20 has been shown to be required for formation of the ventricular septum in the four-chambered chick heart (Liberatore et al., 2000; Takeuchi et al., 2003). Therefore, we hypothesize that some differences in the TBX5 proteome between the mouse and *Xenopus* may be proteins that are required for ventricular septation.

We could further utilize this *Xenopus* line to determine the role of phosphorylation in TBX5 regulation. By isolating endogenous TBX5, we could determine whether TBX5 is phosphorylated in the adult heart. Furthermore, we could generate a T278 mutation in TBX5^{Avi} using gene editing in the *Tbx5*^{Avi} line. Our lab has generated mutations in *Xenopus* using Transcription Activator-like Effector nucleases (TALENs) (Boch et al., 2009; Moscou and Bogdanove, 2009). Classical genetic experiments are not normally performed in *Xenopus* because of the ploidy; *Xenopus laevis* is a pseudotetraploid. However, gene editing using TALENs can target multiple alleles. Assuming characterization of the number of transgene insertions, one could utilize gene editing to introduce the T278A point mutation by altering the sequence in the *Tbx5*^{Avi} line and conduct quantitative proteomics analysis to determine the interactions that are ablated by this point mutation.

The TBX5-NuRD complex interaction

In Chapter 3 we established that TBX5 and the NuRD complex interact in both the adult and the E9.5 heart. We demonstrated that TBX5 acts to repress gene transcription in both a NuRD-dependent and NuRD-independent manner, providing a novel role for TBX5 in cardiogenesis. We show that the TBX5-NuRD interaction is required for septation, and correlate TBX5 genotypes that ablate the NuRD interaction to the AVSD phenotype. In light of these findings, several exciting future directions are described below.

The roles of TBX5 and TBX5-NuRD in the adult heart

We conducted proteomics analysis of TBX5 complexes in the hearts of 4 week old mice, but we characterized the role of the TBX5-NuRD complex in the developing heart at E9.5. It is likely that TBX5-NuRD acts via a different mechanism in the adult heart than in the developing heart. TBX5 is required for the formation of the cardiac conduction system (Bruneau et al., 2001; Moskowitz et al., 2007; Moskowitz et al., 2004), but GWAS studies of conduction system function have shown TBX5 to be associated with PR- and/or QRS- interval variation in humans, suggesting that TBX5 is required in the adult heart to maintain proper conduction system function (Holm et al., 2010; Pfeufer et al., 2010; Smith et al., 2011; Sotoodehnia et al., 2010). Furthermore, removal of TBX5 from the mature ventricular conduction system using the *minKCreER*^{T2} driver results in a slowing of conduction system activity, arrhythmia, and sudden death within 5 weeks. Arnolds et al demonstrated that TBX5 drives the expression of *Scn5a* to regulate the cardiac

conduction system function (Arnolds et al., 2012), but further analysis of the adult heart and adult conduction system could provide additional information about the mechanism of TBX5 function in the adult heart. As an example, we could utilize the *Tbx5*^{Avi} mouse line to determine conduction system-specific interactors and targets of TBX5 by conducting proteomics and ChIP- experiments in dissected conduction system tissues.

TBX5-NuRD in atrial/atrioventricular septation

We demonstrated that interaction between TBX5 and the NuRD complex (*Mta1)* is crucial for atrioventricular septation. Mice that are compound heterozygous for both *Tbx5* and *Mta1* expression display a significantly higher prevalence of AVSD than either heterozygote alone. Furthermore, human patients with mutations in TBX5 that ablate the TBX5 NuRD-interacting domain are significantly more likely to have AVSD. These are the first data to show a correlation between TBX5 genotype and phenotype (Brassington et al., 2003), and the effect of the TBX5-NuRD interaction and septation should be expanded upon.

AVSD is caused by malformation of the AV septal complex. The most prominent structure in this complex is the DMP, which is derived from the SHF (Snarr et al., 2007). The DMP was notably absent in our compound heterozygous mice, suggesting that the interaction between TBX5 and the NuRD complex may occur in the SHF. To further address this question we would need to deplete both *Tbx5* and *Mta1* in the SHF using an *Isl1-Cre* (Yang et al., 2006), or, to look specifically at the posterior SHF, a *Gli1-Cre* (Ahn and Joyner, 2004). These

experiments would begin to define a requirement for the TBX5-NuRD interaction in the SHF as it relates to atrio-ventricular septation.

Phylogenetic analysis of 48 orthologs of TBX5 demonstrates conservation of the NuRD interaction domain in organisms with a septated heart (*Xenopus* to human). Zebrafish have the amino acid substitution K266R, which is a mutation seen in patients with AVSD. When *Xenopus* TBX5 K266 is mutated to arginine, TBX5 can no longer interact with CHD4. Therefore, we conclude that the TBX5-NuRD interaction evolved concurrently with atrial septation. Now that gene editing is possible in *Xenopus*, it would be interesting to generate the K266R mutation to determine the effect on septation. This would further validate the importance of the TBX5-NuRD interaction and the requirement for this interaction in septation.

The role of the NuRD complex in cardiac development

Our data demonstrate that the TBX5-NuRD complex is required for proper atrio-ventricular septation. Our lab has further demonstrated that a NuRD/Gro/TLE complex interacts with TBX20 and this interaction is important for cardiac development (Kaltenbrun et al., 2013). Recently, other labs have demonstrated that the NuRD complex interacts with other factors such as BAF250a (Singh and Archer, 2014) and FOG2 (Garnatz et al., 2014; Roche et al., 2008) in the heart to regulate cardiogenesis. However, the exact requirement of the NuRD complex in cardiogenesis remains unknown.

Toward this end, I initiated a project to determine the role of *Chd4* in the developing heart. I obtained a *Chd4* floxed mouse (Williams et al., 2004) from Katia

Georgopaulos at Harvard University. Depletion of *Chd4* using an *Nkx2.5-Cre (*Moses et al., 2001) mouse results in formation of all four chambers, but the hearts are malformed and lethality occurs by E10.5 (data not shown). This project will be continued by graduate student Caralynn Wilczewski. Currently, she is investigating the cause of embryonic lethality in the myocardial depleted *Chd4*$^{-/-}$ mice. Furthermore, she seeks to determine the role of *Chd4* in the second heart field by depleting *Chd4* in the SHF using an *Isl1-Cre* driver (Yang et al., 2006). These studies will define a requirement for the NuRD complex in the developing heart. Furthremore, the combination of phenotypic and biochemical analyses (e.g. CHD4 ChIP-seq and RNA-seq) will help to discern a mechanism for the NuRD complex in cardiogenesis.

The repression activity of TBX5 and TBX5-NuRD

The overlay of ChIP-seq and RNA-seq data shows that TBX5 acts as both a transcriptional activator and a transcriptional repressor. We validated 11 transcriptional targets that were repressed by TBX5. Overall, these genes are genes misregulated in cancer, and genes required for the development of the neural lineage. It would be interesting to follow up on the role that TBX5 plays in repression of the neural program, potentially by promoting the proper propagation of electrical impulses through the developing heart. As a number of TBX5 repressed target genes (*Kcne3, Kctd16)* are potassium channels, and potassium signaling is required for repolarization of cell membranes after the heart beats (Hu et al., 2014), we hypothesize that misregulation of these channels leads to improper conduction system propagation, a phenotype of HOS patients.

Additionally, we had originally envisioned a model for TBX5 in the regulation of the proper growth and differentiation of cardiomyocytes through repression of those genes misregulated in cancer. TBX5 contributes to regulation of the cell cycle, and interacts with Osr1 to regulate pSHF cell cycle progression. Misregulation of this interaction leads to AVSD (Goetz et al., 2006; Zhou et al., 2015). We observe that about half of the TBX5 repressed target genes are misregulated in cancer, but most of these genes are also required for neurogenesis. As we do not observe misregulation of cell cycle genes (cyclins, Cdks, MCMs) in *Tbx5*$^{-/-}$ embryos, we do not believe that TBX5 represses genes required for proliferation. The two TBX5-repressed "cancer" genes that are unrelated to neurogenesis are *Col20a1* and *Mef2b*. The function of *Col20a1* is currently unknown, but we hypothesize that *Mef2b* repression is important for the cooperative roles of the other MEF2 family members in cardiogenesis. Overexpression analysis of *Mef2b* can address this hypothesis. Therefore, we hypothesize that the role of TBX5 in proliferation, cell cycle, and cancer is likely unrelated to the role of TBX5-mediated repression.

Our data shows that TBX5 acts to repress transcription in combination with the NuRD complex. TBX5 represses the transcriptional targets *Kctd16* and *Mef2b.* In contrast, the S261C HOS point mutant that ablates the TBX5/NuRD interaction, fails to repress these targets. We concluded that TBX5 represses these targets in a NuRD-dependent manner. However, the other nine genes repressed by TBX5 were not repressed in a NuRD-dependent manner. It would be interesting to be able to separate genes repressed by TBX5 alone from those repressed by TBX5-NuRD. We have begun the experiments to answer this question by generating a mouse line that

is depleted of *Chd4* and contains a biotinylated *Tbx5* allele (*Tbx5*$^{Avi/Avi}$; *Rosa26*$^{BirA/BirA}$; *Chd4*$^{fl/fl}$; *Nkx2.5Cre/+)*. We will utilize the *Tbx5*^{Avi} allele to perform TBX5 ChIP-seq experiments in both *Chd4* wild-type and null embryonic hearts to determine the TBX5 targets that are regulated by NuRD dependent and NuRD independent mechanisms.

TBX5 target gene activation versus repression

Given that TBX5 acts to both activate and repress target genes, our studies have created new avenues of research onTBX5. We would like to know how TBX5 can repress certain genes and activate others. While the NuRD complex is generally considered to be a transcriptional repressor complex, NuRD has been found present at active promoters as well (Shimbo et al., 2013), and plays a role in the activating functions of factors like GATA1 and FOG1 (Miccio et al., 2010; Wade et al., 1998; Xue et al., 1998; Zhang et al., 1998). To address this question, we performed a genome-wide bioinformatics analysis of target genes both activated and repressed by TBX5. Pathway analysis of genes repressed by TBX5 implicates several pathways involved in cancer, which is consistent with our earlier findings. We also performed a binding motif analysis of our activated and repressed gene sets. We found the TBX5 motif present in approximately 50% of the ChIP peaks for both gene sets. These data suggest that there may be an alternate motif or an alternate, indirect mechanism for TBX5-dependent regulation of genes that do not have a TBX5-binding motif.

To uncover alternative motifs present in the TBX5 data sets we performed motif enrichment analysis (Figure 4.1.) We found multiple motifs present in genes activated by TBX5: *Rela*, a gene in the NFκB complex (*NfκB3/NfκB-65*) involved in cancer (Gannon et al., 2013; Gao and Zhang, 2015; Kochupurakkal et al., 2015; Koh et al., 2015; Liu and Brown, 2012; Pyo et al., 2013; Trecca et al., 1997), *Egr3,* a gene involved in muscle development and muscle innervation (Chen et al., 2002; Li et al., 2011; Tourtellotte et al., 2001; Tourtellotte and Milbrandt, 1998), *Rhox11*, a homeobox gene with no known function, and *Ctcf*, a gene responsible for chromatin looping (Guo et al., 2012; Junier et al., 2012; Rao et al., 2014; Sanyal et al., 2012; Splinter et al., 2006; Tark-Dame et al., 2014). We also found multiple motifs present in genes repressed by TBX5: *Hic1,* a gene involved in tumor suppression, methylation and cancer (Chen et al., 2005; Cheng et al., 2014; Dehennaut et al., 2013; Lindsey et al., 2004; Svedlund et al., 2012; Yu et al., 2011; Zhang et al., 2010; Zheng et al., 2013)*, Uncx,* a homeobox transcription factor involved in the proliferation of neural progenitor cells (Sammeta et al., 2010)*, Hnf4a*, a liver-expressed nuclear receptor and endoderm marker (Dean et al., 2010) and *Pax7,* a satellite cell marker in skeletal muscle development (Joung et al., 2014; Knappe et al., 2015; von Maltzahn et al., 2013; Zammit et al., 2006) and important factor for neural crest development (Murdoch et al., 2012; Vadasz et al., 2013). Figure 4.2 depicts an example of these other binding motifs relative to the TBX5 motif in a TBX5-activated (*Scn5a*) (Figure 4.2A) and a TBX5-repressed (*Kctd16*) (Figure 4.2B) gene.

The presence of these other factors near TBX5 binding motifs may work in concert to activate or repress gene transcription (Figure 4.3A). However, it is also possible that the presence of TBX5 at its target genes may rearrange the chromatin structure so that these other factors cannot bind to the target genes (Figure 4.3B). We hypothesize that, while either possibility may be correct, it is specific to the binding factor. To address this question, we could overlay previously published ChIP-seq data from each of the other binding factors on the TBX5 ChIP-seq results and look for other binding factors that are present at the TBX5 target genes. Ideally, the ChIP-seq data should be from the same or comparable cell line (e.g. HL-1, E9.5 heart). There are ChIP-seq data available for a number of these factors in several different cell types (Table 4.1).

There are also available knockout mice for the genes whose binding sites are next to TBX5 binding sites (Table 4.2). We could breed the $TBX5^{Avi}$ mouse to one of these knockout mouse lines and conduct streptavidin ChIP-seq to determine the effect of TBX5 occupancy in the absence of the other binding protein. The reciprocal experiment could also be completed: ChIP-seq of the other binding protein in a *Tbx5* knockout mouse would determine the effect of gene occupancy in the absence of TBX5. This would begin to address the relationship between TBX5 and the other binding proteins. One could then utilize these knockout mice to determine the effect that this binding mechanism may have on the developing heart. This exciting finding is the beginning of a new project in our laboratory designed to test what makes TBX5 “choose” to activate or repress gene transcription.

Table 4.1. ChIP-seq data available for proteins with binding motifs enriched in TBX5-bound regions.

Motifs in regions activated or repressed by TBX5?	Protein	Tissue Type	Reference/ENCODE
Activated	RelA/p65	Lymphoblast cells	(Kasowski et al., 2010; Satoh, 2014; Zhao et al., 2014)
Activated	RelA/p65	Smooth Muscle cells	(Cookson et al., 2015)
Activated	RelA/p65	Airway epithelial cells	(Yang et al., 2013)
Activated	RelA/p65	HeLa cells	(Rao et al., 2011)
Activated	RelA/p65	TNF stimulated HeLa cells	(Xing et al., 2013)
Activated	RelA/p65	Dendritic cells	(Garber et al., 2012)
Activated	RelA/p65	KB cells	(Jurida et al., 2015)
Activated	RelA/p65	C26 cancer induced muscle	(Cornwell et al., 2014)
Activated	RelA/p65	HEK293 cells	(Lu et al., 2013)
Activated	**CTCF**	**Primary cardiomyocyte**	**ENCSR000DTI**
Activated	CTCF	Skeletal muscle myoblast	ENCSR000ANE
Activated	CTCF	Mouse embryonic fibroblasts (MEFs)	ENCSR000CBW (Gerstein et al., 2012)
Activated	CTCF	Bone Marrow Macrophage	ENCSR000CFJ
Activated	CTCF	HeLa cells, immortalized lymphoblast cells, leukemia cells, ESCs, BMP4 induced ESCs	(Heintzman et al., 2009)
Activated	CTCF	Various tissues (mouse- 8 week): cortical plate, **heart**, thymus, lung, testis, olfactory bulb, cerebellum, kidney, small	ENCSR000CBO, ENCSR000CBI, ENCSR000CDZ, ENCSR000CBV, ENCSR000CDX, ENCSR000CBN, ENCSR000CBY, ENCSR000CBU

		intestine, spleen, liver, brain, limb	ENCSR000CEH
Activated	CTCF	MEL cells	ENCSR000CFH, ENCSR000ETE
Activated	CTCF	Neural cells	ENCSR822CEA
Activated	CTCF	C2C12	ENCSR000AIJ
Activated	CTCF	19 different cell types	(Wang et al., 2012)
Activated	CTCF	Liver (human, macaque, dog, mouse, rat, opossum)	(Schmidt et al., 2012)
Repressed	HNF4α	HepG2 liver cells	(Wallerman et al., 2009) ENCSR000EEU ENCSR000BLF
Repressed	HNF4a	Livers (human, mouse, dog)	(Schmidt et al., 2010)
Repressed	PAX7	Mouse skeletal muscle cell line	(Soleimani et al., 2012)
Repressed	PAX7	Pituitary corticotrope cells (AtT-20)	(Budry et al., 2012)

Table 4.2. Mouse models available for genes that have binding motifs enriched in TBX5-bound regions.

Motifs in regions activated or repressed by TBX5?	Gene	Mouse model available?	Reference
Activated	*RelA/p65*	Yes	(Gao et al., 2015), (Beg et al., 1995)
Activated	*Egr3*	Yes	(Tourtellotte and Milbrandt, 1998)
Activated	*Rhox11*	No	
Activated	*Ctcf*	Yes	(Heath et al., 2008)
Repressed	*Hic1*	Yes	(Carter et al., 2000)
Repressed	*Uncx*	Yes	(Mansouri et al., 2000)
Repressed	*Hnf4*α	Yes	(Hayhurst et al., 2001; Walesky et al., 2013)
Repressed	*Pax7*	Yes	(Mansouri et al., 1996)

Figure 4.1. Identification of differential motifs in TBX5 activated genes vs repressed genes. TBX5 peaks associated with differentially regulated genes were also analyzed for motif enrichment using HOMER (Heinz et al., 2010). Differential motif enrichment at regions associated with activated genes (left) and repressed genes (right).

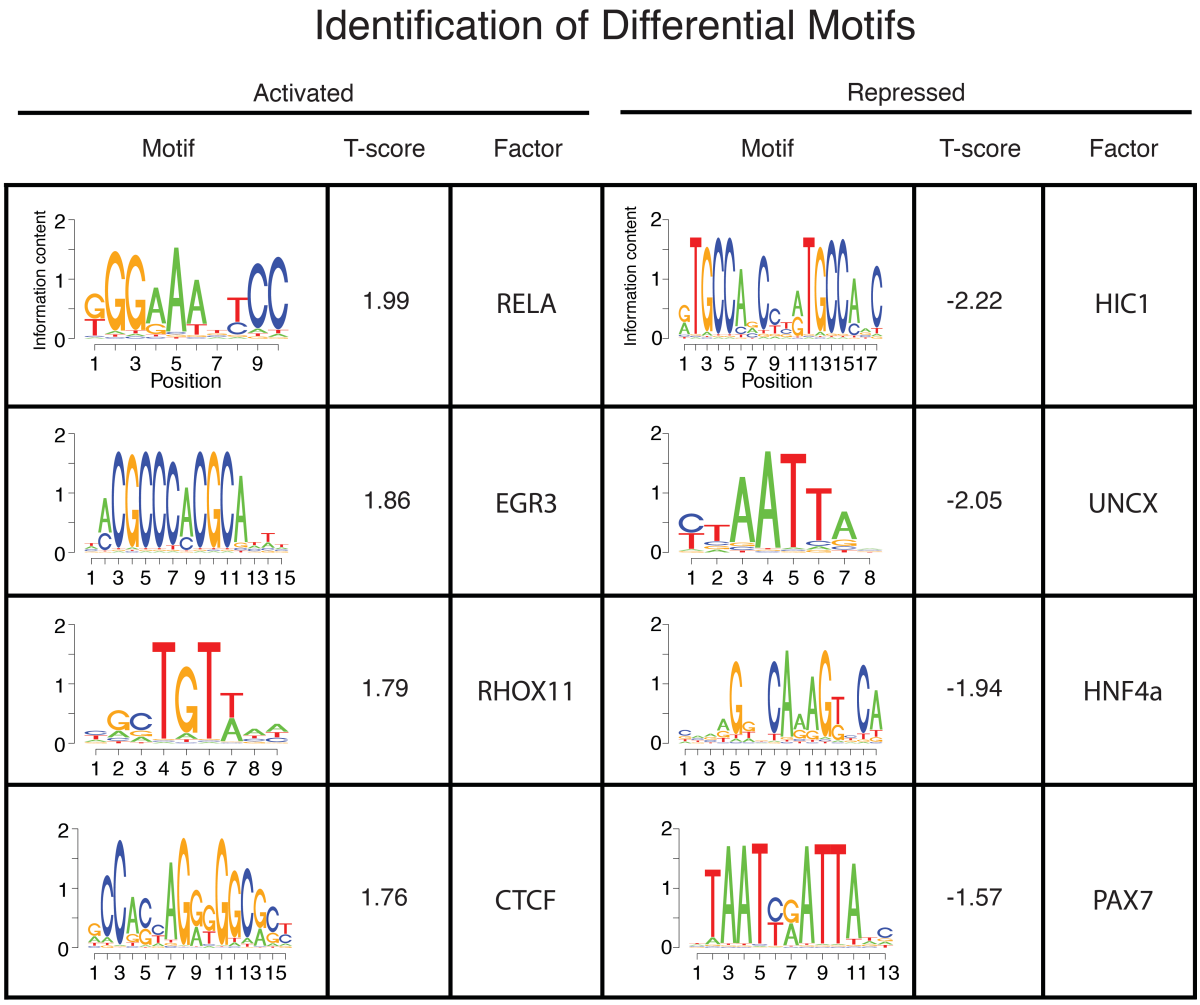

Figure 4.2. Presence of alternative binding motifs in TBX5 bound genes. (A) *(Top)* Schematic of the TBX5-activated target gene *Scn5a* ChIP-peak element. Binding sites for EGR3 (blue), CTCF (brown), TBX5 (orange), RHOX11 (green), and RELA (beige) are depicted. *(Bottom)* Sequence specific binding motifs in the *Scn5a* element. **(B)** *(Top)* Schematic of the TBX5-repressed target gene *Kctd16* ChIP-peak element. Binding sites for HIC1 (light blue), PAX7 (purple), and TBX5 (orange) are depicted. *(Bottom)* Sequence specific binding motifs in the *Kctd16* element. Motif sequences were identified using the Motif-based interval screener with PSSM Cistrome Analysis Pipeline (Liu et al., 2011)

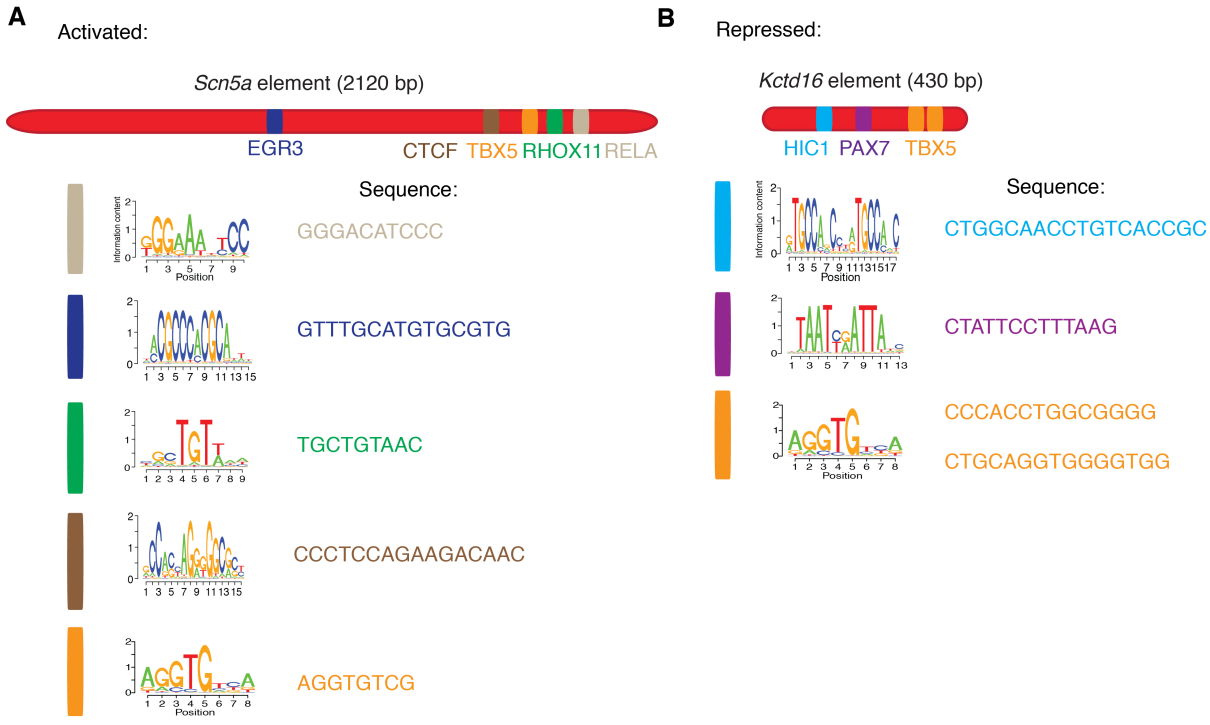

Figure 4.3. Possible mechanisms of TBX5 regulation of target genes. (A) The presence of these other factors (EGR3 in this example) near TBX5 binding motifs may combinatorially activate or repress gene transcription. **(B)** It is also possible that the presence of TBX5 at its target genes may rearrange the chromatin structure so that these other factors cannot bind to the target genes.

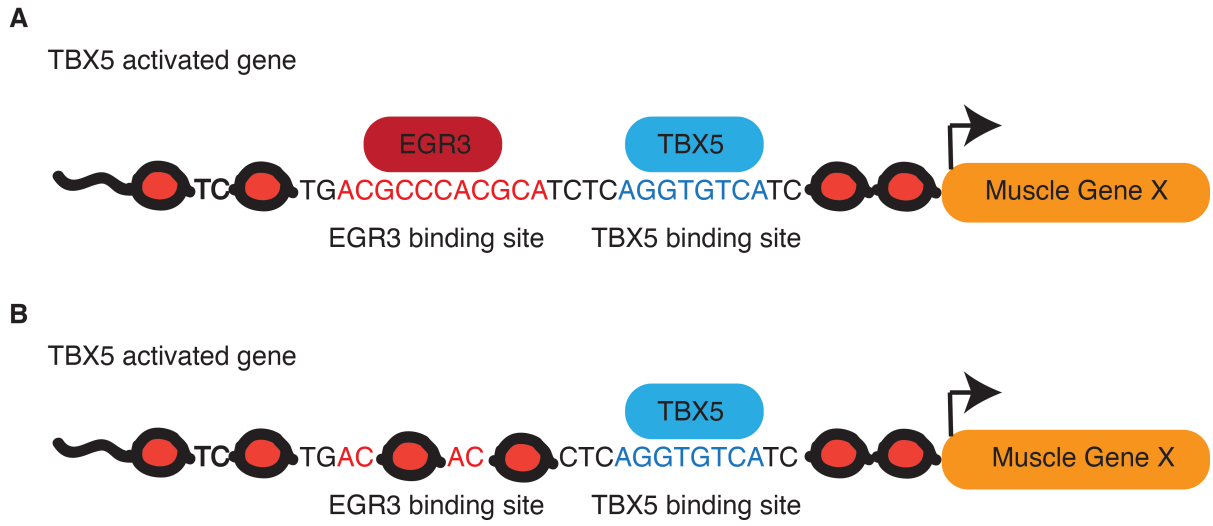

REFERENCES

Ahn, S., and Joyner, A.L. (2004). Dynamic changes in the response of cells to positive hedgehog signaling during mouse limb patterning. Cell *118*, 505-516.

Amaya, E., and Kroll, K.L. (1999). A method for generating transgenic frog embryos. Methods Mol Biol *97*, 393-414.

Arnolds, D.E., Liu, F., Fahrenbach, J.P., Kim, G.H., Schillinger, K.J., Smemo, S., McNally, E.M., Nobrega, M.A., Patel, V.V., and Moskowitz, I.P. (2012). TBX5 drives Scn5a expression to regulate cardiac conduction system function. J Clin Invest *122*, 2509-2518.

Basson, C.T., Bachinsky, D.R., Lin, R.C., Levi, T., Elkins, J.A., Soults, J., Grayzel, D., Kroumpouzou, E., Traill, T.A., Leblanc-Straceski, J.*, et al.* (1997). Mutations in human TBX5 [corrected] cause limb and cardiac malformation in Holt-Oram syndrome. Nat Genet *15*, 30-35.

Basson, C.T., Huang, T., Lin, R.C., Bachinsky, D.R., Weremowicz, S., Vaglio, A., Bruzzone, R., Quadrelli, R., Lerone, M., Romeo, G.*, et al.* (1999). Different TBX5 interactions in heart and limb defined by Holt-Oram syndrome mutations. Proc Natl Acad Sci U S A *96*, 2919-2924.

Beg, A.A., Sha, W.C., Bronson, R.T., Ghosh, S., and Baltimore, D. (1995). Embryonic lethality and liver degeneration in mice lacking the RelA component of NF-kappa B. Nature *376*, 167-170.

Boch, J., Scholze, H., Schornack, S., Landgraf, A., Hahn, S., Kay, S., Lahaye, T., Nickstadt, A., and Bonas, U. (2009). Breaking the code of DNA binding specificity of TAL-type III effectors. Science *326*, 1509-1512.

Brassington, A.M., Sung, S.S., Toydemir, R.M., Le, T., Roeder, A.D., Rutherford, A.E., Whitby, F.G., Jorde, L.B., and Bamshad, M.J. (2003). Expressivity of Holt-Oram syndrome is not predicted by TBX5 genotype. Am J Hum Genet *73*, 74-85.

Brown, D.D., Martz, S.N., Binder, O., Goetz, S.C., Price, B.M., Smith, J.C., and Conlon, F.L. (2005). Tbx5 and Tbx20 act synergistically to control vertebrate heart morphogenesis. Development *132*, 553-563.

Bruneau, B.G., Logan, M., Davis, N., Levi, T., Tabin, C.J., Seidman, J.G., and Seidman, C.E. (1999). Chamber-specific cardiac expression of Tbx5 and heart defects in Holt-Oram syndrome. Dev Biol *211*, 100-108.

Bruneau, B.G., Nemer, G., Schmitt, J.P., Charron, F., Robitaille, L., Caron, S., Conner, D.A., Gessler, M., Nemer, M., Seidman, C.E.*, et al.* (2001). A murine model of Holt-Oram syndrome defines roles of the T-box transcription factor Tbx5 in cardiogenesis and disease. Cell *106*, 709-721.

Budry, L., Balsalobre, A., Gauthier, Y., Khetchoumian, K., L'Honore, A., Vallette, S., Brue, T., Figarella-Branger, D., Meij, B., and Drouin, J. (2012). The selector gene Pax7 dictates alternate pituitary cell fates through its pioneer action on chromatin remodeling. Genes Dev *26*, 2299-2310.

Carter, M.G., Johns, M.A., Zeng, X., Zhou, L., Zink, M.C., Mankowski, J.L., Donovan, D.M., and Baylin, S.B. (2000). Mice deficient in the candidate tumor suppressor gene Hic1 exhibit developmental defects of structures affected in the Miller-Dieker syndrome. Hum Mol Genet *9*, 413-419.

Chen, H.H., Tourtellotte, W.G., and Frank, E. (2002). Muscle spindle-derived neurotrophin 3 regulates synaptic connectivity between muscle sensory and motor neurons. J Neurosci *22*, 3512-3519.

Chen, W.Y., Wang, D.H., Yen, R.C., Luo, J., Gu, W., and Baylin, S.B. (2005). Tumor suppressor HIC1 directly regulates SIRT1 to modulate p53-dependent DNA-damage responses. Cell *123*, 437-448.

Cheng, G., Sun, X., Wang, J., Xiao, G., Wang, X., Fan, X., Zu, L., Hao, M., Qu, Q., Mao, Y.*, et al.* (2014). HIC1 silencing in triple-negative breast cancer drives progression through misregulation of LCN2. Cancer Res *74*, 862-872.

Christoffels, V.M., Habets, P.E., Franco, D., Campione, M., de Jong, F., Lamers, W.H., Bao, Z.Z., Palmer, S., Biben, C., Harvey, R.P.*, et al.* (2000). Chamber formation and morphogenesis in the developing mammalian heart. Dev Biol *223*, 266-278.

Cookson, V.J., Waite, S.L., Heath, P.R., Hurd, P.J., Gandhi, S.V., and Chapman, N.R. (2015). Binding loci of RelA-containing nuclear factor-kappaB dimers in promoter regions of PHM1-31 myometrial smooth muscle cells. Mol Hum Reprod *21*, 865-883.

Cornwell, E.W., Mirbod, A., Wu, C.L., Kandarian, S.C., and Jackman, R.W. (2014). C26 cancer-induced muscle wasting is IKKbeta-dependent and NF-kappaB-independent. PLoS One *9*, e87776.

Dale, L., and Slack, J.M. (1987). Fate map for the 32-cell stage of Xenopus laevis. Development *99*, 527-551.

de Boer, B.A., van den Berg, G., de Boer, P.A., Moorman, A.F., and Ruijter, J.M. (2012). Growth of the developing mouse heart: an interactive qualitative and quantitative 3D atlas. Dev Biol *368*, 203-213.

Dean, S., Tang, J.I., Seckl, J.R., and Nyirenda, M.J. (2010). Developmental and tissue-specific regulation of hepatocyte nuclear factor 4-alpha (HNF4-alpha) isoforms in rodents. Gene Expr *14*, 337-344.

Dehennaut, V., Loison, I., Boulay, G., Van Rechem, C., and Leprince, D. (2013). Identification of p21 (CIP1/WAF1) as a direct target gene of HIC1 (Hypermethylated In Cancer 1). Biochem Biophys Res Commun *430*, 49-53.

Fijnvandraat, A.C., Lekanne Deprez, R.H., Christoffels, V.M., Ruijter, J.M., and Moorman, A.F. (2003). TBX5 overexpression stimulates differentiation of chamber myocardium in P19C16 embryonic carcinoma cells. J Muscle Res Cell Motil *24*, 211-218.

Gannon, P.O., Lessard, L., Stevens, L.M., Forest, V., Begin, L.R., Minner, S., Tennstedt, P., Schlomm, T., Mes-Masson, A.M., and Saad, F. (2013). Large-scale independent validation of the nuclear factor-kappa B p65 prognostic biomarker in prostate cancer. Eur J Cancer *49*, 2441-2448.

Gao, H., and Zhang, Z. (2015). Systematic Analysis of Endometrial Cancer-Associated Hub Proteins Based on Text Mining. Biomed Res Int *2015*, 615825.

Gao, Z., Zhang, J., Henagan, T.M., Lee, J.H., Ye, X., Wang, H., and Ye, J. (2015). P65 inactivation in adipocytes and macrophages attenuates adipose inflammatory response in lean but not in obese mice. Am J Physiol Endocrinol Metab *308*, E496-505.

Garber, M., Yosef, N., Goren, A., Raychowdhury, R., Thielke, A., Guttman, M., Robinson, J., Minie, B., Chevrier, N., Itzhaki, Z.*, et al.* (2012). A high-throughput

chromatin immunoprecipitation approach reveals principles of dynamic gene regulation in mammals. Mol Cell *47*, 810-822.

Garg, V., Kathiriya, I.S., Barnes, R., Schluterman, M.K., King, I.N., Butler, C.A., Rothrock, C.R., Eapen, R.S., Hirayama-Yamada, K., Joo, K.*, et al.* (2003). GATA4 mutations cause human congenital heart defects and reveal an interaction with TBX5. Nature *424*, 443-447.

Garnatz, A.S., Gao, Z., Broman, M., Martens, S., Earley, J.U., and Svensson, E.C. (2014). FOG-2 mediated recruitment of the NuRD complex regulates cardiomyocyte proliferation during heart development. Dev Biol *395*, 50-61.

Garriock, R.J., Meadows, S.M., and Krieg, P.A. (2005). Developmental expression and comparative genomic analysis of Xenopus cardiac myosin heavy chain genes. Dev Dyn *233*, 1287-1293.

Garrity, D.M., Childs, S., and Fishman, M.C. (2002). The heartstrings mutation in zebrafish causes heart/fin Tbx5 deficiency syndrome. Development *129*, 4635-4645.

Gerstein, M.B., Kundaje, A., Hariharan, M., Landt, S.G., Yan, K.K., Cheng, C., Mu, X.J., Khurana, E., Rozowsky, J., Alexander, R.*, et al.* (2012). Architecture of the human regulatory network derived from ENCODE data. Nature *489*, 91-100.

Goetz, S.C., Brown, D.D., and Conlon, F.L. (2006). TBX5 is required for embryonic cardiac cell cycle progression. Development *133*, 2575-2584.

Guo, Y., Monahan, K., Wu, H., Gertz, J., Varley, K.E., Li, W., Myers, R.M., Maniatis, T., and Wu, Q. (2012). CTCF/cohesin-mediated DNA looping is required for protocadherin alpha promoter choice. Proc Natl Acad Sci U S A *109*, 21081-21086.

Hayhurst, G.P., Lee, Y.H., Lambert, G., Ward, J.M., and Gonzalez, F.J. (2001). Hepatocyte nuclear factor 4alpha (nuclear receptor 2A1) is essential for maintenance of hepatic gene expression and lipid homeostasis. Mol Cell Biol *21*, 1393-1403.

Heath, H., Ribeiro de Almeida, C., Sleutels, F., Dingjan, G., van de Nobelen, S., Jonkers, I., Ling, K.W., Gribnau, J., Renkawitz, R., Grosveld, F.*, et al.* (2008). CTCF regulates cell cycle progression of alphabeta T cells in the thymus. EMBO J *27*, 2839-2850.

Heintzman, N.D., Hon, G.C., Hawkins, R.D., Kheradpour, P., Stark, A., Harp, L.F., Ye, Z., Lee, L.K., Stuart, R.K., Ching, C.W.*, et al.* (2009). Histone modifications at human enhancers reflect global cell-type-specific gene expression. Nature *459*, 108-112.

Heinz, S., Benner, C., Spann, N., Bertolino, E., Lin, Y.C., Laslo, P., Cheng, J.X., Murre, C., Singh, H., and Glass, C.K. (2010). Simple combinations of lineage-determining transcription factors prime cis-regulatory elements required for macrophage and B cell identities. Mol Cell *38*, 576-589.

Hiroi, Y., Kudoh, S., Monzen, K., Ikeda, Y., Yazaki, Y., Nagai, R., and Komuro, I. (2001). Tbx5 associates with Nkx2-5 and synergistically promotes cardiomyocyte differentiation. Nat Genet *28*, 276-280.

Hoffmann, A.D., Yang, X.H., Burnicka-Turek, O., Bosman, J.D., Ren, X., Steimle, J.D., Vokes, S.A., McMahon, A.P., Kalinichenko, V.V., and Moskowitz, I.P. (2014). Foxf genes integrate tbx5 and hedgehog pathways in the second heart field for cardiac septation. PLoS Genet *10*, e1004604.

Holm, H., Gudbjartsson, D.F., Arnar, D.O., Thorleifsson, G., Thorgeirsson, G., Stefansdottir, H., Gudjonsson, S.A., Jonasdottir, A., Mathiesen, E.B., Njolstad, I.*, et al.* (2010). Several common variants modulate heart rate, PR interval and QRS duration. Nat Genet *42*, 117-122.

Horb, M.E., and Thomsen, G.H. (1999). Tbx5 is essential for heart development. Development *126*, 1739-1751.

Hu, Z., Crump, S.M., Anand, M., Kant, R., Levi, R., and Abbott, G.W. (2014). Kcne3 deletion initiates extracardiac arrhythmogenesis in mice. FASEB J *28*, 935-945.

Joung, H., Eom, G.H., Choe, N., Lee, H.M., Ko, J.H., Kwon, D.H., Nam, Y.S., Min, H., Shin, S., Kook, J.*, et al.* (2014). Ret finger protein mediates Pax7-induced ubiquitination of MyoD in skeletal muscle atrophy. Cell Signal *26*, 2240-2248.

Junier, I., Dale, R.K., Hou, C., Kepes, F., and Dean, A. (2012). CTCF-mediated transcriptional regulation through cell type-specific chromosome organization in the beta-globin locus. Nucleic Acids Res *40*, 7718-7727.

Jurida, L., Soelch, J., Bartkuhn, M., Handschick, K., Muller, H., Newel, D., Weber, A., Dittrich-Breiholz, O., Schneider, H., Bhuju, S.*, et al.* (2015). The Activation of IL-

1-Induced Enhancers Depends on TAK1 Kinase Activity and NF-kappaB p65. Cell Rep.

Kaltenbrun, E., Greco, T.M., Slagle, C.E., Kennedy, L.M., Li, T., Cristea, I.M., and Conlon, F.L. (2013). A Gro/TLE-NuRD corepressor complex facilitates Tbx20-dependent transcriptional repression. J Proteome Res *12*, 5395-5409.

Kasowski, M., Grubert, F., Heffelfinger, C., Hariharan, M., Asabere, A., Waszak, S.M., Habegger, L., Rozowsky, J., Shi, M., Urban, A.E.*, et al.* (2010). Variation in transcription factor binding among humans. Science *328*, 232-235.

Knappe, S., Zammit, P.S., and Knight, R.D. (2015). A population of Pax7-expressing muscle progenitor cells show differential responses to muscle injury dependent on developmental stage and injury extent. Front Aging Neurosci *7*, 161.

Kochupurakkal, B.S., Wang, Z.C., Hua, T., Culhane, A.C., Rodig, S.J., Rajkovic-Molek, K., Lazaro, J.B., Richardson, A.L., Biswas, D.K., and Iglehart, J.D. (2015). RelA-Induced Interferon Response Negatively Regulates Proliferation. PLoS One *10*, e0140243.

Koh, D.I., An, H., Kim, M.Y., Jeon, B.N., Choi, S.H., Hur, S.S., and Hur, M.W. (2015). Transcriptional activation of APAF1 by KAISO (ZBTB33) and p53 is attenuated by RelA/p65. Biochim Biophys Acta *1849*, 1170-1178.

Kolker, S.J., Tajchman, U., and Weeks, D.L. (2000). Confocal imaging of early heart development in Xenopus laevis. Dev Biol *218*, 64-73.

Koshiba-Takeuchi, K., Mori, A.D., Kaynak, B.L., Cebra-Thomas, J., Sukonnik, T., Georges, R.O., Latham, S., Beck, L., Henkelman, R.M., Black, B.L.*, et al.* (2009). Reptilian heart development and the molecular basis of cardiac chamber evolution. Nature *461*, 95-98.

Latinkić , B.V., Cooper, B., Smith, S., Kotecha, S., Towers, N., Sparrow, D., and Mohun, T.J. (2004). Transcriptional regulation of the cardiac-specific MLC2 gene during Xenopus embryonic development. Development *131*, 669-679.

Latinkić, B.V., Cooper, B., Towers, N., Sparrow, D., Kotecha, S., and Mohun, T.J. (2002). Distinct enhancers regulate skeletal and cardiac muscle-specific expression programs of the cardiac alpha-actin gene in Xenopus embryos. Dev Biol *245*, 57-70.

Lawson, K.A., Meneses, J.J., and Pedersen, R.A. (1991). Clonal analysis of epiblast fate during germ layer formation in the mouse embryo. Development *113*, 891-911.

Li, L., Eldredge, L.C., Quach, D.H., Honasoge, A., Gruner, K., and Tourtellotte, W.G. (2011). Egr3 dependent sympathetic target tissue innervation in the absence of neuron death. PLoS One *6*, e25696.

Li, Q.Y., Newbury-Ecob, R.A., Terrett, J.A., Wilson, D.I., Curtis, A.R., Yi, C.H., Gebuhr, T., Bullen, P.J., Robson, S.C., Strachan, T.*, et al.* (1997). Holt-Oram syndrome is caused by mutations in TBX5, a member of the Brachyury (T) gene family. Nat Genet *15*, 21-29.

Liberatore, C.M., Searcy-Schrick, R.D., and Yutzey, K.E. (2000). Ventricular expression of tbx5 inhibits normal heart chamber development. Dev Biol *223*, 169-180.

Lindsey, J.C., Lusher, M.E., Anderton, J.A., Bailey, S., Gilbertson, R.J., Pearson, A.D., Ellison, D.W., and Clifford, S.C. (2004). Identification of tumour-specific epigenetic events in medulloblastoma development by hypermethylation profiling. Carcinogenesis *25*, 661-668.

Liu, J., and Brown, R.E. (2012). Morphoproteomic confirmation of an activated nuclear factor-small ka, CyrillicBp65 pathway in follicular thyroid carcinoma. Int J Clin Exp Pathol *5*, 216-223.

Liu, T., Ortiz, J.A., Taing, L., Meyer, C.A., Lee, B., Zhang, Y., Shin, H., Wong, S.S., Ma, J., Lei, Y.*, et al.* (2011). Cistrome: an integrative platform for transcriptional regulation studies. Genome Biol *12*, R83.

Lu, T., Yang, M., Huang, D.B., Wei, H., Ozer, G.H., Ghosh, G., and Stark, G.R. (2013). Role of lysine methylation of NF-kappaB in differential gene regulation. Proc Natl Acad Sci U S A *110*, 13510-13515.

Mandel, E.M., Kaltenbrun, E., Callis, T.E., Zeng, X.X., Marques, S.R., Yelon, D., Wang, D.Z., and Conlon, F.L. (2010). The BMP pathway acts to directly regulate Tbx20 in the developing heart. Development *137*, 1919-1929.

Mansouri, A., Stoykova, A., Torres, M., and Gruss, P. (1996). Dysgenesis of cephalic neural crest derivatives in Pax7-/- mutant mice. Development *122*, 831-838.

Mansouri, A., Voss, A.K., Thomas, T., Yokota, Y., and Gruss, P. (2000). Uncx4.1 is required for the formation of the pedicles and proximal ribs and acts upstream of Pax9. Development *127*, 2251-2258.

Miccio, A., Wang, Y., Hong, W., Gregory, G.D., Wang, H., Yu, X., Choi, J.K., Shelat, S., Tong, W., Poncz, M.*, et al.* (2010). NuRD mediates activating and repressive functions of GATA-1 and FOG-1 during blood development. EMBO J *29*, 442-456.

Misra, C., Chang, S.W., Basu, M., Huang, N., and Garg, V. (2014). Disruption of myocardial Gata4 and Tbx5 results in defects in cardiomyocyte proliferation and atrioventricular septation. Hum Mol Genet *23*, 5025-5035.

Mohun, T.J., Leong, L.M., Weninger, W.J., and Sparrow, D.B. (2000). The morphology of heart development in Xenopus laevis. Dev Biol *218*, 74-88.

Moody, S.A. (1987). Fates of the blastomeres of the 32-cell-stage Xenopus embryo. Dev Biol *122*, 300-319.

Moorman, A., Webb, S., Brown, N.A., Lamers, W., and Anderson, R.H. (2003). Development of the heart: (1) formation of the cardiac chambers and arterial trunks. Heart *89*, 806-814.

Moscou, M.J., and Bogdanove, A.J. (2009). A simple cipher governs DNA recognition by TAL effectors. Science *326*, 1501.

Moses, K.A., DeMayo, F., Braun, R.M., Reecy, J.L., and Schwartz, R.J. (2001). Embryonic expression of an Nkx2-5/Cre gene using ROSA26 reporter mice. Genesis *31*, 176-180.

Moskowitz, I.P., Kim, J.B., Moore, M.L., Wolf, C.M., Peterson, M.A., Shendure, J., Nobrega, M.A., Yokota, Y., Berul, C., Izumo, S.*, et al.* (2007). A molecular pathway including Id2, Tbx5, and Nkx2-5 required for cardiac conduction system development. Cell *129*, 1365-1376.

Moskowitz, I.P., Pizard, A., Patel, V.V., Bruneau, B.G., Kim, J.B., Kupershmidt, S., Roden, D., Berul, C.I., Seidman, C.E., and Seidman, J.G. (2004). The T-Box transcription factor Tbx5 is required for the patterning and maturation of the murine cardiac conduction system. Development *131*, 4107-4116.

Murdoch, B., DelConte, C., and Garcia-Castro, M.I. (2012). Pax7 lineage contributions to the mammalian neural crest. PLoS One *7*, e41089.

Parameswaran, M., and Tam, P.P. (1995). Regionalisation of cell fate and morphogenetic movement of the mesoderm during mouse gastrulation. Dev Genet *17*, 16-28.

Pfeufer, A., van Noord, C., Marciante, K.D., Arking, D.E., Larson, M.G., Smith, A.V., Tarasov, K.V., Muller, M., Sotoodehnia, N., Sinner, M.F.*, et al.* (2010). Genome-wide association study of PR interval. Nat Genet *42*, 153-159.

Pyo, J.S., Kang, G., Kim, D.H., Chae, S.W., Park, C., Kim, K., Do, S.I., Lee, H.J., Kim, J.H., and Sohn, J.H. (2013). Activation of nuclear factor-kappaB contributes to growth and aggressiveness of papillary thyroid carcinoma. Pathol Res Pract *209*, 228-232.

Rao, N.A., McCalman, M.T., Moulos, P., Francoijs, K.J., Chatziioannou, A., Kolisis, F.N., Alexis, M.N., Mitsiou, D.J., and Stunnenberg, H.G. (2011). Coactivation of GR and NFKB alters the repertoire of their binding sites and target genes. Genome Res *21*, 1404-1416.

Rao, S.S., Huntley, M.H., Durand, N.C., Stamenova, E.K., Bochkov, I.D., Robinson, J.T., Sanborn, A.L., Machol, I., Omer, A.D., Lander, E.S.*, et al.* (2014). A 3D map of the human genome at kilobase resolution reveals principles of chromatin looping. Cell *159*, 1665-1680.

Roche, A.E., Bassett, B.J., Samant, S.A., Hong, W., Blobel, G.A., and Svensson, E.C. (2008). The zinc finger and C-terminal domains of MTA proteins are required for FOG-2-mediated transcriptional repression via the NuRD complex. J Mol Cell Cardiol *44*, 352-360.

Rothschild, S.C., Easley, C.A.t., Francescatto, L., Lister, J.A., Garrity, D.M., and Tombes, R.M. (2009). Tbx5-mediated expression of Ca(2+)/calmodulin-dependent protein kinase II is necessary for zebrafish cardiac and pectoral fin morphogenesis. Dev Biol *330*, 175-184.

Sammeta, N., Hardin, D.L., and McClintock, T.S. (2010). Uncx regulates proliferation of neural progenitor cells and neuronal survival in the olfactory epithelium. Mol Cell Neurosci *45*, 398-407.

Sanyal, A., Lajoie, B.R., Jain, G., and Dekker, J. (2012). The long-range interaction landscape of gene promoters. Nature *489*, 109-113.

Sater, A.K., and Jacobson, A.G. (1989). The specification of heart mesoderm occurs during gastrulation in Xenopus laevis. Development *105*, 821-830.

Satoh, J. (2014). Molecular network of ChIP-Seq-based NF-kappaB p65 target genes involves diverse immune functions relevant to the immunopathogenesis of multiple sclerosis. Mult Scler Relat Disord *3*, 94-106.

Schmidt, D., Schwalie, P.C., Wilson, M.D., Ballester, B., Goncalves, A., Kutter, C., Brown, G.D., Marshall, A., Flicek, P., and Odom, D.T. (2012). Waves of retrotransposon expansion remodel genome organization and CTCF binding in multiple mammalian lineages. Cell *148*, 335-348.

Schmidt, D., Wilson, M.D., Ballester, B., Schwalie, P.C., Brown, G.D., Marshall, A., Kutter, C., Watt, S., Martinez-Jimenez, C.P., Mackay, S.*, et al.* (2010). Five-vertebrate ChIP-seq reveals the evolutionary dynamics of transcription factor binding. Science *328*, 1036-1040.

Shimbo, T., Du, Y., Grimm, S.A., Dhasarathy, A., Mav, D., Shah, R.R., Shi, H., and Wade, P.A. (2013). MBD3 localizes at promoters, gene bodies and enhancers of active genes. PLoS Genet *9*, e1004028.

Singh, A.P., and Archer, T.K. (2014). Analysis of the SWI/SNF chromatin-remodeling complex during early heart development and BAF250a repression cardiac gene transcription during P19 cell differentiation. Nucleic Acids Res *42*, 2958-2975.

Small, E.M., and Krieg, P.A. (2003). Transgenic analysis of the atrialnatriuretic factor (ANF) promoter: Nkx2-5 and GATA-4 binding sites are required for atrial specific expression of ANF. Dev Biol *261*, 116-131.

Smith, J.G., Magnani, J.W., Palmer, C., Meng, Y.A., Soliman, E.Z., Musani, S.K., Kerr, K.F., Schnabel, R.B., Lubitz, S.A., Sotoodehnia, N.*, et al.* (2011). Genome-wide association studies of the PR interval in African Americans. PLoS Genet *7*, e1001304.

Smith, S.J., Ataliotis, P., Kotecha, S., Towers, N., Sparrow, D.B., and Mohun, T.J. (2005). The MLC1v gene provides a transgenic marker of myocardium formation within developing chambers of the Xenopus heart. Dev Dyn *232*, 1003-1012.

Smith, S.J., Fairclough, L., Latinkic, B.V., Sparrow, D.B., and Mohun, T.J. (2006). Xenopus laevis transgenesis by sperm nuclear injection. Nat Protoc *1*, 2195-2203.

Snarr, B.S., O'Neal, J.L., Chintalapudi, M.R., Wirrig, E.E., Phelps, A.L., Kubalak, S.W., and Wessels, A. (2007). Isl1 expression at the venous pole identifies a novel role for the second heart field in cardiac development. Circ Res *101*, 971-974.

Soleimani, V.D., Punch, V.G., Kawabe, Y., Jones, A.E., Palidwor, G.A., Porter, C.J., Cross, J.W., Carvajal, J.J., Kockx, C.E., van, I.W.F.*, et al.* (2012). Transcriptional dominance of Pax7 in adult myogenesis is due to high-affinity recognition of homeodomain motifs. Dev Cell *22*, 1208-1220.

Sotoodehnia, N., Isaacs, A., de Bakker, P.I., Dorr, M., Newton-Cheh, C., Nolte, I.M., van der Harst, P., Muller, M., Eijgelsheim, M., Alonso, A.*, et al.* (2010). Common variants in 22 loci are associated with QRS duration and cardiac ventricular conduction. Nat Genet *42*, 1068-1076.

Sparrow, D.B., Cai, C., Kotecha, S., Latinkic, B., Cooper, B., Towers, N., Evans, S.M., and Mohun, T.J. (2000). Regulation of the tinman homologues in Xenopus embryos. Dev Biol *227*, 65-79.

Splinter, E., Heath, H., Kooren, J., Palstra, R.J., Klous, P., Grosveld, F., Galjart, N., and de Laat, W. (2006). CTCF mediates long-range chromatin looping and local histone modification in the beta-globin locus. Genes Dev *20*, 2349-2354.

Svedlund, J., Koskinen Edblom, S., Marquez, V.E., Akerstrom, G., Bjorklund, P., and Westin, G. (2012). Hypermethylated in cancer 1 (HIC1), a tumor suppressor gene epigenetically deregulated in hyperparathyroid tumors by histone H3 lysine modification. J Clin Endocrinol Metab *97*, E1307-1315.

Takeuchi, J.K., Ohgi, M., Koshiba-Takeuchi, K., Shiratori, H., Sakaki, I., Ogura, K., Saijoh, Y., and Ogura, T. (2003). Tbx5 specifies the left/right ventricles and ventricular septum position during cardiogenesis. Development *130*, 5953-5964.

Tam, P.P., Parameswaran, M., Kinder, S.J., and Weinberger, R.P. (1997). The allocation of epiblast cells to the embryonic heart and other mesodermal lineages: the role of ingression and tissue movement during gastrulation. Development *124*, 1631-1642.

Tark-Dame, M., Jerabek, H., Manders, E.M., Heermann, D.W., and van Driel, R. (2014). Depletion of the chromatin looping proteins CTCF and cohesin causes chromatin compaction: insight into chromatin folding by polymer modelling. PLoS Comput Biol *10*, e1003877.

Tourtellotte, W.G., Keller-Peck, C., Milbrandt, J., and Kucera, J. (2001). The transcription factor Egr3 modulates sensory axon-myotube interactions during muscle spindle morphogenesis. Dev Biol *232*, 388-399.

Tourtellotte, W.G., and Milbrandt, J. (1998). Sensory ataxia and muscle spindle agenesis in mice lacking the transcription factor Egr3. Nat Genet *20*, 87-91.

Trecca, D., Guerrini, L., Fracchiolla, N.S., Pomati, M., Baldini, L., Maiolo, A.T., and Neri, A. (1997). Identification of a tumor-associated mutant form of the NF-kappaB RelA gene with reduced DNA-binding and transactivating activities. Oncogene *14*, 791-799.

Vadasz, S., Marquez, J., Tulloch, M., Shylo, N.A., and Garcia-Castro, M.I. (2013). Pax7 is regulated by cMyb during early neural crest development through a novel enhancer. Development *140*, 3691-3702.

von Maltzahn, J., Jones, A.E., Parks, R.J., and Rudnicki, M.A. (2013). Pax7 is critical for the normal function of satellite cells in adult skeletal muscle. Proc Natl Acad Sci U S A *110*, 16474-16479.

Wade, P.A., Jones, P.L., Vermaak, D., and Wolffe, A.P. (1998). A multiple subunit Mi-2 histone deacetylase from Xenopus laevis cofractionates with an associated Snf2 superfamily ATPase. Curr Biol *8*, 843-846.

Walesky, C., Edwards, G., Borude, P., Gunewardena, S., O'Neil, M., Yoo, B., and Apte, U. (2013). Hepatocyte nuclear factor 4 alpha deletion promotes diethylnitrosamine-induced hepatocellular carcinoma in rodents. Hepatology *57*, 2480-2490.

Wallerman, O., Motallebipour, M., Enroth, S., Patra, K., Bysani, M.S., Komorowski, J., and Wadelius, C. (2009). Molecular interactions between HNF4a, FOXA2 and GABP identified at regulatory DNA elements through ChIP-sequencing. Nucleic Acids Res *37*, 7498-7508.

Wang, H., Maurano, M.T., Qu, H., Varley, K.E., Gertz, J., Pauli, F., Lee, K., Canfield, T., Weaver, M., Sandstrom, R.*, et al.* (2012). Widespread plasticity in CTCF occupancy linked to DNA methylation. Genome Res *22*, 1680-1688.

Williams, C.J., Naito, T., Arco, P.G., Seavitt, J.R., Cashman, S.M., De Souza, B., Qi, X., Keables, P., Von Andrian, U.H., and Georgopoulos, K. (2004). The chromatin remodeler Mi-2beta is required for CD4 expression and T cell development. Immunity *20*, 719-733.

Xie, L., Hoffmann, A.D., Burnicka-Turek, O., Friedland-Little, J.M., Zhang, K., and Moskowitz, I.P. (2012). Tbx5-hedgehog molecular networks are essential in the second heart field for atrial septation. Dev Cell *23*, 280-291.

Xing, Y., Yang, Y., Zhou, F., and Wang, J. (2013). Characterization of genome-wide binding of NF-kappaB in TNFalpha-stimulated HeLa cells. Gene *526*, 142-149.

Xue, Y., Wong, J., Moreno, G.T., Young, M.K., Cote, J., and Wang, W. (1998). NURD, a novel complex with both ATP-dependent chromatin-remodeling and histone deacetylase activities. Mol Cell *2*, 851-861.

Yang, J., Mitra, A., Dojer, N., Fu, S., Rowicka, M., and Brasier, A.R. (2013). A probabilistic approach to learn chromatin architecture and accurate inference of the NF-kappaB/RelA regulatory network using ChIP-Seq. Nucleic Acids Res *41*, 7240-7259.

Yang, L., Cai, C.L., Lin, L., Qyang, Y., Chung, C., Monteiro, R.M., Mummery, C.L., Fishman, G.I., Cogen, A., and Evans, S. (2006). Isl1Cre reveals a common Bmp pathway in heart and limb development. Development *133*, 1575-1585.

Yu, J., Liu, P., Cui, X., Sui, Y., Ji, G., Guan, R., Sun, D., Ji, W., Liu, F., Liu, A.*, et al.* (2011). Identification of novel subregions of LOH in gastric cancer and analysis of the HIC1 and TOB1 tumor suppressor genes in these subregions. Mol Cells *32*, 47-55.

Zammit, P.S., Relaix, F., Nagata, Y., Ruiz, A.P., Collins, C.A., Partridge, T.A., and Beauchamp, J.R. (2006). Pax7 and myogenic progression in skeletal muscle satellite cells. J Cell Sci *119*, 1824-1832.

Zhang, W., Zeng, X., Briggs, K.J., Beaty, R., Simons, B., Chiu Yen, R.W., Tyler, M.A., Tsai, H.C., Ye, Y., Gesell, G.S.*, et al.* (2010). A potential tumor suppressor role

for Hic1 in breast cancer through transcriptional repression of ephrin-A1. Oncogene *29*, 2467-2476.

Zhang, Y., LeRoy, G., Seelig, H.P., Lane, W.S., and Reinberg, D. (1998). The dermatomyositis-specific autoantigen Mi2 is a component of a complex containing histone deacetylase and nucleosome remodeling activities. Cell *95*, 279-289.

Zhao, B., Barrera, L.A., Ersing, I., Willox, B., Schmidt, S.C., Greenfeld, H., Zhou, H., Mollo, S.B., Shi, T.T., Takasaki, K.*, et al.* (2014). The NF-kappaB genomic landscape in lymphoblastoid B cells. Cell Rep *8*, 1595-1606.

Zheng, J., Wang, J., Sun, X., Hao, M., Ding, T., Xiong, D., Wang, X., Zhu, Y., Xiao, G., Cheng, G.*, et al.* (2013). HIC1 modulates prostate cancer progression by epigenetic modification. Clin Cancer Res *19*, 1400-1410.

Zhou, L., Liu, J., Olson, P., Zhang, K., Wynne, J., and Xie, L. (2015). Tbx5 and Osr1 interact to regulate posterior second heart field cell cycle progression for cardiac septation. J Mol Cell Cardiol *85*, 1-12.

Appendix 1

Xenopus: An emerging model for studying congenital heart disease

Overview

This work was published as a review article in the journal *Birth Defects Research A: Clinical and Molecular Teratology.* I wrote sections on Tbx5 and Holt-Oram Syndrome as well as utilizing Xenopus transgenesis to study congenital heart disease. The manuscript was written primarily by Erin Kaltenbrun and finalized by Frank Conlon and Chris Showell.

Kaltenbrun E.,Tandon P., Amin N.M., Waldron L. Showell C., and Conlon F.L. Xenopus: An emerging model for studing congenital heart disease (2011) *Birth Defects Res A Clin Mol Teratol.* Jun;91(6):495-510.

Congenital heart defects affect nearly 1% of all newborns and are a significant cause of infant death. Clinical studies have identified a number of congenital heart syndromes associated with mutations in genes that are involved in the complex process of cardiogenesis. The African clawed frog, *Xenopus*, has been instrumental in studies of vertebrate heart development and provides a valuable tool to investigate the molecular mechanisms underlying human congenital heart

diseases. In this review, we discuss the methodologies that make *Xenopus* an ideal model system to investigate heart development and disease. We also outline congenital heart conditions linked to cardiac genes that have been well-studied in *Xenopus* and describe some emerging technologies that will further aid in the study of these complex syndromes.

INTRODUCTION

Xenopus as a Model System for Human Congenital Heart Disease

It is becoming increasingly clear that many forms of human disease are associated with defects in genes required for early steps in embryonic development. The African clawed frog, *Xenopus* shares surprising similarities with humans both genetically and anatomically. Thus, the molecular and cellular pathways through which these genes function can be elucidated using *Xenopus* to model vertebrate heart development and disease. *Xenopus* has numerous advantages as a model system in which to identify and characterize cellular and developmental processes. Unlike the mouse, the *Xenopus* embryo develops externally, and its early patterning and morphogenesis have been extensively studied. The *Xenopus* embryo is relatively large and is amenable to surgical manipulations, allowing defined regions to be excised and cultured in simple salt solutions in which the developmental and downstream transcriptional effects of exogenous growth factors can be determined. These classical approaches are complemented by molecular techniques that allow the overexpression or knockdown of specific gene products in the early embryo (Harvey and Melton, 1988; Heasman et al., 2000). In addition, transgenesis

techniques are well established and technologies are continually being optimized (Chesneau et al., 2008). Moreover, recent sequence annotation and assembly of the *Xenopus tropicalis* genome has demonstrated that it has long regions in which genes exhibit remarkably similar synteny relationships to those found in the human genome (Showell and Conlon, 2007; Hellsten et al., 2010). Specifically, regarding human congenital heart disease (CHD), *Xenopus* has unique advantages for studying cardiovascular development (Warkman and Krieg, 2006; Bartlett and Weeks, 2008; Evans et al., 2010). First, early *Xenopus* development can proceed in the absence of a functional circulation system, allowing defects to be extensively analyzed in living embryos. Second, *Xenopus* has a pulmonary system and a two-chambered atrium. Third, *Xenopus* has a well-established fate map that is not confounded by extensive cell mixing (Dale and Slack, 1987; Moody, 1987). Only three hours after fertilization, it is possible to identify the blastomeres that will give rise to the adult heart. Collectively, this unique set of attributes places *Xenopus* as an ideal model system for studying congenital heart defects and in this review we will describe the experimental tools available to researchers, together with the existing *Xenopus* models of human CHDs (Table A1.1).

METHODS FOR STUDYING HEART DEVELOPMENT AND DISEASE IN *XENOPUS*

Protein Depletion and Overexpression

The advent of effective antisense techniques has enabled researchers to associate developmental processes with the genes that control them. The most

extensively used of these techniques are the use of morpholino oligonucleotides (MOs), which inhibit the function of specific genes by preventing translation or splicing of messenger RNA (mRNA). This technique has resulted in the publication of many studies of heart development in *Xenopus* that have advanced our understanding of this process in vertebrates (Brown et al., 2005; Garriock et al., 2005a; Small et al., 2005; Zhang et al., 2005; Inui et al., 2006; Kumano et al., 2006; Brown et al., 2007; Hilton et al., 2007; Bartlett and Weeks, 2008; Christine and Conlon, 2008; Movassagh and Philpott, 2008; Nagao et al., 2008). MO antisense oligonucleotides are neutrally charged synthetic nucleic acid analogs that are stable, soluble, and bind to RNA with high affinity (Heasman et al., 2000; Moulton, 2007). In addition, they are resistant to nuclease degradation and have limited interaction with proteins (Summerton, 2007; Eisen and Smith, 2008; Bill et al., 2009). MOs are designed to reduce gene function in two ways. First, the MO can be designed to target sequences in the 5′ untranslated region close to the translation initiation codon of the gene to sterically block the attachment of the ribosomal machinery and inhibit protein translation (Heasman et al., 2000). Alternatively, MOs can be designed to target the splice junctions in the pre-mRNA strand, resulting in the incorporation of intron-encoded amino acids and, in many cases, early termination of translation via premature stop codons or by a shift in the reading frame of the subsequent sequence (Morcos, 2007).

Strategies other than MOs have been employed to inhibit gene function. These include antisense RNA injection (Harland and Weintraub, 1985; Melton, 1985; Dagle and Weeks, 2001), RNA interference in which the RNA is targeted for degradation by the binding of small inhibitory RNA molecules and recruitment of the RNA-induced

silencing complex (Zhou and others, 2002; Summerton, 2007), DNA with chemically modified phosphate linkages that employs cellular RNase H to cleave the target RNA strand (Summerton, 2007), and peptide nucleic acid nucleotides which sterically block RNA translation in a similar way to MOs (Harland and Weintraub, 1985; Melton, 1985; Dagle and Weeks, 2001; Zhou et al., 2002; Summerton, 2007). However, due to few off-target effects, their binding success and their commercial availability, MOs have become a favored tool for studying gene function in vertebrate models (Knudsen and Nielsen, 1996; Summerton, 2007).

Protein overexpression can be as valuable a technique as protein depletion to determine the role of a particular gene in development. The microinjection of capped mRNA into the *Xenopus* embryo has commonly been used to study heart development in the context of globally increased function of the protein under investigation, the effects of lateral- and lineage-specific overexpression, and to study isoform-specific phenotypes (Campione et al., 1999; Kitaguchi et al., 2000; Stennard et al., 2003; Goetz et al., 2006). Overexpression of truncated or mutated proteins can also be utilized to reproduce and investigate phenotypes caused by mutations identified in human patients with CHD (Ataliotis et al., 2005; Bartlett et al., 2007). Furthermore, protein function can be manipulated in a spatio-temporal manner by injecting hormone-inducible constructs with timed dexamethasone application (Kitaguchi et al., 2000; Afouda et al., 2008).

Xenopus Explants for Cardiogenic Assays

The *Xenopus* embryo is particularly amenable to tissue explant assays due to its unique ability to heal after microsurgery. In addition, *Xenopus* embryonic tissue

can survive in the absence of added nutrients (due to the yolk contained in embryonic cells) allowing culture of tissue explants in a simple saline solution. The first use of *Xenopus* explants in a cardiogenic assay was performed by Horst Grunz in 1992 (Grunz, 1992) who demonstrated that the isolated blastopore lip, fated to give rise to notochord and somites but not the heart, gives rise to differentiated cardiac tissue when cultured in the presence of the growth factor-blocking compound suramin. This demonstrated the importance of growth factor signaling in negatively regulating the induction of cardiac cell fate in the dorsal marginal zone (DMZ), which restricts cardiac cell fate to two bilateral groups of cells in the dorsoanterior mesoderm of the gastrula. Similar experiments by Schneider and Mercola have shown that Wnt signaling can antagonize cardiac specification in DMZ explants. When an arc of dorsal marginal zone mesoderm containing the heart progenitors is excised from the equatorial region of the gastrula and cultured in isolation it gives rise to differentiated, beating cardiac tissue. However, overexpression of *wnt3A* and *wnt8* in these DMZ explants by injection of plasmid DNA into dorsal blastomeres results in a downregulation of cardiac marker expression, suggesting that inhibition of endogenous Wnt signaling might be required for proper heart induction (Schneider and Mercola, 2001). Indeed, when the Wnt inhibitors *dickkopf1* or *crescent* are expressed ectopically in non-cardiogenic ventral marginal zone (VMZ) explants, cardiac terminal differentiation can be induced. This results in the striking observation of beating cardiac tissue within the cultured explants (Schneider and Mercola, 2001). A role has also been identified for *wnt11*, encoding a non-canonical Wnt antagonist, in the induction of heart formation

by the observation that it is sufficient to induce expression of cardiac markers and differentiation of contractile cardiac tissue in VMZ explants (Pandur et al., 2002). As WNT11 both inhibits β-catenin through the canonical pathway and activates JNKAs WNT11 also inhibits β-catenin through the canonical pathway, Pandur *et al.* injected mRNA encoding a dominant negative LEF-1 and observed that disruption of β-catenin signaling alone fails to induce a contractile phenotype in VMZ explants. s. This result indicates that heart induction may require both 1) low levels of Wnt/**β**-catenin activity and, 2) activation of non-canonical Wnt/JNK signaling through WNT11 activation of the non-canonical Wnt signaling cascade through WNT11 is required for cardiac differentiation in this assay (Pandur et al., 2002). Alternately, it could reflect activity differences between TCF and LEF factors in β-catenin inhibition as another group demonstrated that injection of a dominant negative TCF3 was indeed sufficient to induce cardiogenesis in *Xenopus* animal caps.

Explants have also been used to investigate factors required for induction of cardiogenesis via a loss-of-function approach. For example, MO knockdown of *hex* (a transcription factor induced by antagonists of the canonical Wnt pathway) in DMZ explants resulted in loss of cardiac markers, indicating that heart induction by Wnt antagonists relies upon activation of *hex* (Foley and Mercola, 2005).

The *Xenopus* animal cap also serves as a useful tissue for cardiogenic assays and can be used to examine the ability of various molecules to affect cardiac gene expression and differentiation. The animal cap consists of prospective ectoderm at the animal pole of a blastula embryo and is fated to become epidermal and neural tissues. Because the ectodermal cells of the animal pole are pluripotent,

they can be induced to give rise to alternate cell lineages, including mesodermal derivatives such as the heart. Logan and Mohun demonstrated that cardiac muscle is induced in animal caps treated with high concentrations of the mesoderm-inducing factor activin (Logan and Mohun, 1993). A more recent protocol involving the dissociation and reaggregation of animal caps in the presence of activin results in beating animal cap explants that can form ectopic hearts in *Xenopus* adults following transplantation into the hosts at embryonic stages (Ariizumi et al., 2003). As with DMZ and VMZ explants, animal caps have been used to advance our understanding of the role of WNT signaling during cardiogenesis. Activin-induced expression of GATA factors in animal caps is abolished upon injection of an inducible form of β-catenin, suggesting that Wnt signaling may act to repress *gata* gene expression to restrict cardiogenesis (Afouda et al., 2008). In addition, inhibition of *gata4* and *gata6* by MO injection in animal cap explants results in decreased *wnt11* expression, whereas injection of inducible versions of *Gata4* and *Gata6* results in upregulation of *wnt11* expression, placing GATA factors in a regulatory pathway that links canonical and non-canonical Wnt signaling during cardiogenesis (Pandur et al., 2002; Afouda et al., 2008).

Finally, prospective cardiac tissue itself can be explanted from the embryo and used for cardiogenic assays in the absence of the rest of the embryo. This technique is particularly useful when it is necessary to bypass an early embryonic requirement for a gene to assess its later role in the developing heart. In short, tissue posterior to the cement gland including the heart field can be excised starting at stage 22 when the cardiac precursor populations form a ridge of tissue on top of

underlying endoderm. In isolation, these explants will go on to form beating hearts in culture (Raffin et al., 2000; Langdon et al., 2007). Using this assay, a recent study identified a role for SHP-2, a protein tyrosine phosphatase that is disrupted in human CHD, in the maintenance of cardiac progenitors (Langdon et al., 2007).

Xenopus Transgenesis

The development of transgenesis in *Xenopus* has allowed investigators to introduce heritable genetic modifications into the frog genome, propelling *Xenopus* forward as both a genetic and developmental model. Transgenic procedures in *Xenopus* have primarily been used for promoter/enhancer analyses and for expressing transgenes in a tissue-specific manner with defined promoters. Early experiments involving microinjection of circular or linear DNA demonstrated that integration into the genome occurred in a significant number of injected embryos (Rusconi and Schaffner, 1981; Etkin and Roberts, 1983; Andres et al., 1984; Bendig and Williams, 1984; Etkin et al., 1984). The first characterization of transgenic frogs produced by this method showed that the resulting animals were mosaic and that the copy number was highly variable, even within cells from the same animal (Etkin and Pearman, 1987). It was not until the development of the Restriction Enzyme Mediated Integration (REMI) strategy that the problem of mosaicism was overcome (Kroll and Amaya, 1996b). Using this method, sperm nuclei are incubated with linearized DNA and a restriction enzyme along with egg extracts which promote DNA decondensation. The modified sperm nuclei are then injected into unfertilized eggs, where the foreign DNA is believed to integrate randomly into the genomic

DNA during the DNA repair process prior to the first cell division (Amaya and Kroll, 1999; Smith et al., 2006).

Other methods of transgenesis that utilize different core insertion techniques have been used with varying success. Transposable elements such as *Sleeping Beauty* or the *Tol2* transposon have been used as an alternative to REMI to facilitate transgene integration in *Xenopus* (Kawakami et al., 2000; Kawakami et al., 2004; Parinov et al., 2004; Choo et al., 2006; Hamlet et al., 2006; Sinzelle et al., 2006; Yergeau and Mead, 2007; Yergeau et al., 2009). The more commonly used transposon *Tol2* is an active and autonomous transposable element that can integrate into one or multiple sites in the genome and has been used successfully in zebrafish for insertional mutagenesis, although this method of transgenesis in *Xenopus* has not been as efficient as expected. Other groups have optimized the use of integrase-mediated transgenesis utilizing the bacteriophage ΦC31 and the more frequently used *I-SceI* meganuclease (Allen and Weeks, 2005; Allen and Weeks, 2009). The *I-SceI* meganuclease, originally isolated from *Saccharomyces cerevisiae,* is used to digest transgene DNA containing *I-SceI* 18-bp recognition sites and this reaction mixture is injected into unfertilized eggs where it integrates randomly into the host genome. Copy number of integrated transgenes is relatively low, ranging from one to four, compared to the REMI method which typically results in the integration of transgene concatemers (two to six copies) at four to eight sites in the genome (Kroll and Amaya, 1996a). (Jacquier and Dujon, 1985; Ogino et al., 2006; Pan et al., 2006).

The developmental regulation of several cardiac genes has been characterized with *Xenopus* transgenesis, leading to a clearer picture of the complex gene regulatory networks that guide heart development. This commonly involves *in vivo* analysis of *cis*-regulatory regions that drive cardiac expression in the heart and is accomplished by inserting the promoter of interest upstream of a reporter transgene, such as green fluorescent protein (GFP), to follow transgene expression in the live embryo. This approach has been used to identify cardiac-specific regulatory elements for *atrial natriuretic factor* (*anf*), *cardiac α-Actin*, *myosin Light Chain 2* (*mlc2*), *myosin light chain 1v* (*mlc1v*), *nkx2-5*, *alpha myosin heavy chain* (*α-mhc*), and *tbx20* (Sparrow et al., 2000; Latinkić et al., 2002; Small and Krieg, 2003; Latinkić et al., 2004; Garriock et al., 2005b; Smith et al., 2005; Mandel et al., 2010). Additional studies examining the mechanisms of regulating these cardiac elements have revealed much about the signaling pathways that act on cardiac genes during development. Importantly, many of these regulatory elements are evolutionarily conserved as they are sufficient for cardiac-specific expression in other vertebrates including mice.

One of the benefits of transgenesis is the ability to tightly control the spatial and temporal expression of a transgene during development with tissue-specific promoters. Several cardiac promoters that drive expression throughout the developing heart have been used with great success to misexpress a gene of interest specifically in the heart-forming region. Using transgenic embryos expressing *bmp4* under the control of the *mlc2* promoter, Breckenridge *et al.* demonstrated that ectopic expression throughout the developing heart results in

randomization of the direction of cardiac looping, indicating that asymmetric BMP4 signaling is required for proper cardiac looping (Breckenridge et al., 2001).

CONGENITAL HEART DISEASE

Atrial Septal Defects: *Nkx2.5* and *Gata4*

Atrial Septal Defects (ASD) are relatively common and account for 10% of all human congenital heart defects (Hoffman and Kaplan, 2002). ASD refers to a failure of the atrial septum to fully separate the right and left atrial chambers after birth and is often accompanied by other forms of CHD including cardiac conduction system abnormalities. The cardiac transcription factor *Nkx2.5* is mutated in a number of patients with non-syndromic ASD, suggesting a critical function for this gene in the septogenesis process (Schott et al., 1998; Benson et al., 1999).

Nkx2.5 encodes a homeodomain protein that is highly conserved from *Drosophila* to human. *Nkx2.5* is expressed early in development, and in combination with other cardiac transcription factors, helps define the cardiogenic field in which it plays an essential role in the specification of cardiac progenitors from the cardiogenic mesoderm. Cardiac expression of *Nkx2.5* persists into adulthood, however, a complete understanding of the role NKX2.5 plays during the later stages of heart formation has been complicated by the fact that targeted disruption of murine *Nkx2.5* results in embryonic lethality at E9-E10, prior to heart looping (Lyons, 1995). Interestingly, a recent study in *Xenopus* demonstrated that injection of two truncated forms of *Xenopus laevis* NKX2.5, corresponding to two human NKX2.5 point mutations identified in patients with cardiac defects including ASD and

atrioventricular conduction delays, results in atrial septal and conduction system defects (Schott et al., 1998; Bartlett et al., 2007). Significantly, this study focused on the effects of injecting mutant forms of *nkx2.5*on internal changes to the hearts of stage 46 embryos when the *Xenopus* heart is fully looped with chambers, septae, valves, and a functional conduction system (Bartlett et al., 2007). The results suggest that early expression of mutant *nkx2.5* in the frog can lead to a late phenotype that includes cardiac defects consistent with those seen in human disease.

NKX2.5 has also been shown to physically interact with the cardiac zinc finger transcription factor GATA4, an additional gene mutated in in patients with ASD (Durocher et al., 1997; Lee et al., 1998; Sepulveda et al., 1998; Pehlivan et al., 1999; Garg et al., 2003). The NKX2.5-GATA4 interaction synergistically activates cardiac promoters during the cardiogenic program, suggesting that deficiencies in either member of this transcriptional complex can result in ASDs (Durocher et al., 1997; Lee et al., 1998; Sepulveda et al., 1998). Studies utilizing the embryonic carcinoma P19 cell line have shown *Gata4* to be essential for cardiac differentiation. However, *Gata4* null mice can generate differentiated cardiac myocytes that express contractile proteins but are deficient in ventral morphogenesis, resulting in a failure of cardiomyocytes to form a linear heart tube at the ventral midline (cardia bifida) (Grepin et al., 1995; Grepin et al., 1997; Kuo et al., 1997; Molkentin et al., 1997). Recent studies in *Xenopus* complement the mouse work and demonstrate with MOs that *gata4* is dispensable for cardiac specification but essential for proper heart morphogenesis downstream of the induction of the myocardium (Haworth et al.,

2008). Interestingly, when GATA4, GATA5, and GATA6 are all depleted from *Xenopus* embryos, *myosin heavy chain* expression is completely lost from most morphant embryos, suggesting that there is GATA factor redundancy in the regulation of myocardial differentiation, providing a possible explanation for the persistent presence of differentiated cardiomyocytes in *Gata4*$^{-/-}$ mice (Peterkin et al., 2007).

DiGeorge Syndrome: *Tbx1*

DiGeorge syndrome (DGS) is a congenital disorder that has many overlapping characteristics with velo-cardio-facial syndrome and conotruncal anomaly face syndrome due to shared deletions within chromosome band *22q11.2* (Yamagishi and Srivastava, 2003; Baldini, 2004). For this reason, these syndromes are collectively known as *22q11* deletion syndrome (*del22q11DS*). Approximately 80% of neonates displaying *del22q11DS* have congenital heart defects that include Tetralogy of Fallot, persistent truncus arterious, and cardio-facial abnormalities (Epstein, 2001; Yamagishi and Srivastava, 2003; Baldini, 2004; Di Felice and Zummo, 2009; Momma, 2010; Starr, 2010).

DGS is one of the most prevalent chromosomal microdeletion genetic disorders. The region of chromosome *22q11.2* that is deleted in DGS encompasses 1.5 to 3 Mb and includes 24-30 genes (Epstein, 2001; Yamagishi and Srivastava, 2003; Baldini, 2004). A heterozygous mouse genetic model in which the orthologous chromosomal region affected in DGS is deleted displays similar phenotypes as

those in human patients (Lindsay et al., 1999; Lindsay and Baldini, 2001). The deleted region frequently includes the locus encoding the T-box transcription factor *Tbx1*. In a genetic analysis screen, five patients were identified who exhibited DGS phenotypes and had *Tbx1* mutations but not chromosomal microdeletions, suggesting that *Tbx1* may be contributing to the DGS phenotype in these individuals (Yagi et al., 2003). DGS abnormalities have been correlated with disrupted pharyngeal and neural crest patterning during development. Subsequently, *Tbx1* was shown to be expressed in the pharyngeal arches, and mouse genetic models have demonstrated that *Tbx1* haplo-insufficiency disrupts the development of the fourth pharyngeal arch arteries, possibly in conjunction with FGF8 signaling (Chapman et al., 1996; Lindsay et al., 2001b; Merscher et al., 2001; Kochilas et al., 2002; Sauka-Spengler et al., 2002; Vitelli et al., 2002; Kochilas et al., 2003; Baldini, 2004; Ataliotis et al., 2005; Showell et al., 2006). In addition, *Tbx1* plays a role in growth and septation of the outflow tract (OFT). Conditionally ablating *Tbx1* in the *Nkx2.5* domain of the secondary heart field results in mild pharyngeal defects and a severe defect in aorto-pulmonary septation of the OFT that is associated with neural crest migration defects and reduced proliferation of cells in the secondary heart field (Waldo et al., 2001; Xu et al., 2004). FGF signaling may be involved in the latter event as there is a reduction in *Fgf10* expression in the secondary heart field in *Tbx1*-null mice. Further, *Fgf10* is a direct transcriptional target of *Tbx1 in vitro* (Waldo et al., 2001; Xu et al., 2004). Interestingly, the defect in OFT septation suggests a dose-dependent role for *Tbx1* because this phenotype can be partially

rescued upon reestablishing *Tbx1* expression (Jerome and Papaioannou, 2001; Lindsay et al., 2001a; Xu et al., 2004).

Tbx1 has been identified in many vertebrates including *Xenopus laevis* and *Xenopus tropicalis*. In these model systems, the expression domains of *tbx1* replicate those seen in other vertebrates, namely the pharyngeal arches, otic vesicle, and mesenchyme surrounding the OFT (Chapman et al., 1996; Sauka-Spengler et al., 2002; Kochilas et al., 2003; Ataliotis et al., 2005; Showell et al., 2006). A dominant interfering mutant of *tbx1* injected into *Xenopus* embryos results in very similar phenotypes to those of mice deficient in *Tbx1*, including pharyngeal defects, unlooped heart, pericardial edema, and a reduction in anterior structures. These defects can be rescued by co-injecting wild-type *tbx1* mRNA. To lineage trace the fate of TBX1-deficient cells, Ataliotis *et al.* co-injected *β-galactosidase* mRNA and the dominant interfering mutant *tbx1* mRNA into *Xenopus* embryos and identified a requirement for TBX1 in cells that contribute to pharyngeal mesoderm (Ataliotis et al., 2005). Additionally, recent advances in *Xenopus* transgenesis have enabled researchers to analyze cardiac and craniofacial phenotypes in embryos with reduced functions of specific genes, effectively generating models of CHD such as DGS. Using the active promoter of *mlc1v* to drive GFP, craniofacial and cardiac muscle formation was followed in *Xenopus* embryos injected with the dominant interfering mutant of *tbx1*, enabling real-time visualization of cardiac structural defects in developing embryos (Smith et al., 2005).

Holt-Oram Syndrome: *Tbx5*

Holt-Oram Syndrome (HOS), also known as heart-hand syndrome, is a congenital autosomal dominant disorder that primarily affects the heart and upper limbs (Holt and Oram, 1960). HOS is the most common heart-hand syndrome, affecting nearly 1 in 100,000 total births (Basson et al., 1994). Approximately 75% of patients with HOS experience cardiac defects, most commonly ASD, ventricular septal defects (VSD), and/or defects in the cardiac conduction system (Basson et al., 1994; Benson et al., 1996; Newbury-Ecob et al., 1996; Cross et al., 2000; McDermott et al., 2005). Atypical phenotypes have also been discovered and characterized, and phenotypic expression is variable even within families (Newbury-Ecob et al., 1996; Sletten and Pierpont, 1996; Brassington et al., 2003; Lehner et al., 2003; McDermott et al., 2005; Garavelli et al., 2008). HOS is often caused by mutations in the coding region of the T-box transcription factor *Tbx5* on chromosome *12q.24.1* (Basson et al., 1997; Li et al., 1997; Basson et al., 1999). More than 70% of patients with HOS have a mutation in the *Tbx5* coding exons, and 85% of these mutations are *de novo* (McDermott et al., 2005). Most HOS mutations are predicted to result in haploinsufficiency of *Tbx5* (Li et al., 1997; Basson et al., 1999).

Mice lacking *Tbx5* do not survive past E10.5 due to arrested cardiac development caused by impaired cardiac differentiation (Bruneau et al., 2001). Heterozygous *Tbx5*$^{del/+}$ mice display subtle defects in the paw and wrist, enlarged hearts with ASD, cardiac conduction defects, and a variety of additional complex cardiac defects reminiscent of patients with HOS. The expression of several cardiac genes is reduced in mice lacking *Tbx5*. Two of these genes, *ANF* and *Cx40,* are also reduced in mice expressing 50% of the normal TBX5 levels (Moskowitz et al., 2004).

Similar heart and limb defects are observed in the orthologous *Tbx5* zebrafish mutant *heartstrings*, suggesting that both the expression domain and protein function of *Tbx5* are conserved among vertebrates (Garrity et al., 2002). In *Xenopus, tbx5* is first expressed in the migrating heart primordia and eye anlage of the late neurula embryo. Its expression is maintained in the primitive heart tube, although its expression becomes more graded after looping of the heart, with higher expression in the ventricle than the atria (Horb and Thomsen, 1999; Showell et al., 2006). Consistent with work in other organisms, *Tbx5* was demonstrated to be critical for proper heart morphogenesis in *Xenopus* (Horb and Thomsen, 1999; Brown et al., 2005). Overexpression of a dominant negative hormone-inducible form of TBX5 blocks heart tube formation, whereas knockdown of *tbx5* expression by MO results in reduced cardiac cell number and an unlooped heart tube (Horb and Thomsen, 1999; Brown et al., 2005). The decrease in cardiac cell number in the *tbx5* morphant embryos was demonstrated to result from a proliferation defect caused by a delay or arrest in the G1/S phase of the cell cycle, implicating a role for TBX5 in cardiac cell cycle control (Goetz et al., 2006). These results from *Xenopus* as well as those from human studies (Hatcher et al., 2001), suggest that HOS defects may in part arise from a decrease in cell cycle progression and cardiac cell proliferation in *Tbx5*-expressing regions. In addition, work in a number of model systems has demonstrated a conserved role for *Tbx5* in the regulation of cardiac-specific gene expression (Liberatore et al., 2000; Bruneau et al., 2001; Hatcher et al., 2001; Hiroi et al., 2001; Garrity et al., 2002; Plageman and Yutzey, 2004; Brown et al., 2005).

Spectrum of Congenital Heart Defects: *Tbx20*

Tbx20 is a member of the T-box family of transcription factors and is one of the first genes to be expressed in the cardiac lineage along with *Nkx2.5*, *Gata4*, and *Tbx5*. In all species examined, expression of *Tbx20* is maintained throughout the primary heart field, in both myocardium and endocardium, as development proceeds and persists in the adult heart. Kirk *et al.* were the first group to identify mutations in human *Tbx20* in patients with familial CHD (Kirk et al., 2007). The two mutations identified are both in the T-box DNA binding domain and segregate with a spectrum of cardiac pathologies including ASD, VSD, valve disease, pulmonary hypertension, and cardiomyopathy. Loss-of-function mutations were the first to be identified. However, several other groups have since identified new *Tbx20* mutations with both loss- and gain-of-function that are associated with CHD (Posch et al.; Liu et al., 2008; Qian et al., 2008). In addition, upregulation of *Tbx20* expression has been noted in patients with Tetralogy of Fallot (Hammer et al., 2008). The wide range of defects associated with mutant or misregulated *Tbx20* may be the result of the expression of *Tbx20* in both myocardium and endocardium, where endocardial cushions give rise to valves and the interventricular septum.

Although the early expression of *Tbx20* in cardiogenic mesoderm suggests a role in the specification, migration, and/or differentiation of cardiac progenitors, a requirement for TBX20 is not evident until the early stages of heart morphogenesis, as shown by studies in fish and frogs (Szeto et al., 2002; Brown et al., 2005). Upon MO knockdown of *Tbx20* in zebrafish and *Xenopus* embryos, morphant embryos display unlooped heart tubes and pericardial edema, but express markers of cardiac

specification and differentiation, indicating an essential role for TBX20 in cardiac morphogenesis. In addition, TBX20-depleted *Xenopus* hearts have reduced cardiomyocyte cell numbers and fail to properly form chambers (Brown et al., 2005). Likewise, mice lacking *Tbx20* undergo normal cardiac specification and differentiation, but development is arrested in the primary linear heart tube stage, and chamber differentiation is not initiated (Cai et al., 2005; Singh et al., 2005; Stennard et al., 2005; Takeuchi et al., 2005). There also appears to be a proliferation defect in *Tbx20* null hearts that is thought to be mediated by a loss of repression of *Tbx2*, thereby allowing aberrant repression of the cell cycle gene *N-Myc* in chamber myocardium (Cai et al., 2005; Singh et al., 2005). The misregulation of *Tbx2* in *Tbx20* mutant hearts may partially explain the loss of cardiomyocytes seen in *Xenopus* and mouse *Tbx20* mutants.

The frequent occurrence of cardiac defects resulting from perturbations in the complex regulatory network guiding the cardiomyogenic program highlights the importance of understanding the interactions that occur between members of this network. *Xenopus* embryos co-injected with MOs against *tbx20* and *tbx5* display a more severe cardiac phenotype than single mutants, indicating that TBX20 and TBX5 cooperate to regulate cardiac morphogenesis (Brown et al., 2005). TBX20 physically interacts with the cardiac transcription factors NKX2.5, GATA4, GATA5, and TBX5 and, in transcription assays, TBX20 synergistically activates cardiac promoters in the presence of NKX2.5, GATA4, and ISLET1 (Stennard et al., 2003; Brown et al., 2005; Takeuchi et al., 2005). Surprisingly, in transient transcription assays, the shorter TBX20b isoform, which is terminated shortly after the T-box

domain, is more effective at activating reporter gene expression than the longer TBX20a that is the predominant isoform expressed in the heart during development (Stennard et al., 2003). To determine which TBX20 isoform promotes changes in morphogenesis and gene expression *in vivo*, *Tbx20a* and *Tbx20b* mRNAs were injected into *Xenopus* embryos . Overexpression of *Tbx20a*, but not *Tbx20b*, results in multiple developmental defects, including shortening of the anterior/posterior axis and secondary axis formation (Stennard and others, 2003). *Tbx20* mRNAs were also injected into explanted *Xenopus* animal pole caps resulting in an upregulation of the early mesoderm marker *Xbra* and the cardiac marker *Nkx2.5* in the *Tbx20a*-injected, but not *Tbx20b*-injected, caps (Stennard and others, 2003). These studies suggest that the C-terminal domain of TBX20a is essential for TBX20 activity in the embryo and highlight the utility of *Xenopus* embryo assays for investigating the biological relevance of *in vitro* findings.

Noonan Syndrome: *Shp-2*

Noonan syndrome is one of the most common forms of CHD. The disorder leads to several cardiac developmental abnormalities including ASD, VSD, pulmonary stenosis, and hypertrophic cardiomyopathy (Noonan, 1968; Noonan, 1994). Noonan syndrome was shown to be associated with mis-sense mutations in *SHP-2* in approximately half of affected individuals (Tartaglia et al., 2001; Kosaki et al., 2002; Maheshwari et al., 2002; Tartaglia et al., 2002). *Shp-2* mis-sense mutations are associated with a gain-of-function and are thought to result in prolonged downstream activation of several growth factors including epidermal

growth factors (EGFs), fibroblast growth factors (FGFs), and platelet-derived growth factor (Feng et al., 1994; Van Vactor et al., 1998; Feng, 1999; Qu, 2000; Zhang et al., 2000; Tartaglia et al., 2001). Interestingly, patients with acute myelogenous leukemia (AML), acute lymphoblastic leukemia (ALL), and juvenile myelomonocytic leukemia (JMML) carry a second, mostly mutually exclusive, somatically introduced subset of mis-sense mutations in *Shp-2*, strongly suggesting a genotype-phenotype relationship between *Shp-2* mis-sense mutations and disease (Musante et al., 2003; Tartaglia et al., 2003; Bentires-Alj et al., 2004; Loh et al., 2004; Kratz et al., 2005). However, the cellular and biochemical basis for the role of SHP-2 in Noonan syndrome, AML, ALL, and JMML is unknown.

Shp-2 is a widely expressed non-receptor tyrosine phosphatase comprised of two tandemly arranged SH2 domains and a protein tyrosine phosphatase (PTP) domain. *Shp-2*, also known as *Sh-Ptp2*, *Ptpn11*, *Ptp1d*, and *Ptp2c*, is the vertebrate homologue of the Drosophila gene *corkscrew* (*csw*). The sequence, expression pattern, and function of *Shp-2* are highly conserved throughout evolution. For example, *Xenopus* and human orthologues display 94% sequence identity, and as in fly and mouse, *Xenopus shp-2* is believed to be ubiquitously expressed (Tang et al., 1995; Langdon et al., 2007). Moreover, several animal models have suggested a critical role for *Shp-2* in vertebrate development. For example, mice expressing an internal deletion of the amino-terminal (N-SH2) domain of *Shp-2* die at late gastrulation and display several mesodermal abnormalities including heart and vascular defects (Saxton et al., 1997; Saxton and Pawson, 1999; Yang et al., 2006). In addition *Shp-2* mutant cells derived from homozygous mutant embryos show that

Shp-2 is required for full and sustained activation of the MAPK pathway in response to FGF, thus demonstrating that SHP-2 functions downstream of the FGF/MAPK pathway *in vivo* (Saxton et al., 1997; Saxton and Pawson, 1999). Consistent with these findings, studies in *Xenopus* have shown that a dominant negative form of *Xenopus Shp-2* can completely block mesoderm formation in response to both MAPK and FGF (Tang et al., 1995). Furthermore, *in vitro* and tissue culture studies have shown that *csw/Shp-2* interacts directly with the FGF inhibitor SPROUTY, leading to SPROUTY phosphorylation and inactivation (Hanafusa et al., 2004; Jarvis et al., 2006).

In the mouse and chick, SHP-2 is required in the EGF pathway for formation of cardiac valves. However, because approximately one-third of patients with Noonan-associated heart defects appear to undergo normal valvulogenesis (Chen et al., 2000; Krenz et al., 2005), it remains unclear if SHP-2 is required downstream of other receptor tyrosine kinase receptors for other aspects of heart development. To address whether SHP-2 functions in cardiac pathways in addition to EGF and valvulogenesis and to bypass the early embryonic requirements for SHP-2, Langdon et al. (2007) used a *Xenopus* cardiac explant assay and chemical SHP-2 inhibitors to demonstrate that SHP-2 is required for the survival of actively proliferating cardiac progenitor populations but not those that have exited the cell cycle. It was further demonstrated that SHP-2 is directly phosphorylated on specific residues *in vivo* in response to FGF signaling, that SHP-2 co-immunoprecipitates with the FGF receptor adaptor, and that a constitutively active Noonan-associated *Shp-2* mutation can rescue cardiac defects induced by FGF inhibition. Collectively, these studies imply

that SHP-2 functions in the FGF/MAPK pathway to maintain survival of proliferating populations of cardiac progenitor cells. However, it remains to be determined why mis-sense mutations in *Shp-2* lead to a tissue-specific effect in animals and humans.

Heterotaxy and Cardiac Looping Defects: *Zic3*

Heterotaxy (*situs ambiguus*) is a spectrum disorder in which the position of thoracic and abdominal organs is abnormal. Heterotaxy malformations are thought to arise from defective left-right patterning during embryonic development.

Establishing laterality in the embryo is a complex process involving a multitude of spatio-temporal signaling events (Mercola, 1999; Boorman and Shimeld, 2002). Initially, cells in the left-right coordinator (posterior notochord in mammals, gastrocoel roof plate in *Xenopus*, and Kupffer's vesicle in zebrafish) adjacent to the organizing node develop specialized motile cilia that generate a leftward fluid flow and an asymmetrical morphogen gradient (Tabin and Vogan, 2003; Blum et al., 2009; Sutherland and Ware, 2009). The subsequent lateralized expression of nodal, a member of the transforming growth factor β (TGFβ) family, is then thought to be involved in specifying left-right asymmetry via the notch signaling pathway (Krebs et al., 2003; Raya et al., 2003). *Pitx2*, a paired homeobox transcription factor, also plays a crucial role in organ symmetry, particularly in heart looping, downstream of nodal signaling (Ryan et al., 1998).

One of the first major morphological symmetry-breaking events in vertebrates occurs when the relatively symmetrical heart tube undergoes a rightward (dextral) bend, after which a complex process of looping and septation results in the mature

multi-chambered heart (Mercola, 1999; Manner, 2000; Boorman and Shimeld, 2002; Manner, 2009). Cardiac looping defects are commonly observed in cases of heterotaxy, and these defects account for approximately 3% of all CHDs. Other common heart phenotypes seen in heterotaxic patients include ASD, VSD, transposition of the great arteries, double outlet right ventricle, single ventricle, and aortic arch defects (Bowers et al., 1996; Lin et al., 2000; Belmont et al., 2004; Sutherland and Ware, 2009). Numerous cases of familial clustering of heterotaxy have been identified, suggesting autosomal inheritance of the disorder. However, X-linked inheritance has also been shown, involving mutations in the conserved zinc-finger transcription factor gene, *Zic3* (Gebbia et al., 1997; Ware et al., 2004). Heart defects and altered nodal expression are observed in *Zic3* mutant mice (Purandare et al., 2002). In *Xenopus* embryos, *zic3* is expressed in the mesoderm of the gastrulating embryo in a left-right (L-R) symmetrical fashion, however, unilateral right-sided overexpression of *zic3* is sufficient to disturb the L-R axis, resulting in abnormal heart and gut looping and affecting the lateral expression of *pitx2* and *nodal related 1 (Xnrl)* (Kitaguchi and others, 2000). *Xenopus zic3* is therefore considered to have a conserved early role in transducing signals from the left-right organizer and establishing asymmetry (Kitaguchi et al., 2000; Kitaguchi et al., 2002).

The amphibian model system has historically been used to study left-right patterning since the early 1900s by Spemann and colleagues. Subsequently, the *Xenopus* model was established, and has proven ideally suited to study the role of left-right laterality, using well-accepted techniques such as lineage tracing and fate mapping, in the process of heart development (Gormley and Nascone-Yoder, 2003;

Blum et al., 2009). One of the first events in *Xenopus* embryonic development is cleavage at the one-cell stage to form two blastomeres, the descendents of which will contribute almost exclusively to either the left or the right side of the embryo. This feature enables researchers to independently alter signaling events or gene expression unilaterally to determine their effect on asymmetry and to conduct left-right lineage tracing experiments, particularly of the heart region (Branford et al., 2000; Kitaguchi et al., 2000; Kitaguchi et al., 2002; Dagle et al., 2003; Chen et al., 2004; Ramsdell et al., 2006; Toyoizumi et al., 2006; Jahr et al., 2008). Recent work in *Xenopus* has demonstrated that cell lineages in the heart display a high degree of asymmetry, and that defects in left-right patterning alter cardiomyocyte allocation and differentiation in the heart, leading to cardiac malformations (Chen et al., 2004; Ramsdell et al., 2006). The *Xenopus* model is therefore an optimal organism to study the fate of cardiac cell populations and to determine how specific genes such as *Zic3* may be involved in establishing laterality in the heart and their roles in heterotaxic phenotypes.

Axenfeld-Reiger Syndrome: *Pitx2* and *FoxC1*

Axenfeld-Rieger syndrome (ARS) is a complex autosomal dominant disorder primarily characterized by anomalies of the anterior segment of the eye, face, teeth, and umbilical stump. Congenital heart defects, including ASD, pseudotruncus arteriosus, and mitral valve and intraventricular septal defects have also been reported in a number of patients with ARS (Cunningham et al., 1998; Mammi et al., 1998; Davies et al., 1999; Bekir and Gungor, 2000; Baruch and Erickson, 2001; Grosso et al., 2002; Maclean et al., 2005; Calcagni et al., 2006; Aysenur Pac et al.,

2008; Weisschuh et al., 2008; Antevil et al., 2009; Akkus and Argin, 2010). Linkage analyses have identified four different loci in humans, *4q25*, *6p25*, *13q14*, and *16q24*, each of which has been independently associated with ARS. Further analyses of *4q25* and *6p25* in patients with ARS have uncovered mutations in two genes, *Pitx2* and *Foxc1,* respectively (Amendt et al., 2000; Hjalt and Semina, 2005; Maclean et al., 2005).

Pitx2 is a highly conserved homeodomain transcription factor that is expressed asymmetrically in the left lateral plate mesoderm in chick, zebrafish, *Xenopus*, and mouse embryos (Ryan et al., 1998; Campione et al., 1999). At heart-forming stages, *pitx2* expression continues to be restricted to the left half of the heart tube in *Xenopus* embryos. In mouse, *Pitx2* is expressed in the left side of the heart tube and in the left ventricle, OFT, and atrium during heart looping (Ryan et al., 1998). The defects observed in *Pitx2* null and hypomorphic mice, such as altered looping of the heart, absence of atrial septation, and dysmorphic ventricular septation, recapitulate the defects observed in human ARS patients with *Pitx2* dysfunction (Gage et al., 1999; Lin et al., 1999; Lu et al., 1999).

The use of *Xenopus* has been instrumental in understanding the dual role of *Pitx2* in heart development, firstly in directing the looping of the heart tube and secondly in controlling the morphogenesis of the cardiac chambers. Misexpression of *pitx2* by injection of its mRNA on the right side of the *Xenopus* embryo results in a reversal of heart looping, showing the conserved role of *pitx2* in directing this event. The restricted expression of *pitx2* is likely to be downstream of the TGFβ signaling family, as bilateral injections of mRNA encoding nodal or activin results in bilateral

expression of the gene (Campione et al., 1999). Further, injection of a dominant negative form of the activin type II receptor into *Xenopus* embryos alters *pitx2* expression levels and subsequent heart looping. These findings are supported by similar experiments in chick (Ryan et al., 1998). Of the three isoforms of *Pitx2* present during development, experiments in *Xenopus*, zebrafish, and mouse demonstrate that *Pitx2*c is the isoform that is specifically expressed in heart (Essner et al., 2000; Schweickert et al., 2000). The injection of modified antisense oligonucleotides that mediate degradation of *pitx2*c mRNA in *Xenopus* embryos results in cardiac defects that are very similar to phenotypes observed in *Pitx2* mutant mice, including abnormal atrial septation, extracellular matrix restriction, abnormal positioning of the atrial and ventricular chambers, and restriction of ventricular development. These tadpoles also exhibit dramatic straightening of the OFT, followed by a rightward migration (Dagle et al., 2003). This study demonstrates the conservation of *pitx2* function in *Xenopus* cardiac development and its relationship to ARS. It has recently been shown that *Pitx2* patterns the second heart field and is required to specify the left versus right atrium (Liu et al., 2002; Ai et al., 2006; Galli et al., 2008). It will be interesting to determine if *Xenopus* can be exploited as a useful model for testing the effects of various ARS-derived mutations on *Pitx2* function during second heart field development and for further identifying the mechanisms by which *Pitx2* functions.

Foxc1 is a member of the forkhead family of transcription factors and is expressed in endothelial and mesenchymal cells of the developing heart as well as in endocardial cushions derived from cardiac neural crest cells (Iida et al., 1997;

Winnier et al., 1999; Kume et al., 2001; Seo et al., 2006). *Foxc1* transcripts have also been detected in the second heart field and in the proepicardium (Seo and Kume, 2006). In the newly formed heart, *Foxc1* is expressed in the atrial septum, the venous, aortic and pulmonary valves, and the mitral and tricuspid valves (Swiderski et al., 1999). Consistent with its widespread expression in the heart, FOXC1 plays a critical role in heart valve formation and atrial septation as suggested by the cardiac defects noted in mice mutant for *Foxc1.* Specifically, *Foxc1* homozygous mutants display interruption or coarctation of the aortic arch, VSD, and pulmonary and aortic valve dysplasia (Winnier et al., 1999). Mice lacking both *Foxc1* and the closely related Fox transcription factor *Foxc2* have even more severe cardiac abnormalities consisting of hypoplasia or lack of the OFT and right ventricle as well as the inflow tract, and dysplasia of the OFT and atrioventricular cushions. These mice also have an abnormally formed epicardium, reduced cell proliferation, and increased apoptosis of neural crest cells (Winnier et al., 1999; Kume et al., 2001; Seo and Kume, 2006).

Foxc1 has been identified in *Xenopus* and is present in cardiac lineages (Koster et al., 1998; Gessert and Kuhl, 2009). Depletion of *foxc1* during early *Xenopus* development results in downregulation of adhesion molecules involved in mesoderm development and increased apoptosis, correlating with the phenotypes observed in the mouse mutants (Cha et al., 2007). It remains to be determined if reduction of FOXC1 levels in *Xenopus* has similar effects on cardiac morphology to those observed in mouse knockouts and patients with ARS. However, the early

phenotypes of FOXC1 depletion during *Xenopus* development provide a model in which to investigate the phenotypic changes that result from *Foxc1* disruption.

CHARGE Syndrome: *Chd7*

CHARGE syndrome (Coloboma, Heart defects, choanal Atresia, Retarded growth and development, Genital abnormalities, and Ear anomalies) is a complex disease associated with a number of cardiac abnormalities including Tetralogy of Fallot, atrioventricular canal defects, and aortic arch anomalies (Davenport et al., 1986). The majority of individuals with CHARGE syndrome have mutations in the coding region of *chromodomain helicase DNA binding protein 7* (*Chd7)* (Vissers et al., 2004; Aramaki et al., 2006; Jongmans et al., 2006; Lalani et al., 2006; Delahaye et al., 2007; Wincent et al., 2008; Kaliakatsos et al., 2010; Wessels et al., 2010).

Chd7 expression has been characterized in the chick and mouse, where it has been found to be expressed mainly in the neural ectoderm and branchial arches (Bosman et al., 2005; Aramaki et al., 2007; Hurd et al., 2007). Mutant *Chd7* mice display defects in neural stem cell proliferation, olfaction, and some cardiac defects, including formation of the interventricular septum (Bosman et al., 2005; Adams et al., 2007; Hurd et al., 2007; Layman et al., 2009). It has been proposed that the multiple phenotypes in CHARGE syndrome are caused by defects in neural crest cell (NCC) migration (Siebert et al., 1985). Recently, *Chd7* was found to be expressed in *Xenopus* NCCs as well as in human NC-like cells. MO knockdown of *chd7* in *Xenopus* perturbs the migration of NCCs to the pharyngeal arches. This phenotype is partially rescued by injecting human *Chd7* mRNA, suggesting that the molecular

function of CHD7 is well-conserved. In addition, overexpression of human *Chd7* with a substitution of a conserved lysine residue in its ATPase domain results in a dominant-negative effect (Bajpai et al., 2010). This dominant negative effect recapitulates the major features of CHARGE syndrome described above, including abnormal positioning of the truncus arteriosus and OFT. Analysis of markers associated with NCCs reveal that *chd7* is not required for the induction or survival of NCCs, but for their specification. The expression of *sox9*, *twist*, and *slug*, genes that mark multipotent, migrating NCCs, is severely perturbed in *chd7* downregulated embryos (Sauka-Spengler and Bronner-Fraser, 2008; Bajpai et al., 2010). These studies in *Xenopus* have provided a powerful *in vivo* model in which to study the role of NCCs in heart development and the CHDs that result from improper NCC migration and specification. More recently, the chromatin remodeling factors CHD8 and BRG1 have been shown to physically interact with CHD7 (Bajpai et al., 2010; Batsukh et al., 2010) and *Brg1* was demonstrated to play a role in regulating cardiac growth and differentiation (Hang et al., 2010). The roles of *Chd8* and *Brg1* in a *Xenopus* model of CHARGE syndrome could aid in the understanding of this complex syndrome.

FUTURE DIRECTIONS AND EMERGING TECHNOLOGIES IN *XENOPUS*

Investigating a Role for the Epicardium in Congenital Heart Disease

The epicardium is a mesothelial sheet of cells surrounding the myocardium of the developing looped heart in many vertebrate organisms (Ho and Shimada, 1978; Viragh and Challice, 1981; Hirakow, 1992; Manner et al., 2001; Jahr et al., 2008;

Pombal et al., 2008; Serluca, 2008). The epicardial structure arises from the pro-epicardial organ (PEO), which is situated on the sinus venosus. These mesothelial cells cluster and bridge over towards the ventricular surface of the heart and migrate onto the myocardial surface as an epithelial-like sheet. Subsequently, subsets of epicardial cells undergo epithelial-mesenchymal transition (EMT) and migrate into the sub-epicardial space and myocardium where they differentiate into various cell populations including fibroblasts and smooth muscle cells of the coronary vasculature (Manner et al., 2001; Lie-Venema et al., 2007; Winter and Gittenberger-de Groot, 2007). The epicardium is thought to play a mitogenic role in cardiomyocyte growth and has been shown to be important for cardiac repair in adult zebrafish (Lepilina et al., 2006). Recently, adult human epicardium-derived cells (EPDCs) were demonstrated to have a paracrine role in improving mammalian cardiac function when co-transfected with cardiomyocytes into an infarcted murine heart (Winter et al., 2007; Winter et al., 2009). Thus, the epicardium may have the potential to stimulate cardiac repair and regeneration, given the right conditions.

Various congenital heart diseases display abnormalities that may arise from improper epicardium formation or differentiation of EPDCs. In avian embryos in which either the pro-epicardial organ is ablated or the epithelial-mesenchymal transition of EPDCs is disrupted, defects are seen in the compact layer of the myocardium, while the inner curvature of the heart is wider and often displays a double outlet right ventricle, indicative of a heart looping defect (Gittenberger-de Groot et al., 2000; Lie-Venema et al., 2005; Manner et al., 2005). Ventricular non-compaction is also seen when genes involved in epicardium formation, e.g., *Wt1* and

RXRα, are knocked out in the mouse (Moore et al., 1998; Merki et al., 2005). In addition to their roles in regulating the development of the compact ventricular and atrial myocardia, EPDCs are involved in the development of cardiac structures associated with the conduction system. The annulus fibrosus, which plays an important insulating role in the cardiac conduction system, is derived from the epicardium, and EPDCs also influence the formation of the peripheral Purkinje fiber network from ventricular cardiomyocytes (Eralp et al., 2006; Zhou et al., 2010). Electrophysiological cardiac defects, such as Wolff-Parkinson-White syndrome and Mahaim tachycardia, may therefore have an origin in improper epicardium or EPDC formation.

EPDCs also contribute cells to the atrioventricular cushions and valves, and disrupting epicardium formation can lead to aberrant valve formation (Gittenberger-de Groot et al., 1998; Gittenberger-de Groot et al., 2000; Perez-Pomares et al., 2002; Manner et al., 2005). It is conceivable that disorders in which the valve leaflet has not fully delaminated - for example, Ebstein's anomaly (tricuspid valve leaflet) - might result from defects in epicardial patterning or signaling (Attenhofer Jost et al., 2005; Lie-Venema et al., 2007). Ventricular non-compaction may also be indicative of an epicardial defect as shown by mouse knockout models of genes involved in epicardium formation, e.g., *Wt1* and *RXRα*, or in PEO ablation studies in chick (Moore et al., 1998; Manner et al., 2005; Merki et al., 2005; Sucov et al., 2009). Interestingly, the *Fog-2* knockout mouse, which has an epicardial defect phenotype, displays many of the anomalies described above - including tricuspid atresia, thin

myocardium, double outlet right ventricles, and VSD (Svensson et al., 2000; Tevosian et al., 2000; Clark et al., 2006).

To date, little is known about how the epicardium develops and functions in *Xenopus* embryos. Scanning electron microscopy has demonstrated the presence of the PEO on the right side of the septum transversum in *Xenopus* embryos, similar to other vertebrates (Jahr et al., 2008). Furthermore, genes characteristic of the vertebrate PEO and epicardium are conserved in *Xenopus* (Jahr et al., 2008). The *Xenopus* model lends itself to studying the epicardium and potential defects in valve formation and conduction systems due to the ease of manipulating gene function and the established techniques of tissue explanting, antisense MO microinjection, lineage tracing, and transgenics. Recent advances in live imaging have enabled researchers to utilize the *Xenopus* model to visualize cardiac development in real time and to use non-invasive electrical recording, Doppler optical cardiograms, and optical coherence tomography to study heart structure, conduction, and blood flow to determine the role of the epicardium in these processes (Bartlett et al., 2004; Mariampillai et al., 2007; Yelin et al., 2007; Kieserman et al., 2010).

In Vivo Imaging of the Developing *Xenopus* Heart

Xenopus embryos are very well-suited for live imaging of dynamic developmental processes due to their large size and external development. Because of the large size of the embryos, individual cells in the embryo are larger, which allows visualization of the subcellular localization and dynamics of a given fluorescent fusion protein. For example, live confocal imaging has been successfully

used to demonstrate the dispersal of individual fluorescent myeloid cells throughout the *Xenopus* embryo (Kieserman et al., 2010). A combination of transgenesis and advanced imaging tools makes this type of approach feasible in the living animal. Yolk opacity in the early *Xenopus* embryo presents a challenge for imaging of deeper tissues. However, cells and/or deep tissues can be visualized easily after microsurgery and subsequent culture of tissue explants. High resolution imaging of the structure and function of the developing myocardium will be critical to complete our understanding of how the heart develops in three and four dimensions, and thus how developmental defects can arise in this system.

Historically, the morphology of the *Xenopus* embryonic heart has been studied in fixed embryos with a combination of confocal microscopy and 3D reconstruction of serial sections through the heart (Kolker et al., 2000; Mohun, 2000). As even slight morphological or dynamic changes in the heart can result in myocardial dysfunction, it is of vital importance to examine these changes *in vivo* in the developing embryo. One area in which this is particularly relevant is in the characterization of defects in the cardiac conduction system. Human CHD is often complicated by atrioventricular conduction abnormalities. However, a thorough understanding of the defects in embryonic heart contraction as they result from a genetic or morphological abnormality is lacking due to the difficulty of examining these defects *in vivo*. It has recently been demonstrated that the *Xenopus* embryo is amenable to noninvasive live video analysis of the conduction system, allowing one to examine the properties of chamber contraction *in vivo* (Bartlett et al., 2004). Moreover, *Xenopus* cardiac electrophysiology shares many characteristics with the

human conduction system, making it an ideal model in which to analyze the physiology of cardiac conduction defects. As a proof of principle, this methodology has been used to examine the microscopic timing of heart contraction in embryos injected with two human *Nkx2.5* mutants and resulted in the identification of a number of conduction defects including a delay in the AV interval and a distinct tachycardia (Bartlett et al., 2007). This type of study, when applied to other human mutations such as those in *Tbx5* that cause Holt-Oram Syndrome, can improve our understanding of these complex human pathologies.

Protein Interactions and Biochemical Function

As discussed previously, transgenesis has primarily been used to study the regulation of gene expression and has revealed much about the transcriptional regulation of cardiac development. However, it has been used relatively little as a tool for isolating protein complexes. Because protein complexes mediate the majority of cellular processes, knowledge of the composition and function of cardiac-specific protein complexes will provide key insights into their tissue-specific activity in the heart. With the advent of proteomics-based approaches to identify endogenous protein complexes, there are a variety of convenient *in vivo* tags such as GFP that can be used to genomically label any protein of interest. Thus, the generation of transgenic *Xenopus* lines that express tagged versions of proteins will provide virtually unlimited material for applications such as mass spectrometry and protein localization studies. Additionally, tagged proteins carrying known CHD-causing mutations could be utilized to characterize changes in their ability to form

complexes with other cardiac proteins. As discussed previously, deficiencies in members of cardiac transcriptional complexes often lead to congenital heart malformations, illuminating the need to investigate the functional role of these complexes during cardiac development.

Genetic Approaches in *Xenopus tropicalis*

To date, most studies that have used *Xenopus* as a model system to examine cardiac development have used the pseudotetraploid species *Xenopus laevis* and have relied upon well-established nucleic acid microinjection techniques for depletion or over-expression of proteins in the developing embryo. As our understanding of the genetic basis of inherited cardiac disease increases, there will be a greater need to use genetic approaches in *Xenopus*. Genetic techniques enable precise experimental manipulation that can be used to gain a deeper understanding not just of individual gene functions, but also of the interconnectivity between genes in genetic networks (through enhancer/suppressor gene interaction studies, for example). These interconnections, coupled with variation in the genetic background, may ultimately explain the range of disease type and severity often observed in patients with particular CHDs (Basson et al., 1994; Newbury-Ecob et al., 1996; Sznajer et al., 2007). The use of loss-of-function or gain-of-function alleles of endogenous genes that are generated by mutagenesis also circumvents the undesirable features of MO-based inhibition and mRNA-based expression that result from the inherent limitations in controlling where and when MOs or mRNAs are active in the embryo. Specifically, the role of mutations that affect the biochemical

function of a protein can be examined without inappropriately expressing the mutant protein in cells in which the native protein is not expressed, or at times at which it would not normally be present.

The diploid *Xenopus tropicalis* is much more amenable to genetic analysis than the pseudotetraploid *X. laevis*. Fortunately, the vast majority of reagents and techniques developed by researchers for *X. laevis* can be adapted for use with *X. tropicalis*, primarily due to the extremely close similarities between the two species at the genetic and embryonic levels. Even complex reagents such as microarrays developed in one *Xenopus* species have been shown to be usable in both, although species-specific reagents are becoming increasingly available (Chalmers et al., 2005). A key factor encouraging researchers to adopt *X. tropicalis* is the availability of a high-quality genome sequence and the resources that have stemmed from it, including a simple-sequence repeat map of more than 1,500 polymorphic markers that allows mutations to be mapped to relatively small regions of the genome following their isolation in forward genetic screens (Xu et al., 2008; Hellsten et al., 2010) (http://tropmap.biology.uh.edu/index.html). The first two mutations mapped in *X. tropicalis, Muzak* and *Dicky Ticker*, both affect cardiac function and are located in the myosin heavy chain gene *myh6* and the muscle-specific chaperone gene *unc45b*, respectively (Abu-Daya et al., 2009; Geach and Zimmerman, 2010). These early successes validate *X. tropicalis* as a model in which novel cardiac genes can be identified through phenotype-based forward genetic screens. The primary importance of this work will be to gain a better understanding of the developmental

genetics of cardiac cell type differentiation and morphogenesis. However, studying the effects of mutations in disease-associated genes is also likely to advance our understanding of the etiology of congenital heart abnormalities.

Table A1.1. *Xenopus* models of human congenital heart disease.

Gene Name	Disease	Cardiovascular Manifestations	*Xenopus* Model	*Xenopus* Cardiac Phenotype	Refs
Tbx1	DiGeorge Syndrome	TOF, persistent truncus arteriosus	overexpression of dominant negative	unlooped heart, pericardial edema	(Ataliotis et al., 2005)
Tbx5	Holt-Oram Syndrome	ASD, VSD, cardiac conduction system defects	overexpression of dominant negative protein depletion	unlooped heart unlooped heart, loss of cardiac cells	(Horb and Thomsen, 1999) (Brown et al., 2005)
Tbx20	NA	ASD, VSD, valve disease, pulmonary hypertension, cardiomyopathy, TOF	protein depletion	unlooped heart, pericardial edema, loss of cardiac cells	(Brown et al., 2005)
Nkx2.5	NA	ASD, cardiac conduction system defects	overexpression overexpression of dominant negative overexpression of mutant mRNA	enlarged heart reduced heart ASD, cardiac conduction system defects	(Cleaver, 1996) (Fu, 1998; Grow and Krieg, 1998) (Bartlett et al., 2007)
Gata4	NA	ASD	protein depletion	partial fusion of heart fields, cardiac bifida, abnormal cardiac looping	(Haworth et al., 2008)
Shp2	Noonan Syndrome	ASD, VSD, pulmonary stenosis, hypertrophic cardiomyopathy	chemical inhibition	unfused heart fields, loss of cardiac cells	(Langdon et al., 2007)
Zic3	Heterotaxy	cardiac looping defects, ASD, VSD, transposition of the great arteries,	overexpression	abnormal cardiac looping	(Kitaguchi et al., 2000; Kitaguchi et al.,

		double outlet right ventricle, ventricle and aortic arch defects			2002)
Pitx2	Axonfeld-Reiger Syndrome	ASD, pseudotruncus arteriosus, mitral valve and intraventricular septal defects	overexpression overexpression of dominant negative protein depletion	abnormal cardiac looping abnormal cardiac looping abnormal atrial septation, defects in atrial and ventricular chamber position, restriction of ventricular development	(Campione et al., 1999) (Campione et al., 1999) (Dagle et al., 2003)
Chd7	CHARGE Syndrome	TOF, atrioventricular canal defects, aortic arch defects	protein depletion overexpression of mutant mRNA	defects in neural crest cell migration abnormal positioning of truncus arteriosus and OFT	(Bajpai et al., 2010) (Bajpai et al., 2010)

TOF, Tetralogy of Fallot; ASD, atrial septal defects; VSD, ventricular septal defects;

NA, Not Applicable; OFT, outflow tract

REFERENCES

Abu-Daya, A., Sater, A. K., Wells, D. E., Mohun, T. J. and Zimmerman, L. B. (2009) 'Absence of heartbeat in the Xenopus tropicalis mutation muzak is caused by a nonsense mutation in cardiac myosin myh6', *Dev Biol*.

Adams, M. E., Hurd, E. A., Beyer, L. A., Swiderski, D. L., Raphael, Y. and Martin, D. M. (2007) 'Defects in vestibular sensory epithelia and innervation in mice with loss of Chd7 function: implications for human CHARGE syndrome', *J Comp Neurol* 504(5): 519-32.

Afouda, B. A., Martin, J., Liu, F., Ciau-Uitz, A., Patient, R. and Hoppler, S. (2008) 'GATA transcription factors integrate Wnt signalling during heart development', *Development* 135(19): 3185-90.

Ai, D., Liu, W., Ma, L., Dong, F., Lu, M. F., Wang, D., Verzi, M. P., Cai, C., Gage, P. J., Evans, S. et al. (2006) 'Pitx2 regulates cardiac left-right asymmetry by patterning second cardiac lineage-derived myocardium', *Dev Biol* 296(2): 437-49.

Akkus, M. N. and Argin, A. (2010) 'Congenital heart defects in two siblings in an Axenfeld-Rieger syndrome family', *Clin Dysmorphol* 19(2): 56-61.

Allen, B. G. and Weeks, D. L. (2005) 'Transgenic Xenopus laevis embryos can be generated using phiC31 integrase', *Nat Methods* 2(12): 975-9.

Allen, B. G. and Weeks, D. L. (2009) 'Bacteriophage phiC31 integrase mediated transgenesis in Xenopus laevis for protein expression at endogenous levels', *Methods Mol Biol* 518: 113-22.

Amaya, E. and Kroll, K. L. (1999) 'A method for generating transgenic frog embryos', *Methods Mol Biol* 97: 393-414.

Amendt, B. A., Semina, E. V. and Alward, W. L. (2000) 'Rieger syndrome: a clinical, molecular, and biochemical analysis', *Cell Mol Life Sci* 57(11): 1652-66.

Andres, A. C., Muellener, D. B. and Ryffel, G. U. (1984) 'Persistence, methylation and expression of vitellogenin gene derivatives after injection into fertilized eggs of Xenopus laevis', *Nucleic Acids Res* 12(5): 2283-302.

Antevil, J., Umakanthan, R., Leacche, M., Brewer, Z., Solenkova, N., Byrne, J. G. and Greelish, J. P. (2009) 'Idiopathic mitral valve disease in a patient presenting with Axenfeld-Rieger syndrome', *J Heart Valve Dis* 18(3): 349-51.

Aramaki, M., Kimura, T., Udaka, T., Kosaki, R., Mitsuhashi, T., Okada, Y., Takahashi, T. and Kosaki, K. (2007) 'Embryonic expression profile of chicken CHD7,

the ortholog of the causative gene for CHARGE syndrome', *Birth Defects Res A Clin Mol Teratol* 79(1): 50-7.
Aramaki, M., Udaka, T., Kosaki, R., Makita, Y., Okamoto, N., Yoshihashi, H., Oki, H., Nanao, K., Moriyama, N., Oku, S. et al. (2006) 'Phenotypic spectrum of CHARGE syndrome with CHD7 mutations', *J Pediatr* 148(3): 410-4.

Ariizumi, T., Kinoshita, M., Yokota, C., Takano, K., Fukuda, K., Moriyama, N., Malacinski, G. M. and Asashima, M. (2003) 'Amphibian in vitro heart induction: a simple and reliable model for the study of vertebrate cardiac development', *Int J Dev Biol* 47(6): 405-10.

Ataliotis, P., Ivins, S., Mohun, T. J. and Scambler, P. J. (2005) 'XTbx1 is a transcriptional activator involved in head and pharyngeal arch development in Xenopus laevis', *Dev Dyn* 232(4): 979-91.

Attenhofer Jost, C. H., Connolly, H. M., Edwards, W. D., Hayes, D., Warnes, C. A. and Danielson, G. K. (2005) 'Ebstein's anomaly - review of a multifaceted congenital cardiac condition', *Swiss Med Wkly* 135(19-20): 269-81.

Aysenur Pac, F., Cagdas, D. N. and Necati Demir, M. (2008) 'Axenfeld-Rieger syndrome and pseudotruncus arteriosus', *Int J Cardiol* 126(1): e4-7.

Bajpai, R., Chen, D. A., Rada-Iglesias, A., Zhang, J., Xiong, Y., Helms, J., Chang, C. P., Zhao, Y., Swigut, T. and Wysocka, J. (2010) 'CHD7 cooperates with PBAF to control multipotent neural crest formation', *Nature* 463(7283): 958-62.

Baldini, A. (2004) 'DiGeorge syndrome: an update', *Curr Opin Cardiol* 19(3): 201-4.
Bartlett, H. L., Scholz, T. D., Lamb, F. S. and Weeks, D. L. (2004) 'Characterization of embryonic cardiac pacemaker and atrioventricular conduction physiology in Xenopus laevis using noninvasive imaging', *Am J Physiol Heart Circ Physiol* 286(6): H2035-41.

Bartlett, H. L., Sutherland, L., Kolker, S. J., Welp, C., Tajchman, U., Desmarais, V. and Weeks, D. L. (2007) 'Transient early embryonic expression of Nkx2-5 mutations linked to congenital heart defects in human causes heart defects in Xenopus laevis', *Dev Dyn* 236(9): 2475-84.

Bartlett, H. L. and Weeks, D. L. (2008) 'Lessons from the lily pad: Using Xenopus to understand heart disease', *Drug Discov Today Dis Models* 5(3): 141-146.

Baruch, A. C. and Erickson, R. P. (2001) 'Axenfeld-Rieger anomaly, hypertelorism, clinodactyly, and cardiac anomalies in sibs with an unbalanced translocation der(6)t(6;8)', *Am J Med Genet* 100(3): 187-90.

Basson, C. T., Bachinsky, D. R., Lin, R. C., Levi, T., Elkins, J. A., Soults, J., Grayzel, D., Kroumpouzou, E., Traill, T. A., Leblanc-Straceski, J. et al. (1997) 'Mutations in

human TBX5 [corrected] cause limb and cardiac malformation in Holt-Oram syndrome', *Nat Genet* 15(1): 30-5.
Basson, C. T., Cowley, G. S., Solomon, S. D., Weissman, B., Poznanski, A. K., Traill, T. A., Seidman, J. G. and Seidman, C. E. (1994) 'The clinical and genetic spectrum of the Holt-Oram syndrome (heart-hand syndrome)', *N Engl J Med* 330(13): 885-91.

Basson, C. T., Huang, T., Lin, R. C., Bachinsky, D. R., Weremowicz, S., Vaglio, A., Bruzzone, R., Quadrelli, R., Lerone, M., Romeo, G. et al. (1999) 'Different TBX5 interactions in heart and limb defined by Holt-Oram syndrome mutations', *Proc Natl Acad Sci U S A* 96(6): 2919-24.

Batsukh, T., Pieper, L., Koszucka, A. M., von Velsen, N., Hoyer-Fender, S., Elbracht, M., Bergman, J. E., Hoefsloot, L. H. and Pauli, S. (2010) 'CHD8 interacts with CHD7, a protein which is mutated in CHARGE syndrome', *Hum Mol Genet* 19(14): 2858-66.

Bekir, N. A. and Gungor, K. (2000) 'Atrial septal defect with interatrial aneurysm and Axenfeld-Rieger syndrome', *Acta Ophthalmol Scand* 78(1): 101-3.

Belmont, J. W., Mohapatra, B., Towbin, J. A. and Ware, S. M. (2004) 'Molecular genetics of heterotaxy syndromes', *Curr Opin Cardiol* 19(3): 216-20.

Bendig, M. M. and Williams, J. G. (1984) 'Differential expression of the Xenopus laevis tadpole and adult beta-globin genes when injected into fertilized Xenopus laevis eggs', *Mol Cell Biol* 4(3): 567-70.

Benson, D. W., Basson, C. T. and MacRae, C. A. (1996) 'New understandings in the genetics of congenital heart disease', *Curr. Opin. Pediatr.* 8(5): 505-511.

Benson, D. W., Silberbach, G. M., Kavanaugh-McHugh, A., Cottrill, C., Zhang, Y., Riggs, S., Smalls, O., Johnson, M. C., Watson, M. S., Seidman, J. G. et al. (1999) 'Mutations in the cardiac transcription factor NKX2.5 affect diverse cardiac developmental pathways', *J Clin Invest* 104(11): 1567-73.

Bentires-Alj, M., Paez, J. G., David, F. S., Keilhack, H., Halmos, B., Naoki, K., Maris, J. M., Richardson, A., Bardelli, A., Sugarbaker, D. J. et al. (2004) 'Activating mutations of the noonan syndrome-associated SHP2/PTPN11 gene in human solid tumors and adult acute myelogenous leukemia', *Cancer Res* 64(24): 8816-20.

Bill, B. R., Petzold, A. M., Clark, K. J., Schimmenti, L. A. and Ekker, S. C. (2009) 'A primer for morpholino use in zebrafish', *Zebrafish* 6(1): 69-77.

Blum, M., Beyer, T., Weber, T., Vick, P., Andre, P., Bitzer, E. and Schweickert, A. (2009) 'Xenopus, an ideal model system to study vertebrate left-right asymmetry', *Dev Dyn* 238(6): 1215-25.

Boorman, C. J. and Shimeld, S. M. (2002) 'The evolution of left-right asymmetry in chordates', *BioEssays* 24(11): 1004-11.
Bosman, E. A., Penn, A. C., Ambrose, J. C., Kettleborough, R., Stemple, D. L. and Steel, K. P. (2005) 'Multiple mutations in mouse Chd7 provide models for CHARGE syndrome', *Hum Mol Genet* 14(22): 3463-76.

Bowers, P. N., Brueckner, M. and Yost, H. J. (1996) 'The genetics of left-right development and heterotaxia', *Semin Perinatol* 20(6): 577-88.

Branford, W. W., Essner, J. J. and Yost, H. J. (2000) 'Regulation of gut and heart left-right asymmetry by context-dependent interactions between xenopus lefty and BMP4 signaling', *Dev Biol* 223(2): 291-306.

Brassington, A. M., Sung, S. S., Toydemir, R. M., Le, T., Roeder, A. D., Rutherford, A. E., Whitby, F. G., Jorde, L. B. and Bamshad, M. J. (2003) 'Expressivity of Holt-Oram syndrome is not predicted by TBX5 genotype', *Am J Hum Genet* 73(1): 74-85.

Breckenridge, R. A., Mohun, T. J. and Amaya, E. (2001) 'A role for BMP signalling in heart looping morphogenesis in Xenopus', *Dev Biol* 232(1): 191-203.

Brown, D. D., Christine, K. S., Showell, C. and Conlon, F. L. (2007) 'Small heat shock protein Hsp27 is required for proper heart tube formation', *Genesis* 45(11): 667-78.

Brown, D. D., Martz, S. N., Binder, O., Goetz, S. C., Price, B. M. J., Smith, J. C. and Conlon, F. L. (2005) 'Tbx5 and Tbx20 act synergistically to control vertebrate heart morphogenesis', *Development* 132(3): 553-563.

Bruneau, B. G., Nemer, G., Schmitt, J. P., Charron, F., Robitaille, L., Caron, S., Conner, D. A., Gessler, M., Nemer, M., Seidman, C. E. et al. (2001) 'A Murine Model of Holt-Oram Syndrome Defines Roles of the T-Box Transcription Factor Tbx5 in Cardiogenesis and Disease', *Cell* 106(6): 709-721.

Cai, C. L., Zhou, W., Yang, L., Bu, L., Qyang, Y., Zhang, X., Li, X., Rosenfeld, M. G., Chen, J. and Evans, S. (2005) 'T-box genes coordinate regional rates of proliferation and regional specification during cardiogenesis', *Development*.

Calcagni, G., Digilio, M. C., Capolino, R., Dallapiccola, B. and Marino, B. (2006) 'Concordant familial segregation of atrial septal defect and Axenfeld-Rieger anomaly in father and son', *Clin Dysmorphol* 15(4): 203-6.

Campione, M., Steinbeisser, H., Schweickert, A., Deissler, K., van Bebber, F., Lowe, L. A., Nowotschin, S., Viebahn, C., Haffter, P., Kuehn, M. R. et al. (1999) 'The homeobox gene Pitx2: mediator of asymmetric left-right signaling in vertebrate heart and gut looping', *Development* 126(6): 1225-34.

Cha, J. Y., Birsoy, B., Kofron, M., Mahoney, E., Lang, S., Wylie, C. and Heasman, J. (2007) 'The role of FoxC1 in early Xenopus development', *Dev Dyn* 236(10): 2731-41.
Chalmers, A. D., Goldstone, K., Smith, J. C., Gilchrist, M., Amaya, E. and Papalopulu, N. (2005) 'A Xenopus tropicalis oligonucleotide microarray works across species using RNA from Xenopus laevis', *Mech Dev* 122(3): 355-63.

Chapman, D. L., Garvey, N., Hancock, S., Alexiou, M., Agulnik, S. I., Gibson-Brown, J., Cebra-Thomas, J., Bollag, R., Silver, L. M. and Papaionnou, V. E. (1996) 'Expression of the T-box family genes, *Tbx1-Tbx5*, during early mouse development', *Dev. Dynam.* 206: 379-390.

Chen, B., Bronson, R. T., Klaman, L. D., Hampton, T. G., Wang, J. F., Green, P. J., Magnuson, T., Douglas, P. S., Morgan, J. P. and Neel, B. G. (2000) 'Mice mutant for Egfr and Shp2 have defective cardiac semilunar valvulogenesis', *Nat Genet* 24(3): 296-9.

Chen, Y., Mironova, E., Whitaker, L. L., Edwards, L., Yost, H. J. and Ramsdell, A. F. (2004) 'ALK4 functions as a receptor for multiple TGF beta-related ligands to regulate left-right axis determination and mesoderm induction in Xenopus', *Dev Biol* 268(2): 280-94.

Chesneau, A., Sachs, L. M., Chai, N., Chen, Y., Du Pasquier, L., Loeber, J., Pollet, N., Reilly, M., Weeks, D. L. and Bronchain, O. J. (2008) 'Transgenesis procedures in Xenopus', *Biol Cell* 100(9): 503-21.

Choo, B. G., Kondrichin, I., Parinov, S., Emelyanov, A., Go, W., Toh, W. C. and Korzh, V. (2006) 'Zebrafish transgenic Enhancer TRAP line database (ZETRAP)', *BMC Dev Biol* 6: 5.
Christine, K. S. and Conlon, F. L. (2008) 'Vertebrate CASTOR is required for differentiation of cardiac precursor cells at the ventral midline', *Dev Cell* 14(4): 616-23.
Clark, K. L., Yutzey, K. E. and Benson, D. W. (2006) 'Transcription factors and congenital heart defects', *Annu Rev Physiol* 68: 97-121.

Cleaver, O. B., PAtterson, K. D. and Krieg, P. A. (1996) 'Overexpressoin of the *tinman*-related genes XNkx-2.5 and XNkx-2.3 in *Xenopus* embryos results in myocardial hyperplasia.', *Development* 122: 3549-3556.

Cross, S. J., Ching, Y. H., Li, Q. Y., Armstrong-Buisseret, L., Spranger, S., Lyonnet, S., Bonnet, D., Penttinen, M., Jonveaux, P., Leheup, B. et al. (2000) 'The mutation spectrum in Holt-Oram syndrome', *J Med Genet* 37(10): 785-7.

Cunningham, E. T., Jr., Eliott, D., Miller, N. R., Maumenee, I. H. and Green, W. R. (1998) 'Familial Axenfeld-Rieger anomaly, atrial septal defect, and sensorineural hearing loss: a possible new genetic syndrome', *Arch Ophthalmol* 116(1): 78-82.

Dagle, J. M., Sabel, J. L., Littig, J. L., Sutherland, L. B., Kolker, S. J. and Weeks, D. L. (2003) 'Pitx2c attenuation results in cardiac defects and abnormalities of intestinal orientation in developing Xenopus laevis', *Dev Biol* 262(2): 268-81.

Dagle, J. M. and Weeks, D. L. (2001) 'Oligonucleotide-based strategies to reduce gene expression', *Differentiation* 69(2-3): 75-82.

Dale, L. and Slack, J. M. (1987) 'Fate map for the 32-cell stage of Xenopus laevis', *Development* 99(4): 527-51.

Davenport, S. L., Hefner, M. A. and Mitchell, J. A. (1986) 'The spectrum of clinical features in CHARGE syndrome', *Clin Genet* 29(4): 298-310.

Davies, A. F., Mirza, G., Sekhon, G., Turnpenny, P., Leroy, F., Speleman, F., Law, C., van Regemorter, N., Vamos, E., Flinter, F. et al. (1999) 'Delineation of two distinct 6p deletion syndromes', *Hum Genet* 104(1): 64-72.

Delahaye, A., Sznajer, Y., Lyonnet, S., Elmaleh-Berges, M., Delpierre, I., Audollent, S., Wiener-Vacher, S., Mansbach, A. L., Amiel, J., Baumann, C. et al. (2007) 'Familial CHARGE syndrome because of CHD7 mutation: clinical intra- and interfamilial variability', *Clin Genet* 72(2): 112-21.

Di Felice, V. and Zummo, G. (2009) 'Tetralogy of fallot as a model to study cardiac progenitor cell migration and differentiation during heart development', *Trends Cardiovasc Med* 19(4): 130-5.

Durocher, D., Charron, F., Warren, R., Schwartz, R. J. and Nemer, M. (1997) 'The cardiac transcription factors Nkx2-5 and GATA-4 are mutual cofactors', *EMBO J* 16(18): 5687-96.

Eisen, J. S. and Smith, J. C. (2008) 'Controlling morpholino experiments: don't stop making antisense', *Development* 135(10): 1735-43.

Epstein, J. A. (2001) 'Developing models of DiGeorge syndrome', *Trends Genet* 17(10): S13-7.

Eralp, I., Lie-Venema, H., Bax, N. A., Wijffels, M. C., Van Der Laarse, A., Deruiter, M. C., Bogers, A. J., Van Den Akker, N. M., Gourdie, R. G., Schalij, M. J. et al. (2006) 'Epicardium-derived cells are important for correct development of the Purkinje fibers in the avian heart', *Anat Rec A Discov Mol Cell Evol Biol* 288(12): 1272-80.

Essner, J. J., Branford, W. W., Zhang, J. and Yost, H. J. (2000) 'Mesendoderm and left-right brain, heart and gut development are differentially regulated by pitx2 isoforms', *Development* 127(5): 1081-93.

Etkin, L., Pearman, B., Roberts, M. and Bektesh, S. L. (1984) 'Replication, integration and expression of exogenous DNA injected into fertilized eggs of Xenopus laevis', *Differentiation* 26(3): 194-202.
Etkin, L. D. and Pearman, B. (1987) 'Distribution, expression, and germline transmission of exogenous DNA sequences following microinjection into Xenopus eggs', *Development* 99: 15-23.

Etkin, L. D. and Roberts, M. (1983) 'Transmission of integrated sea urchin histone genes by nuclear transplantation in Xenopus laevis', *Science* 221(4605): 67-9.

Evans, S. M., Yelon, D., Conlon, F. L. and Kirby, M. L. (2010) 'Myocardial lineage development', *Circ Res* 107(12): 1428-44.

Feng, G. S. (1999) 'Shp-2 tyrosine phosphatase: signaling one cell or many', *Exp Cell Res* 253(1): 47-54.

Feng, G. S., Shen, R., Heng, H. H., Tsui, L. C., Kazlauskas, A. and Pawson, T. (1994) 'Receptor-binding, tyrosine phosphorylation and chromosome localization of the mouse SH2-containing phosphotyrosine phosphatase Syp', *Oncogene* 9(6): 1545-50.

Foley, A. C. and Mercola, M. (2005) 'Heart induction by Wnt antagonists depends on the homeodomain transcription factor Hex', *Genes Dev* 19(3): 387-96.

Fu, Y., Yan, W., Mohun, T. J., and Evans, S. M. (1998) 'Vertebrate tinman homologues XNkx2-3 and XNkx2-5 are required for heart formation in a functionally redundant manner', *Development* 125: 4439-4449.

Gage, P. J., Suh, H. and Camper, S. A. (1999) 'Dosage requirement of Pitx2 for development of multiple organs', *Development* 126(20): 4643-51.

Galli, D., Dominguez, J. N., Zaffran, S., Munk, A., Brown, N. A. and Buckingham, M. E. (2008) 'Atrial myocardium derives from the posterior region of the second heart field, which acquires left-right identity as Pitx2c is expressed', *Development* 135(6): 1157-67.

Garavelli, L., De Brasi, D., Verri, R., Guareschi, E., Cariola, F., Melis, D., Calcagno, G., Salvatore, F., Unger, S., Sebastio, G. et al. (2008) 'Holt-Oram syndrome associated with anomalies of the feet', *Am J Med Genet A* 146A(9): 1185-9.

Garg, V., Kathiriya, I. S., Barnes, R., Schluterman, M. K., King, I. N., Butler, C. A., Rothrock, C. R., Eapen, R. S., Hirayama-Yamada, K., Joo, K. et al. (2003) 'GATA4 mutations cause human congenital heart defects and reveal an interaction with TBX5', *Nature* 424(6947): 443-7.

Garriock, R. J., D'Agostino, S. L., Pilcher, K. C. and Krieg, P. A. (2005a) 'Wnt11-R, a protein closely related to mammalian Wnt11, is required for heart morphogenesis in Xenopus', *Dev Biol* 279(1): 179-92.

Garriock, R. J., Meadows, S. M. and Krieg, P. A. (2005b) 'Developmental expression and comparative genomic analysis of Xenopus cardiac myosin heavy chain genes', *Dev Dyn* 233(4): 1287-93.

Garrity, D. M., Childs, S. and Fishman, M. C. (2002) 'The heartstrings mutation in zebrafish causes heart/fin Tbx5 deficiency syndrome', *Development* 129(19): 4635-45.

Geach, T. J. and Zimmerman, L. B. (2010) 'Paralysis and delayed Z-disc formation in the Xenopus tropicalis unc45b mutant dicky ticker', *BMC Dev Biol* 10: 75.

Gebbia, M., Ferrero, G. B., Pilia, G., Bassi, M. T., Aylsworth, A., Penman-Splitt, M., Bird, L. M., Bamforth, J. S., Burn, J., Schlessinger, D. et al. (1997) 'X-linked situs abnormalities result from mutations in ZIC3', *Nat Genet* 17(3): 305-8.

Gessert, S. and Kuhl, M. (2009) 'Comparative gene expression analysis and fate mapping studies suggest an early segregation of cardiogenic lineages in Xenopus laevis', *Dev Biol* 334(2): 395-408.

Gittenberger-de Groot, A. C., Vrancken Peeters, M. P., Bergwerff, M., Mentink, M. M. and Poelmann, R. E. (2000) 'Epicardial outgrowth inhibition leads to compensatory mesothelial outflow tract collar and abnormal cardiac septation and coronary formation', *Circ Res* 87(11): 969-71.

Gittenberger-de Groot, A. C., Vrancken Peeters, M. P., Mentink, M. M., Gourdie, R. G. and Poelmann, R. E. (1998) 'Epicardium-derived cells contribute a novel population to the myocardial wall and the atrioventricular cushions', *Circ Res* 82(10): 1043-52.

Goetz, S. C., Brown, D. D. and Conlon, F. L. (2006) 'TBX5 is required for embryonic cardiac cell cycle progression', *Development*.

Gormley, J. P. and Nascone-Yoder, N. M. (2003) 'Left and right contributions to the Xenopus heart: implications for asymmetric morphogenesis', *Dev Genes Evol* 213(8): 390-8.

Grepin, C., Nemer, G. and Nemer, M. (1997) 'Enhanced cardiogenesis in embryonic stem cells overexpressing the GATA-4 transcription factor', *Development* 124(12): 2387-95.

Grepin, C., Robitaille, L., Antakly, T. and Nemer, M. (1995) 'Inhibition of transcription factor GATA-4 expression blocks in vitro cardiac muscle differentiation', *Mol Cell Biol* 15(8): 4095-102.

Grosso, S., Farnetani, M. A., Berardi, R., Vivarelli, R., Vanni, M., Morgese, G. and Balestri, P. (2002) 'Familial Axenfeld-Rieger anomaly, cardiac malformations, and sensorineural hearing loss: a provisionally unique genetic syndrome?', *Am J Med Genet* 111(2): 182-6.

Grow, M. W. and Krieg, P. A. (1998) 'Tinman function is essential for vertebrate heart development: elimination of cardiac differentiation by dominant inhibitory mutants of the tinman-related genes, XNkx2-3 and XNkx2-5', *Dev Biol* 204(1): 187-96.

Grunz, H. (1992) 'Suramin changes the fate of Spemann's organizer and prevents neural induction in Xenopus laevis', *Mech Dev* 38(2): 133-41.

Hamlet, M. R., Yergeau, D. A., Kuliyev, E., Takeda, M., Taira, M., Kawakami, K. and Mead, P. E. (2006) 'Tol2 transposon-mediated transgenesis in Xenopus tropicalis', *Genesis* 44(9): 438-45.

Hammer, S., Toenjes, M., Lange, M., Fischer, J. J., Dunkel, I., Mebus, S., Grimm, C. H., Hetzer, R., Berger, F. and Sperling, S. (2008) 'Characterization of TBX20 in human hearts and its regulation by TFAP2', *J Cell Biochem* 104(3): 1022-33.

Hanafusa, H., Torii, S., Yasunaga, T., Matsumoto, K. and Nishida, E. (2004) 'Shp2, an SH2-containing protein-tyrosine phosphatase, positively regulates receptor tyrosine kinase signaling by dephosphorylating and inactivating the inhibitor Sprouty', *J Biol Chem* 279(22): 22992-5.

Hang, C. T., Yang, J., Han, P., Cheng, H. L., Shang, C., Ashley, E., Zhou, B. and Chang, C. P. (2010) 'Chromatin regulation by Brg1 underlies heart muscle development and disease', *Nature* 466(7302): 62-7.

Harland, R. and Weintraub, H. (1985) 'Translation of mRNA injected into Xenopus oocytes is specifically inhibited by antisense RNA', *J Cell Biol* 101(3): 1094-9.

Harvey, R. P. and Melton, D. A. (1988) 'Microinjection of synthetic Xhox-1A homeobox mRNA disrupts somite formation in developing Xenopus embryos', *Cell* 53(5): 687-97.

Hatcher, C. J., Kim, M. S., Mah, C. S., Goldstein, M. M., Wong, B., Mikawa, T. and Basson, C. T. (2001) 'TBX5 transcription factor regulates cell proliferation during cardiogenesis', *Dev. Biol.* 230(2): 177-188.

Haworth, K. E., Kotecha, S., Mohun, T. J. and Latinkic, B. V. (2008) 'GATA4 and GATA5 are essential for heart and liver development in Xenopus embryos', *BMC Dev Biol* 8: 74.

Heasman, J., Kofron, M. and Wylie, C. (2000) 'Beta-catenin signaling activity dissected in the early Xenopus embryo: a novel antisense approach', *Dev Biol* 222(1): 124-34.

Hellsten, U., Harland, R. M., Gilchrist, M. J., Hendrix, D., Jurka, J., Kapitonov, V., Ovcharenko, I., Putnam, N. H., Shu, S., Taher, L. et al. (2010) 'The genome of the Western clawed frog Xenopus tropicalis', *Science* 328(5978): 633-6.

Hilton, E. N., Manson, F. D., Urquhart, J. E., Johnston, J. J., Slavotinek, A. M., Hedera, P., Stattin, E. L., Nordgren, A., Biesecker, L. G. and Black, G. C. (2007) 'Left-sided embryonic expression of the BCL-6 corepressor, BCOR, is required for vertebrate laterality determination', *Hum Mol Genet* 16(14): 1773-82.

Hirakow, R. (1992) 'Epicardial formation in staged human embryos', *Kaibogaku Zasshi* 67(5): 616-22.

Hiroi, Y., Kudoh, S., Monzen, K., Ikeda, Y., Yazaki, Y., Nagai, R. and Komuro, I. (2001) 'Tbx5 associates with Nkx2-5 and synergisticallly promotes cardiomyocyte differentiation', *Nature Genetics* 28(3): 276-280.

Hjalt, T. A. and Semina, E. V. (2005) 'Current molecular understanding of Axenfeld-Rieger syndrome', *Expert Rev Mol Med* 7(25): 1-17.

Ho, E. and Shimada, Y. (1978) 'Formation of the epicardium studied with the scanning electron microscope', *Dev Biol* 66(2): 579-85.

Hoffman, J. I. and Kaplan, S. (2002) 'The incidence of congenital heart disease', *J Am Coll Cardiol* 39(12): 1890-900.

Holt, M. and Oram, S. (1960) 'Familial heart disease with skeletal malformations', *Br Heart J* 22: 236-42.

Horb, M. E. and Thomsen, G. H. (1999) 'Tbx5 is essential for heart development', *Development* 126: 1739-1751.

Hurd, E. A., Capers, P. L., Blauwkamp, M. N., Adams, M. E., Raphael, Y., Poucher, H. K. and Martin, D. M. (2007) 'Loss of Chd7 function in gene-trapped reporter mice is embryonic lethal and associated with severe defects in multiple developing tissues', *Mamm Genome* 18(2): 94-104.

Iida, K., Koseki, H., Kakinuma, H., Kato, N., Mizutani-Koseki, Y., Ohuchi, H., Yoshioka, H., Noji, S., Kawamura, K., Kataoka, Y. et al. (1997) 'Essential roles of the

winged helix transcription factor MFH-1 in aortic arch patterning and skeletogenesis', *Development* 124(22): 4627-38.

Inui, M., Fukui, A., Ito, Y. and Asashima, M. (2006) 'Xapelin and Xmsr are required for cardiovascular development in Xenopus laevis', *Dev Biol* 298(1): 188-200.

Jacquier, A. and Dujon, B. (1985) 'An intron-encoded protein is active in a gene conversion process that spreads an intron into a mitochondrial gene', *Cell* 41(2): 383-94.

Jahr, M., Schlueter, J., Brand, T. and Manner, J. (2008) 'Development of the proepicardium in Xenopus laevis', *Dev Dyn* 237(10): 3088-96.
Jarvis, L. A., Toering, S. J., Simon, M. A., Krasnow, M. A. and Smith-Bolton, R. K. (2006) 'Sprouty proteins are in vivo targets of Corkscrew/SHP-2 tyrosine phosphatases', *Development* 133(6): 1133-42.

Jerome, L. A. and Papaioannou, V. E. (2001) 'DiGeorge syndrome phenotype in mice mutant for the T-box gene, Tbx1', *Nat. Genet.* 27(3): 286-291.

Jongmans, M. C., Admiraal, R. J., van der Donk, K. P., Vissers, L. E., Baas, A. F., Kapusta, L., van Hagen, J. M., Donnai, D., de Ravel, T. J., Veltman, J. A. et al. (2006) 'CHARGE syndrome: the phenotypic spectrum of mutations in the CHD7 gene', *J Med Genet* 43(4): 306-14.

Kaliakatsos, M., Giannakopoulos, A., Fryssira, H., Kanariou, M., Skiathitou, A. V., Siahanidou, T., Giannikou, K., Makrythanasis, P., Kanavakis, E. and Tzetis, M. (2010) 'Combined microdeletions and CHD7 mutation causing severe CHARGE/DiGeorge syndrome: clinical presentation and molecular investigation by array-CGH', *J Hum Genet*.

Kawakami, K., Imanaka, K., Itoh, M. and Taira, M. (2004) 'Excision of the Tol2 transposable element of the medaka fish Oryzias latipes in Xenopus laevis and Xenopus tropicalis', *Gene* 338(1): 93-8.

Kawakami, K., Shima, A. and Kawakami, N. (2000) 'Identification of a functional transposase of the Tol2 element, an Ac-like element from the Japanese medaka fish, and its transposition in the zebrafish germ lineage', *Proc Natl Acad Sci U S A* 97(21): 11403-8.

Kieserman, E. K., Lee, C., Gray, R. S., Park, T. J. and Wallingford, J. B. (2010) 'High-magnification in vivo imaging of Xenopus embryos for cell and developmental biology', *Cold Spring Harb Protoc* 2010(5): pdb prot5427.

Kirk, E. P., Sunde, M., Costa, M. W., Rankin, S. A., Wolstein, O., Castro, M. L., Butler, T. L., Hyun, C., Guo, G., Otway, R. et al. (2007) 'Mutations in cardiac T-box factor gene TBX20 are associated with diverse cardiac pathologies, including

defects of septation and valvulogenesis and cardiomyopathy', *Am J Hum Genet* 81(2): 280-91.

Kitaguchi, T., Mizugishi, K., Hatayama, M., Aruga, J. and Mikoshiba, K. (2002) 'Xenopus Brachyury regulates mesodermal expression of Zic3, a gene controlling left-right asymmetry', *Dev Growth Differ* 44(1): 55-61.

Kitaguchi, T., Nagai, T., Nakata, K., Aruga, J. and Mikoshiba, K. (2000) 'Zic3 is involved in the left-right specification of the Xenopus embryo', *Development* 127(22): 4787-95.

Knudsen, H. and Nielsen, P. E. (1996) 'Antisense properties of duplex- and triplex-forming PNAs', *Nucleic Acids Res* 24(3): 494-500.

Kochilas, L., Merscher-Gomez, S., Lu, M. M., Potluri, V., Liao, J., Kucherlapati, R., Morrow, B. and Epstein, J. A. (2002) 'The role of neural crest during cardiac development in a mouse model of DiGeorge syndrome', *Dev Biol* 251(1): 157-66.

Kochilas, L. K., Potluri, V., Gitler, A., Balasubramanian, K. and Chin, A. J. (2003) 'Cloning and characterization of zebrafish tbx1', *Gene Expr Patterns* 3(5): 645-51.

Kolker, S. J., Tajchman, U. and Weeks, D. L. (2000) 'Confocal imaging of early heart development in Xenopus laevis', *Dev Biol* 218(1): 64-73.

Kosaki, K., Suzuki, T., Muroya, K., Hasegawa, T., Sato, S., Matsuo, N., Kosaki, R., Nagai, T., Hasegawa, Y. and Ogata, T. (2002) 'PTPN11 (protein-tyrosine phosphatase, nonreceptor-type 11) mutations in seven Japanese patients with Noonan syndrome', *J Clin Endocrinol Metab* 87(8): 3529-33.

Koster, M., Dillinger, K. and Knochel, W. (1998) 'Expression pattern of the winged helix factor XFD-11 during Xenopus embryogenesis', *Mech Dev* 76(1-2): 169-73.

Kratz, C. P., Niemeyer, C. M., Castleberry, R. P., Cetin, M., Bergstrasser, E., Emanuel, P. D., Hasle, H., Kardos, G., Klein, C., Kojima, S. et al. (2005) 'The mutational spectrum of PTPN11 in juvenile myelomonocytic leukemia and Noonan syndrome/myeloproliferative disease', *Blood* 106(6): 2183-5.

Krebs, L. T., Iwai, N., Nonaka, S., Welsh, I. C., Lan, Y., Jiang, R., Saijoh, Y., O'Brien, T. P., Hamada, H. and Gridley, T. (2003) 'Notch signaling regulates left-right asymmetry determination by inducing Nodal expression', *Genes Dev* 17(10): 1207-12.

Krenz, M., Yutzey, K. E. and Robbins, J. (2005) 'Noonan syndrome mutation Q79R in Shp2 increases proliferation of valve primordia mesenchymal cells via extracellular signal-regulated kinase 1/2 signaling', *Circ Res* 97(8): 813-20.

Kroll, K. L. and Amaya, E. (1996a) 'Transgenic Xenopus embryos from sperm nuclear transplantations reveal FGF signaling requirements during gastrulation', *Development* 122(10): 3173-83.

Kroll, K. L. and Amaya, E. (1996b) 'Transgenic *Xenopus* embryos from sperm nuclear transplantations reveal FGF signalling requirements during gastrulation', *Development* 122: 3173-3183.

Kumano, G., Ezal, C. and Smith, W. C. (2006) 'ADMP2 is essential for primitive blood and heart development in Xenopus', *Dev Biol* 299(2): 411-23.

Kume, T., Jiang, H., Topczewska, J. M. and Hogan, B. L. (2001) 'The murine winged helix transcription factors, Foxc1 and Foxc2, are both required for cardiovascular development and somitogenesis', *Genes Dev* 15(18): 2470-82.
Kuo, C. T., Morrisey, E. E., Anandappa, R., Sigrist, K., Lu, M. M., Parmacek, M. S., Soudais, C. and Leiden, J. M. (1997) 'GATA4 transcription factor is required for ventral morphogenesis and heart tube formation', *Genes Dev* 11(8): 1048-60.

Lalani, S. R., Safiullah, A. M., Fernbach, S. D., Harutyunyan, K. G., Thaller, C., Peterson, L. E., McPherson, J. D., Gibbs, R. A., White, L. D., Hefner, M. et al. (2006) 'Spectrum of CHD7 mutations in 110 individuals with CHARGE syndrome and genotype-phenotype correlation', *Am J Hum Genet* 78(2): 303-14.
Langdon, Y. G., Goetz, S. C., Berg, A. E., Swanik, J. T. and Conlon, F. L. (2007) 'SHP-2 is required for the maintenance of cardiac progenitors', *Development* 134(22): 4119-30.

Latinkić , B. V., Cooper, B., Smith, S., Kotecha, S., Towers, N., Sparrow, D. and Mohun, T. J. (2004) 'Transcriptional regulation of the cardiac-specific MLC2 gene during Xenopus embryonic development', *Development* 131(3): 669-79.

Latinkić, B. V., Cooper, B., Towers, N., Sparrow, D., Kotecha, S. and Mohun, T. J. (2002) 'Distinct enhancers regulate skeletal and cardiac muscle-specific expression programs of the cardiac alpha-actin gene in Xenopus embryos', *Dev Biol* 245(1): 57-70.

Layman, W. S., McEwen, D. P., Beyer, L. A., Lalani, S. R., Fernbach, S. D., Oh, E., Swaroop, A., Hegg, C. C., Raphael, Y., Martens, J. R. et al. (2009) 'Defects in neural stem cell proliferation and olfaction in Chd7 deficient mice indicate a mechanism for hyposmia in human CHARGE syndrome', *Hum Mol Genet* 18(11): 1909-23.

Lee, Y., Shioi, T., Kasahara, H., Jobe, S. M., Wiese, R. J., Markham, B. E. and Izumo, S. (1998) 'The cardiac tissue-restricted homeobox protein Csx/Nkx2.5 physically associates with the zinc finger protein GATA4 and cooperatively activates atrial natriuretic factor gene expression', *Mol Cell Biol* 18(6): 3120-9.

Lehner, R., Goharkhay, N., Tringler, B., Fasching, C. and Hengstschlager, M. (2003) 'Pedigree analysis and descriptive investigation of three classic phenotypes associated with Holt-Oram syndrome', *J Reprod Med* 48(3): 153-9.

Lepilina, A., Coon, A. N., Kikuchi, K., Holdway, J. E., Roberts, R. W., Burns, C. G. and Poss, K. D. (2006) 'A dynamic epicardial injury response supports progenitor cell activity during zebrafish heart regeneration', *Cell* 127(3): 607-19.

Li, Q. Y., Newbury Ecob, R. A., Terrett, J. A., Wilson, D. I., Curtis, A. R., Yi, C. H., Gebuhr, T., Bullen, P. J., Robson, S. C., Strachan, T. et al. (1997) 'Holt-Oram syndrome is caused by mutations in TBX5, a member of the Brachyury (T) gene family', *Nat. Genet.* 15(1): 21-29.

Liberatore, C. M., Searcy-Schrick, R. D. and Yutzey, K. E. (2000) 'Ventricular expression of tbx5 inhibits normal heart chamber development', *Dev Biol* 223(1): 169-80.

Lie-Venema, H., Eralp, I., Maas, S., Gittenberger-De Groot, A. C., Poelmann, R. E. and DeRuiter, M. C. (2005) 'Myocardial heterogeneity in permissiveness for epicardium-derived cells and endothelial precursor cells along the developing heart tube at the onset of coronary vascularization', *Anat Rec A Discov Mol Cell Evol Biol* 282(2): 120-9.

Lie-Venema, H., van den Akker, N. M., Bax, N. A., Winter, E. M., Maas, S., Kekarainen, T., Hoeben, R. C., deRuiter, M. C., Poelmann, R. E. and Gittenberger-de Groot, A. C. (2007) 'Origin, fate, and function of epicardium-derived cells (EPDCs) in normal and abnormal cardiac development', *ScientificWorldJournal* 7: 1777-98.

Lin, A. E., Ticho, B. S., Houde, K., Westgate, M. N. and Holmes, L. B. (2000) 'Heterotaxy: associated conditions and hospital-based prevalence in newborns', *Genet Med* 2(3): 157-72.

Lin, C. R., Kioussi, C., O'Connell, S., Briata, P., Szeto, D., Liu, F., Izpisua-Belmonte, J. C. and Rosenfeld, M. G. (1999) 'Pitx2 regulates lung asymmetry, cardiac positioning and pituitary and tooth morphogenesis', *Nature* 401(6750): 279-82.

Lindsay, E. A. and Baldini, A. (2001) 'Recovery from arterial growth delay reduces penetrance of cardiovascular defects in mice deleted for the DiGeorge syndrome region', *Hum Mol Genet* 10(9): 997-1002.

Lindsay, E. A., Botta, A., Jurecic, V., Carattini-Rivera, S., Cheah, Y. C., Rosenblatt, H. M., Bradley, A. and Baldini, A. (1999) 'Congenital heart disease in mice deficient for the DiGeorge syndrome region', *Nature* 401(6751): 379-83.

Lindsay, E. A., Vitelli, F., Su, H., Morishima, M., Huynh, T., Pramparo, T., Jurecic, V., Ogunrinu, G., Sutherland, H. F., Scambler, P. J. et al. (2001a) 'Tbx1 haploinsufficiency in the DiGeorge syndrome region causes aortic arch defects in mice', *Nature* 410(6824): 97-101.

Lindsay, E. A., Vitelli, F., Su, H., Morishima, M., Huynh, T., Pramparo, T., Jurecic, V., Ogunrinu, G., Sutherland, H. F., Scambler, P. J. et al. (2001b) 'Tbx1 haploinsufficieny in the DiGeorge syndrome region causes aortic arch defects in mice', *Nature* 410(6824): 97-101.

Liu, C., Liu, W., Palie, J., Lu, M. F., Brown, N. A. and Martin, J. F. (2002) 'Pitx2c patterns anterior myocardium and aortic arch vessels and is required for local cell movement into atrioventricular cushions', *Development* 129(21): 5081-91.

Liu, C., Shen, A., Li, X., Jiao, W., Zhang, X. and Li, Z. (2008) 'T-box transcription factor TBX20 mutations in Chinese patients with congenital heart disease', *Eur J Med Genet* 51(6): 580-7.

Logan, M. and Mohun, T. (1993) 'Induction of cardiac muscle differentiation in isolated animal pole explants of Xenopus laevis embryos', *Development* 118(3): 865-875.

Loh, M. L., Reynolds, M. G., Vattikuti, S., Gerbing, R. B., Alonzo, T. A., Carlson, E., Cheng, J. W., Lee, C. M., Lange, B. J. and Meshinchi, S. (2004) 'PTPN11 mutations in pediatric patients with acute myeloid leukemia: results from the Children's Cancer Group', *Leukemia* 18(11): 1831-4.

Lu, M. F., Pressman, C., Dyer, R., Johnson, R. L. and Martin, J. F. (1999) 'Function of Rieger syndrome gene in left-right asymmetry and craniofacial development', *Nature* 401(6750): 276-8.

Lyons, I., et al. (1995) 'Myogenic and morphogenic defects in the heart tubes of murine embrryos lacking thehomeobox gene Nkx-2.5', *Genes Dev.* 9: 1654-1666.

Maclean, K., Smith, J., St Heaps, L., Chia, N., Williams, R., Peters, G. B., Onikul, E., McCrossin, T., Lehmann, O. J. and Ades, L. C. (2005) 'Axenfeld-Rieger malformation and distinctive facial features: Clues to a recognizable 6p25 microdeletion syndrome', *Am J Med Genet A* 132(4): 381-5.

Maheshwari, M., Belmont, J., Fernbach, S., Ho, T., Molinari, L., Yakub, I., Yu, F., Combes, A., Towbin, J., Craigen, W. J. et al. (2002) 'PTPN11 mutations in Noonan syndrome type I: detection of recurrent mutations in exons 3 and 13', *Hum Mutat* 20(4): 298-304.

Mammi, I., De Giorgio, P., Clementi, M. and Tenconi, R. (1998) 'Cardiovascular anomaly in Rieger Syndrome: heterogeneity or contiguity?', *Acta Ophthalmol Scand* 76(4): 509-12.

Mandel, E. M., Kaltenbrun, E., Callis, T. E., Zeng, X. X., Marques, S. R., Yelon, D., Wang, D. Z. and Conlon, F. L. (2010) 'The BMP pathway acts to directly regulate Tbx20 in the developing heart', *Development* 137(11): 1919-29.

Manner, J. (2000) 'Cardiac looping in the chick embryo: a morphological review with special reference to terminological and biomechanical aspects of the looping process', *Anat Rec* 259(3): 248-62.

Manner, J. (2009) 'The anatomy of cardiac looping: a step towards the understanding of the morphogenesis of several forms of congenital cardiac malformations', *Clin Anat* 22(1): 21-35.

Manner, J., Perez-Pomares, J. M., Macias, D. and Munoz-Chapuli, R. (2001) 'The origin, formation and developmental significance of the epicardium: a review', *Cells Tissues Organs* 169(2): 89-103.

Manner, J., Schlueter, J. and Brand, T. (2005) 'Experimental analyses of the function of the proepicardium using a new microsurgical procedure to induce loss-of-proepicardial-function in chick embryos', *Dev Dyn* 233(4): 1454-63.

Mariampillai, A., Standish, B. A., Munce, N. R., Randall, C., Liu, G., Jiang, J. Y., Cable, A. E., Vitkin, I. A. and Yang, V. X. (2007) 'Doppler optical cardiogram gated 2D color flow imaging at 1000 fps and 4D in vivo visualization of embryonic heart at 45 fps on a swept source OCT system', *Opt Express* 15(4): 1627-38.

McDermott, D. A., Bressan, M. C., He, J., Lee, J. S., Aftimos, S., Brueckner, M., Gilbert, F., Graham, G. E., Hannibal, M. C., Innis, J. W. et al. (2005) 'TBX5 genetic testing validates strict clinical criteria for Holt-Oram syndrome', *Pediatr Res* 58(5): 981-6.

Melton, D. A. (1985) 'Injected anti-sense RNAs specifically block messenger RNA translation in vivo', *Proc Natl Acad Sci U S A* 82(1): 144-8.

Mercola, M. (1999) 'Embryological basis for cardiac left-right asymmetry', *Semin Cell Dev Biol* 10(1): 109-16.

Merki, E., Zamora, M., Raya, A., Kawakami, Y., Wang, J., Zhang, X., Burch, J., Kubalak, S. W., Kaliman, P., Belmonte, J. C. et al. (2005) 'Epicardial retinoid X receptor alpha is required for myocardial growth and coronary artery formation', *Proc Natl Acad Sci U S A* 102(51): 18455-60.

Merscher, S., Funke, B., Epstein, J. A., Heyer, J., Puech, A., Lu, M. M., Xavier, R. J., Demay, M. B., Russell, R. G., Factor, S. et al. (2001) 'TBX1 is responsible for cardiovascular defects in velo-cardio- facial/DiGeorge syndrome', *Cell* 104(4): 619-29.

Mohun, T. J., Leong, L.M., Weninger, W. J., and Sparrow, D. B. (2000) 'The Morphology of Heart Development in Xenopus laevis', *Developmental Biology* 218: 74-88.

Molkentin, J. D., Lin, Q., Duncan, S. A. and Olson, E. N. (1997) 'Requirement of the transcription factor GATA4 for heart tube formation and ventral morphogenesis', *Genes Dev* 11(8): 1061-72.

Momma, K. (2010) 'Cardiovascular anomalies associated with chromosome 22q11.2 deletion syndrome', *Am J Cardiol* 105(11): 1617-24.

Moody, S. A. (1987) 'Fates of the blastomeres of the 32-cell-stage Xenopus embryo', *Dev Biol* 122(2): 300-19.

Moore, A. W., Schedl, A., McInnes, L., Doyle, M., Hecksher-Sorensen, J. and Hastie, N. D. (1998) 'YAC transgenic analysis reveals Wilms' tumour 1 gene activity in the proliferating coelomic epithelium, developing diaphragm and limb', *Mech Dev* 79(1-2): 169-84.

Morcos, P. A. (2007) 'Achieving targeted and quantifiable alteration of mRNA splicing with Morpholino oligos', *Biochem Biophys Res Commun* 358(2): 521-7.

Moskowitz, I. P., Pizard, A., Patel, V. V., Bruneau, B. G., Kim, J. B., Kupershmidt, S., Roden, D., Berul, C. I., Seidman, C. E. and Seidman, J. G. (2004) 'The T-Box transcription factor Tbx5 is required for the patterning and maturation of the murine cardiac conduction system', *Development* 131(16): 4107-16.

Moulton, J. D. (2007) 'Using morpholinos to control gene expression', *Curr Protoc Nucleic Acid Chem* Chapter 4: Unit 4 30.

Movassagh, M. and Philpott, A. (2008) 'Cardiac differentiation in Xenopus requires the cyclin-dependent kinase inhibitor, p27Xic1', *Cardiovasc Res* 79(3): 436-47.

Musante, L., Kehl, H. G., Majewski, F., Meinecke, P., Schweiger, S., Gillessen-Kaesbach, G., Wieczorek, D., Hinkel, G. K., Tinschert, S., Hoeltzenbein, M. et al. (2003) 'Spectrum of mutations in PTPN11 and genotype-phenotype correlation in 96 patients with Noonan syndrome and five patients with cardio-facio-cutaneous syndrome', *Eur J Hum Genet* 11(2): 201-6.

Nagao, K., Taniyama, Y., Kietzmann, T., Doi, T., Komuro, I. and Morishita, R. (2008) 'HIF-1alpha signaling upstream of NKX2.5 is required for cardiac development in Xenopus', *J Biol Chem* 283(17): 11841-9.

Newbury-Ecob, R. A., Leanage, R., Raeburn, J. A. and Young, I. D. (1996) 'Holt-Oram syndrome: a clinical genetic study', *J Med Genet* 33(4): 300-7.

Noonan, J. A. (1968) 'Hypertelorism with Turner phenotype. A new syndrome with associated congenital heart disease', *Am J Dis Child* 116(4): 373-80.

Noonan, J. A. (1994) 'Noonan syndrome. An update and review for the primary pediatrician', *Clin Pediatr (Phila)* 33(9): 548-55.

Ogino, H., McConnell, W. B. and Grainger, R. M. (2006) 'Highly efficient transgenesis in Xenopus tropicalis using I-SceI meganuclease', *Mech Dev* 123(2): 103-13.

Pan, F. C., Chen, Y., Loeber, J., Henningfeld, K. and Pieler, T. (2006) 'I-SceI meganuclease-mediated transgenesis in Xenopus', *Dev Dyn* 235(1): 247-52.

Pandur, P., Lasche, M., Eisenberg, L. M. and Kuhl, M. (2002) 'Wnt-11 activation of a non-canonical Wnt signalling pathway is required for cardiogenesis', *Nature* 418(6898): 636-41.

Parinov, S., Kondrichin, I., Korzh, V. and Emelyanov, A. (2004) 'Tol2 transposon-mediated enhancer trap to identify developmentally regulated zebrafish genes in vivo', *Dev Dyn* 231(2): 449-59.

Pehlivan, T., Pober, B. R., Brueckner, M., Garrett, S., Slaugh, R., Van Rheeden, R., Wilson, D. B., Watson, M. S. and Hing, A. V. (1999) 'GATA4 haploinsufficiency in patients with interstitial deletion of chromosome region 8p23.1 and congenital heart disease', *Am J Med Genet* 83(3): 201-6.

Perez-Pomares, J. M., Phelps, A., Sedmerova, M., Carmona, R., Gonzalez-Iriarte, M., Munoz-Chapuli, R. and Wessels, A. (2002) 'Experimental studies on the spatiotemporal expression of WT1 and RALDH2 in the embryonic avian heart: a model for the regulation of myocardial and valvuloseptal development by epicardially derived cells (EPDCs)', *Dev Biol* 247(2): 307-26.

Peterkin, T., Gibson, A. and Patient, R. (2007) 'Redundancy and evolution of GATA factor requirements in development of the myocardium', *Dev Biol* 311(2): 623-35.

Plageman, T. F., Jr. and Yutzey, K. E. (2004) 'Differential expression and function of tbx5 and tbx20 in cardiac development', *J Biol Chem* 279(18): 19026-34.

Pombal, M. A., Carmona, R., Megias, M., Ruiz, A., Perez-Pomares, J. M. and Munoz-Chapuli, R. (2008) 'Epicardial development in lamprey supports an evolutionary origin of the vertebrate epicardium from an ancestral pronephric external glomerulus', *Evol Dev* 10(2): 210-6.

Posch, M. G., Gramlich, M., Sunde, M., Schmitt, K. R., Lee, S. H., Richter, S., Kersten, A., Perrot, A., Panek, A. N., Al Khatib, I. H. et al. 'A gain-of-function TBX20 mutation causes congenital atrial septal defects, patent foramen ovale and cardiac valve defects', *J Med Genet* 47(4): 230-5.

Purandare, S. M., Ware, S. M., Kwan, K. M., Gebbia, M., Bassi, M. T., Deng, J. M., Vogel, H., Behringer, R. R., Belmont, J. W. and Casey, B. (2002) 'A complex syndrome of left-right axis, central nervous system and axial skeleton defects in Zic3 mutant mice', *Development* 129(9): 2293-302.

Qian, L., Mohapatra, B., Akasaka, T., Liu, J., Ocorr, K., Towbin, J. A. and Bodmer, R. (2008) 'Transcription factor neuromancer/TBX20 is required for cardiac function in Drosophila with implications for human heart disease', *Proc Natl Acad Sci U S A* 105(50): 19833-8.

Qu, C. K. (2000) 'The SHP-2 tyrosine phosphatase: signaling mechanisms and biological functions', *Cell Res* 10(4): 279-88.

Raffin, M., Leong, L. M., Rones, M. S., Sparrow, D., Mohun, T. and Mercola, M. (2000) 'Subdivision of the cardiac Nkx2.5 expression domain into myogenic and nonmyogenic compartments', *Dev Biol* 218(2): 326-40.

Ramsdell, A. F., Bernanke, J. M. and Trusk, T. C. (2006) 'Left-right lineage analysis of the embryonic Xenopus heart reveals a novel framework linking congenital cardiac defects and laterality disease', *Development* 133(7): 1399-410.

Raya, A., Kawakami, Y., Rodriguez-Esteban, C., Buscher, D., Koth, C. M., Itoh, T., Morita, M., Raya, R. M., Dubova, I., Bessa, J. G. et al. (2003) 'Notch activity induces Nodal expression and mediates the establishment of left-right asymmetry in vertebrate embryos', *Genes Dev* 17(10): 1213-8.

Rusconi, S. and Schaffner, W. (1981) 'Transformation of frog embryos with a rabbit beta-globin gene', *Proc Natl Acad Sci U S A* 78(8): 5051-5.

Ryan, A. K., Blumberg, B., Rodriguez-Esteban, C., Yonei-Tamura, S., Tamura, K., Tsukui, T., de la Pena, J., Sabbagh, W., Greenwald, J., Choe, S. et al. (1998) 'Pitx2 determines left-right asymmetry of internal organs in vertebrates', *Nature* 394(6693): 545-51.

Sauka-Spengler, T. and Bronner-Fraser, M. (2008) 'A gene regulatory network orchestrates neural crest formation', *Nat Rev Mol Cell Biol* 9(7): 557-68.

Sauka-Spengler, T., Le Mentec, C., Lepage, M. and Mazan, S. (2002) 'Embryonic expression of Tbx1, a DiGeorge syndrome candidate gene, in the lamprey Lampetra fluviatilis', *Gene Expr Patterns* 2(1-2): 99-103.

Saxton, T. M., Henkemeyer, M., Gasca, S., Shen, R., Rossi, D. J., Shalaby, F., Feng, G. S. and Pawson, T. (1997) 'Abnormal mesoderm patterning in mouse embryos mutant for the SH2 tyrosine phosphatase Shp-2', *EMBO J* 16(9): 2352-64.

Saxton, T. M. and Pawson, T. (1999) 'Morphogenetic movements at gastrulation require the SH2 tyrosine phosphatase Shp2', *Proc Natl Acad Sci U S A* 96(7): 3790-5.

Schneider, V. A. and Mercola, M. (2001) 'Wnt antagonism initiates cardiogenesis in Xenopus laevis', *Genes Dev* 15(3): 304-15.

Schott, J., Benson, D. W., Bassson, C. T., Pease, W., Silberbach, S., Moak, J. P., Maron, B. J., Seidman, C. E. and Seidman, J. G. (1998) 'Congenital Heart Disease Caused by Mutations in the Transcription Factor NKX2-5', *Science* 281: 108-111.

Schweickert, A., Campione, M., Steinbeisser, H. and Blum, M. (2000) 'Pitx2 isoforms: involvement of Pitx2c but not Pitx2a or Pitx2b in vertebrate left-right asymmetry', *Mechanisms of Development* 90(1): 41-51.

Seo, S., Fujita, H., Nakano, A., Kang, M., Duarte, A. and Kume, T. (2006) 'The forkhead transcription factors, Foxc1 and Foxc2, are required for arterial specification and lymphatic sprouting during vascular development', *Dev Biol* 294(2): 458-70.

Seo, S. and Kume, T. (2006) 'Forkhead transcription factors, Foxc1 and Foxc2, are required for the morphogenesis of the cardiac outflow tract', *Dev Biol* 296(2): 421-36.

Sepulveda, J. L., Belaguli, N., Nigam, V., Chen, C. Y., Nemer, M. and Schwartz, R. J. (1998) 'GATA-4 and Nkx-2.5 coactivate Nkx-2 DNA binding targets: role for regulating early cardiac gene expression', *Mol Cell Biol* 18(6): 3405-15.
Serluca, F. C. (2008) 'Development of the proepicardial organ in the zebrafish', *Dev Biol* 315(1): 18-27.

Showell, C., Christine, K. S., Mandel, E. M. and Conlon, F. L. (2006) 'Developmental expression patterns of Tbx1, Tbx2, Tbx5, and Tbx20 in Xenopus tropicalis', *Dev Dyn* 235(6): 1623-30.

Showell, C. and Conlon, F. L. (2007) 'Decoding development in Xenopus tropicalis', *Genesis* 45(6): 418-26.

Siebert, J. R., Graham, J. M., Jr. and MacDonald, C. (1985) 'Pathologic features of the CHARGE association: support for involvement of the neural crest', *Teratology* 31(3): 331-6.
Singh, M. K., Christoffels, V. M., Dias, J. M., Trowe, M. O., Petry, M., Schuster-Gossler, K., Burger, A., Ericson, J. and Kispert, A. (2005) 'Tbx20 is essential for cardiac chamber differentiation and repression of Tbx2', *Development* 132(12): 2697-707.

Sinzelle, L., Vallin, J., Coen, L., Chesneau, A., Du Pasquier, D., Pollet, N., Demeneix, B. and Mazabraud, A. (2006) 'Generation of trangenic Xenopus laevis using the Sleeping Beauty transposon system', *Transgenic Res* 15(6): 751-60.

Sletten, L. J. and Pierpont, M. E. (1996) 'Variation in severity of cardiac disease in Holt-Oram syndrome', *Am J Med Genet* 65(2): 128-32.

Small, E. M. and Krieg, P. A. (2003) 'Transgenic analysis of the atrialnatriuretic factor (ANF) promoter: Nkx2-5 and GATA-4 binding sites are required for atrial specific expression of ANF', *Dev Biol* 261(1): 116-31.

Small, E. M., Warkman, A. S., Wang, D. Z., Sutherland, L. B., Olson, E. N. and Krieg, P. A. (2005) 'Myocardin is sufficient and necessary for cardiac gene expression in Xenopus', *Development* 132(5): 987-97.

Smith, S. J., Ataliotis, P., Kotecha, S., Towers, N., Sparrow, D. B. and Mohun, T. J. (2005) 'The MLC1v gene provides a transgenic marker of myocardium formation within developing chambers of the Xenopus heart', *Dev Dyn* 232(4): 1003-12.

Smith, S. J., Fairclough, L., Latinkic, B. V., Sparrow, D. B. and Mohun, T. J. (2006) 'Xenopus laevis transgenesis by sperm nuclear injection', *Nat Protoc* 1(5): 2195-203.

Sparrow, D. B., Cai, C., Kotecha, S., Latinkic, B., Cooper, B., Towers, N., Evans, S. M. and Mohun, T. J. (2000) 'Regulation of the tinman homologues in Xenopus embryos', *Dev Biol* 227(1): 65-79.

Starr, J. P. (2010) 'Tetralogy of fallot: yesterday and today', *World J Surg* 34(4): 658-68.

Stennard, F. A., Costa, M. W., Elliott, D. A., Rankin, S., Haast, S. J., Lai, D., McDonald, L. P., Niederreither, K., Dolle, P., Bruneau, B. G. et al. (2003) 'Cardiac T-box factor Tbx20 directly interacts with Nkx2-5, GATA4, and GATA5 in regulation of gene expression in the developing heart', *Dev Biol* 262(2): 206-24.

Stennard, F. A., Costa, M. W., Lai, D., Biben, C., Furtado, M. B., Solloway, M. J., McCulley, D. J., Leimena, C., Preis, J. I., Dunwoodie, S. L. et al. (2005) 'Murine T-box transcription factor Tbx20 acts as a repressor during heart development, and is essential for adult heart integrity, function and adaptation', *Development*.

Sucov, H. M., Gu, Y., Thomas, S., Li, P. and Pashmforoush, M. (2009) 'Epicardial control of myocardial proliferation and morphogenesis', *Pediatr Cardiol* 30(5): 617-25.

Summerton, J. E. (2007) 'Morpholino, siRNA, and S-DNA compared: impact of structure and mechanism of action on off-target effects and sequence specificity', *Curr Top Med Chem* 7(7): 651-60.

Sutherland, M. J. and Ware, S. M. (2009) 'Disorders of left-right asymmetry: heterotaxy and situs inversus', *Am J Med Genet C Semin Med Genet* 151C(4): 307-17.

Svensson, E. C., Huggins, G. S., Dardik, F. B., Polk, C. E. and Leiden, J. M. (2000) 'A functionally conserved N-terminal domain of the friend of GATA-2 (FOG-2) protein represses GATA4-dependent transcription', *J Biol Chem* 275(27): 20762-9.

Swiderski, R. E., Reiter, R. S., Nishimura, D. Y., Alward, W. L., Kalenak, J. W., Searby, C. S., Stone, E. M., Sheffield, V. C. and Lin, J. J. (1999) 'Expression of the Mf1 gene in developing mouse hearts: implication in the development of human congenital heart defects', *Dev Dyn* 216(1): 16-27.

Szeto, D. P., Griffin, K. J. and Kimelman, D. (2002) 'HrT is required for cardiovascular development in zebrafish', *Development* 129(21): 5093-101.

Sznajer, Y., Keren, B., Baumann, C., Pereira, S., Alberti, C., Elion, J., Cave, H. and Verloes, A. (2007) 'The spectrum of cardiac anomalies in Noonan syndrome as a result of mutations in the PTPN11 gene', *Pediatrics* 119(6): e1325-31.

Tabin, C. J. and Vogan, K. J. (2003) 'A two-cilia model for vertebrate left-right axis specification', *Genes Dev* 17(1): 1-6.

Takeuchi, J. K., Mileikovskaia, M., Koshiba-Takeuchi, K., Heidt, A. B., Mori, A. D., Arruda, E. P., Gertsenstein, M., Georges, R., Davidson, L., Mo, R. et al. (2005) 'Tbx20 dose-dependently regulates transcription factor networks required for mouse heart and motoneuron development', *Development*.

Tang, T. L., Freeman, R. M., Jr., O'Reilly, A. M., Neel, B. G. and Sokol, S. Y. (1995) 'The SH2-containing protein-tyrosine phosphatase SH-PTP2 is required upstream of MAP kinase for early Xenopus development', *Cell* 80(3): 473-83.
Tartaglia, M., Kalidas, K., Shaw, A., Song, X., Musat, D. L., van der Burgt, I., Brunner, H. G., Bertola, D. R., Crosby, A., Ion, A. et al. (2002) 'PTPN11 mutations in Noonan syndrome: molecular spectrum, genotype-phenotype correlation, and phenotypic heterogeneity', *Am J Hum Genet* 70(6): 1555-63.

Tartaglia, M., Mehler, E. L., Goldberg, R., Zampino, G., Brunner, H. G., Kremer, H., van der Burgt, I., Crosby, A. H., Ion, A., Jeffery, S. et al. (2001) 'Mutations in PTPN11, encoding the protein tyrosine phosphatase SHP-2, cause Noonan syndrome', *Nat Genet* 29(4): 465-8.

Tartaglia, M., Niemeyer, C. M., Fragale, A., Song, X., Buechner, J., Jung, A., Hahlen, K., Hasle, H., Licht, J. D. and Gelb, B. D. (2003) 'Somatic mutations in PTPN11 in juvenile myelomonocytic leukemia, myelodysplastic syndromes and acute myeloid leukemia', *Nat Genet* 34(2): 148-50.

Tevosian, S. G., Deconinck, A. E., Tanaka, M., Schinke, M., Litovsky, S. H., Izumo, S., Fujiwara, Y. and Orkin, S. H. (2000) 'FOG-2, a cofactor for GATA transcription factors, is essential for heart morphogenesis and development of coronary vessels from epicardium', *Cell* 101(7): 729-39.

Toyoizumi, R., Takeuchi, S. and Mogi, K. (2006) 'Subtilisin-like proprotein convertase activity is necessary for left-right axis determination in Xenopus neurula embryos', *Dev Genes Evol* 216(10): 607-22.

Van Vactor, D., O'Reilly, A. M. and Neel, B. G. (1998) 'Genetic analysis of protein tyrosine phosphatases', *Curr Opin Genet Dev* 8(1): 112-26.

Viragh, S. and Challice, C. E. (1981) 'The origin of the epicardium and the embryonic myocardial circulation in the mouse', *Anat Rec* 201(1): 157-68.

Vissers, L. E., van Ravenswaaij, C. M., Admiraal, R., Hurst, J. A., de Vries, B. B., Janssen, I. M., van der Vliet, W. A., Huys, E. H., de Jong, P. J., Hamel, B. C. et al. (2004) 'Mutations in a new member of the chromodomain gene family cause CHARGE syndrome', *Nat Genet* 36(9): 955-7.

Vitelli, F., Taddei, I., Morishima, M., Meyers, E. N., Lindsay, E. A. and Baldini, A. (2002) 'A genetic link between Tbx1 and fibroblast growth factor signaling', *Development* 129(19): 4605-11.

Waldo, K. L., Kumiski, D. H., Wallis, K. T., Stadt, H. A., Hutson, M. R., Platt, D. H. and Kirby, M. L. (2001) 'Conotruncal myocardium arises from a secondary heart field', *Development* 128(16): 3179-88.

Ware, S. M., Peng, J., Zhu, L., Fernbach, S., Colicos, S., Casey, B., Towbin, J. and Belmont, J. W. (2004) 'Identification and functional analysis of ZIC3 mutations in heterotaxy and related congenital heart defects', *Am J Hum Genet* 74(1): 93-105.
Warkman, A. S. and Krieg, P. A. (2006) 'Xenopus as a model system for vertebrate heart development', *Semin Cell Dev Biol*.

Weisschuh, N., Wolf, C., Wissinger, B. and Gramer, E. (2008) 'A novel mutation in the FOXC1 gene in a family with Axenfeld-Rieger syndrome and Peters' anomaly', *Clin Genet* 74(5): 476-80.

Wessels, K., Bohnhorst, B., Luhmer, I., Morlot, S., Bohring, A., Jonasson, J., Epplen, J. T., Gadzicki, D., Glaser, S., Gohring, G. et al. (2010) 'Novel CHD7 mutations contributing to the mutation spectrum in patients with CHARGE syndrome', *Eur J Med Genet*.

Wincent, J., Holmberg, E., Stromland, K., Soller, M., Mirzaei, L., Djureinovic, T., Robinson, K., Anderlid, B. and Schoumans, J. (2008) 'CHD7 mutation spectrum in 28 Swedish patients diagnosed with CHARGE syndrome', *Clin Genet* 74(1): 31-8.

Winnier, G. E., Kume, T., Deng, K., Rogers, R., Bundy, J., Raines, C., Walter, M. A., Hogan, B. L. and Conway, S. J. (1999) 'Roles for the winged helix transcription factors MF1 and MFH1 in cardiovascular development revealed by nonallelic noncomplementation of null alleles', *Dev Biol* 213(2): 418-31.

Winter, E. M. and Gittenberger-de Groot, A. C. (2007) 'Epicardium-derived cells in cardiogenesis and cardiac regeneration', *Cell Mol Life Sci* 64(6): 692-703.

Winter, E. M., Grauss, R. W., Hogers, B., van Tuyn, J., van der Geest, R., Lie-Venema, H., Steijn, R. V., Maas, S., DeRuiter, M. C., deVries, A. A. et al. (2007) 'Preservation of left ventricular function and attenuation of remodeling after transplantation of human epicardium-derived cells into the infarcted mouse heart', *Circulation* 116(8): 917-27.

Winter, E. M., van Oorschot, A. A., Hogers, B., van der Graaf, L. M., Doevendans, P. A., Poelmann, R. E., Atsma, D. E., Gittenberger-de Groot, A. C. and Goumans, M. J. (2009) 'A new direction for cardiac regeneration therapy: application of synergistically acting epicardium-derived cells and cardiomyocyte progenitor cells', *Circ Heart Fail* 2(6): 643-53.

Xu, H., Morishima, M., Wylie, J. N., Schwartz, R. J., Bruneau, B. G., Lindsay, E. A. and Baldini, A. (2004) 'Tbx1 has a dual role in the morphogenesis of the cardiac outflow tract', *Development* 131(13): 3217-27.

Xu, Z., Gutierrez, L., Hitchens, M., Scherer, S., Sater, A. K. and Wells, D. E. (2008) 'Distribution of polymorphic and non-polymorphic microsatellite repeats in Xenopus tropicalis', *Bioinform Biol Insights* 2: 157-69.

Yagi, H., Furutani, Y., Hamada, H., Sasaki, T., Asakawa, S., Minoshima, S., Ichida, F., Joo, K., Kimura, M., Imamura, S. et al. (2003) 'Role of TBX1 in human del22q11.2 syndrome', *Lancet* 362(9393): 1366-73.
Yamagishi, H. and Srivastava, D. (2003) 'Unraveling the genetic and developmental mysteries of 22q11 deletion syndrome', *Trends Mol Med* 9(9): 383-9.

Yang, W., Klaman, L. D., Chen, B., Araki, T., Harada, H., Thomas, S. M., George, E. L. and Neel, B. G. (2006) 'An Shp2/SFK/Ras/Erk signaling pathway controls trophoblast stem cell survival', *Dev Cell* 10(3): 317-27.

Yelin, R., Yelin, D., Oh, W. Y., Yun, S. H., Boudoux, C., Vakoc, B. J., Bouma, B. E. and Tearney, G. J. (2007) 'Multimodality optical imaging of embryonic heart microstructure', *J Biomed Opt* 12(6): 064021.

Yergeau, D. A., Johnson Hamlet, M. R., Kuliyev, E., Zhu, H., Doherty, J. R., Archer, T. D., Subhawong, A. P., Valentine, M. B., Kelley, C. M. and Mead, P. E. (2009)

'Transgenesis in Xenopus using the Sleeping Beauty transposon system', *Dev Dyn* 238(7): 1727-43.

Yergeau, D. A. and Mead, P. E. (2007) 'Manipulating the Xenopus genome with transposable elements', *Genome Biol* 8 Suppl 1: S11.

Zhang, C., Basta, T. and Klymkowsky, M. W. (2005) 'SOX7 and SOX18 are essential for cardiogenesis in Xenopus', *Dev Dyn* 234(4): 878-91.

Zhang, J., Somani, A. K. and Siminovitch, K. A. (2000) 'Roles of the SHP-1 tyrosine phosphatase in the negative regulation of cell signalling', *Semin Immunol* 12(4): 361-78.

Zhou, B., von Gise, A., Ma, Q., Hu, Y. W. and Pu, W. T. (2010) 'Genetic fate mapping demonstrates contribution of epicardium-derived cells to the annulus fibrosis of the mammalian heart', *Dev Biol* 338(2): 251-61.

Zhou, Y., Ching, Y. P., Kok, K. H., Kung, H. F. and Jin, D. Y. (2002) 'Post-transcriptional suppression of gene expression in Xenopus embryos by small interfering RNA', *Nucleic Acids Res* 30(7): 1664-9.

Appendix 2

Immunoisolation of protein complexes from *Xenopus*

Overview

This work was published as an in-depth technical article as part of the series *Xenopus Protocols: Post-Genomic Approaches* (ed. Stefan Hoppler and Peter D. Vize) in the journal *Methods in Molecular Biology*. It is based on an ongoing collaboration between our laboratory and Ileana Cristea's lab at Princeton University to optimize the isolation of protein complexes from *Xenopus* embryonic tissue. I contributed an IP-western blot demonstrating assessment of isolation efficiency of an endogenous protein (Shp2) and to the writing of the manuscript itself. The article was conceived and finalized by Frank Conlon and Ileana Cristea.

Conlon F.L., Miteva Y., Kaltenbrun E., Waldron L., Greco T.M., and Cristea I.M. (2012) Immunoisolation of protein complexes from *Xenopus*. *Methods in Molecular Biology*, vol 917: 369-390.

The immunoaffinity isolation of protein complexes is an essential technique for the purification and concentration of protein complexes from cells and tissues. In this chapter we present the methodologies for the purification of proteins and protein

complexes from *Xenopus laevis* and *Xenopus tropicalis.* Specific to this protocol are the techniques for the cryolysis of *Xenopus* cells and tissues, a procedure that limits contamination from yolk proteins while preserving endogenous protein complexes, the methodologies for immunoaffinity purification of proteins using magnetic beads, and the protocols for western blot analysis. In addition, the procedures in this chapter can be extended to use with proteomic analysis of protein complexes as presented in the following chapter.

INTRODUCTION

It is becoming increasingly clear that many forms of human disease are associated with defects in genes that are required for early steps in embryonic development. Moreover, the molecular and cellular pathways through which these genes function can be elucidated using established model systems such as the African clawed frog, *Xenopus*. *Xenopus* has numerous advantages as a model system in which to identify and characterize cellular and developmental processes particularly in regards to proteomic-based approaches. Most critically, unlike the mouse, the *Xenopus* embryo develops externally and the embryo is relatively large and is amenable to surgical manipulations, allowing defined regions to be excised and cultured in simple salt solutions. These classical approaches are complemented by molecular techniques that allow the ectopic expression, overexpression, or knock-down of specific gene transcripts in the early embryo, and transgenic technologies.

Complementary to these approaches are emerging biochemical approaches. In this regard, *Xenopus* offers a unique model system for the identification and characterization of protein complexes *in vivo*. However, the use of these approaches has been limited due to the lack of optimized protocols for isolation of early stage *Xenopus* tissues and the large abundance of yolk proteins. As shown in Figure A2.1, this chapter describes methods for conducting immuno-precipitation of endogenous protein complexes in *Xenopus laevis* and *Xenopus tropicalis* which combines the cryogenic lysis of tissues with immunoisolation on magnetic beads. An overview of the approach is shown in Figure A2.1. Collectively, these approaches function to preserve endogenous protein complexes, limit problems associated with yolk platelets, and proved a specific isolation of a given protein.

METHODS AND EQUIPMENT

Obtaining *Xenopus laevis* embryonic tissue

1. Fine watchmaker's forceps such as Dumont number 5 forceps.
2. X. *laevis* embryos cultured to desired stage of development (Nieuwkoop, 1994)
3. 10X Modified Barth's Saline (MBS), pH 7.8: 880 mM NaCl, 10 mM KCl, 10 mM $MgSO_4$, 50 mM HEPES pH 7.8, 25 mM $NaHCO_3$. 1X MBS is made by mixing 100 mL of 10X stock solution with 700 µL 1 M $CaCl_2$ and adjusting the volume to 1 L with dH_2O. Store at room temperature.
4. 1% agarose plates for dissections: Weigh 1 g agarose and transfer to 250 mL Erlenmeyer flask containing 100 mL dH_2O. Heat flask in microwave until agarose has completely dissolved. Cool molten agarose until cool enough to

hold flask. Pour a layer of agarose into small plastic petri dishes (5 cm). Allow agarose to set. Store plates at 4°C.

5. Plastic transfer pipettes
6. Liquid nitrogen
7. Syringe needle (19G1½)
8. 50 mL conical tubes
9. A dissecting microcope (e.g. Leica MZ6)

Tissue lysis and protein extraction

1. Retsch MM 301 Mixer Mill with 2 X 25 mL jars and 2 X 20 mm (tungsten carbide or stainless steel) grinding balls (Retsch, Newtown, PA).
2. Liquid nitrogen, Styrofoam container and a pair of long forceps
3. Windex
4. Methanol
5. 50 mL conical tubes
6. Ultrapure water

Immunoaffinity purification of protein complexes

Conjugation of magnetic beads

Unless otherwise stated all solutions can be stored at room temperature

1. Dynabeads M-270 Epoxy (Invitrogen).

2. Affinity purified antibodies against a protein of interest or tag (e.g., anti-GFP antibodies as shown below for the isolation of GFP-tagged proteins), or Immunoglobulin G (for isolation of Protein A-tagged proteins).
3. 0.1 M Sodium Phosphate buffer, pH 7.4: Prepare as 19 mM NaH_2PO_4, 81 mM Na_2HPO_4 in water and adjust pH to 7.4, if necessary. Filter sterilize (0.2 µm filter (Millipore)). Store at 4°C.
4. 3 M Ammonium Sulfate: Prepare in 0.1 M Sodium Phosphate buffer, pH 7.4. Filter sterilize (0.2 µm filter (Millipore)).
5. 100 mM Glycine-HCl, pH 2.5: Prepare in water. Adjust pH to 2.5 with HCl. Filter sterilize (0.2 µm filter (Millipore)). Store at 4°C.
6. 10 mM Tris, pH 8.8: Prepare in water. Adjust pH to 8.8 with HCl. Filter sterilize (0.2 µm filter (Millipore)).
7. 100 mM Triethylamine: Prepare fresh in water. CAUTION: toxic and extremely flammable. Must handle in a chemical hood and dispose of appropriately.
8. DPBS, pH 7.4 (Dulbecco's Phosphate-Buffered Saline (1X), liquid), (Invitrogen): Store at 4°C.
9. 0.5% Triton X-100: Prepare in DPBS. Store at 4°C.
10. 0.02% Sodium azide (NaN_3): Prepare in DPBS. Store at 4°C. CAUTION: NaN_3 is a toxic solid compound. Must handle in a chemical hood and dispose of appropriately.
11. Rotator (at 30°C)
12. Magnetic separation tube rack (Invitrogen)
13. Tube shaker (Tomy shaker)

14. Round bottom 2 mL Safe-Lock tubes (Eppendorf)
15. Ultrapure water (e.g., from a Milli-Q Integral Water Purification System)

Immunoaffinity purification

1. Frozen tissue powder (see section *Obtaining Xenopus laevis embryonic tissue*)
2. Optimized lysis buffer (See section *Tissue lysis and protein extraction*) prepared fresh prior to each experiment.
3. Magnetic beads conjugated with antibodies (see section *Conjugation of magnetic beads*)
4. 50 mL conical tubes
5. Polytron for tissue homogenization (e.g., PT 10-35 Polytron from Kinematica)
6. Centrifuge and rotor, compatible with 50 mL conical tubes and capable of 8000 x g at 4°C
7. Tube rotator at 4°C
8. Ultrapure dH_2O
9. Round bottom eppendorf tubes (Fisher)
10. Axygen Maxymum Recovery microcentrifuge tubes, 1.5 mL (VWR)
11. Bar magnets (for conical tubes) and magnetic separation rack (for eppendorf tubes) (Invitrogen)
12. Ammonium hydroxide, 14.8 M (Sigma). Store at 4°C.
13. Base elution buffer: Mix 4.826 mL of ultrapure H_2O, 5 µL of 0.5 M EDTA, pH 8.0, and 169 µL of ammonium hydroxide. Prepare fresh before use.

14. 4X LDS elution buffer: Dissolve 0.666 g of Tris-HCl, 0.682 g of Tris-Base, 0.8 g of LDS, and 0.006 g of EDTA (free acid) in ultrapure dH_2O to a final volume of 10 mL. Aliquot and store at -20°C.
15. 10X Reducing Agent (Invitrogen)
16. 1M iodoacetamide (IAA) (Sigma): Dissolve 0.185 g of iodoacetamide in 1 mL HPLC grade water. Dispense into 50 x 20 ml aliquots and store at -20°C
17. Heat block at 70°C

Assessment of immunoaffinity purification: Sample preparation

1. Reserved fractions (from section *Basic elution of immunoisolates*)
   a. Cell pellet (step 7)
   b. Input Supernatant (step 7)
   c. Flow-through (step 11)
   d. Primary eluate (step 21)
   e. Secondary eluate (step 18)
2. Ultrapure dH_2O
3. Acetone (-20°C)
4. 1.7 mL eppendorf tubes (Fisher)
5. Microcentrifuge
6. NuPAGE 4-12% Bis-Tris pre-cast SDS-PAGE gel, 10 well (Invitrogen)
7. Xcell SureLock Mini-Cell electrophoresis system (Invitrogen)

1. 20X NuPAGE MOPS SDS Running Buffer (Invitrogen)
8. 4X NuPAGE LDS Sample Buffer (Invitrogen)

9. 10X Reducing Agent (Invitrogen)
10. Heat block at 70°C

Assessment of immunoaffinity purification: SDS-PAGE and western blot analysis

1. Prepared fractions (from section *Assessment of immunoaffinity purification: Sample preparation*)
   a. Cell pellet (step 1)
   b. Input supernatant (step 2)
   c. Flow-through (step 3)
   d. Secondary eluate (step 4)
   e. Primary eluate (step 5)
2. NuPAGE 4-12% Bis-Tris gel, 10 well (Invitrogen)
3. Xcell SureLock Mini-Cell electrophoresis system (Invitrogen)
4. 20X NuPAGE MOPS SDS Running Buffer (Invitrogen)
5. 1X Running Buffer: Dilute 20X NuPAGE MOPS SDS Running Buffer in 700 mL of ultrapure water.
6. Precision Plus Protein Dual Color Molecular Weight Standards (BioRad)
7. 4X NuPAGE LDS Sample Buffer (Invitrogen)
8. 10X Reducing Reagent (Invitrogen)
9. PVDF membrane (BioRad)
10. Methanol
11. Transfer apparatus (e.g. Mini Trans-blot Cell from BioRad)

12. 10X Transfer Buffer: Dissolve 144 g glycine and 30.3 g Tris base in final volume of 1 L dH_2O. Prepare 1L of 1X Transfer Buffer containing 20% methanol. Chill at 4°C for 30min before use.
13. 2 x Whatman filter paper and 2 x sponges for transfer
14. 20X TBST: 200 mM Tris-HCl pH 8, 3 M NaCl, 2% Tween-20 in dH_20. Dilute to 1X with dH_20 for use.
15. Blocking Buffer: 5% non-fat dry milk powder in 1X TBST.
16. Appropriate primary and secondary antibodies, diluted in Blocking Buffer
17. Autoradiography cassette (FisherBiotech Cat# FBCA 57)
18. ECL chemiluminescent substrate kit (Thermo Scientific)
19. Autoradiography film (Kodak)

METHODS AND PROCEDURES

Obtaining *Xenopus laevis* embryonic tissue

Of all the proteins in *X. laevis* embryonic tissue, yolk proteins are among the most abundant, especially at earlier developmental stages when the embryo is still dependent on yolk for nutrients. The abundance of yolk proteins can be problematic when performing immunoaffinity purifications, as these proteins can nonspecifically react with antibodies and mask a less abundant interaction. For this reason, it is desirable to remove as much of the yolk from the embryo as possible.

1. Fill a 1% agarose plate with cold 1X MBS. Transfer *X. laevis* embryos to MBS in agarose plate.

2. Using fine forceps and a dissecting microscope, remove as much of the yolk as possible from the rest of the embryo. Using a plastic transfer pipette, transfer the embryo to a new agarose plate containing fresh 1X MBS. Keep tissue on ice until all dissections are completed. Collect appropriate number of embryos for each immunopurification to be performed (See Note 1).
3. Using a syringe needle, poke 4 holes in the cap of a 50 mL conical tube. Remove cap and secure tube into a rack in a styrofoam cooler. Fill cooler and tube with liquid nitrogen.
4. Using a plastic transfer pipette, drop embryos one by one into liquid nitrogen in conical tube (see Note 4). When finished, replace the cap and screw on tightly. Remove the tube from the cooler (using a paper towel for protection) and invert to remove the liquid nitrogen. Store frozen tissue at -80°C.

Tissue lysis and protein extraction

Tissue lysis can be carried out utilizing several approaches, including homogenization in a detergent-containing lysis buffer, passage through a needle (different needle gauges can be tested for efficiency of lysis), and cryogenic tissue disruption using traditional mortar and pestle or a Mixer Mill. While the procedures described below for immunoaffinity purification of protein complexes utilize as starting material tissue disrupted cryogenically using a Mixer Mill, the other types of tissue lysis can also be incorporated. We prefer the type of cryogenic disruption described below as it leads to an increased efficiency of extraction (i.e., isolation of the targeted protein) and decreased level of non-specific associations. This method

has provided us with a reliable and effective means of cell lysis for isolating varied protein complexes (Cristea et al., 2005; Cristea et al., 2006; Carabetta et al., 2010; Goldberg et al., 2010; Moorman et al., 2010; Greco et al., 2011). In circumstances that require a mild tissue lysis, such as the maintenance of intact organelles or large structures, e.g postsynaptic densities (Selimi et al., 2009), cryogenic disruption may not be the method of choice.

Cryogenic tissue disruption

1. Clean one spatula, the Retsch Mixer Mill jars, and the grinding balls sequentially with ultrapure dH_2O, Windex, ultrapure dH_2O, and 100% methanol. Allow all parts to dry completely in a chemical hood.
2. Cool the jars and balls in liquid nitrogen (e.g., using a Styrofoam container filled with liquid nitrogen). Once cooled (i.e., liquid nitrogen no longer appears to be bubbling) remove them from the liquid nitrogen container using a pair of long forceps and place the frozen tissue into the jar. The tissue can fill up to a maximum of one third of the total volume of the jar for optimal cryogenic grinding (e.g., ~7 g frozen tissue pellets per 25 mL jar). Add the chilled ball on top of the tissue (use one ball per jar), close the jar, and place it back into the liquid nitrogen container to cool.
3. Place the filled jars in the Retsch Mixer Mill holders. If only one jar contains frozen tissue for grinding, then use the other empty jar (without a ball) as a balance. Grind the tissue using 20 cycles of 2 minutes 30 seconds each at a

frequency of 30 Hz. Place the jars in liquid nitrogen in between cycles to cool, and ensure that the jars are still tightly closed.

4. Open the jar and use a chilled spatula to transfer the frozen tissue powder to a 50 mL conical tube kept on dry ice. Work as quickly as possible to avoid thawing of the ground sample. Periodically chill the spatula in liquid nitrogen. Store the powder at -80°C until immunopurification is to be performed.

Optimization of lysis buffer and isolation conditions

Successful isolation of a protein of interest and its interacting partners is dependent on several criteria including protein abundance and subcellular localization, sample amount, affinity of the antibody used for immunoaffinity purification, efficiency of bead conjugation, and lysis buffer conditions for immunoaffinity purification. During the cell lysis and protein isolation steps it is crucial to extract and preserve the targeted protein with its interactions in a soluble fraction. Therefore, the lysis buffer conditions utilized prior and during the affinity purification have to be optimized for each protein of interest before proceeding with larger scale immunoaffinity purifications for proteomics studies. This can be done by performing small scale experiments (i.e., 20 embryos per immunopurification) that use western blotting to assess 1) the efficiency of protein solubilization (see procedure below) and 2) efficiency of isolation (see section *Assessment of immunoaffinity purification*). It is recommended to compare at least three lysis buffer conditions with varied levels of stringency. Generally, the stringency of a lysis buffer is determined by the concentrations and combinations of detergents and salts. Table

A2.1 provides examples of frequently used detergents, and Table A2.2 lists several lysis buffers that differ slightly in their compositions and were successfully utilized in immunoaffinity purifications of protein complexes from varied species.

1. Split cryogenically ground tissue into equal small aliquots (e.g., 0.1 g) (see Note 2). Ensure that the tissue power does not thaw during the weighing.
2. Place the small aliquots on ice (4°C) and add a different lysis buffer (5 mL buffer per 1 g cells) to each sample.
3. Homogenize the tissue powder in the buffer by vortexing for 1 min with intermittent cooling. This step is different than the usual homogenization for immunoaffinity purifications, which uses a polytron and a larger volume for the starting material.
4. Separate the soluble and insoluble fractions by centrifugation at 8000 x g at 4°C for 10 minutes. Recover soluble fraction and label “supernatant”
5. Wash the pellet in water and discard supernatant. Extract pellet by sequential sonication then boiling at 95°C for 5 min in 50 mM Tris-HCl, pH 7.4, containing 2% SDS. Centrifuge at 20,000 x g for 10 min. Recover supernatant and label “Pellet”.
6. Assess the levels of bait protein in the supernatant and pellet fractions (5 – 10% aliquots) using western blotting and antibodies against either the affinity tag (if present) or the endogenous protein.
7. To proceed with a larger scale immunoaffinity purification for proteomics analyses, select the lysis buffer condition that provides the highest proportion of

bait protein in the soluble fraction, at the lowest necessary stringency. This will allow for a balance between an efficient extraction of the protein of interest and maintenance of interacting partners (see Note 3).

Immunoaffinity purification of protein complexes

Conjugation of magnetic beads

This protocol has been optimized for conjugation of Dynabeads M-270 Epoxy, however it can also be applied for conjugation of other types of magnetic beads with larger or smaller diameters. In such cases, it is important to adjust the amount of antibody used for conjugation, depending on the bead capacity of binding. This protocol can be utilized for conjugating beads with high-affinity purified in-house developed antibodies as well as commercially available ones, provided their storage buffer doesn't hinder covalent conjugation to Epoxy.

It is best to start this protocol in the late afternoon and perform all washing steps (Step 7-10) in the morning of the following day. Unless otherwise stated all steps should be performed at room temperature. Do not allow the beads to dry out (i.e., do not keep the beads without a washing solution in between the steps).

1. Weigh out the necessary amount of magnetic Dynabeads in a round-bottom tube.
   a. Round-bottom tubes are preferred to avoid the trapping of beads in conical-shape tubes during the conjugation.

b. The necessary amount of beads is dependent on the purpose of the experiment and the abundance of the protein that will be immunoaffinity purified. An approximate guidance: 1-2 mg beads are appropriate for small-scale optimization experiments, 5-7 mg beads are usually sufficient for performing single immunoaffinity purifications, and 10-20 mg beads are suitable for highly abundant proteins.

2. Add 1 mL Sodium Phosphate buffer pH 7.4 to the beads; mix by vortexing for 30 sec, followed by 15 min on a tube shaker (vigorous setting).
3. Place the tube on a magnetic rack. After all the beads settle towards the magnetic side, discard the buffer.
4. Remove the tube from the rack. Add 1 mL Sodium Phosphate buffer pH 7.4. Mix by vortexing for 30 sec and remove the buffer in the same manner as above.
5. Remove the tube from the rack. Add, in this order, the necessary amount of antibodies, Sodium Phosphate buffer, and Ammonium Sulfate solution.
   a. The optimal total volume during the beads conjugation (that includes the antibody, Sodium Phosphate buffer, and Ammonium Sulfate solution) is ~ 20 µl/mg beads
   b. As a guideline of amounts of antibodies or IgG that we routinely use: 8-10 µg Ab/mg beads for commercially available antibodies and IgG, and 3-5 µg Ab/mg beads for purified high-affinity antibodies (e.g., in-house developed anti-GFP antibodies).

c. The 3 M Ammonium Sulfate solution is added last and will be one third of total volume to give a final concentration of 1 M.

d. For example, to conjugate 18 mg beads, use a total volume of 360 µL. For this, add 54 µg antibody to beads (if using 3 µg Ab/mg beads), then add 0.1 M Sodium Phosphate Buffer (volume 0.1 M Sodium Phosphate Buffer = 360 µL – volume of antibody used – 66.7 µL 3M Ammonium Sulfate), then add 66.7 µL of 3 M Ammonium Sulfate.

6. Secure the tube with parafilm and rotate bead slurry overnight on rotator at 30°C.

7. The next morning, place the tube with bead slurry on a magnetic rack. Remove and reserve the supernatant to assess the efficiency of bead conjugation by SDS-PAGE (See Note 4).

8. Wash the beads sequentially with the following buffers. For each wash, gently resuspend the beads in 1 mL of the buffer, then place the tube on the magnet and remove buffer. “FAST” indicates that buffer should not be in contact with beads for longer than it takes to resuspend them:

   a. 1 mL of Sodium Phosphate buffer

   b. 1 mL 100 mM Glycine-HCl, pH 2.5 (FAST)

   c. 1 mL 10 mM Tris-HCl pH 8.8

   d. 1 mL 100 mM Triethylamine solution (FAST)

   e. 4 x 1 mL DPBS

   f. 1 mL DPBS containing 0.5% Triton X-100. Leave the tube on a Tomy shaker (gentle setting) for 15 min.

g. 1 mL DPBS

9. Beads can be used immediately or stored at 4°C in DPBS containing 0.02% NaN_3. For beads stored for future use, measure the final volume of the bead slurry (the bead size will contribute to the final volume) and make a note of the volume required for one mg beads as this will permit known aliquots of beads to be removed for multiple immunoaffinity purifications. Beads should be used within 2 weeks of conjugation. After 1 month of storage, their efficiency for isolation decreases by approximately 40%.

Immunoaffinity purification: Basic elution of immunoisolates

It is important to prepare all necessary reagents beforehand. Carry out all procedures on ice unless otherwise noted. At several steps during the protocol aliquots of samples (indicated with "RESERVE") are taken to assess bait protein extraction and isolation efficiency (see section *Assessment of immunoaffinity purification*).

Day 1

1. Prepare appropriate volume of optimized lysis buffer as determined in section 3.2.2. Pre-cool to 4°C. Add protease inhibitors just before use. Prepare 10 mL of wash buffer per sample (used in steps 6, 11 – 13), which is usually identical in composition to the optimized lysis buffer, except protease and phosphatase inhibitors cocktails are not included.

2. Incubate the frozen tissue powder on ice for 1 - 2 min, but do not thaw. Proceed immediately to step 3.
3. Resuspend the frozen tissue powder in appropriate volume of lysis buffer by first adding a small amount of lysis buffer and swirling homogenate to solubilize pellet. Continue to add lysis buffer and gently mixing by hand until tissue powder has been completely solubilized (see Note 5).
4. Run Polytron 10 sec in ultrapure dH_2O to wash. Ensure that the tissue homogenate occupies ≤ 1/3 of the conical tube volume. Subject tissue lysates to Polytron homogenization for 2 x 15 second (speed = 22.5k), resting the sample on ice for a few minutes between homogenizations. If processing additional samples, rinse and run Polytron in ultrapure dH_2O to wash out excess lysate. When finished, perform a final rinse with methanol.
5. Centrifuge the lysate at 8000 x g at 4°C for 10 minutes.
6. During centrifugation, place tube containing antibody-conjugated magnetic beads on a magnetic rack for 30 – 60 secs. Discard the storage buffer and wash with 3 x 1 mL wash buffer by gently pipeting up and down to resuspend the beads. Do not vortex antibody-conjugated beads. Suspend beads in 100 – 200 mL of wash buffer.
7. Carefully pour the clarified lysates (supernatant) into new 50 mL conical tubes (see Note 6). RESERVE (i) the cell pellet and (ii) 40 mL of the input supernatant (See section *Assessment of immunoaffinity purification* for analysis).

8. Gently flick tube of antibody-conjugated beads to mix beads in solution. Pipet the appropriate amount of beads into the clarified lysates.
9. Rotate the lysates with beads on a rotator at 4°C for 1 hour. Do not use longer incubation times as this promotes the accumulation of non-specific binding and loss of weak interacting partners.
10. During incubation, prepare base elution buffer and 1X LDS elution buffer (see Note 7).
11. Attach a bar magnet to the lysates/bead suspension tube using a rubber band. Incubate on ice for 5 min. RESERVE the flow-through (unbound) fraction by pouring the supernatant into a clean conical tube (see section *Assessment of immunoaffinity purification* for analysis)
12. Resuspend the beads in 1 mL of wash buffer and transfer the bead slurry to a round-bottom eppendorf tube.
13. Place on a magnetic rack for 30 sec to pellet the beads and discard wash buffer. Perform this procedure between all subsequent wash steps.
14. Wash the beads 3 x 1 mL wash buffer. On the third wash, transfer the bead slurry to a clean round-bottom eppendorf tube, then pellet beads and discard wash buffer.
15. Wash the beads 2 x 1 mL with wash buffer.
16. Add 1 mL DPBS to beads and transfer slurry to clean round-bottom eppendorf tube. Repeat wash once with 1 mL of DPBS to remove residual detergent. Quantitatively remove DPBS wash.

17. Add 750 ml of base elution buffer. Incubate at RT for 20 min while shaking (see Note 8).
18. Place the tube on the magnetic rack and transfer the eluate to an Axygen microcentrifuge tube. Freeze primary eluate in liquid nitrogen and evaporate to dryness overnight by vacuum centrifugation.
19. Perform a second elution from the beads by suspending the beads in 40 µL of 1X LDS elution buffer containing 50 mM DTT, incubating at 70°C for 10 min, and then at RT for 10 min while shaking. Place the tube on a magnetic rack and transfer the eluate to a clean microcentrifuge tube. RESERVE 10% (4 µl) of the secondary eluate in a clean microcentrifuge tube (see section *Assessment of immunoaffinity purification* for analysis). Freeze remaining 90% of secondary eluate in liquid nitrogen and store at -20°C.
20. Proceed to *Assessment of immunoaffinity purification* to prepare reserved samples for Western blot analysis. Continue with step 21 the following day.

Day 2

21. Remove dried eluate from the Speedvac.
    a. If performing SDS-PAGE-in-gel digestion (see Note 4), suspend dried eluate in 40 mL of 1X NuPAGE sample buffer containing 1X reducing agent and heat at 70°C for 10 min. RESERVE 10% (4 µl) of the eluate in a clean microcentrifuge tube. Add 4 ml of 1 M iodoacetamide to remaining 90% of primary eluate and incubate 30 min at RT protected from light. Freeze in

liquid nitrogen and store at -20°C or proceed immediately to proteomic analysis (see (Greco et al., 2012)

b. If in-solution digestion is to be performed (see Note 4), suspend dried eluate in 40 mL of 1X LDS elution buffer containing 50 mM DTT and heat at 70°C for 10 min. RESERVE 10% (4 µl) of the eluate in a clean microcentrifuge tube. Freeze remaining 90% of primary eluate in liquid nitrogen and store at -20°C or proceed immediately to proteomic analysis (see (Greco et al., 2012).

Immunoaffinity purification: Alternate procedure (detergent elution of immunoisolates; see Note 7)

Day 1

1. Perform steps 1 – 16 as described above, except preparation of base elution buffer can be omitted (step 10).
2. Add 40 µl of 1X LDS elution buffer to beads. Incubate 10 min at 70°C, then 10 min at RT while shaking.
3. Pellet beads on magnetic rack and transfer primary eluate to an Axygen microcentrifuge tube.
4. Repeat Steps 2 and 3, transferring secondary eluate to an Axygen microcentrifuge tube.
5. Add 2.0 mL of 1 M DTT to primary and secondary eluates. Heat at 70°C for 10 min. RESERVE 10% (4 µl) of eluates in clean microcentrifuge tubes.

6. If performing in-gel digestion (see Note 8), add 4 µl of 1 M iodoacetamide to remaining 90% of eluates and incubate at RT for 30 min protected from light. If performing in-solution digestion (see Note 8), proceed directly to step 7.
7. Freeze remaining 90% of eluates in liquid nitrogen and store at -20°C or proceed immediately to proteomic analysis (see (Greco et al., 2012).

Assessment of immunoaffinity purification: Sample preparation

Reserved sample aliquots from section *Immunoaffinity purification* are prepared for SDS-PAGE and Western blot analysis. The recommended amount of each aliquot analyzed is provided as a starting point, and may need further optimization for differences in input material and bait protein abundance.

1. Cell Pellet
    a. Wash the cell pellet with 1.0 mL dH_2O. Homogenize washed cell pellet in 1.0 mL of 2% SDS, transfer to microcentrifuge tube, and heat at 70°C for 10 min. Centrifuge at maximum speed for 5 minutes at RT (see Note 9).
    b. Remove aliquot of SDS-soluble pellet fraction that corresponds to an identical percent of the input supernatant. For example, assuming a 40 µL aliquot of input supernatant was reserved from a total lysis volume of 10 mL, a 4 µL aliquot of the pellet sample should be removed.
    c. Dilute aliquot of SDS-soluble pellet fraction to a final volume of 60 µL containing 1X NuPAGE LDS Sample Buffer/1X Reducing Agent.
2. Input Supernatant

a. Dilute 40 µL of reserved input supernatant to a final volume of 60 µL containing 1X NuPAGE LDS Sample Buffer/1X Reducing Agent.

3. Flow-through (see Note 10)
   a. Transfer 10% of flow-through to clean tube. Slowly add 4 volumes of -20°C acetone. Vortex briefly. Incubate at -20°C for at least 1 hr.
   b. Centrifuge at 3000 x g at 4°C for 10 min. Pour off supernatant
   c. Briefly wash pellet with 4 volumes of 80% acetone/20% dH_2O and discard.
   d. Air dry pellet for 5 min, then partially solubilize in 40 µL of 1X NuPAGE LDS Sampler Buffer/1X Reducing Agent by gentle agitation.
4. Secondary Eluate
   a. Dilute 4 µL (10%) of the secondary eluate into a final volume of 40 µL 1x NuPAGE LDS Sample Buffer/1X Reducing Agent.
5. Primary Eluate (prepared the following day, see Note 11)
   a. Dilute 4 µL (10%) of the primary eluate into a final volume of 40 µL 1x NuPAGE LDS Sample Buffer/1X Reducing Agent.
6. Heat all samples at 70°C for 10 minutes. Freeze the samples at -20°C until ready to proceed with SDS-PAGE and western blot analysis.

Assessment of immunoaffinity purification: SDS-PAGE and western blot analysis

In this protocol the efficiency of immunoaffinity isolation of the bait protein is assessed by comparing 5 samples reserved at progressing stages of the immunoaffinity purification procedure: 1) cell pellet, 2) input supernatant, 3) flow-through, 4) secondary eluate, and 5) primary eluate (see section *Immunoaffinity*

purification). While the amount of sample prepared (see section *Sample preparation*) is sufficient for duplicates analyses, the protocol below details a single experiment. A representative western blot is shown below (Figure A2.2A) indicating efficient isolation (no protein remaining in the flow-through) and recovery of the intended GFP-tagged bait protein (a majority of the protein was in the primary eluate).

1. Set up the Xcell SureLock Mini-Cell electrophoresis system:
    a. Remove the white strip and the upper comb from the NuPAGE 4-12% Bis-Tris pre-cast SDS-PAGE gel and rinse wells with ultrapure dH_20. Place the gel in the apparatus, using a buffer dam for the opposing side, then lock the assembly in place.
    b. Fill the inner chamber with 200 mL and the outer chamber with 500 mL of 1X Running Buffer.
2. Thaw fractions if previously frozen and load into wells as follows: Lane 2, 10 µL Molecular Weight Standards; Lane 3, 30 µl of input supernatant; Lane 4, 30 µl of cell pellet; Lane 5, 20 µl of primary eluate; Lane 6, 20 µl of secondary eluate; Lane 8, 20 µl of flow-through; Empty lanes, 20 µL of 1X LDS Sample Buffer.
3. Electrophorese for 5 min at 100 V, then 45 - 50 min at 200 V, or until the dye front has migrated all the way down the gel.
4. While the gel is running, cut 2 pieces of Whatman filter paper and one PVDF membrane to the appropriate gel size. Always handle the membrane with tweezers.

5. Pre-wet PVDF in methanol and soak along with 2 transfer sponges, 2 filter papers, in pre-cooled 1X Transfer Buffer at least 15 min at 4°C.
6. Open gel cassette to expose gel and discard the wells. Working with wet gloves, transfer gel (by the thick ridge at the bottom) into a plastic tray containing 1X Transfer buffer. Remove bottom ridge.
7. Assemble a WB "sandwich" in the tray with pre-soaked items. Layer them in a transfer cassette as follows, starting from the clear side of the cassette: sponge, filter paper, PVDF membrane, SDS-PAGE gel, filter paper (gently roll out any bubbles using a 15ml conical tube), sponge. Close the sandwich and place into transfer apparatus with black side of cassette (gel side) facing black (anode) side transfer core. Place ice tray and stir bar into apparatus. Pour ice-cold 1X Transfer Buffer into the apparatus until it covers fully the cassette.
8. Transfer at 100 V for 1.5 hrs at 4°C while stirring.
9. Open transfer cassette and discard the filter papers and gel. Verify the pre-stained Molecular Weight Standards transferred to the membrane.
10. Wash PVDF membrane with 1X TBST, discard, then add Blocking Buffer and incubate for 1 hour at RT on a rocking platform. Do not let the membrane dry.
11. Discard Blocking Buffer and add the primary antibody diluted in Blocking Buffer. Incubate for 1-2 hours at RT or overnight at 4°C.
12. Wash the membrane 3 x 20 mL in 1X TBST for 5 min while rocking at RT.
13. Add the secondary horseradish peroxidase-conjugated antibody diluted in Blocking Buffer. Incubate for 1 hour at RT.
14. Wash the membrane 4 x 20 mL in 1X TBST for 5 min while rocking at RT.

15. Mix ECL chemiluminescence substrates in 1:1 ratio (a total volume of 1 mL is usually sufficient to cover the membrane). Using tweezers, place the membrane on a dry plastic surface and apply the ECL solution, incubating for 1 minute. Blot off the excess substrate and place the membrane between a sheet protector or Saran-wrap and tape into a film cassette.
16. Carefully place a piece of autoradiography film on top of the membrane and close the cassette avoiding any film shifts as this will result in smeared bands. An initial exposure of 30 sec will indicate whether subsequent exposures of longer or shorter duration are required.

Appropriate controls

To assess the specificity of immunoaffinity isolation it is critical to have a control sample analyzed in parallel, beginning from tissue lysis through the isolation of the target protein. The controls described below account for non-specific binding of proteins to magnetic beads, antibody, and affinity tag (when present).

GFP-tagged

Often the bait protein is expressed as a GFP fusion protein. Here, parallel isolations of the GFP-tagged protein and GFP alone are highly desirable. If the GFP-tagged protein is stably overexpressed by mRNA injection into embryos, it is necessary to generate a GFP-only tissue/animal in the same manner as the GFP fusion protein, i.e. mRNA injection of a GFP-only expression construct. Moreover, all treatment conditions and experimental variables, such as lysis buffer composition,

should be identical between the two isolations. Thus both the tag alone and the fusion protein can be immunoaffinity purified using identical preparations of antibody-conjugated magnetic beads. If lysis buffer conditions or other isolation variables are altered, such as incubation time of sample with antibody, an additional control should be performed.

FLAG-tagged

If the bait protein is tagged with FLAG, then a more appropriate control (compared to the GFP tag), is the respective cell/tissue/animal but under wild type conditions. For both FLAG-tagged and wild-type conditions, magnetic beads conjugated with an antibody against the FLAG tag should be utilized. Although this doesn't control for proteins that bind non-specifically to FLAG itself, non-specificity due to the antibody and beads can be determined.

Endogenous, non-tagged protein

In many experiments it is essential to immunoaffinity purify the bait protein at an endogenous level of expression (under its native promoter). Here, the control sample will use the identical cell/tissue/animal as for the experimental condition. In contrast to an affinity tag, the beads for the negative control are conjugated with either non-specific IgG or an IgG that lacks reactivity towards the endogenous bait protein. The control protein isolation will reveal interactions that bind non-specifically to the antibody and magnetic beads. A representative western blot from an

immunoisolation of endogenous Shp2 from *X. tropicalis* embryos is shown in Figure A2.2B.

NOTES

1. The number of embryos needed for each immunopurification is dependent on a number of criteria including protein abundance and solubility as well as the affinity of the antibody used for immunoisolation. For this reason, the optimal number of embryos and resulting amount of tissue must be optimized individually for each protein studied. Generally, 20-50 embryos per immunoisolation is a good starting point for small-scale experiments and may be scaled up for larger immunoaffinity purifications for proteomics studies.

2. If starting directly with a small amount of tissue, the sample could be ground using round-bottom eppendorf tubes or used directly for incubation with the various lysis buffers. While performing the cryogenic grinding is preferred to mimic the conditions that will be utilized for protein isolation, direct resuspension in lysis buffer is an alternative that can adequately guide selection of an optimal buffer composition.

3. The balance between extraction efficiency and maintenance of interacting partners can be further optimized by increasing the stringency of the buffer used to wash the magnetic beads relative to the buffer used for tissue homogenization.

4. To test the efficiency of bead conjugation, prepare the following samples for SDS-PAGE analysis: 1) Dilute ≥1 µg neat antibody with 2.5 µL 10x Reducing Agent and 6.25 µL 4x NuPAGE LDS Sample Buffer. Bring the sample to 25 µL total volume with dH_2O. 2) Calculate the amount of bead supernatant that is equivalent to the amount of neat antibody in the previous sample, assuming that no antibody successfully conjugated to the beads. Dilute this amount with 2.5 µL 10X Reducing Agent and 6.25 µL 4X NuPAGE LDS Sample Buffer. Bring sample to 25 µL with ultrapure H_2O. Heat samples for 10 minutes at 70°C. Centrifuge the samples at 20,000 x g for 3 minutes at room temperature and load onto an SDS-PAGE gel. Stain the gel with SimplyBlue SafeStain and look for a reduction in the amount of antibody in the lane containing the bead supernatant. Refer to Cristea *et al.* 2005 (Cristea et al., 2005) for the expected amount of unbound antibody resulting from differing amounts of antibody used in the conjugation.

5. After suspending tissue powder in lysis buffer, the solution may be slightly turbid, but should be devoid of tissue "clumps". Do not proceed to Polytron (step 4) until a homogenous suspension is observed. If necessary, additional rotation for 10 – 20 min at 4°C can be performed.

6. If insoluble particles are present in supernatant after centrifugation, a pipet can be used to selectively transfer supernatant to clean 50 mL conical tube.

7. The base elution buffer is preferred as significantly less background protein contamination is observed under these elution conditions. However, if low recovery of bait protein is observed, e.g. when a high affinity antibody is used, an “Alternate Procedure” can be followed that uses a harsher detergent-based elution buffer (see above).

8. The selection of an in-gel or in-solution digestion approach depends largely on the properties and nature of the proteins within the samples, e.g. pI, molecular weight, hydrophobicity, complexity, dynamic range, and total yield. In general, for high complexity and large yield and/or dynamic range of protein abundances, an in-gel approach is often desired. For further discussion, see (Greco et al., 2012).

9. For viscous samples, brief sonication can be used to aid solubilization of cell pellet.

10. As the flow-through fraction often has higher protein concentration, the percent of material analyzed may need to be adjusted to prevent overloading of the SDS gel. For NuPAGE gels of 1.0 mm thickness, between 100 – 150 mg is recommended.

11. If base elution buffer is used, processing of the primary eluate and its reserved fraction is not performed until the day after the immunoisolation was started (see section *Immunoaffinity purification: Base elution*, step 20).

Figure A2.1. Immunoisolation of protein complexes from *Xenopus*.

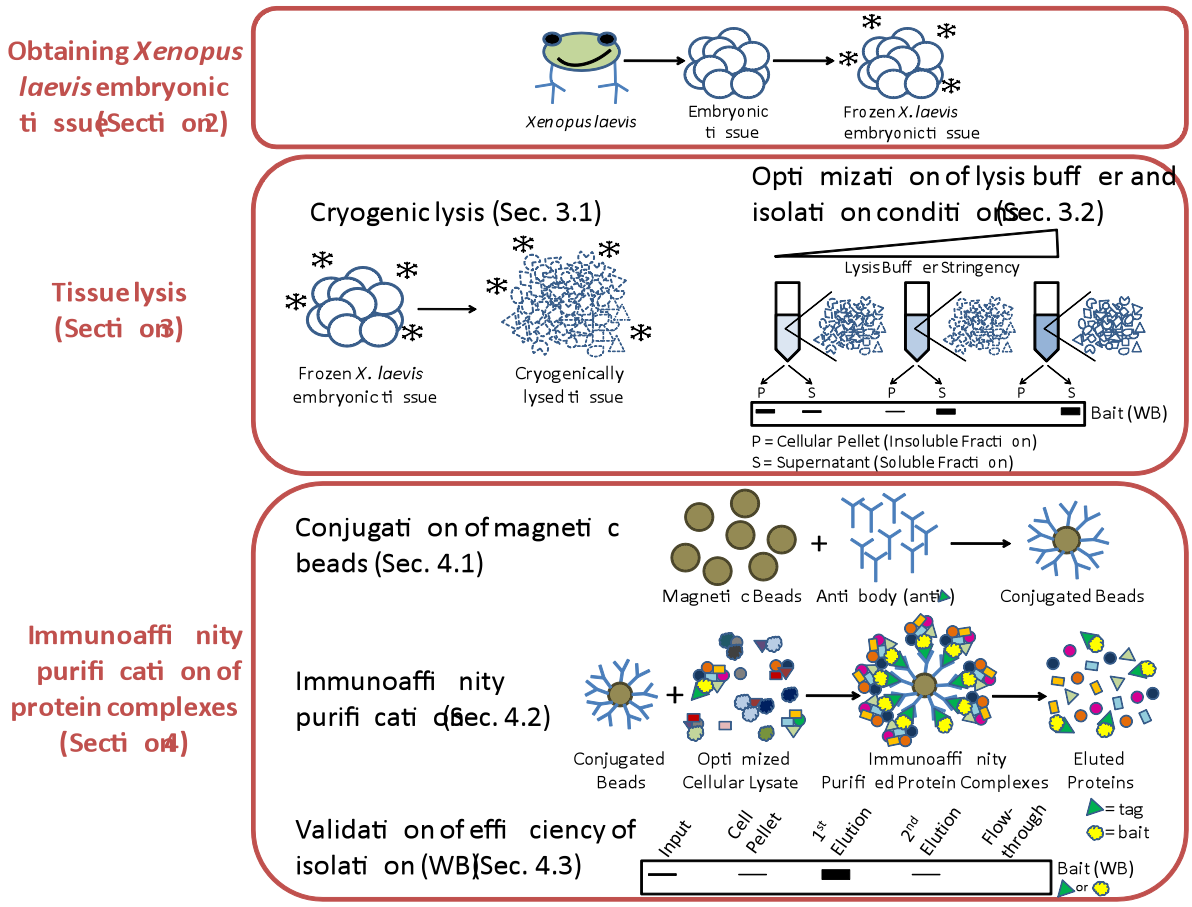

Figure A2.2. Assessment of isolation efficiency and specificity of immunoaffinity purification. (A) A GFP-tagged bait protein was isolated and eluted with the alternate detergent-based procedure. 10% of the following fractions were analyzed to assess the efficiency of isolation: FT, flow-through; PE, primary eluate; SE, secondary eluate. The majority of bait protein was found in the primary eluate. (B) Immunoaffinity purification of endogenous Shp2 protein from 100 stage 40 *Xenopus tropicalis* whole embryos. As a control for the specificity of the Shp2 antibody, a second immunopurification was performed using anti-V5 antibody-conjugated beads.

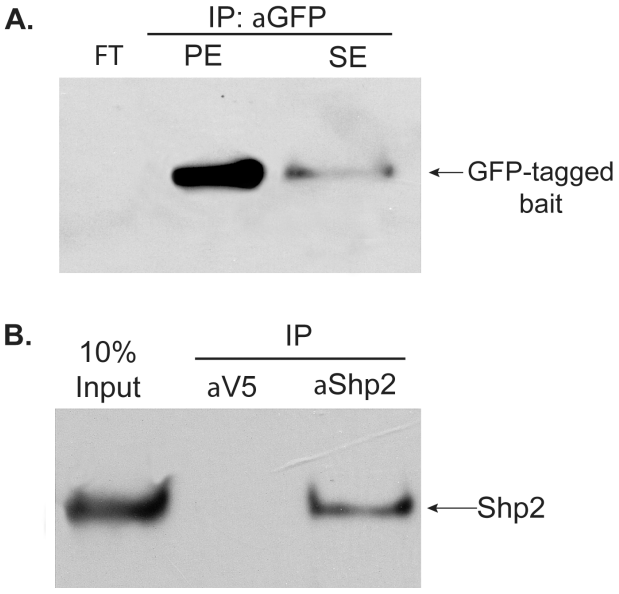

Table A2.1. Examples of detergents commonly used for cell lysis and their properties.

Detergent	Properties	Notes
Triton X-100	• Nonionic detergent • pH 6.0 to 8.0 (5% aqueous solution) • Critical micelle concentration (CMC): 0.22-24 mM • Soluble at 25°C in all proportions; Soluble in water, benzene, toluene, xylene, trichloroethylene, ethylene glycol, ethyl ether, ethanol, isopropanol, ethylene dichloride	• Depending on the utilized concentration, Triton is considered a relatively mild, non-denaturing detergent. Many enzymes remain active in 0.1%-0.5% Triton X-100 solution (e.g. Proteinase K is still active in 1% solution). • Can be used to preserve protein-lipid interactions
Sodium deoxycholate (DOC)	• Anionic detergent • pH 5.0 to 9.0 (1% aqueous solution) • CMC: 2-6 mM (0.083 to 0.249%, w/v). Micelle Molecular Weight: 2000 g (average), at concentrations above 2 mM • Soluble at 20°C; Soluble in water in less than 5% solution	• Common component of RIPA lysis buffer. • Suitable for isolating membrane associated proteins, and liposome preparation. Disrupts protein-lipid interactions.
Digitonin	• Nonionic detergent • pH: data not available • CMC: <0.5 mM, at 20-25°C. Micelle Molecular Weight: 70,000 g (average) • Soluble in water at ~5% (w/v); Must be heated to 95-98°C first, then cooled to room temperature. Soluble in	• Suitable for analyzing membrane-bound proteins and solubilizing lipids.

	ethanol at 10 mg/mL	
Octyl-beta-glucoside	• Nonionic detergent • pH: data not available • CMC: 23-25 mM (0.6716 to 0.7300%, w/v); Micelle Molecular Weight: 8000 g • Soluble in water	• Suitable for studying membrane-associated proteins • Readily integrated with mass spectrometry studies (i.e.., does not interfere as much as other detergents with ionization in MALDI MS experiments)
Nonidet P-40	• Nonionic detergent • pH 5.0 to 8.0 (5% aqueous solution) • CMC: 0.059 mM (20-25C) • Soluble in water	• Milder alternative to Triton X-100; depending on the concentration it may not penetrate nuclear membranes.

Table A2.2. Examples of lysis buffers used for immunoaffinity purification of protein complexes.

Bait (GFP-tagged)	Description & Localization	Species & Sample type	Optimized Lysis Buffer	Ref.
Apl1	beta-adaptin of AP-2 complex; cellular membrane	*S. cerevisiae* cells	20 mM K-HEPES, pH 7.4, 110 mM KOAc, 2 mM $MgCl_2$, 0.1% Tween, 0.4% Triton, 200 mM NaCl, 1/100 (v/v) protease inhibitor mixture (20 mg/mL PMSF + 0.4 mg/mL pepstatin A), and 1/200 (v/v) protease inhibitor cocktail)	(Cristea et al., 2005)
Nup37	Member of nuclear pore complex; subunit of Nup107-160 subcomplex	*Homo sapiens* cells	20 mM K-HEPES, pH 7.4, 110 mM KOAc, 2 mM $MgCl_2$, 0.1% Tween, 0.5% Triton, 200 mM NaCl, 1/100 (v/v) protease inhibitor mixture (20 mg/mL PMSF + 0.4 mg/mL pepstatin A), and 1/200 (v/v) protease inhibitor cocktail)	(Cristea et al., 2005)
HDAC5	Histone deacetylase 5; Nucleus and Cytoplasm	*Homo sapiens* cells	20 mM HEPES-KOH, pH 7.4, 0.1 M potassium acetate, 2 mM $MgCl_2$, 0.1% Tween-20, 1 µM $ZnCl_2$, 1 µM $CaCl_2$, 0.5% Triton X-100, 250 mM NaCl, 4 µg/mL DNase, 1/100 (v/v) protease and phosphatase inhibitor cocktails	(Greco et al., 2011)
PAP I	poly(A) polymerase I; Cytoplasm and inner membrane	*Escherichia coli* cells	20 mM HEPES, pH 7.4, 0.11 M KOAc, 2 mM $MgCl_2$, 0.1% Tween-20 (v/v), 1 µM $ZnCl_2$, 1 µM $CaCl_2$, 1% Triton X-100, 0.5% Deoxycholate, 150 mM NaCl, 1:100 protease inhibitor cocktail, 1:200 phenylmethylsulphonyl fluoride	(Carabetta et al., 2010)

H3	Histone 3 isoforms; Nucleus	*Mus musculus* ES cells	20 mM K-HEPES, pH 7.4, 110 mM K-acetate, 0.1% Tween 20, 0.5% Triton, 300 mM NaCl, and 1/100 (v/v) protease inhibitor cocktail	(Goldberg et al., 2010)
nsP3	Sindbis nonstructural protein 3; Cytoplasm	Sindbis-infected *Rattus Norvegicus* cells	20 mM K-HEPES, pH 7.4, 110 mM KOAc, 2 mm $MgCl_2$, 0.1% Tween 20, 1% Triton, 0.5% deoxycholate, 500 mM NaCl, 25 units/mL DNase, 1/100 (v/v) protease inhibitor mixture	(Cristea et al., 2006)
PSD (via VGluRδ 2)	postsynaptic densities; cerebellar excitatory synapses	*Mus musculus* tissue	10 mM HEPES, pH 7.4, 2 mM $CaCl_2$, 132 mM NaCl, 3 mM KCl, 2 mM $MgSO_4$, 1.2 mM NaH_2PO_4, 0.5% Triton X-100, 1/100 (v/v/) protease inhibitor cocktail	(Selimi et al., 2009)

REFERENCES

Carabetta, V. J., Silhavy, T. J. and Cristea, I. M. (2010) 'The response regulator SprE (RssB) is required for maintaining poly(A) polymerase I-degradosome association during stationary phase', *J Bacteriol* 192(14): 3713-21.

Cristea, I. M., Carroll, J. W., Rout, M. P., Rice, C. M., Chait, B. T. and MacDonald, M. R. (2006) 'Tracking and elucidating alphavirus-host protein interactions', *J Biol Chem* 281(40): 30269-78.

Cristea, I. M., Williams, R., Chait, B. T. and Rout, M. P. (2005) 'Fluorescent proteins as proteomic probes', *Mol Cell Proteomics* 4(12): 1933-41.

Goldberg, A. D., Banaszynski, L. A., Noh, K. M., Lewis, P. W., Elsaesser, S. J., Stadler, S., Dewell, S., Law, M., Guo, X., Li, X. et al. (2010) 'Distinct factors control histone variant H3.3 localization at specific genomic regions', *Cell* 140(5): 678-91.

Greco, T. M., Miteva, Y., Conlon, F. L. and Cristea, I. M. (2012) 'Complementary proteomic analysis of protein complexes', *Methods in molecular biology* 917: 391-407.

Greco, T. M., Yu, F., Guise, A. J. and Cristea, I. M. (2011) 'Nuclear import of histone deacetylase 5 by requisite nuclear localization signal phosphorylation', *Mol Cell Proteomics* 10(2): M110 004317.

Moorman, N. J., Sharon-Friling, R., Shenk, T. and Cristea, I. M. (2010) 'A targeted spatial-temporal proteomics approach implicates multiple cellular trafficking pathways in human cytomegalovirus virion maturation', *Mol Cell Proteomics* 9(5): 851-60.

Nieuwkoop, P., Faber, J. (1994) *Normal Table of Xenopus laevis*, New York: Garland Publishing.

Selimi, F., Cristea, I. M., Heller, E., Chait, B. T. and Heintz, N. (2009) 'Proteomic studies of a single CNS synapse type: the parallel fiber/purkinje cell synapse', *PLoS Biol* 7(4): e83.